



GEOLOGICAL SURVEY OF CANADA
COMMISSION GÉOLOGIQUE DU CANADA

PAPER 77-1C

This document was produced
by scanning the original publication.

Ce document est le produit d'une
numérisation par balayage
de la publication originale.

**REPORT OF ACTIVITIES
PART C**





**GEOLOGICAL SURVEY
PAPER 77-1C**

REPORT OF ACTIVITIES PART C

Minister of Supply and Services Canada 1977

Printing and Publishing
Supply and Services Canada,
Ottawa, Canada K1A 0S9,

from the Geological Survey of Canada
601 Booth St., Ottawa, K1A 0E8.

or through your bookseller.

Catalogue No. M44-77-1C
ISBN - 0-660-01500-5

Price: Canada: \$3.00
Other Countries: \$3.60

Price subject to change without notice

CONTENTS

	Page
1. C.T. SCHAFER, F.E. COLE, and F.J.E. WAGNER: Relationship of foraminifera distribution patterns to sedimentary processes in the Miramichi Estuary, New Brunswick	1
2. G.A. FOWLER, C.T. SCHAFER, and K.S. MANCHESTER: PORTAVIBE: A tool for coring from an ice platform	9
3. E.D. GHENT, and P.S. SIMONY; and W. MITCHELL, J. PERRY, D. ROBBINS, and J. WAGNER: Structure and metamorphism in southeast Canoe River area, British Columbia	13
4. A. OVERTON: Seismic determinations of basement depths, Athabasca Basin, Saskatchewan	19
5. C.T. SCHAFER and J.A. YOUNG: Experiments on mobility and transportability of some nearshore benthonic foraminifera species	27
6. P.J. KURFURST: Geotechnical study of rock heave, central Arctic Canada	33
7. J.A. HEGINBOTTOM, P.J. KURFURST, and J.S.O. LAU: Evaluation of regional occurrence of ground ice and frozen ground, Mackenzie Valley, District of Mackenzie	35
8. R.B. TAYLOR: The summer climate of Cunningham Inlet, Somerset Island, District of Franklin	39
9. D.C. FORD and H.P. SCHWARCZ: Radiometric age studies of speleothem	49
10. J. BRIAN BIRD: Coastal morphology and terrain studies, Kivito Peninsula, Baffin Island	53
11. F.J.E. WAGNER: Mollusc distribution, Chaleur Bay, New Brunswick-Quebec	57
12. R.L. GRASTY: A general calibration procedure for airborne gamma-ray spectrometers	61
13. A.K. SINHA: Charts for the correction of airborne E-Phase data	63
14. F.G. YOUNG: The mid-Cretaceous flysch and phosphatic ironstone sequence, northern Richardson Mountains, Yukon Territory	67
15. J.W.M. KERR: Frost and glacially deformed bedrock on Somerset Island, Northwest Territories	75
16. J.W.M. KERR: An unusual sea stack at high elevation on northwest Devon Island, District of Franklin	79
17. D.K. NORRIS: Geology and hydrocarbon resources, northern mainland and Offshore Canada	81
18. W. DYCK and J.C. PELCHAT: A semiportable helium analysis facility	85
19. D.J. TEMPELMAN-KLUIT and R.G. CURRIE: Uranium in Nisling Range alaskite and related rocks of Yukon crystalline terrane	89
20. J. RIMSAITE: Occurrences of rare secondary U- and Pb-bearing mineral aggregates in uranium deposits, northern Saskatchewan: A progress report	95
21. G.B. LEECH: Notes on a report evaluating the regional mineral potential (non-hydrocarbon) of the western Arctic region, Yukon and Northwest Territories	99
22. J.L. JAMBOR and J.M. BEAULNE: Exploration possibilities for porphyry deposits in the central part of Highland Valley, British Columbia	101
23. W. BLAKE, JR.: Glacial sculpture along the east-central coast of Ellesmere Island, Arctic Archipelago	107
Author Index	117

The Geological Survey of Canada

D.J. McLAREN, Director General

J.O. WHEELER, Deputy Director General

E. HALL, Scientific Executive Officer

M.J. KEEN, Director, Atlantic Geoscience Centre, Dartmouth Nova Scotia

J.A. MAXWELL, Director, Central Laboratories and Administrative Services Division

PETER HARKER, Director, Geological Information Division

D.F. STOTT, Director, Institute of Sedimentary and Petroleum Geology, Calgary Alberta

J.E. REESOR, Director, Regional and Economic Geology Division

A.G. DARNLEY, Director, Resource Geophysics and Geochemistry Division

J.S. SCOTT, Director, Terrain Sciences Division

INTRODUCTION

Since 1962 the Geological Survey has released the results of its current studies by means of brief reports grouped together in volumes titled "Report of Activities". Between 1963 and 1974 these were issued twice yearly; since 1974 the number of papers submitted for publication has necessitated the addition of a third part.

The present volume is the last to be issued under the present title. Commencing with Paper 78-1A, the series will be designated "Current Research" to better reflect the nature of the papers that make up the series. Material published in "Current Research" will be divided into scientific and technical papers and scientific and technical notes. There will also be a discussion and communications section. With few exceptions papers will be limited to 5000 words and, as in the past, will be subject to a time-limited critical review. "Current Research" will be issued at intervals best suited to meet the Geological Survey's obligations to its users. Thus, to meet the need to release promptly information obtained during the field season, Parts C and A will come out only a few months apart — November and January.

The Geological Survey has always welcomed comments on the scientific content of its publications but there has never been a forum for general discussion. The addition of a "Discussion and Communications" section will fill this gap. It will also enable those who wish to communicate new data or interpretations that would supplement the informations in our reports, to do so. Discussions will be limited to 1500 words and to reports issued not more than two years earlier. The section is for discussion of scientific content; general discussions on policy will not be accepted. Every effort will be made to publish both "Discussion" and "Reply" in the same issue. Contributions, which will be subject to editorial review, should be sent to me at the Ottawa office of the Geological Survey.

The "Report of Activities" has changed considerably since first issued and in 1977 comprised some 200 articles and more than 1000 pages. The change in format will enable us to be still more flexible and yet continue to meet the prime purpose of the publication — the rapid release of new information for use by industry, other government agencies and the general public.

Ottawa, October 3, 1977

R.G. Blackadar,
Chief Scientific Editor.

Reprints

A limited number of the reprints of the papers that appear in this volume are available by direct request to the individual authors. The addresses of the Geological Survey of Canada offices follow:

601 Booth Street,
OTTAWA, Ontario
K1A 0E8

Institute of Sedimentary and Petroleum Geology,
3303-33rd St. N.W.,
CALGARY, Alberta
T2L 2A7

British Columbia Office,
100 West Pender Street,
VANCOUVER, B.C.
V6B 1R8

Atlantic Geoscience Centre,
Bedford Institute of Oceanography,
P.O. Box 1006,
DARTMOUTH, N.S.
B2Y 4A2

When no location accompanies an author's name in the title of a paper, the Ottawa address should be used.

RELATIONSHIP OF FORAMINIFERA DISTRIBUTION PATTERNS TO SEDIMENTARY
PROCESSES IN THE MIRAMICHI ESTUARY, NEW BRUNSWICK

Project 750048

C.T. Schafer, F.E. Cole, and F.J.E. Wagner
Atlantic Geoscience Centre, Dartmouth

Introduction

An analysis of total Foraminifera populations in the Miramichi estuary has shown the presence of three distinct assemblages that are indicative of upper estuarine, lower estuarine and marginal marine environments respectively (Schafer and Scott, 1976; Scott et al. in press). The results of an analysis of total molluscan assemblages (Wagner, 1976) suggests distribution patterns that are comparable to the observed foraminiferal biotopes. Reinson (1976) recognized five major sedimentary environments in the estuary. His "river channel", "inner bay" and "tidal delta complex" are related to the foraminiferal biotopes noted above. This report summarizes some results obtained from a quantitative subsampling program carried out by SCUBA divers in each of the three distinctive environments. The aim of this study is to determine the local patterns of species distribution in each biotope and relate these observations to ecological and environmental factors.

Methodology

Sediment subsamples were collected at one station within each foraminiferal biotope (Fig. 1.1). The subsample locations at each station were located using a 3m x 3m grid made from weighted 6 mm polypropylene rope. This grid was staked to the bottom at two of its corners and then carefully spread over the area that was to be sampled. Nine areas each being one square metre were thus defined (see Fig. 1.2) and each of these was sampled across its diagonal to a depth of 1-2 cm using a 15-cm-wide shovel. The sediment was transferred to a 4.5 l container until about 3 l of material had been collected. This procedure was repeated for each of the nine areas at each station and, in each instance, the nine containers were sealed and lifted to the surface. On the research vessel the subsamples were fixed with buffered formalin and thoroughly mixed to provide a homogeneous sample for the analysis. Thus the subsamples from each

station reflect the distribution patterns of the Foraminifera at a scale greater than one m.

Analytical Method

In each subsample living and total populations of Foraminifera and molluscs were determined using standard methods (Schafer et al., 1975; Walker et al., 1974). Relatively ubiquitous Foraminifera species that were present in at least six of the nine subsamples collected at each station were used for the distribution pattern analysis. The pattern data thus account for both presence-absence and absolute abundance variations of these species. The Foraminifera species that conformed to this frequency criterion represented 50 per cent of the total population at station 6A, 44 per cent at station 12A and 38 per cent at the upper estuarine station (42A). Mollusc data are not suited to this type of analysis because the variation in specimen size (from 4-6 mm for *Acteocina canaliculata* up to about 150 mm for *Crassostrea virginica* and *Mya arenaria*) precludes obtaining representative specimen counts from the subsample volumes that were collected.

An approximation of the degree of randomness in the spatial distribution pattern of comparatively abundant species of Foraminifera was estimated using the Coefficient of Variation (V). $V = \frac{100SD}{\bar{x}_i}$ where \bar{x}_i is the mean number of specimens of species i per cc of the subsamples collected at each station and SD_i is the standard deviation \bar{x}_i . Greig-Smith (1967) described two basic examples of departure from a random or Poisson distribution pattern, that have been observed repeatedly in natural systems. In the first example individuals tend to be clumped or aggregated so that a species collected at N sites on a sampling grid may be absent or found in comparatively high numbers compared to the expectation for a random distribution. This type of pattern is termed overdispersed, clumped or contagious and V is greater

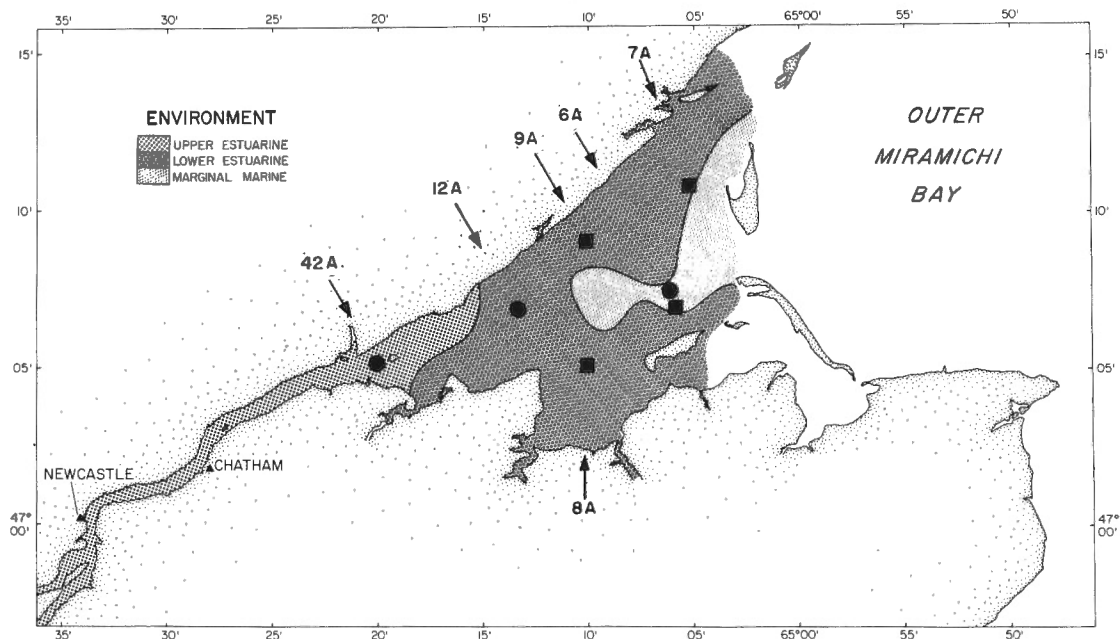


Figure 1.1. Station locations and major foraminiferal biotopes in the Miramichi estuary. Circles indicate grid stations and squares indicate location of sediment traps.

than 100 per cent. In the second example individuals of a species tend to be equal in abundance in a series of N subsamples. Sampling this pattern yields a deficiency of subsamples where the species is absent and the mean number of specimens per cc approaches the mean in more cases compared to a random distribution. This distribution pattern is referred to as underdispersed or regular and V is less than 100 per cent. Coefficient of Variation data were compared with a Poisson distribution (VE) to determine the relative departure of species patterns from a random distribution. In the ideal case of random (Poisson) distribution the mean count of specimens of a given species in a group of subsamples is equal to its variance (Q^2) and in this case VE = 100 per cent. The difference between V and VE is expressed as ΔV here and it accounts for interspecies differences in population density at each grid site. ΔV for species $i = 100 \cdot (SD_i - \sqrt{Q^2_i}) / \bar{x}$ where $Q^2_i = \bar{x}_i$. When ΔV is positive the distribution pattern is termed relatively overdispersed and when ΔV is negative the pattern is considered to be relatively underdispersed.

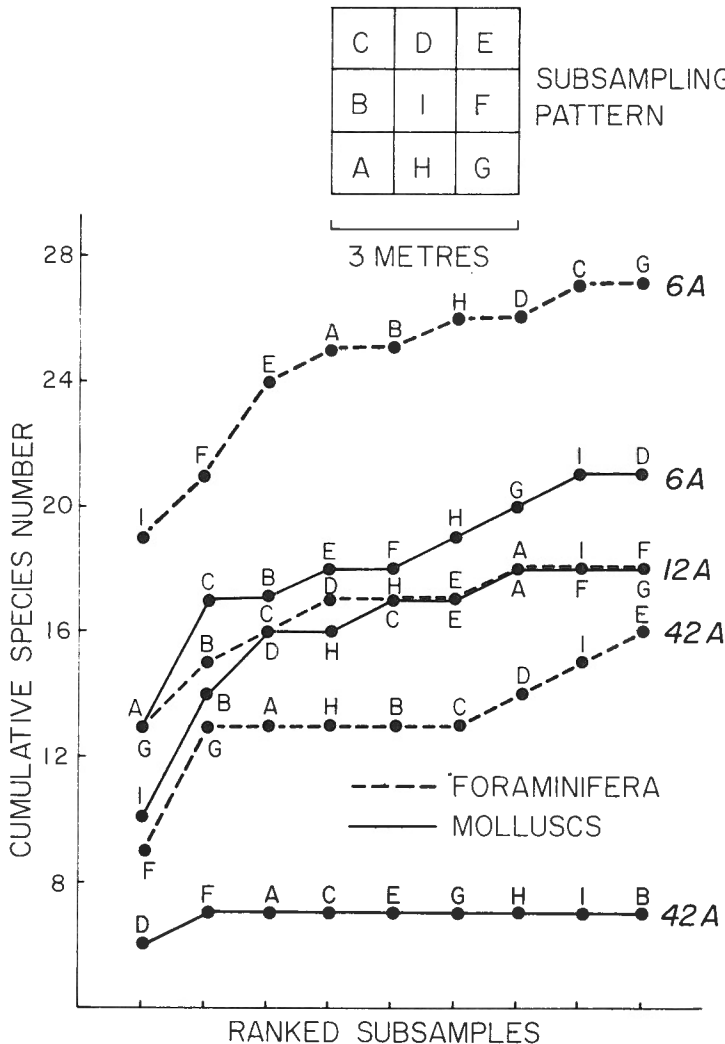


Figure 1.2. Cumulative species curves for molluscs and foraminifera at the three grid sample sites in Miramichi Bay. Subsamples are ranked in terms of decreasing total species number. Letters on each curve identify the position of the subsample on the sampling grid. The slope of each curve reflects the number of new species acquired in each successive subsample. The sampling sequence A-I is shown in the diagram at the top of the figure.

Similarity of ubiquitous species assemblages (total counts) between each subsample was estimated using an index of similarity (S) introduced by Berger and Soutar (1970). The similarity between two subsamples (e.g., A and B) is

$$S_{AB} = \frac{\sum_{i=1}^n A_i B_i}{\sum_{i=1}^n (A_i/2 + B_i/2)^2}$$

where A_i and B_i are the proportions of the i th species in the two subsamples being compared expressed in terms of the number of specimens per cc of wet sediment (FN); n is the total number of species observed in both subsamples.

Environmental Setting and Total Population Species Diversity

Station 42A is located in a water depth of about 1.5 m and falls within the area designated as the Upper Estuarine biotope (Schafer and Scott, 1976). The predominant ecological feature of the flat bottom in this area is the dense population of eel grass (*Zostera* sp.) which forms a favourable habitat for several larger invertebrates including the gastropod *Littorina saxatilis* and the pelecypod *Geukensia demissa*. Muddy sands and gravel comprise the substrate for this community. The area is subject to hydrodynamic forces as a result of river and tidal currents and wave generated turbulence. Comparatively low salinities of less than 10 to 20‰ and low sedimentation rates favour the settling and growth of species such as the oyster *Crassostrea virginica* which is presently restricted to this part of the Upper Estuarine biotope. On the whole, the total species diversity of the Foraminifera and mollusc populations (rare + ubiquitous species) is relatively low here compared to the other two biotopes (Fig. 1.2) and rare Foraminifera species tend to occur in those subsamples characterized by relatively low total species diversity. The mean total FN (i.e., the number of specimens per cc of wet sediment of plant-related Foraminifera species such as *Miliammina fusca* is exceptionally high compared to that noted at the two other stations. The distribution pattern of the total mollusc population is relatively regular at this site compared to the Foraminifera and may reflect the unique nature of the eel grass environment. The prominent plateau of the mollusc total species cumulative curve suggests a relatively underdispersed pattern of species (i.e., relatively few subsamples are needed to detect all the new species) compared to the other two grid stations. The pelecypod *Macoma balthica* is restricted to this station.

Station 12A is located within the Lower Estuarine biotope in a water depth of 3.5 m. The sediment at this location is primarily mud (Reinson, 1976) and the area is considered to be the main depositional sink for fine grained fluvial detritus. The dispersal pattern of the mud facies in this part of the bay suggests that current velocities are relatively low in comparison to those of the other two biotopes. The results of a pollen analysis of two replicate cores from station 12A indicate a comparatively low sedimentation rate in this mud-dominated environment. At this station the C3c (European) pollen zone is apparently restricted to the upper 20 cm of the bottom sediment (McAndrews, pers. comm.). The lower boundary of this zone is estimated to about 200 to 250 years old in this area. Consequently, the relatively low FN values recorded at this grid station must be ascribed to a low level of productivity which may be related to sedimentological and other environmental characteristics of this part of the bay. Preliminary sediment pH data indicate that interstitial water values are all above 7 in this area so that the low numbers of specimens per cc wet sediment (FN) cannot be related to the post-mortem solution of specimens. The per cent of organic carbon in sediments at both station 42A and 12A ranges between 2 and 3, a concentration that is about four times as high as that observed in the Marginal Marine foraminiferal biotope (station 6A). These high organic carbon values are

also indicative of geochemical conditions that favour the post-mortem preservation of specimens (see Rashid et al., 1975; Berger and Soutar, 1970).

Station 6A is situated within a sand-dominated environment that occurs on both sides of the barrier island complex. The station falls within the flood-tidal delta complex described by Reinson (1976) and is characterized by comparatively high energy conditions that favour sediment transport and reworking. Under these conditions niche diversity might initially be expected to be comparatively low and total Foraminifera species distribution patterns should be relatively underdispersed, both in response to a uniform substrate character, and because of the physical redistribution of foraminiferal tests. Cumulative total species curves suggest, however, that this is not the case especially with respect to the mollusc species occurrences which are comparatively heterogeneous. The large number of Foraminifera and mollusc species observed at station 6A, and their seemingly heterogeneous distribution pattern, suggests that the Marginal Marine foraminiferal biotope may be the most ecologically complex part of the bay and is indicative of a faunal response to both open gulf and estuarine influences.

The species diversity at each station is related generally to substrate and tends to be low at 12A and 42A where the mud component of the sediment is high compared to 6A (Reinson, 1976). Gray (1974) noted that although coarser sediments may not be structurally more complex (i.e., poorly sorted) this is usually the case since small grains can fit between large grains, thus giving more potential niches.

Cluster analysis of the molluscan faunas places this station in a subdivision of the Lower Estuarine molluscan biotope which borders on the Marginal Marine molluscan biotope (Wagner, 1976). The Marginal Marine molluscan biotope is characterized by a less diverse fauna (7 species in all compared with 27 species for the Lower Estuarine molluscan biotope). Twenty-two species of molluscs were noted at station 6A.

Abundance Distribution Patterns

Relative-abundance distribution patterns (ΔV) were determined for foraminiferal species that were observed in at least 6 of the 9 subsamples at each station. As explained previously, mollusc data do not lend themselves to this particular analysis. An obvious correlation between ΔV and \overline{FN} is evident in both the total and the living foraminiferal assemblages at station 6A (Table 1.1). Relatively underdispersed abundance patterns are evident when $\overline{FN} \leq 2$. This pattern-abundance relationship agrees with observations described by Schafer and Cole in the Restigouche estuary (1976) and those noted by Buzas (1968). In the Restigouche estuary total species populations that were underdispersed were characterized by \overline{FN}_T values less than 4. The ΔV values at station 6A indicate an underdispersed relative abundance pattern for those comparatively rare forms that have estuarine, nearshore and/or open gulf affinities. These patterns are superimposed on the relatively overdispersed patterns of the major indigenous forms. The underdispersed abundance pattern of some species, as well as the occurrence of other members of the total population in relatively brackish environments (e.g. *Diffugia oblonga*, a thecamoebid), suggests seaward and bayward passive transport of specimens between adjacent environments in this part of the bay. When subsample D is omitted from the matrix the mean similarity of abundant species proportions improves considerably as might be expected in an area where bedload transport processes are significant ($\overline{S} = 0.75$ but $\overline{S}_{N-D} = 0.95$).

Table 1.1

Living and total foraminiferal distribution patterns and subsample similarity based on populations of ubiquitous species at station 6A

STATION 6A	\overline{FN}_T	ΔV_T	\overline{FN}_L	ΔV_L
<i>Eggerella advena</i>	66	38	23	59
<i>Elphidium excavatum</i>	38	42	17	44
<i>Protelphidium orbiculare</i>	16	20	9	19
<i>Ammotium cassis</i>	4	14	1	-20
<i>Trochammina lobata</i>	3	13	1	-31
<i>Miliammina fusca</i>	2	-12	1	-92
<i>Ammotium salsum</i>	2	-26	-	-
<i>Ammomarginulina fluvialis</i>	1	-23	-	-
<i>Hemisphaerammina bradyi</i>	1	-23	<1	-96
<i>Buccella frigida</i>	<1	-37	<1	-102
<i>Trochammina macrescens</i>	<1	-12	1	6
<i>Elphidium bartletti</i>	<1	-79	-	-
<i>Trochammina inflata</i>	<1	-63	-	-

\overline{FN}_T - mean number of total specimens per cc wet sediment

\overline{FN}_L - mean number of living specimens per cc wet sediment

ΔV_T - relative pattern values for the total populations of each species

ΔV_L - relative pattern values for the living populations of each species

SIMILARITY BETWEEN SUBSAMPLES								
	6A	6B	6C	6D	6E	6F	6G	6H
6B	0.99							
6C	0.97	0.98						
6D	0.07	0.07	0.05					
6E	0.96	0.96	0.90	0.10				
6F	0.88	0.88	0.95	0.03	0.75			
6G	0.98	0.97	0.99	0.05	0.89	0.95		
6H	0.98	0.96	0.97	0.05	0.89	0.92	0.99	
6I	0.99	1.00	0.99	0.06	0.94	0.92	0.99	0.97
\overline{S}	= 0.75				\overline{S}_{N-D} = 0.95			
$SD_{\overline{S}}$	= 0.38				$SD_{\overline{S}_{N-D}}$ = 0.05			
$V_{\overline{S}}$	= 50.3%				$V_{\overline{S}_{N-D}}$ = 5.2%			
\overline{S}	- mean similarity							
$SD_{\overline{S}}$	- standard deviation of \overline{S}							
$V_{\overline{S}}$	- coefficient of variation of \overline{S}							
N-D	- value of parameters when subsample D is not considered							

Table 1.2

Foraminiferal distribution patterns and total population subsample similarity at station 12A based on ubiquitous species

STATION 12A	\overline{FN}_T	ΔV_T	\overline{FN}_L	ΔV_L
<i>Ammotium cassis</i>	3	55	1	78
<i>Protelphidium orbiculare</i>	2	13	1	-56
<i>Elphidium excavatum</i> Gp.	2	0	1	-23
<i>Ammotium salsum</i>	<1	-58	<1	-185
<i>Hemisphaerammina bradyi</i>	<1	-110	<1	-187
<i>Miliammina fusca</i>	<1	-201	<1	-376
<i>Reophax dentaliniformis</i>	<1	-283	-	-
<i>Trochammina macrescens</i>	<1	-668	-	-

SIMILARITY BETWEEN SUBSAMPLES

	12AA	12AB	12AC	12AD	12AE	12AF	12AG	12AH
12AB	0.99							
12AC	0.60	0.60						
12AD	0.92	0.91	0.29					
12AE	0.94	0.94	0.44	0.98				
12AF	0.40	0.40	0.94	0.95	0.27			
12AG	0.68	0.67	0.97	0.35	0.52	0.84		
12AH	0.99	0.99	0.53	0.95	0.97	0.34	0.61	
12AI	0.65	0.59	0.33	0.66	0.69	0.21	0.43	0.62
	\overline{S}	=	0.65					
	$SD\overline{S}$	=	0.26					
	$V\overline{S}$	=	40.8%					

At station 12A the relationship between ΔV and \overline{FN} is also evident (Table 1.2) and those species having comparatively high negative ΔV values again include nearshore and upper estuarine indigenous forms such as *Miliammina fusca* and *Trochammina macrescens* that may be passively transported into the Transitional biotope. In terms of living species, *Hemisphaerammina bradyi* is confined to station 6A and its occurrence in the total population at 12A suggests some tidal transport processes between the Marginal Marine and Transitional biotopes. The low mean similarity between subsamples at station 12A reflects several factors including the small quantity of specimens observed and the overall suitability of the biotope for Foraminifera.

The typical relative abundance distribution pattern of the species considered at station 42A is approximately random (Table 1.3). This station is also characterized by the highest \overline{S} , lowest $SD\overline{S}$ values, and highest \overline{FN} values. It is interesting to note however that this station ranks only second in terms of the lowest $SD\overline{S}$ and $V\overline{S}$ values if the anomalous subsample D is omitted from the data matrix of station 6A subsamples. The comparatively low standard deviation of \overline{S} values in the 8-subsample matrix of station 6A is most indicative of the redistribution of the abundant species by tidal currents. Living *Protelphidium orbiculare* species that were observed at 42A are most abundant at stations 6A and 12A and their rare occurrence at 42A is suggestive of up-estuary (salt wedge?) transport processes.

Table 1.3

Foraminiferal distribution patterns and subsample similarity at station 42A based on ubiquitous species

STATION 42A	\overline{FN}_T	ΔV_T	\overline{FN}_L	ΔV_L
<i>Miliammina fusca</i>	148	9	40	16
<i>Ammobaculites exiguus</i>	26	4	9	15
<i>A. dilitatus</i>	3	14	<1	-98
<i>Protoschista findens</i>	2	6	-	-
<i>Ammotium salsum</i>	2	147	-	-
<i>Protelphidium orbiculare</i>	<1	-59	-	-

SIMILARITY BETWEEN SUBSAMPLES

	42AA	42AB	42AC	42AD	42AE	42AF	42AG	42AH
42AB	0.99							
42AC	0.97	0.99						
42AD	1.00	0.99	0.97					
42AE	0.99	0.98	0.94	0.99				
42AF	0.99	1.00	0.99	0.99	0.97			
42AG	0.98	1.00	1.00	0.98	0.96	1.00		
42AH	0.99	1.00	1.00	0.99	0.97	1.00	1.00	
42AI	0.99	0.98	0.94	0.99	1.00	0.97	0.96	0.97
	\overline{S}	=	0.96					
	$SD\overline{S}$	=	0.15					
	$V\overline{S}$	=	15.6%					

Discussion

The underdispersed abundance distribution pattern of some upper estuarine and marginal marine species of Foraminifera observed at the Transitional biotope station (12A) is indicative of transport of tests from adjacent environments into this part of the bay. The value of ΔV for these species is negative and is considerably higher than was observed for species in the 0 to 10-m-depth interval in Chaleur Bay (Schafer and Cole, 1976). These transported forms exert their greatest effect on the quantitative similarity of subsamples at the 12A site because of the relatively low population density of the indigenous forms inhabiting this area.

Environmental aspects of the three stations differ significantly in terms of sediment type, mollusc assemblages, the presence of eel grass, and the intensity of hydrodynamic processes. On the basis of the mean foraminiferal number of living specimens (\overline{FN}), the highest level of productivity occurs within the eel grass community which is prominent in the Upper Estuarine foraminiferal biotope (Table 1.4). The next most productive area of the estuary is the Marginal Marine biotope. This biotope also is the most ecologically complex and is characterized by the most diverse population of Foraminifera and molluscs. It represents a major ecotone separating Northumberland Strait and Miramichi estuary assemblages.

The productivity of Foraminifera appears to be comparatively low at station 12A, especially when the \overline{FN} value is considered in conjunction with the low sedimentation rate in this area. This condition may be indicative of several natural

factors peculiar to this part of the estuary including the fine substrate texture and comparably high water turbidity, rather than available food supply since this area is characterized by comparatively high organic carbon concentrations. Myers (1942) observed a reduction in the size of the benthonic Foraminifera populations in those areas of the Java Sea that were characterized by high sedimentation rates and high turbidity. Boltovskoy (1957) noted an increase in the abundance of arenaceous species in turbid waters and surmised that high turbidity may be selectively unfavourable for calcareous forms. Except for *P. orbiculare* the ubiquitous species at 12A are all arenaceous.

Oxygen availability may also be a key factor in this part of the bay in maintaining low population densities. Vernberg and Coull, 1975, indicated that redox discontinuity layers measured in marine bottom sediments in a South Carolina estuary tended to be shallower during the summer months. They concluded that the disappearance of some copepod species could be attributed to their sensitivity to oxygen lack in the sediment in combination with higher water temperatures. An analogous situation would be best developed in the deeper, organic rich environments of inner Miramichi Bay especially near the sediment-water interface. As such, the microfauna of the Transitional biotope would be least affected by the dumping of sediments dredged from the ship channel that passes through this part of the bay because the present environmental setting has already imposed severe limitations.

The relatively overdispersed pattern and abundance of *Ammotium cassis* at station 12A indicates that this form is now indigenous to the Transitional biotope as suggested by Schafer and Scott (1976). Its increase in the uppermost layer (1-2 cm) of bottom sediment in this part of the bay supports the theory of a trend toward increased estuarine conditions (Scott et al., 1977) which developed over several years prior to 1975.

Specimen and Sediment Transport Observations

The transport of Foraminifera and sediment in the bay was monitored in February using 38-cm-diameter dish-shaped



Figure 1.3. Decanting sediment slurry from the sediment bottle. Residual sediment was washed free using a dilute solution of standard automotive antifreeze.

Table 1.4

Mean living foraminiferal number (total no. living specimens/cc wet sediment) and total species number at each grid station

STATION	\overline{FN}	TOTAL SPECIES
42A	16.6	16
6A	6.1	26
12A	1.0	18

sediment traps (Fig. 1.3) similar to the type described by Hakanson (1976). Four traps were placed on the bottom at stations 9A, 6A, 7A, and 8A (Fig. 1.1). The monitoring period ranged from about 4 to 6 days and the samples recovered confirmed that tidal transport rates are highest within, and adjacent to, the flood tidal delta complex at the eastern end of the bay (Table 1.5). This is also indicated by the quantitative similarity of ubiquitous species in the 8 subsample species comparison (station 6A). During periods of ice cover bottom sediment transport in the estuary is controlled primarily by river and tidal currents. However, it is expected that deposition rates in the deeper portion of the western half of the bay will be considerably higher during the ice-free seasons because of the relatively low intensity of wave turbulence in these deeper areas compared to subtidal areas, and because of an increase in the opposing effect of tidal and river-related currents during periods of high river discharge. The high sedimentation rate recorded at station 9A may be related to ice breaker activity that occurred during the experiment since this station was located immediately adjacent to the navigation channel.

Trap samples contained several species of Foraminifera which were transported in suspension or as part of the bedload. Trap stations 6A and 8A were located in environments comparable to grid stations 6A and 12A. Comparison of total grid station species and trap species (Table 1.6) indicates that the trap species are related primarily to the relatively ubiquitous and numerically abundant indigenous forms. This relationship would be expected if the transport mechanism is primarily related to tidal currents and bedload transport, as shown by the similarity of station 6A subsamples, compared to suspended load transport from more distant adjacent or upstream areas. The latter case would be reflected by the presence of rare non-indigenous species in the trap samples.

Table 1.5

Sedimentation rates in the bay based on sediment trap data under total ice cover conditions

STATION	CC/M/day	CM/year
6A	97.8	3.6
9A	95.1	3.5
8A	16.7	0.6
7A	8.0	0.3

Table 1.6

Comparison of the frequency of occurrence (F) of species in all grid subsamples and their presence, (T) in sediment trap samples

STATION 6A	F	6A	STATION 12A	F	T8A
<i>Eggerella advena</i>	100	X	<i>Ammotium cassis</i>	100	X
<i>Elphidium excavatum</i>	100	X	<i>Ammobaculites salsus</i>	100	
<i>Protelphidium orbiculare</i>	100	X	<i>Hemisphaerammina bradyi</i>	100	X
<i>Ammotium cassis</i>	100	X	<i>Miliammina fusca</i>	100	
<i>Trochammina lobata</i>	100	X	<i>Protelphidium orbiculare</i>	89	X
<i>Miliammina fusca</i>	100	X	<i>Elphidium excavatum</i>	89	X
<i>Ammobaculites salsus</i>	100		<i>Reophax dentaliniformis</i>	89	
<i>Hemisphaerammina bradyi</i>	100	X	<i>Trochammina macrescens</i>	78	X
<i>Buccella frigida</i>	100	X	<i>Reophax fusiformis</i>	55	
<i>Ammomarginulina fluvialis</i>	89		<i>Centropyxis arenatus</i>	44*	
<i>Trochammina macrescens</i>	89		<i>Ammobaculites dilatatus</i>	33	
<i>Elphidium bartletti</i>	78		<i>Buccella frigida</i>	33	
<i>Trochammina inflata</i>	67	X	<i>Diffugia capreolata</i>	33*	
<i>Ammobaculites exiguus</i>	44		<i>Ammomarginulina fluvialis</i>	22	
<i>Parafissurina fusuliformis</i>	44		<i>Elphidium margaretaceum</i>	22	
<i>Ammodiscus catinus</i>	44		<i>Ammobaculites exiguus</i>	11	
<i>Quineloculina seminulum</i>	33	X	<i>Reophax scottii</i>	11	
<i>Trochammina ochracea</i>	22		<i>Eggerella advena</i>	11	X
<i>Reophax scottii</i>	22				
<i>Centropyxis arenatus</i>	22*				
<i>Diffugia oblonga</i>	11*				
<i>Trochammina helgolandica</i>	11				
<i>Pateoris hauerinoides</i>	11				
<i>Textularia earlandi</i>	11				
<i>Tiphotrocha comprimata</i>	11				
<i>Reophax dentaliniformis</i>	11				

* Identifies species of *Thecamoebina* observed in Mirimachi sediments.

Conclusions

The analysis of Foraminifera and molluscs within the three major biotopes suggests significant differences in foraminiferal productivity, and in environmental complexity. Foraminifera are most abundant in the Upper Estuarine biotope (Fig. 1.1) and least abundant in the Transitional biotope where high turbidity, fine sediments and low energy conditions may have a significant effect on parameters such as oxygen concentration at the sediment-water interface (i.e., the foraminiferal life zone). The high mollusc and foraminiferal total species diversity at station 6A indicates that the Marginal Marine biotope is the most ecologically complex within the estuary and would show the greatest response to channel dredging activity.

Despite the degree of specimen transport observed during periods of ice cover, the living population abundance distribution pattern of indigenous Foraminifera species is probably relatively overdispersed during this period because of minimal reworking compared to the patterns that might be observed at the grid stations during the summer months. Regional quantitative analysis of ubiquitous species proportions based on a series of grab samples should therefore be more representative during ice-free periods since test transport processes will involve the interaction of wave turbulence

and tidal currents which would act in opposition to the development of clumped patterns at the local level. This process would be most evident for comparatively abundant species and/or populations. Conversely, in the case of the rare species the effect would be one of dilution or burial by sediment. The geographic boundaries of biotopes such as those mapped by Scott and Schafer (1976) should be viewed as being indicative of both the intensity of local transport mechanisms and the geographic influence of controlling ecological parameters. In this regard it is satisfying to note the general regional agreement between mollusc and foraminiferal biotope boundaries in this relatively shallow estuary.

References

- Berger, W.H. and Soutar, A.
1970: Preservation of plankton shells in an anaerobic basin off California; *Geol. Soc. Am. Bull.*, v. 81, p. 275-282.
- Boltovskoy, E.
1957: Los Foraminiferos del Estuario del Rio de la Plata y su zone de Influencia; *Inst. Nac. Cienc. Nat. Rev. Geol.*, v. 6, p. 1-77.

- Buzas, M.A.
1968: On the spatial distribution of foraminifera; Cushman Found. Foraminiferal. Res., Contrib., v. 19, p. 1-11.
- Gray, J.S.
1974: Animal-sediment relationships; Oceanogr. Mar. Biol. Ann. Rev., v. 12, p. 223-261.
- Greig-Smith, P.
1967: Quantitative plant ecology; Butterworth and Co., London, 265 p.
- Hakanson, L.
1976: A bottom sediment trap for recent sedimentary deposits; Limnol. Oceanogr., v. 21, p. 170-174.
- Myers, E.H.
1942: Ecologic relationship of some recent and fossil Foraminifera; Nat. Res. Council, Div. Geol. Geogr., Ann. Rep., Appendix 2.
- Rashid, M.A., Vilks, G., and Leonard, J.D.
1975: Geological environment of a methane-rich Recent sedimentary basin in the Gulf of St. Lawrence; Chem. Geol., v. 15, p. 83-96.
- Reison, G.E.
1976: Surficial sediment distribution in the Miramichi Estuary, New Brunswick; in Report of Activities, Pt. C, Geol. Surv. Can., Paper 76-1C, p. 41-44.
- Schafer, C.T. and Cole, F.E.
1976: Foraminiferal distribution patterns in the Restigouche Estuary; Marit. Sediments Spec. Pub. No. 1, Pt. A, p. 1-24.
- Schafer, C.T. and Scott, D.B.
1976: Multidisciplinary environmental marine geological analysis of a coastal area; in Report of Activities, Pt. C, Geol. Surv. Can., Paper 76-1C, p. 1-3.
- Schafer, C.T., Wagner, F.J.E., and Ferguson, C.
1975: Occurrence of foraminifera, molluscs and ostracods adjacent to the industrialized shoreline of Canso Strait, Nova Scotia; Water, Air, Soil Pollut., v. 5, p. 79-98.
- Scott, D.B., Medioli, F.S., and Schafer, C.T.
1977: Temporal changes in foraminiferal distribution in Miramichi River estuary; Can. J. Earth Sci. (in press).
- Vernberg, W.B. and Coull, B.C.
1975: Multiple factor effects of environmental parameters on the physiology, ecology and distribution of some marine meiofauna; Cah. de Biol. Mar., v. 16, p. 721-732.
- Wagner, F.J.E.
1976: Mollusc distributions, Miramichi estuary, New Brunswick; in Report of Activities, Pt. C, Geol. Surv. Can., Paper 76-1C, p. 45.
- Walker, D.A., Linton, A.E., and Schafer, C.T.
1974: Sudan Black B: A superior stain to Rose Bengal for distinguishing living from non-living foraminifera; J. Foraminiferal Res., v. 4, p. 205-223.

Project 750048

G.A. Fowler¹, C.T. Schafer², and K.S. Manchester²**Introduction**

Coring operations in shallow nearshore marine environments are usually carried out with comparatively light-weight gravity corers or by divers using plastic core liners. These methods normally yield up to 2 m of core depending on sediment texture. In most nearshore areas coarse sediments often underlie a veneer of fine modern sediments, or are interbedded with fine grained layers. These coarse layers may be indicative of storms, high river discharge events or, depending on sedimentation rates, can be formed during a change in relative sea level. The use of vibrocoring techniques is well known for obtaining samples of marine sediments with a high sand content. However, the equipment available does not lend itself to field surveys where portability is of primary importance because of its size, weight and power requirements. This report describes the development and use of a light sampling system 'PORTAVIBE' that can be used to obtain samples from shallow marine environments through holes in the ice. The device was developed at the Bedford Institute of Oceanography and was used in February 1977 to core sediments from an 0.6-m-thick ice surface in inner Miramichi Bay, New Brunswick.

Core Barrel Design

To provide portability it is essential to reduce the weight of a system to the absolute minimum but this cannot be accomplished by simply scaling down existing vibracorer designs. In particular, the diameter of the core barrel cannot be reduced since the effects of sample disturbance increase with decreasing diameter, and for small barrels core entry is stopped almost immediately because of wall friction. In addition, geological information decreases directly with barrel diameter. For these reasons it was decided to maximize the diameter of the cores to be taken and indeed increase it above the size normally used by full scale vibracorer systems (e.g., see Arduş, 1974).

To achieve penetration of the sample tube it is necessary to mobilize the sediment immediately ahead of the core cutter. It follows that the resistance to penetration is directly related to the frontal area of the cutter. Typically the frontal area of the barrel-linear assembly on large vibracorers, such as an 8.25 cm diameter core, is 28 cm². The diameter of the 'PORTAVIBE' barrel is 10 cm and it requires a frontal area of only 22 cm². The design reduces the high deadweight loads required for penetration in large vibracorers in addition to providing a sample 50 per cent larger in cross-sectional area.

In the single tube system described here, a plastic pipe (PVC) was chosen to provide the functions of both the outer and inner tubes and the core cutter cutting shoe of the double tube system (Fig. 2.1). Special attention was paid to the method of mounting the core catcher in the bottom of the tube in a manner which would not restrict core sample entry into the barrel. The system chosen is shown in Figure 2.1 and is similar in concept to that of a 'CIRCLIP' or retaining ring. The core catcher is easily removed or inserted in a groove, which has been cut into the plastic barrel with a hand-held device, using a pair of 'CIRCLIP pliers'.

¹Atlantic Oceanographic Laboratory,
Bedford Institute of Oceanography, Dartmouth, N.S.

²Atlantic Geoscience Centre,
Geological Survey of Canada,
Bedford Institute of Oceanography, Dartmouth, N.S.

Table 2.1

Comparison of jackhammer blow rates with penetration rates

driver	core catcher	core compaction	penetration rate
37 Hz	Rigid plastic with about 90% coverage	-	no penetration
37 Hz	Rigid plastic with about 50% coverage	17%	20 cm/min
37 Hz	No core catcher	6%	90 cm/min
10 Hz	Flexible steel with about 50% coverage	4%	150 cm/min
10 Hz	No core catcher	0	165 cm/min

Core Barrel Driver

It has been noted that when using a large vibracorer (Arduş, 1974) it was possible to increase penetration through stiff sediments by shutting the drive unit off and allowing the vibrations (50 Hz when running) to die out. Before coming to rest the unit changes its frequency of vibration and virtually hammers the sample tube through the sediment.

Since this hammering feature can cause a vibrating system to both increase its penetration capability and decrease sample disturbance (Kogler and Veit, 1974), it was decided to investigate the use of a hammering drive system.

Lab Testing

Two hammers operating at 37 Hz and 10 Hz were evaluated individually with prototype PVC core barrels to determine the best type for field operations. The latter hammer has an input power approximately three times that of the former which draws 5 A at 110 V. Tests were run by driving core barrels into a container filled with 0.5 mm diameter quartz sand and the effect on penetration rate of the two driving frequencies and powers were measured. The degree of compaction of the samples taken was also determined.

It was noted initially that the core catcher configuration had a pronounced effect on both penetration rate and sample compaction. Plastic core catchers, which were glued to the inside of the core barrels, increased the effective frontal area of the core barrel assembly, and resulted in greatly reduced penetration rates compared to tests made with core barrels that were not fitted with core catchers.

Comparison of the tests that did not utilize core catchers showed clearly that the lower blow rate driver was capable of faster penetration rates (Table 2.1). In addition, this low frequency unit did not compact the core sample as much as the high frequency model.

As a result of the tests the low blow rate unit was chosen in conjunction with a steel 'CIRCLIP' core catcher as the system most suited to field operations.

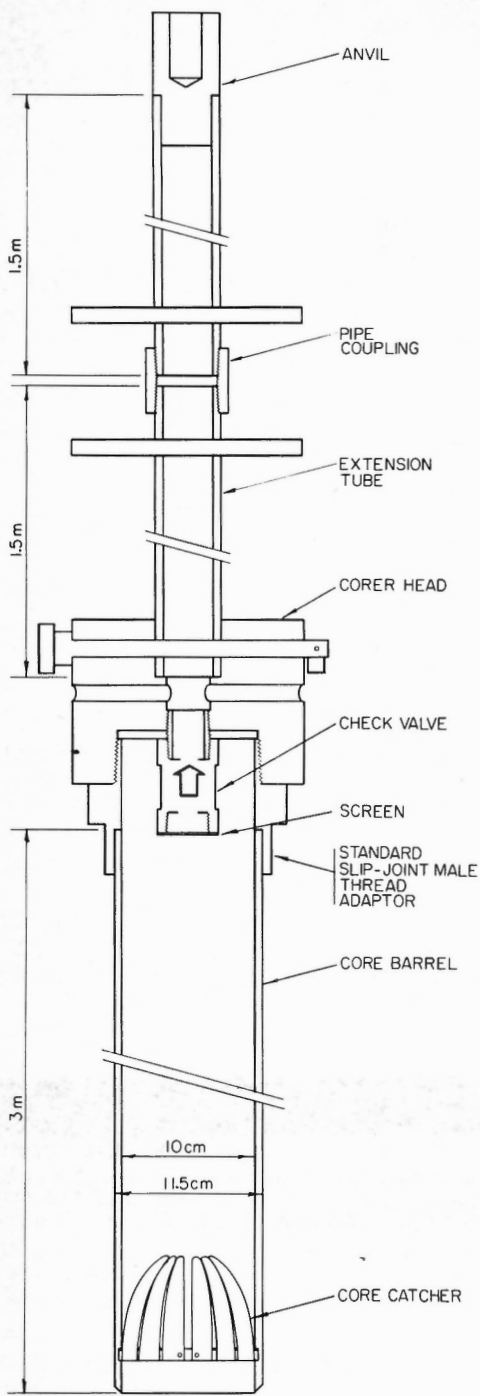


Figure 2.1 (above)
Cross-sectional view of the 'PORTAVIBE' corer.

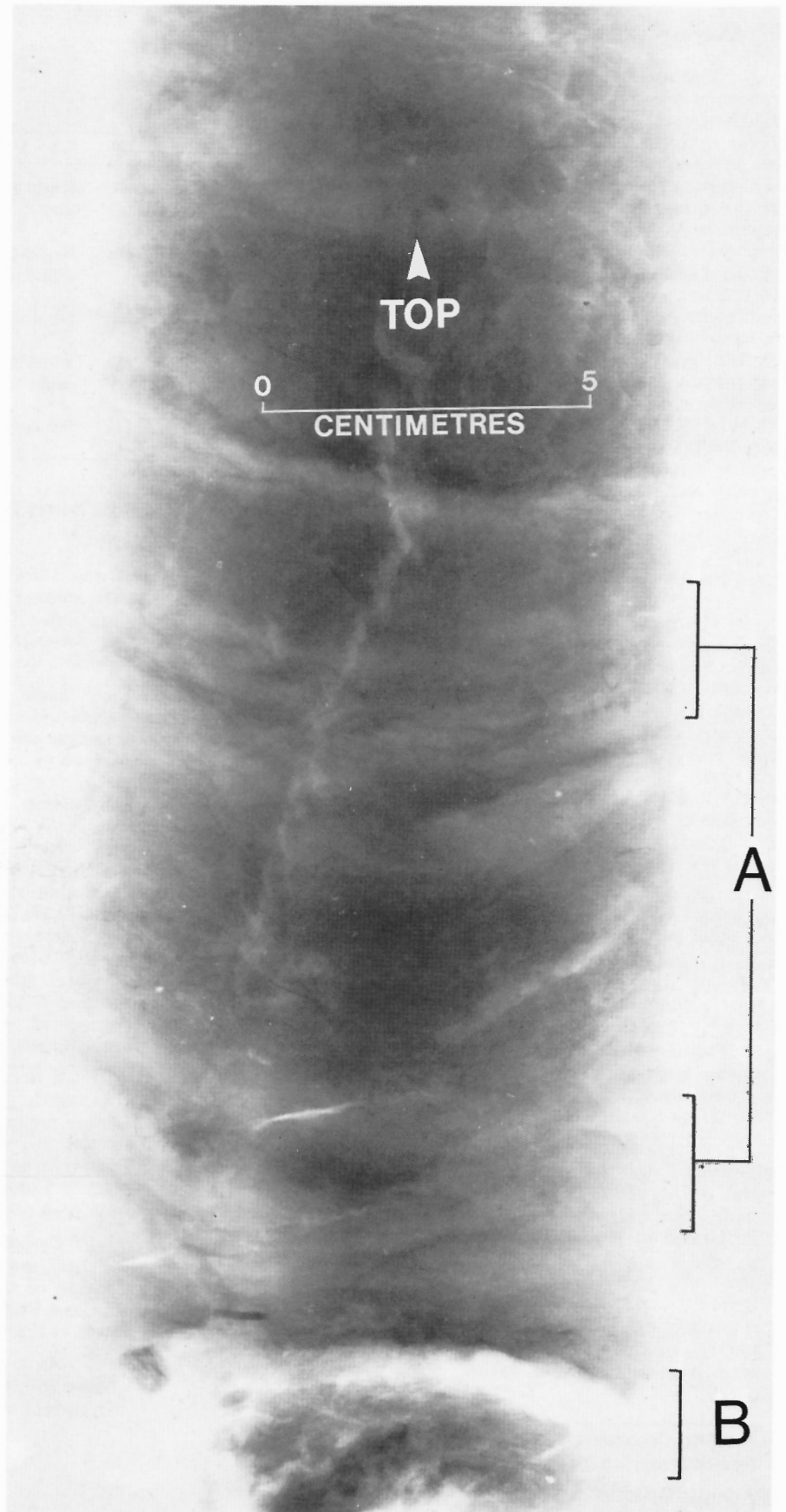


Figure 2.2 (right)
X-ray of section of comparatively sandy core showing orientation of sediment layers. Outline of sediment immediately above the core catcher can be seen at the bottom of the photograph.



Figure 2.3 Sediment coring operation. Portable 3 Kw used to drive the hammer is partially visible on the back of the sled.



Figure 2.4 Core extraction hardware. Chain hoist is attached directly to the core head using a suitable rope which must be retied after each 0.6 m pull.

Field Operations

Six cores were obtained in Miramichi Bay using this device and these ranged in length from 0.6 to 2.9 m. The longest core contains about 2.5 m of sandy silt underlying a 0.4 m layer of silty clay. The penetration depth in this instance was limited by the length of the barrel (3.0 m) and was attained after about 5 minutes of intermittent hammering. The corer was used successfully from the ice platform in water depths of up to 9 m. Distortion of sedimentary structures in most of the cores appears to be minimal especially near the edges of the sample where down drag effects are most easily developed during penetration of a mixed-layered sediment. In one instance the sediment in a comparatively sandy core displayed concave layering that may have developed during extraction from the bottom (Fig. 2.2). However, further x-ray analysis is required to verify the geometry of these structures since dipping layers often show similar features.

Field Methods

The core barrel was first connected to the appropriate number of 1.5 m lengths of aluminum pipe necessary to reach the bottom. The assembly was slowly lowered through a 0.5 m² hole in the ice that had been cut using a conventional chain saw with a 0.9 m blade. After the initial contact with the bottom, the barrel was slowly forced into the sediment to a depth of about 0.5 m by the two operators standing on the overlying ice. Slow penetration allowed adequate time for the water in the barrel to pass through the one-way valve in the coring head. The electric hammer was then mated to the end of the aluminum pipe and activated until the penetration rate was less than 1 cm per minute (Fig. 2.3).

Extracting the Core Barrel

A tripod constructed from 10 x 10 cm x 3 m wood was placed over the hole and the core head was attached to it using 1.5 cm polypropylene rope which was fixed to a one ton capacity lever-actuated chain hoist (Fig. 2.4). The core barrel was raised in 0.6 m intervals until it could be lifted manually onto the ice.

Summary

The 'PORTAVIBE' is both simple in design and operation and can be constructed for a comparatively low cost. The jackhammer used in the prototype was actually rented from a local portable power tool rental agency. The sampler provides a cost effective method of obtaining relatively undisturbed large diameter cores composed of sediments that usually cannot be recovered using gravity corers. The practical water depth limitations of this tool is probably about 30 m however the maximum practical working depth will be heavily dependent on local current conditions.

References

- Ardus, D.A.
1974: Institute of Geological Sciences Vibrocore Developments and Operations; Paper no. 14, in: Exploitation of Vibration Symposium, 8-10 April, 1974. Birniehill Institute, National Engineering Laboratory, East Kilbride, Glasgow.
- Kogler, F.C. and Veit, K.H.
1974: Problems and experiences of sand core sampling by vibration; Paper no. 19, in: 8-10 April, 1974. Birniehill Institute, National Engineering Laboratory, East Kilbride, Glasgow.

3. STRUCTURE AND METAMORPHISM IN SOUTHEAST CANOE RIVER AREA, BRITISH COLUMBIA

EMR Research Agreement 1135-D13-4-83-73

E.D. Ghent, and P.S. Simony; and W. Mitchell, J. Perry, D. Robbins and J. Wagner
Regional and Economic Geology Division

Introduction

A team from the University of Calgary has, since 1973, investigated the structure, stratigraphy and metamorphic petrology of the southeast portion of Canoe River area (NTS 1:250 000 sheet 83D). The area presents the opportunity to investigate the northeast flank of the Selkirk-Monashee metamorphic complex.

Mapping has been carried out on scales of 1:12 000 and 1:24 000 for publication at 1:50 000. Detailed petrographic and mineralogic studies, involving electron microprobe investigations have been carried out in conjunction with the field studies.

While they rely heavily on the work done by the junior authors, the senior authors (Ghent and Simony) have worked in all parts of the area and take full responsibility for the interpretations presented here as well as for any errors that remain in the work.

We wish to acknowledge the financial assistance of the Department of Energy, Mines and Resources and the National Research Council of Canada. It is with much pleasure that we acknowledge the friendly co-operation we have received in the Mica Creek area, from officials of the British Columbia Department of Lands and Forests, B.C. Hydro and Okanagan Helicopters.

The area is underlain primarily by metasedimentary rocks of the Hadrynian Horsethief Creek group. These have been intensely deformed by at least three folding phases and have been affected by Barrovian metamorphism ranging in grade from that of the garnet zone to that of the sillimanite zone. Migmatite and pegmatite constitute 10 per cent to 30 per cent by volume of the rocks in the higher grade portions of the area.

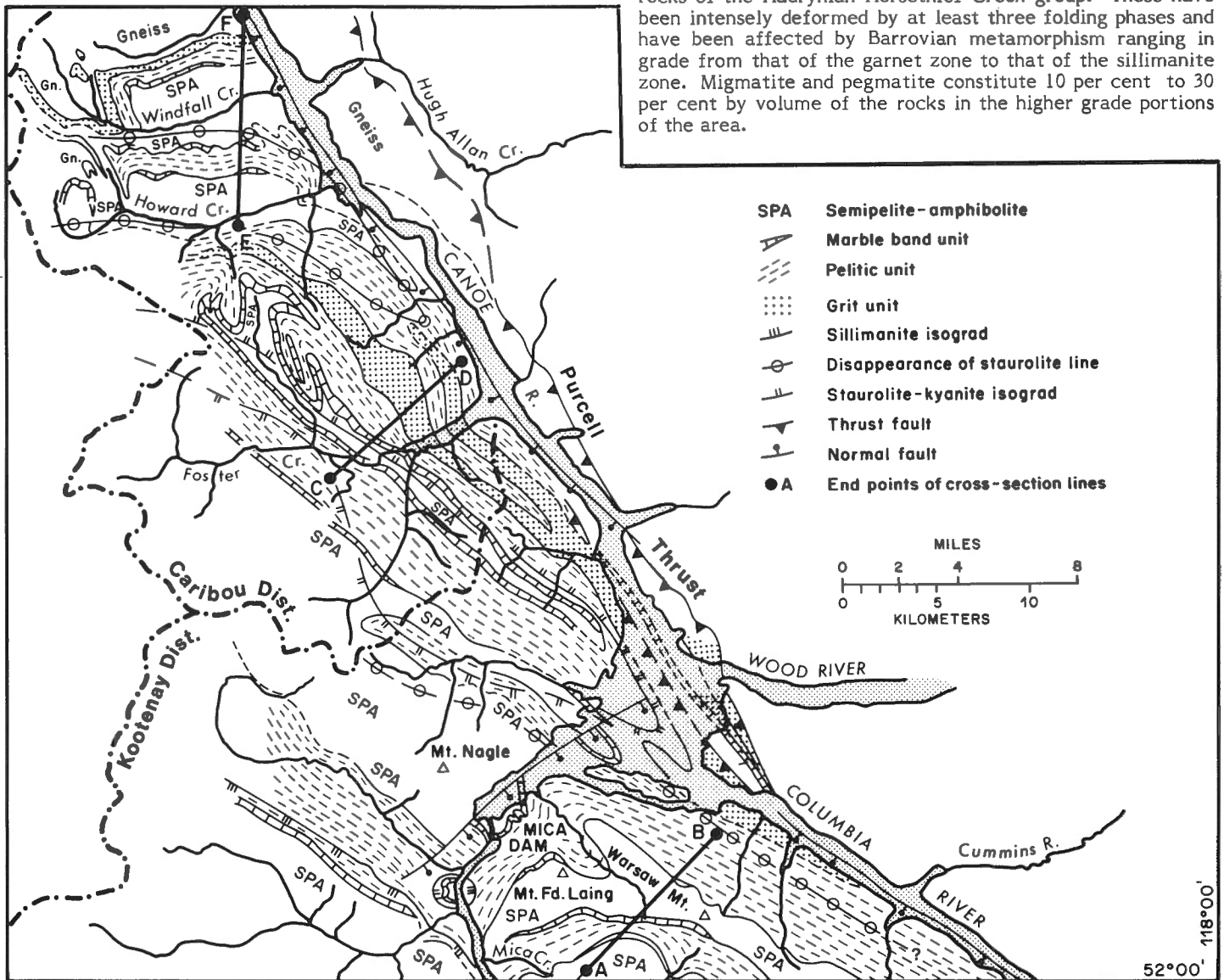


Figure 3.1. Geology of southern Canoe River area.

Authors' address:
Dept. of Geology, Univ. of Calgary,
Calgary, Alberta, Canada, T2N 1N4

From: Report of Activities, Part C;
Geol. Surv. Can., Paper 77-1C (1977)

Stratigraphy

Reconnaissance mapping by Wheeler (1965) and Campbell (1968) in Big Bend and Canoe River areas, had shown that the Hadrynian Horsethief Creek Group extends northward to the area. Our work further shows that the subdivisions that can be recognized in the northern Purcells (Evans, 1933; Wheeler, 1963; Simony and Wind, 1970; Poulton, 1973) can be recognized again in Canoe River area. Table 3.1 summarizes the main features of the stratigraphy. Because of the intense folding, stratigraphic thicknesses have been tectonically modified and the thicknesses presented in the table merely provide a semiquantitative impression.

The association of markers which has proved most helpful to follow the continuity of structures over the whole area is the contact of the pelitic unit with the flaggy semipelite-amphibolite unit. Marble and calcsilicate occur near this contact but they are discontinuous and can be found above, at, or below the contact.

The grit unit is considered to be at the base of the succession because in this way, the sequence has many points of comparison with the Horsethief Creek succession of the northern Purcells as well as with the Hadrynian Miette succession in the Rockies immediately to the east of the map-area.

Along the Cariboo-Kootenay districts boundary, south of Foster Creek inlet, grit is enclosed by the "Brown Zone" and the pelite unit in the core of a fold. Graded bedding and the intersection of bedding with first schistosity on both flanks of the fold indicate that the sequence faces outwards. In other words, the fold is a downward-closing anticline and the grit unit is at the base of the sequence.

Structure

The salient features of the large scale structure are depicted on Figures 3.1 and 3.2. The latter was constructed to illustrate how the structures are connected from Mica Creek to Malton Gneiss.

On the megascopic and mesoscopic scales, it is clear that at least three and possibly four phases of folding have affected the area. Phase 1 and 2 folds are very tight to isoclinal with sharp, narrow hinge zones. They have a style that is approximately similar. Phase 2 folds dominate the map pattern in much of the area and the earlier folds are not obvious. Phase 1 and phase 2 folds have penetrative, axial plane schistosity associated with them. Only locally, in some F_2 hinge zones, does some crenulation remain. In general, the pervasive schistosity of the area can only be described as an S_{1+2} foliation surface and it is approximately parallel to compositional layering.

Table 3.1
Summary of stratigraphy of Southern Canoe River area

<u>Unit</u>	<u>Thickness</u>		<u>Correlation to N. Purcells</u>
Semipelite - amphibolite	1000 m (no top)	Semipelite and pelite with psammite and locally, amphibolite. In the lower part, mostly flaggy semipelite with amphibolite and calc-silicate beds, dark garnet-mica schists and biotite hornblende schists. Some quartzite beds locally. Marble and quartzite near the base.	Lower part of "Upper Slate"
Marble	0-100 m	Grey and brownish laminated marble, coarse massive lenses, quartzose marble and calc-silicate beds. Semipelite and pelite beds are common.	"Carbonate Unit"
Pelite	600 m	Dark mica schist with widespread aluminum silicates, well laminated and with psammite and semipelite interbeds. Locally, calcareous conglomerate near the top. Coarse psammite and grit beds near the base.	"Middle Slate"
"Brown Zone"	5-20 m	Brown-weathering zone with calc-silicate, amphibolite and marble layers in semipelite.	Sandy limestone locally at top of Grit Unit
Grit	100-600 m (no strat. base)	Semipelite with coarse psammite and grit beds, in regular 30 cm to 2 m beds; local pebbly horizons. Much dark mica schist especially near the top.	Upper portion of "Lower Grit"
Malton Gneiss		Grey, granitoid hornblende and biotite gneiss with amphibolitic lenses and layers. Local zones of mica schist of metasedimentary aspect. The contact with the Hadrynian cover in a mylonite zone.	Hudsonian Basement

Phase 3 folds are unevenly distributed across the area. They strongly influence the map pattern north of Foster Creek and, particularly, in the Mica Dam area. There the southeast plunging Mica Dam Antiform, adjacent synform and related smaller folds dominate the structure. The broad and complex core of the antiform is well exposed in the Mount Nagle area, on the northwest, upthrown side of the transverse normal fault that passes near the west abutment of Mica Dam. South of the fault, the folds can be followed southward and upward through a structural stack some 5 km thick (see section AB, Fig. 3.2). The folds die upwards into a southwest-dipping homocline formed of a major phase 2 antiform-synform pair which is crumpled by northeast verging mesoscopic folds with wavelengths of 0.2 to 50 m.

Phase 3 folds generally have southwest-dipping axial surfaces and a steeply dipping crenulation cleavage associated with them. The folds, however, vary greatly in style and attitude. In particular, the dip of the axial surfaces varies from fold to fold; box folds are not uncommon and in many folds the axial surface is markedly curved.

Once the phase 3 and 2 folds are outlined from the map pattern of the markers, the presence of yet earlier and very major folds is strongly suggested. A line can be drawn on the map, and it is shown in section A ... F, which separates two identical stratigraphic packages facing in opposite directions. This line is interpreted as the axial surface trace of a major phase 1 recumbent fold or nappe. If our stratigraphic interpretation is correct then the nappe contains older and older strata to the northeast and eventually roots to the northeast in the Malton Gneiss.

On the ridge north of Windfall Creek, the contact of the Malton Gneiss with the overlying metasediments is exposed. Reading downwards, towards the gneiss, one passes through the same succession established elsewhere in the area. However only 200 to 300 m of the grit-bearing unit overlie the gneiss. On Windfall ridge the Hadrynian metasediments are not migmatized and stand in sharp contrast to the grey granitoid gneisses of the Malton mass. Near the contact the gneiss is highly deformed, streaky and mylonitic. The contact is approximately parallel to layering in metasediments and gneiss, but, near the head of Windfall Creek, as already recognized by Campbell (1968) the contact truncates layering both in the gneiss and in the metasediments. North of the head of Howard Creek, a small body of gneiss and amphibolite lies within the semipelite-amphibolite unit in the core of a phase 2 antiform. The manner of its emplacement is unclear.

The Malton Gneiss mass was a gneiss before the Hadrynian strata were metamorphosed. It further has yielded radiometric ages that suggest it is pre-Hadrynian (R. St. J. Lambert, pers. comm. and Campbell, 1973). It probably represents a portion of the Hudsonian crystalline basement. At an early orogenic stage the mylonite zone marked the cover/basement décollement such that the cover sequence is allochthonous in its present position on the gneiss. Later the décollement ceased to function and cover and basement were folded together. Rather late in the structural evolution, perhaps during phase 3, the Malton gneiss was cut from its root and the Selkirk-Monashee complex moved on the Purcell Thrust upward and northeastward against the Rocky Mountains.

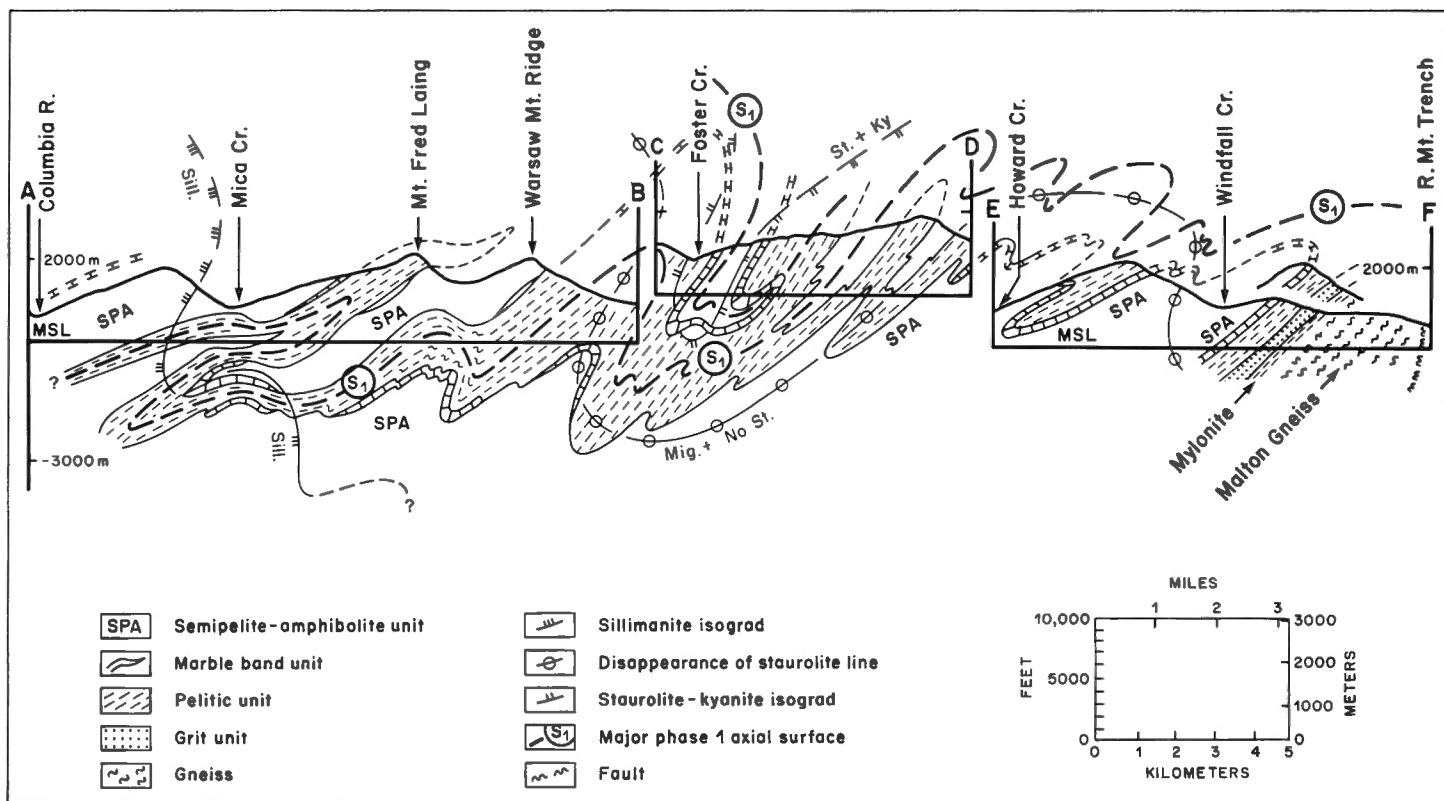


Figure 3.2. Combined cross-sections to illustrate relation of structures from Mica Creek to Malton Gneiss, southern Canoe River area, British Columbia.

Petrology

Isograds and relationship between metamorphic crystallization and deformation

The lines of first appearance of staurolite, kyanite and sillimanite were traced in the field and their position checked petrographically. Their map pattern yields information on the geometry of the metamorphic surfaces which they represent. Staurolite and kyanite appear together and staurolite disappears in a 200-300 m wide belt well within the kyanite zone. The first appearance of leucosome (mostly trondhjemite) coincides with the staurolite disappearance belt. Sillimanite first appears as fibrolite and is found together with kyanite over 100 to 200 m. The kyanite zone is at least 6 km thick (see section AB, Fig. 3.2). These relationships suggest a metamorphic "path" on the high pressure side of the Barrovian facies series.

The metamorphic surfaces outline metamorphic synforms and antiforms, the most notable being the synform outlined by the staurolite-kyanite isograd trending northwestward from the junction of Columbia, Canoe, and Wood rivers (now flooded). No staurolite and kyanite occurs within the synform, nor is any leucosome present. The chemistry of the biotite and garnet in this "lower grade" zone suggests, however, that temperatures were not markedly lower within the synform than on its flanks, where staurolite and kyanite have appeared.

The metamorphic lines turn with the structural grain north of Howard Creek and trend nearly west. On proceeding northward from Windfall Creek towards Malton Gneiss, migmatite, which constitutes 10 to 20 per cent of the rock mass between Howard and Windfall creeks, disappears and staurolite appears in abundance. In other words, grade drops towards the Malton Gneiss. This is a detail inconsistent with the close relationship between metamorphism and the Malton Gneiss envisaged on a regional scale by Price and Mountjoy (1970).

The metamorphic surfaces cut obliquely across phase 1 and 2 folds. On the other hand it is clear that the sillimanite "inlier" in Columbia Valley, north of Mica Creek is related to phase 3 folding and that the metamorphic surfaces are folded during phase 3. The geometry of the metamorphic surfaces cannot, however, be accounted for by phase 3 folding only. One must envisage the metamorphic surfaces, already with important relief, being imprinted on the twice deformed rock mass. The metamorphic surfaces were then folded and otherwise deformed along with the rock mass during phase 3.

The mesoscopic structures and the metamorphic textures indicate a sequence of tectonic and metamorphic events much like the sequence suggested by the map patterns described above. The minor folds and crenulations, which are associated with the large F_3 folds, buckle and kink index minerals such as sillimanite, kyanite and staurolite. Biotite is also locally kinked but it appears to have recrystallized during or after F_3 . Leucosome layers and pegmatite sheets within the migmatitic zones have also been folded and boudiné during the evolution of F_3 folds.

Sillimanite, kyanite and staurolite lie on the S_{1+2} foliation plane but are not aligned parallel to phase 1 or 2 lineations. Trondhjemite leucosomes of essentially unfoliated granitic texture have formed within the S_{1+2} surfaces. It would thus appear that the maximum of metamorphism and migmatization occurred after, or late in, phase 2 but prior to the bulk of phase 3 deformation.

Examination of textural relations of garnet and biotite in the lower grade zones reveals that during F_1 the grade rose at least to biotite and probably to garnet zone conditions. During F_2 the grade increased to reach the maximum late in F_2 . In the higher grade zones, where staurolite has disappeared and where migmatization has set in, the rocks

generally have a coarse texture which is microscopically "simple"; inclusions, internal schistosity, helicitic textures, etc., are rare and it is difficult to decipher the earlier history of the rock.

Obvious retrogressive mineral assemblages are not seen on a regional scale. Phase 3 structures are not accompanied by retrogressive metamorphism and it would seem that the area has not undergone a hydration and diaphoresis associated with some late regional deformation episode.

The temperatures and pressures calculated from the mineral geochemistry of the maximum metamorphic grade mineral assemblages give estimates of the conditions under which the later stages of phase 2 deformation took place.

Mineral assemblages and estimates of physical conditions of metamorphism

Important pelitic mineral assemblages in the Canoe River area include:

biotite-garnet
staurolite-biotite-garnet
staurolite-biotite-garnet-kyanite
kyanite-biotite-garnet
sillimanite-biotite-garnet

All of the above assemblages include quartz, muscovite, and plagioclase. A chemical study of coexisting minerals at the staurolite-kyanite isograd south of Foster Creek (Fig. 3.1) has been completed. Additional studies of the chemistry of coexisting minerals in pelitic and mafic rocks at the sillimanite isograd are in progress. A comprehensive study of calc-silicates from the Canoe River area is also in progress.

Preliminary estimates of pressure, temperature, and fluid composition attending metamorphism have been made for rocks near the staurolite-kyanite isograd. Application of the empirical garnet-biotite geothermometer (Thompson, 1976) to eight garnet rim-biotite assemblages yields temperatures between 545 and 588°C (one sample yielded 502°C). The garnet-biotite geothermometer also appears to yield plausible temperatures in the adjacent southern Park Ranges (D. Craw, pers. comm.). Temperature estimates have also been made from the Mg-content of calcite coexisting with dolomite, using the experimental curves of Goldsmith and Newton (1969). Five samples yield temperature estimates in the range 540 to 565°C which is in reasonable agreement with garnet-biotite temperature estimates. Oxygen isotope temperature estimates based on coexisting quartz and ilmenite are still pending.

The presence of kyanite at a T near 550°C suggests a minimum pressure of metamorphism near 5 kilobars (using the aluminum silicate phase diagram of Holdaway, 1971). The disappearance of staurolite in the kyanite stability field suggests higher pressures than those attending metamorphism in the southern Park Ranges where staurolite breaks down near the sillimanite-kyanite isograd (D. Craw, pers. comm.). Calculation of the distribution coefficients for garnet-plagioclase ($K_D = (X_{gr}^{ga})^3 / (X_{an}^{pl})^3$ where K_D = the distribution coefficient, X_{gr}^{ga} = mol fraction of grossular in garnet, X_{an}^{pl} = mol fraction of anorthite) and application of an ideal solution model to the solid solutions (Ghent, 1976) suggest metamorphic pressures greater than 8 kb.

References

- Campbell, R.B.
1968: Canoe River, British Columbia: Geol. Surv. Can., Map 15-1967.
1973: Structural cross-section and tectonic model of southeastern Canadian Cordillera; Can. J. Earth Sci., v. 10, no. 11, p. 1607-1620.

Evans, C.S.

1933: Brisco-Dogtooth map-area, British Columbia; Geol. Surv. Can., Summ. Rep. 1933, Pt. A.

Ghent, E.D.

1976: Plagioclase-garnet- Al_2SiO_5 -quartz: a potential geobarometer-geothermometer; Am. Mineral., v. 61, p. 710-714.

Goldsmith, J.R. and Newton, R.C.

1969: P-T-X relationships in the system $CaCO_3$ - $MgCO_3$ at high temperatures and pressures; Am. J. Sci. (Schairer Vol.), v. 267-A, p. 160-190.

Holdaway, M.J.

1971: Stability of andalusite and the aluminum silicate phase diagrams; Am. J. Sci., v. 271, p. 97-131.

Poulton, T.P.

1973: Upper Proterozoic "Limestone Unit" Northern Mountains, British Columbia; Can. J. Earth Sci., v. 10, no. 2, p. 292-305.

Price, R.A. and Mountjoy, E.W.

1970: Geologic structure of the Canadian Rocky Mountains between Bow and Athabasca Rivers--a program report; in Structure of the Southern Canadian Cordillera, J.O. Wheeler (Ed) Geol. Assoc. Can., Spec. Paper 6, p. 7-39.

Simony, P.S. and Wind, G.

1970: Structure of the Dogtooth Range and adjacent portions of the Rocky Mountain Trench; in Structure of the Southern Canadian Cordillera, J.O. Wheeler (Ed); Geol. Assoc. Can., Spec. Paper 6, p. 41-51.

Thompson, A.B.

1976: Mineral reactions in pelitic rocks: II Calculations of some P-T-X (Fe-Mg) phase relations; Am. J. Sci., v. 276, p. 425-454.

Wheeler, J.O.

1963: Rogers Pass map-area British Columbia and Alberta (82N west-half) Geol. Surv. Can., Paper 62-32, 32 p.

1965: Big Bend map-area, British Columbia (82M east half); Geol. Surv. Can., Paper 64-32, 37 p.

Introduction

During the spring breakup period in March 1977, the Geological Survey of Canada conducted a seismic refraction study over the southeast edge of the Athabasca basin as part of the Uranium Evaluation Program. The purpose of the study was to measure, by the seismic refraction method, thicknesses of the Athabasca sandstone formation that overlies the Precambrian basement. This work was supplementary and adjacent to an airborne reconnaissance vertical magnetic gradiometer survey (Fig. 4.1) conducted by the Geological Survey of Canada during the summer of 1976 to assess the value of the gradiometer in mapping basement depths and features. The gradiometer results have been described by Kornik (in prep.). The seismic program was designed to be as detailed as possible although confined to the lakes within the area to facilitate aircraft landings, cable layouts and the shooting of small dynamite charges in the water under the ice. The base camp for the seismic program was set up on the southwest shore of Close Lake (Fig. 4.1). A single-engined Otter aircraft equipped with wheel-skis was used to move instruments and personnel to the work sites on the lake. Small charges of Geogel 60% explosive were used as the energy

source in co-operation with the fisheries agency of the Department of Northern Saskatchewan. A Southwestern Industrial Electronics RA-49R amplifier system with 24 Texas Instruments 7.5 Hz seismometers spaced at 36.6 m recorded on a Southwestern Industrial Electronics ERC-10 electrostatic oscillograph. The procedure was to fly the equipment to selected lakes within the area, lay out the cable on the ice using a skidoo, and drill holes in the ice at the ends of the cable and at offset intervals large enough to get seismic penetration to the Precambrian basement. Penetration to basement was assumed to have been effected when seismic velocities approximating 6.1 km/s were recorded. Shots were offset from both ends of the cable to record basement events in both directions where the size of the lake permitted. However, most of the lakes used were only large enough to allow offsets and measurements in one direction, and by far the majority were either too small to allow the landing of the aircraft, or were unusable due to thin ice or open water conditions created by water currents. Other problems encountered were due to anomalous snow conditions and abnormally erratic weather conditions during the spring breakup period. According to previous experience in the area gained by members of the crew and to reports by local

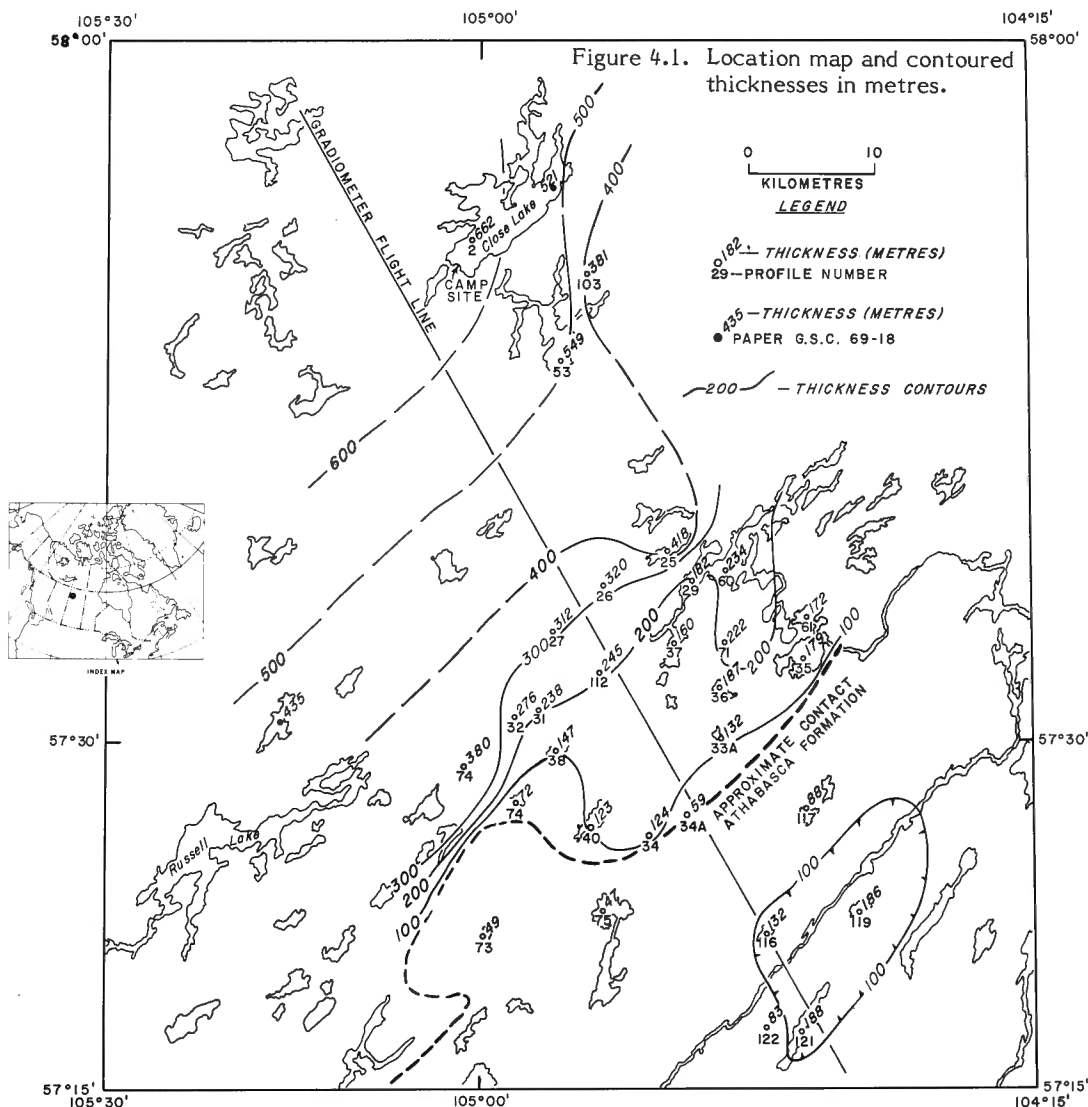


Figure 4.1. Location map and contoured thicknesses in metres.

From: Report of Activities, Part C;
Geol. Surv. Can., Paper 77-1C (1977)

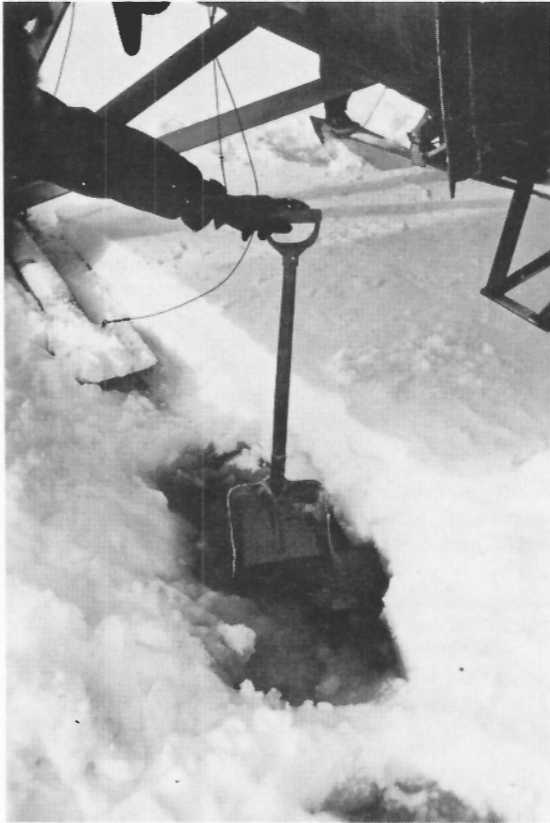


Figure 4.2. Water laden snow covering lake ice, Athabasca area, April 1977.



Figure 4.3. Clearing a path for takeoff on snow covered lake ice, Athabasca area, April 1977. (GSC-203202-F)

agencies the winter of 1976-1977 and the spring breakup in northern Saskatchewan was unusual in many respects. The lakes were all covered with a layer of loose snow varying in thickness from about 0.3 to 1 m. This in itself made landing and takeoff of the heavily loaded aircraft at best difficult, and at worst impossible to the point that loads had to be split between more numerous trips to lighten the aircraft on takeoff. The spring breakup was also marked by cycles of extreme thawing to extreme cold. These variations in temperature caused an accumulation of water on top of the main ice layer, which in turn was covered by a thin crust of ice under the snow. The aircraft and the skidoo would break through the ice crust into the water layer which in the colder weather would freeze onto the skidoo and the aircraft skis substantially increasing the weight of the aircraft. Many times the aircraft had to be dug out and tracks dug by hand to make a runway for takeoff (Figs. 4.2, 4.3).

While the resulting seismic grid was as closely spaced as possible it still constitutes very coarse control. The seismic results have been contoured on Fig. 4.1, but the very general nature of the indicated thicknesses must be emphasized. Some of the seismic profiles show that highly detailed gross and erratic structures are present which cannot be depicted adequately by the resulting seismic grid.

Acknowledgments

R.A. Burns and R. Good ably expedited the field work under extremely adverse conditions. Lamb Airways personnel performed their part very efficiently and effectively. The writer is particularly grateful to those people for their cheerful and efficient performance of the field work, and to R.M. Gagne for drafting the figures.

Brief Description of Geology

The Athabasca basin covers an area of approximately 104 000 km² in northern Saskatchewan. Fahrig (1961) described the Athabasca Formation as the generally flat-lying to very gently dipping predominantly sandstone rocks south of Lake Athabasca. The basinal configuration of the formation has been demonstrated by seismic measurements (Hobson and MacAulay, 1969) which suggest a thickness in the east-central part of the basin as great as 1550 m. Recent drilling has substantiated basinward slopes of the sub-Athabasca surface at the eastern part of the basin. Athabasca sandstones are characteristically buff, white, light grey, pink, or mauve. They are mostly medium- to coarse-grained, and range from friable to very well indurated. Minor beds of coarse conglomerates occupy the lowermost few metres of the formation and minor beds of shale are also present. A pre-Athabasca regolith has been observed in surface exposures (Fahrig, 1961) and has been confirmed in drill cores with some thicknesses exceeding 30 m.

The Athabasca Formation is locally underlain with major unconformity by folded and metamorphosed sediments of the Tazin Group including carbonate rocks, quartzites, argillites and conglomerates (Tremblay, 1968). At some localities, the basement rocks are highly weathered immediately below the unconformity. Drilling programs have provided useful information on the character of the sub-Athabasca rocks (Fraser et al., 1970). Drillholes near the eastern boundary have indicated that the basement gneisses are typically intensely altered for several metres below the unconformity. This intensive alteration gradually decreases with depth but geophysical probes in some holes can detect alteration to a depth of up to a hundred or more metres.

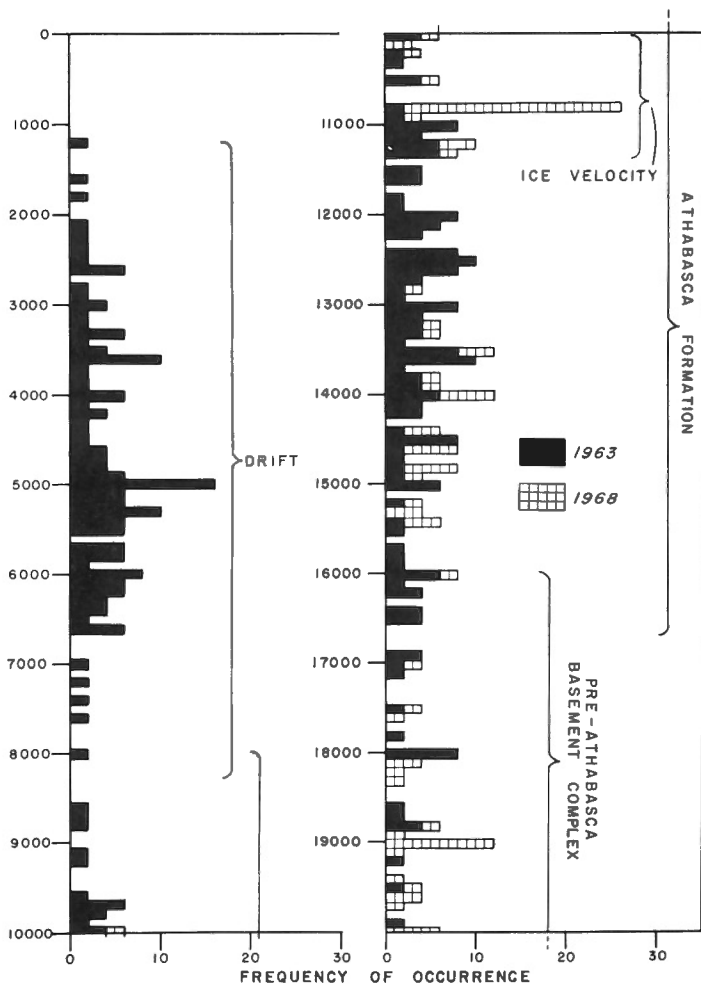


Figure 4.4. Distribution of observed seismic velocities, Athabasca basin. From Hobson and MacAulay (1969).

Near the southeast peripheral contact, basement rocks exposed outside the basin belong to the Wollaston Lake fold belt system. This system was described (Money, 1968) as tightly to isoclinically folded metamorphic and migmatitic rocks which coincide in part with the most extensive zone of magnetic anomalies in the Precambrian of Saskatchewan. On the basis of aeromagnetic data (Kornik, 1977), fault systems observed in this region may be extended under the Athabasca sandstone cover. Previous magnetic interpretations have been described by Kornik (1969, 1970), which suggest that relative movements between fault bounded blocks appear to be the mechanism controlling the present configuration of the southeastern portion of the Athabasca basin. This, in addition to evidence from Sibbald (1976) showing the influence of post-Athabasca faulting on the Rabbit Lake orebody, and from Ramaekers (1976) showing the presence of faulting and crustal movement along the northeast edge of the Athabasca basin, indicates that post-Athabasca faulting and crustal movements have played an important role in shaping the present structures in the Athabasca Formation.

Ramaekers (1975) has described a reconnaissance geological survey of the southeast edge of the Athabasca Formation. The prime objective was to study the formation and to locate its southeastern edge. In this area, the formation is little exposed, being nearly completely covered by glacial deposits. In the Precambrian metamorphic rocks adjacent to and southeast of the Athabasca Formation, four main units were encountered; they are meta-arkose, biotite hornblende, granulite, and diorite. Ramaekers describes the Athabasca Formation in this area as a cross-bedded quartzose sandstone that becomes increasingly conglomeratic near its base.

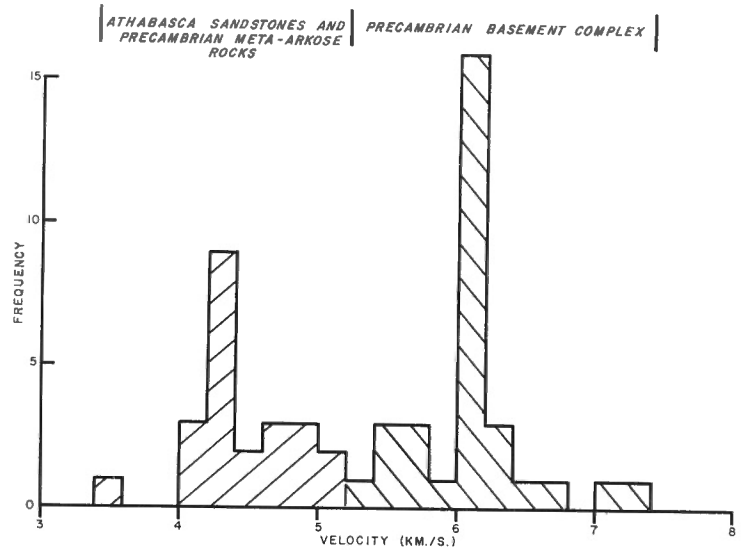


Figure 4.5. Distribution of observed velocities, 1977 data.

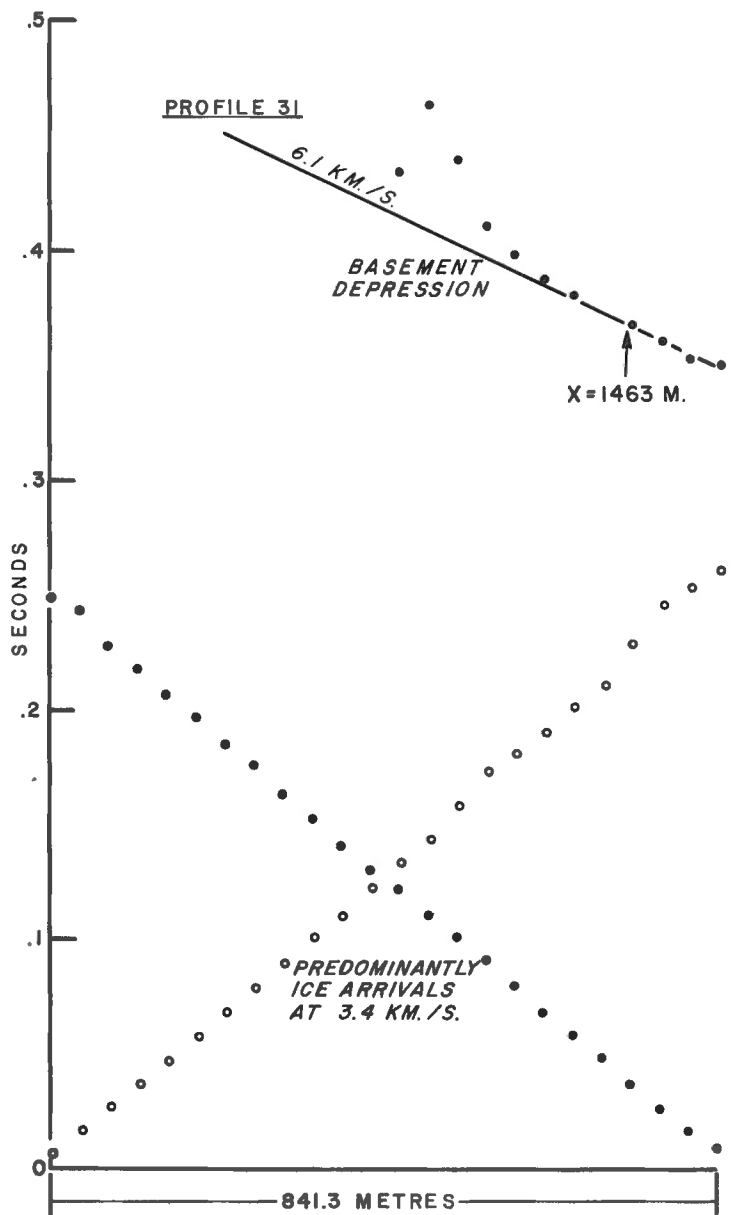


Figure 4.6. Profile 31, time-distance graph.

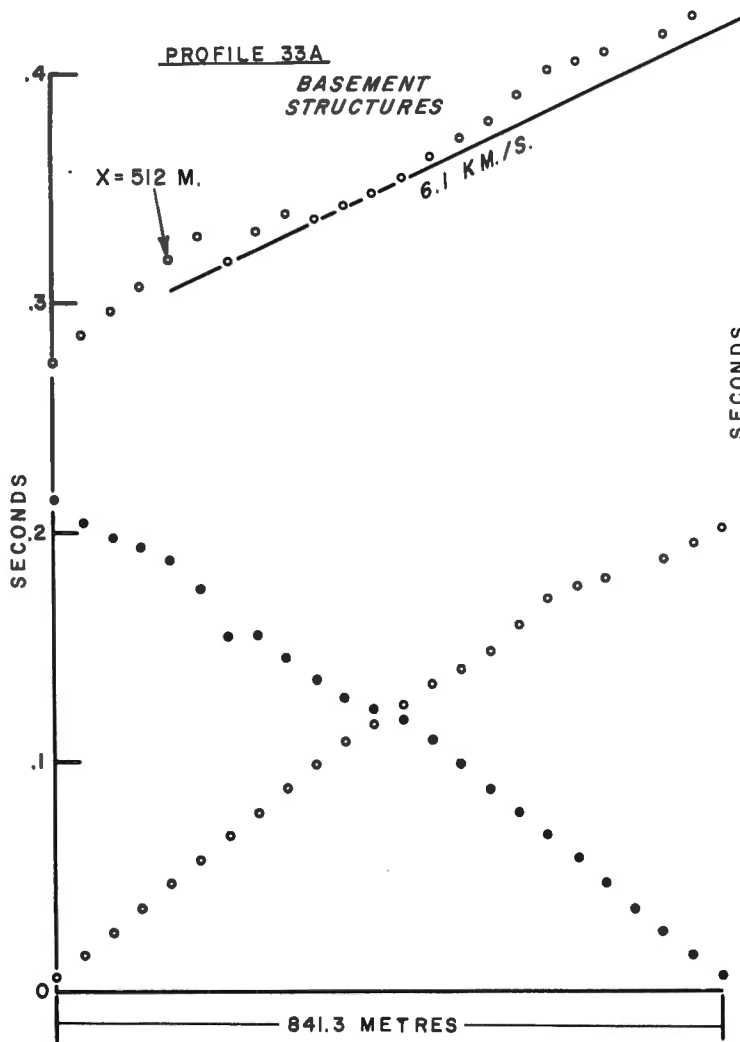


Figure 4.7. Profile 33A, time-distance graph.

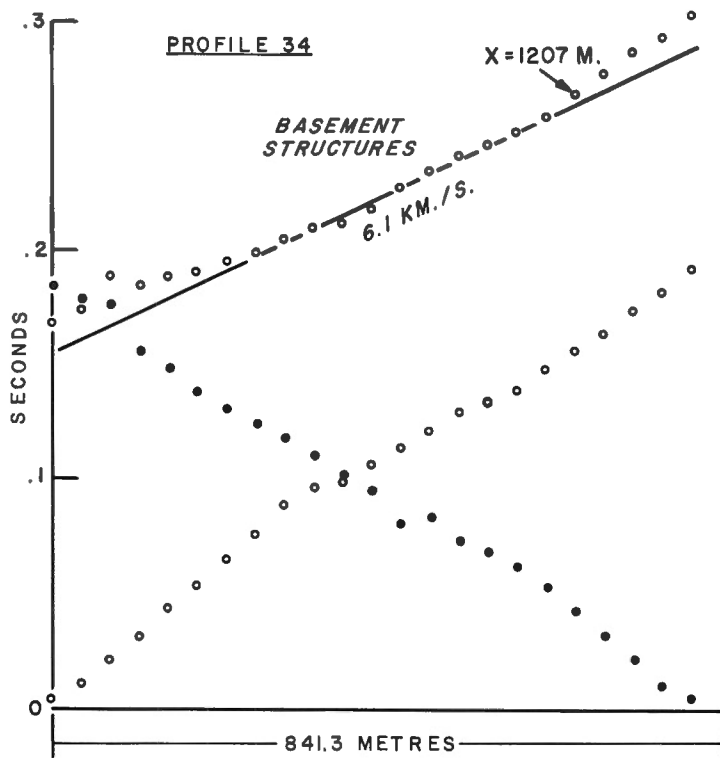


Figure 4.8. Profile 34, time-distance graph.

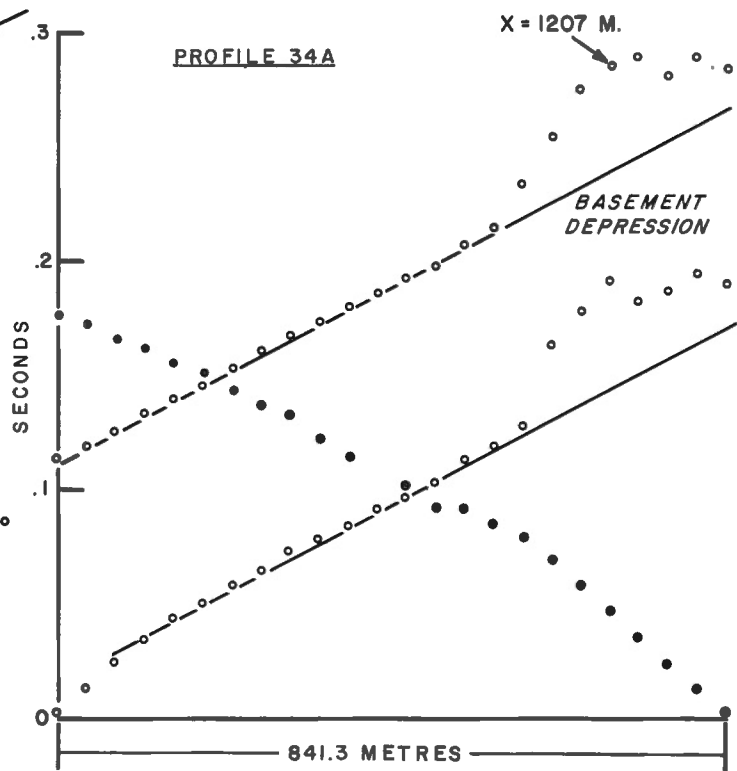


Figure 4.9. Profile 34A, time-distance graph.

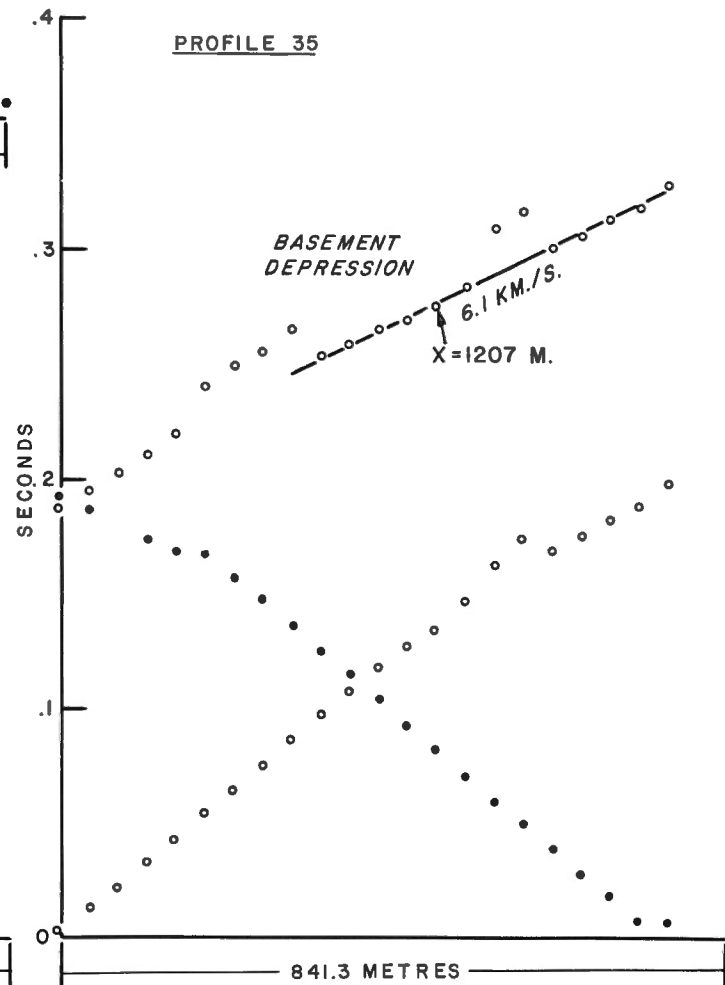


Figure 4.10. Profile 35, time-distance graph.

Previous Work

The Athabasca basin has previously been examined by Hobson and MacAulay (1969) using reconnaissance seismic surveys. This work demonstrated the basal configuration of the Athabasca Formation with a thickness in the east-central part of the basin of 1550 m. The field work was conducted in two seasons; one during the summer of 1963 and the other during the winter of 1968. Distinctly different results were obtained in seismic velocities between the two seasons. The frequency distribution of observed seismic velocities (Fig. 6, Hobson and MacAulay, 1969) shows a comparison of these results (Fig. 4.4). In both cases the frequency distributions are broadly dispersed multimodal. The results obtained during the winter season show a sharp cutoff of velocities below 3.3 km/s attributable to the masking effect of the ice layer present on the lakes in the winter. Above this velocity the

distributions for winter and summer are similar in appearance. Velocities for drift and sediments of values smaller than that for ice are only seen in the summer data. Broad geological correlations have been indicated on the frequency distribution of velocities, showing overlapping ranges for drift (0.3 to 2.5 km/s), Athabasca Formation (2.4 to 5.1 km/s), and pre-Athabasca basement complex (4.9 km/s and higher). The widely dispersed velocities in the Athabasca Formation probably represent different degrees of sorting of grain sizes in different parts of the formation and variations in porosity and water content. The dispersion in velocities for the basement complex represents variations in metamorphism, velocity modifications due to structural dips on the interface, variations in lithology, and differences in composition and texture due to varying degrees of weathering.

Table 4.1

Velocity-thickness summary for the profiles

Profile	Region	Velocities, km/s	Thicknesses, metres	Total thickness, metres
2	Athabasca basin	(1.52), 4.57, 6.10	46, 616	662
25		(1.52), 4.72, 6.40	20, 398	418
26		(1.52), 4.42, (6.10)	52, 268 Min.	320 Min.
27		(1.52), 4.33, 6.64	35, 277	312
29		(1.52), 3.66, 5.79	5, 177	182
31		(1.52), 4.27, 6.10	51, 187	238
32		(1.52), 4.18, 6.10	23, 253	276
33A		(1.52), 4.27, 6.10	19, 113	132
34		(1.52), 5.06, 6.10	9, 115	124
34A		(1.52), (4.27), 5.91	14, 45	59
35		(1.52), (4.27), 6.10	18, 161	179
36		(1.52), 4.36, 6.10	21, 166	187
37		(1.52), 4.27, 6.10	20, 140	160
38		(1.52), 4.27, 6.10	57, 90	147
40		(1.52), 4.69, 5.52	29, 94	123
53		(1.52), 4.27, 6.10	20, 529	549
60		(1.52), 4.27, 6.40	15, 219	234
61		(1.52), 4.08, 5.79	28, 144	172
71		(1.52), 4.27, 6.10	18, 204	222
74		(1.52), 5.12, 6.58	18, 54	72
76	(1.52), 4.11, (6.10)	25, 355	380	
103	(1.52), (4.27), 6.10	33, 348	381	
112	(1.52), 4.27, 6.10	14, 231	245	
73	Wollaston fold belt	(1.52), (4.27), 6.40	11, 38	49
75		(1.52), (4.27), 5.52	34, 13	47
116		(1.52), 4.63, 6.10	22, 110	132
117		(1.52), (4.27), (6.10)	24, 64	88
119		(1.52), 5.00, 6.10	25, 161	186
121		(1.52), 4.27, 7.22	31, 157	188
122		(1.52), 4.27, 5.49	17, 66	83

Parenthetical values are assumed

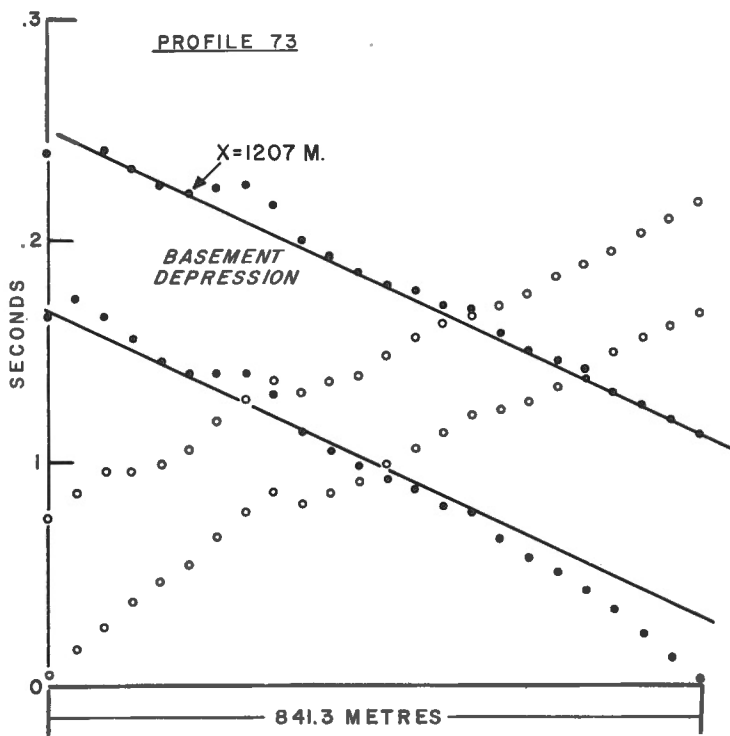


Figure 4.11. Profile 73, time-distance graph.

Results of the 1977 Seismic Program

Thirty locations were surveyed during the 1977 program. Of these, three reversed profile recordings of sub-Athabasca basement velocity were obtained, two gave reversed profile estimates of Athabasca Formation velocities and three gave reversed profile estimates of metamorphosed Precambrian velocities outside the basin. One profile failed to record the basement event because the small size of the lake prevented a sufficiently large offset for the shots. All others were essentially unreversed profiles due to the restrictive sizes of the lakes. In general, the sedimentary events were greatly obscured by events travelling through the ice layer on the lakes, and since the basement depths are relatively small (less than 500 m) only small segments of sedimentary events were commonly observed between the ice arrivals and the basement events. The ice arrivals completely precluded the measurement of drift velocities. The presence of drift, however, is evident from the sedimentary velocity delay times in excess of those accountable by water depths in the lakes. Velocities range from 4.08 km/s to 5.12 km/s for Athabasca Formation, 3.51 km/s to 5.0 km/s for metamorphic rocks of the Wollaston fold belt and 5.52 km/s to 7.22 km/s for sub-Athabasca Precambrian basement rocks. The velocities are shown as a frequency distribution in Figure 4.5. Table 4.1 summarizes velocities and their computed thicknesses for each of the profiles. Thicknesses of water and drift occupying the topmost portion of the section are represented by the assumed velocity of 1.52 km/s. The sedimentary thicknesses, plotted and contoured on Figure 4.1 which shows the general increase into the Athabasca basin, have nowhere been observed to be null. Observed thicknesses even outside the Athabasca Formation on the Wollaston fold belt are substantial. The thicknesses indicated on the Wollaston fold belt may represent partly drift cover, weathered rock material and substantial layers of meta-arkose rocks of the Daly Lake Group (Money, 1968; Ramaekers, 1976). The relationship between seismic and geological models in this region requires further investigation. It is evident from these results that detection of the peripheral contact from seismic velocity information alone would present interpretation problems. However, structural aspects on seismic profiles

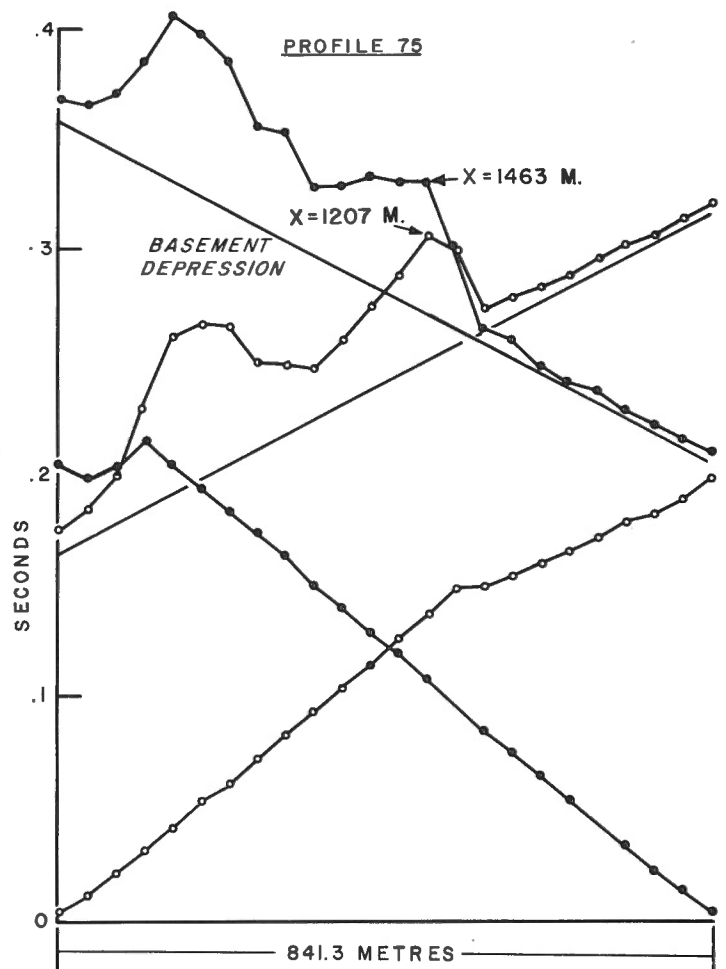


Figure 4.12. Profile 75, time-distance graph.

approximately perpendicular to and crossing the contact may lead to efficient delineation of the contact beneath drift and overburden.

For most of the contoured area overlying the Athabasca basin, the region lying between the peripheral contact and approximately the 400 m thickness contour corresponds with the shelf-like area interpreted as having less than 300 m of sedimentary cover from airborne magnetometer profiles (Kornik, 1977).

The aeromagnetic data also suggest the degree of complexity of basement fault systems which is not evident from the coarse seismic control. For this reason, the very general nature of the contoured seismic thicknesses of Fig. 4.1 must again be emphasized. However, some detailed complexity of the basement surface is also evident on some of the seismic profiles which show large structural effects. The time-distance plots for these profiles are reproduced in Figures 4.6 to 4.13. The large amplitude basement structures are revealed as undulating patterns on the time-distance graphs. Interpretation of the magnitude of these structures depends upon the seismic velocity of the material filling the basement depressions. Magnitudes based on observed velocities averaging 4.3 km/s would require basement structures as large as 460 m for the anomaly on profile 75 (Fig. 4.12). For this model, however, there would have to be 840 m of displacement between the anomalies in reversed recording directions due to the geometry of the headwaves emerging at the critical angle in opposite directions. Figure 4.12 for profile 75 shows no such displacement, but rather a remarkable lateral coincidence in the anomalies as seen in opposite recording directions. This suggests near

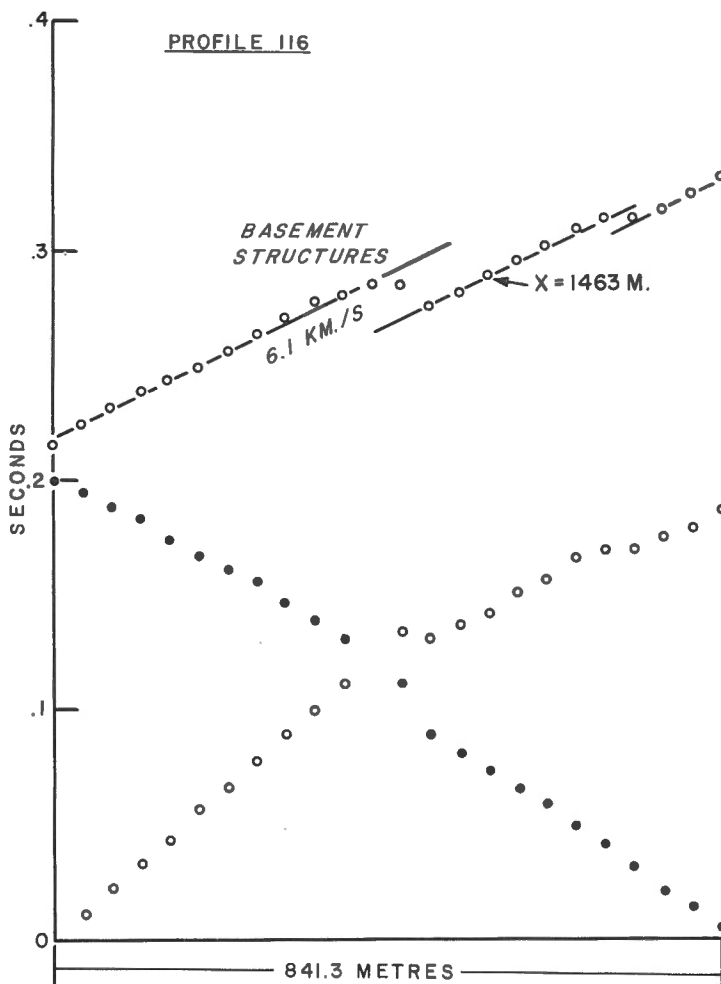


Figure 4.13. Profile 116, time-distance graph.

vertical incidence for the emergent headwaves, a condition that can be met only by the material filling the basement depression having a low seismic velocity. In the presence of the Athabasca sandstone and meta-arkose rocks having seismic velocities averaging 4.3 km/s, the low velocity fill would represent a velocity inversion whose value could not be measured by the seismic refraction method. To estimate the minimum structural effect causing the anomaly on Figure 4.12, it is unlikely that the seismic velocity for the filling material is less than that of water, or 1.5 km/s. At this velocity the structural amplitude would be about 113 m. It is noteworthy that these large structural effects with the suggested low velocity fill are observed on both sides of the Athabasca Formation - Wollaston fold belt peripheral contact. Low velocity materials at the base of the Athabasca Formation may be related to the regolith which has been observed in surface exposures (Fahrig, 1961), and has been confirmed in drill cores with some thicknesses exceeding 30 m, or to highly weathered basement rocks which have also been revealed by drilling programs (Fraser et al., 1970).

Conclusion

The restriction imposed by the use of lakes for conducting seismic surveys results in a coarse grid for defining a structurally complex basement. The complexity of the structures is evident in detail on some of the seismic profiles. Closely spaced continuous seismic profiles not confined to the lakes would yield greater detail and the areal extent of these structures. For definition of the drift and overburden the work should be conducted when these sediments are unfrozen. The seismic reflection method should be evaluated in the Athabasca basin for its capability to provide greater structural detail and definition.

Discussion

K.G. Neave has suggested that the large anomaly associated with profile 75 (Fig. 4.12) may be the effect of included gas (possibly methane) in the lake floor sediments. This possibility would allow the use of still lower (but unknown) seismic velocity for estimating the minimum thickness of the anomaly. For this purpose, a limiting velocity may be assigned as that for air (about 330 m/s) which yields a minimum thickness of 22 m for the anomaly. Low velocities associated with included gas are better able to explain the remarkable coincidence of the structure as seen in opposite recording directions. However, high attenuation of seismic energy caused by included gas zones is not evident on the records of profile 75. The phenomenon requires further investigation.

References

- Fahrig, W.F.
1961: The geology of the Athabasca Formation; Geol. Surv. Can., Bull. 68.
- Fraser, J.A., Donaldson, J.A., Fahrig, W.F., and Tremblay, L.P.
1970: Helikian basins and geosynclines of the northwestern Canadian Shield; in A.J. Baer (editor), Symposium on basins and geosynclines of the Canadian Shield; Geol. Surv. Can., Paper 70-40, p. 213-238.
- Hobson, G.D. and MacAulay, H.A.
1969: A seismic reconnaissance survey of the Athabasca Formation, Alberta and Saskatchewan (part of 74); Geol. Surv. Can., Paper 69-18.
- Kornik, L.J.
1969: A magnetic interpretation of the eastern portion of the Athabasca Formation; in Report of Activities, Part B, Geol. Surv. Can., Paper 69-1B, p. 29-31.
1970: Aeromagnetic survey of the Athabasca Formation; a quantitative interpretation; Can. Min. J., v. 91, p. 50-53.
Athabasca Formation basin: Gradiometer feasibility study; Geol. Surv. Can., Open File Report (in prep.).
- Money, P.L.
1968: The Wollaston Lake fold-belt system, Saskatchewan-Manitoba; Can. J. Earth Sci., v. 5, p. 1489-1504.
- Ramaekers, P.
1975: Athabasca Formation, Southeast Edge (74H): Reconnaissance Geological Mapping, in Summary of Investigations 1975; Sask. Geol. Surv., Sask. Dep. Miner. Res., p. 48-52.
1976: Athabasca Formation, Northeast Edge (64L, 74I, 74P): Part I, Reconnaissance Geology, in Summary of Investigations 1976; Sask. Geol. Surv., Sask. Dep. Miner. Res., p. 73-77.
- Sibbald, T.I.I.
1976: Uranium Metallogenic Studies - Rabbit Lake: in Summary of Investigations 1976; Sask. Geol. Surv., Sask. Dep. Miner. Res., p. 115-123.
- Tremblay, L.P.
1968: Geology of the Beaverlodge mining area, Saskatchewan; Geol. Surv. Can., Mem. 367.

5. EXPERIMENTS ON MOBILITY AND TRANSPORTABILITY OF SOME NEARSHORE BENTHONIC FORAMINIFERA SPECIES

Project 750042

C.T. Schafer and James A. Young
Atlantic Geoscience Centre, Dartmouth

Introduction

The comparatively high diversity, ease of collection and identification, and preservation as fossils, have continued to provide an incentive for the use of benthonic Foraminifera as environmental and process indicators (e.g., Sen Gupta and Kilbourne, 1976; Vilks et al., 1975; Phleger, 1976a, b; Scott et al., in press; Bock, 1976; Muller, 1976). Developing concurrently with this trend is an awareness of the advantage of quantitative approaches in analyzing large amounts of raw foraminiferal data, and in isolating significant environmental factors using one of several well known statistical correlation techniques (see: Parks, 1970; Hazel, 1972; Buzas, 1969). These areas of research have emphasized the need for a better understanding of foraminiferal population dynamics under a variety of environmental conditions so that samples which are not synoptic (the usual case) can be weighted and/or sorted to account for data that might not be representative of ambient conditions. For example, in a cluster analysis of benthonic Foraminifera in Broken Bay, N.S.W. (Albani and Johnson, 1975), it was observed that the more reliable descriptors of subenvironments are the relatively rare but widespread species (i.e., those forms having a relatively regular distribution pattern) compared to locally abundant forms. Albani and Johnson (1975) also concluded that any statistical analysis of foraminiferal populations in which biotopes are to be determined in nearshore marine environments should be based on total rather than living populations. This strategy tends to average out short term temporal and spatial variations in species abundance that have been recognized elsewhere. This report summarizes some experimental observations on the mobility of Foraminifera that could account for species distribution anomalies when data from samples collected in nearshore environments over a given time span are treated in a quasi-synoptic sense. The experiments are also relevant to recolonization rates of certain species on substrates that have been created through anthropogenic activities such as harbour channel dredging, ocean dumping, and ocean mining.

Previous Studies

Research on spatial distribution patterns has been summarized by Murray (1973) who noted that little is known about the means of dispersal of Foraminifera. Wave turbulence, ice, surface tension of seawater, rafting on submarine vegetation, and the inherent locomotive capabilities of species are among some of the mechanisms that have been documented (Richter, 1965; Schafer and Prakash, 1968). Empty tests of benthonic Foraminifera have also been reported from plankton tow samples. The equivalent diameters (i.e., the diameter of a quartz grain having the same settling velocity) of certain common nearshore morphological types of Foraminifera range between 0.10 and 0.14 mm (Haake, 1962; Grabert, 1971). They would thus be within the size range of most easily eroded particles (Shepard, 1963, p. 128), and therefore subject to continuous redistribution in nearshore environments. The redistribution susceptibility is increased for those species that are characterized by a free living unattached epibenthic life style and reduced for attached or infaunal forms.

The experiments discussed in this report were carried out in situ and also with living specimens collected from the St. Georges Bay area of Nova Scotia (Fig. 5.1). Experiments were designed to study factors such as species recolonization

rates, erosion and redeposition of tests, the inherent mobility of certain species, and the quantitative variability of local populations in time and space. Two types of experiments were carried out. The first used an in situ approach in which sterile sand areas were implaced on the bottom of the bay in about 13 m of water and then sampled periodically over about a 200-hour period (see: Schafer, 1976).

During the in situ experiments (Schafer, 1976) many periods of high turbidity were recorded by a portable underwater time-lapse television system that was used to monitor changes in the surface of the emplaced sterile sands (Schafer et al., 1975). Living specimens were observed on the sterile sand after only two days indicating that repopulation is a relatively rapid phenomenon. Major species that ultimately repopulated the sterile sands included *Elphidium incertum/clavatum* Gp., *Quinqueloculina seminulum*, *Ammonia beccarii*, *eggerella advena*, *Hemisphaerammina bradyi*, and *Miliammina fusca*. While the degree of passive versus active transport could not be discerned in the in situ experiment, in situ substrate sampling following a hurricane which passed through the area showed a significant increase in the living population of common nearshore calcareous species. This observation supports the idea of a passive transport mechanism that may be indicative of the typically epibenthic unattached life style as well as the size and shape of certain forms. The results of fish tank experiments described here focus on the active transport capabilities of some of the same species noted above.

The second approach, which is the primary focus of this report, utilizes a laboratory technique in which substrate material comparable to that found at the in situ experimental site is introduced into one side of a fish tank filled with water that was collected at the same site. Sterile sand substrate is added to the other side of the tank bottom following stabilization of the natural sediment and this sand is subsequently sampled. The results of the fish tank technique described here tend to reflect the relative level of biological activity of the species placed in the tank while the in situ experiments account for both passive transport and inherent mobility effects.

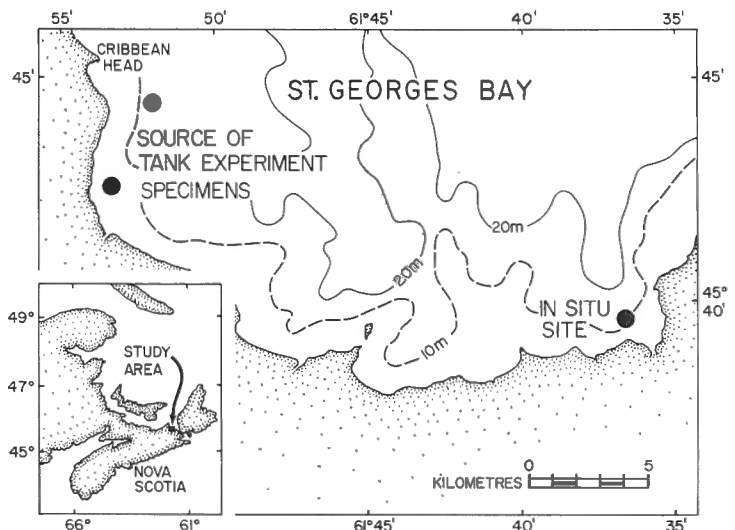


Figure 5.1. Location of source areas of living Foraminifera specimens and of in situ experimental site in St. Georges Bay.

Laboratory Method

Two 45-litre fish tanks were filled with water collected from the sediment sampling sites and held at a constant temperature of $13^{\circ}\text{C} \pm 2^{\circ}\text{C}$. Bottom sediment samples were collected by divers from two locations at water depths of 6 and 15 m. The respective samples were introduced into one half of each tank and allowed to stabilize for 24 hours. The opposite half of each tank was covered with a 4 cm layer of sterile 0.5 mm quartz sand by pouring the material through a 3 cm diameter plastic tube that was initially in contact with

the bottom of the tank. By carefully raising the tube the sand flow could be controlled thus minimizing disturbance to the stabilized natural sediment. A sharp contact between the sterile sand and the natural sediment was also maintained (Fig. 5.2). Two subsamples from each side of both tanks were collected after a seven day period had elapsed. Several hours after the sterile sand was placed in the tank a 25 x 75 mm glass microscope slide was pushed into this material to detect the very active specimens that would be expected to crawl up the slide (see Arnold, 1974, p. 168). The slide was removed



Figure 5.2. Photograph of fish tank substrate showing sterile sand (light coloured) adjacent to natural sediment (dark coloured).

Table 5.1

Summary of results obtained using sediment from the offshore (16 m) site

SPECIES	SOURCE SUBSTRATE MEAN SPEC./SAMPLE	STERILE SUBSTRATE MEAN SPEC./SAMPLE	TOTAL SLIDE SPECIMENS	TOTAL DISH SPECIMENS
<i>Eggerella advena</i>	219	33	11	26
<i>Elphidium incertum/clavatum</i> Gp.	124	37	59	81
<i>Buccella frigida</i>	14	6	3	3
<i>Protelphidium orbiculare</i>	36	3	6	1
<i>Trochammina squamata</i>	5	—	—	—
<i>Ammonia beccarii</i>	5	4	7	—
<i>Saccammina atlantica</i>	27	2	1	—
<i>Elphidium subarcticum</i>	8	—	—	2
<i>Pseudopolymorphina novangliae</i>	2	—	—	—
<i>Ammodiscus catinus</i>	5	2	—	—
<i>Hemisphaerammina bradyi</i>	5	—	—	—
<i>Quinqueloculina arctica</i>	0.5	—	—	2
<i>Trochammina lobata</i>	5	1	—	—
<i>Ammotium cassis</i>	21	—	—	—
<i>Buliminella elegantissima</i>	1	1.5	—	—
<i>Cyclogyra involvens</i>	1	—	—	—
<i>Glomospira gordialis</i>	3	—	—	—

Mean specimen per sample values were determined after a seven day period.

Total slide specimens represent those forms that crawled up the vertical surface of the slide.

Total dish specimens represent counts of specimens that crawled to the surface of the sediment in the petri dish during the seven day period.

from each tank at the end of the seven day period before collecting the two substrate samples and the attached Foraminifera on the slide were identified and counted.

In addition to the tank observations several petri dishes were partially filled with sediment, examined for Foraminifera, and monitored over a seven day period to detect any new specimens that had crawled to the sediment surface.

Results

Tank experiment observations have been summarized in Tables 5.1 and 5.2. The two sites from which the living specimens were collected do not vary significantly with respect to their major species components. However, with decreasing water depth and increasing mean grain size of sediment there is a decrease in the proportion of arenaceous species such as *Eggerella advena* and *Trochammina* sp. These forms are displaced by calcareous forms such as *Ammonia beccarii*, *Buccella frigida*, *Protelphidium orbiculare*, and *Elphidium incertum/clavatum* Gp. that prefer the comparatively warm water temperatures that are developed in shallow water (<10 m) during the summer season (Schafer et al., 1976). With transition from the deep to the shallow site there is also a drop in population density of about 50 per cent which is probably related to dilution of specimens by sediments in the nearshore high energy environment. Mobile species observed in the shallow site sample included *Elphidium incertum/clavatum* Gp., *Buccella frigida*, *Protelphidium orbiculare*, and *Quinqueloculina* cf. *Q. seminulum*. The key active species in the deep site sample were *Eggerella advena*, *Elphidium incertum/clavatum* Gp., *Buccella frigida*, *Protelphidium orbiculare*, *Ammonia beccarii*, and *Saccammina atlantica*.

P. orbiculare and *E. incertum/clavatum* Gp. were especially active in both tanks as evidenced by the ratio of slide specimens to mean sterile substrate specimens (Tables 5.1, 5.2). Most of the active species identified in the tank experiments were also observed in the in situ sterile substrate samples which confirms that the inherently active and the typically epifaunal species are probably also most susceptible to passive transport mechanisms. The transport-susceptible group includes most of the major calcareous rotalid forms. Common shallow water species such as *E. incertum/clavatum* Gp. tend to reflect a somewhat higher level of inherent mobility compared to the indigenous deep water forms.

Discussion

The Foraminifera that have been observed on the sterile sand and on the slide substrates have moved from the natural sediment that was placed in the tanks. This movement may be active or passive. There are several possible sources of passive transport. At the time of introducing the natural sediments, some Foraminifera may have settled on the side of the tank onto which the sterile substrate was to be introduced. This effect was minimized by sampling only from the upper one cm layer of the substrate and by the use of comparatively coarse sand (0.5 mm) which would inhibit vertical burrowing. The other source of contamination originates from the air stones used to maintain homogeneity in the water column. It is possible that sufficient circulation may have been generated to transport some of the Foraminifera specimens although turbid conditions were never observed following stabilization of the natural sediment.

Table 5.2

Summary of results obtained using sediment from the nearshore (6 m) site
Foraminifera listed in both Tables are referenced in Schafer and Cole (1976)

SPECIES	SOURCE SUBSTRATE MEAN SPEC./SAMPLE	STERILE SUBSTRATE MEAN SPEC./SAMPLE	TOTAL SLIDE SPECIMENS	TOTAL DISH SPECIMENS
<i>Eggerella advena</i>	30	1.5	—	6
<i>Elphidium incertum/clavatum</i> Gp.	236	4	29	41
<i>Buccella frigida</i>	62	—	6	12
<i>Protelphidium orbiculare</i>	11	—	9	1
<i>Trochammina squamata</i>	11	—	—	—
<i>Ammonia beccarii</i>	18	—	—	1
<i>Saccammina atlantica</i>	7	—	—	—
<i>Elphidium subarcticum</i>	5	—	—	—
<i>Pseudopolymorphina novangliae</i>	2	—	—	—
<i>Quinqueloculina</i> cf. <i>Q. seminulum</i>	39	0.5	8	30
<i>Hemisphaerammina bradyi</i>	5	—	—	—
<i>Trochammina macrescens</i>	5	—	—	—
<i>Glabratella wrightii</i>	3	—	—	—
<i>Elphidiella arctica</i>	5	—	—	—
<i>Elphidium margaritaceum</i>	4	—	—	1

It should be pointed out that the density of living specimens observed in the sterile substrates is substantially reduced with respect to that noted in the introduced natural substrate samples. If it can be assumed that the population density was high enough in the introduced sediments to necessitate colonization of the sterile substrate, then one could make definite conclusions about the ability of the Foraminifera to move under stress conditions. If this is an invalid assumption we have then learned only about the readiness of certain species to colonize. Despite these considerations, and even though the specimen numbers are relatively low in all of the sterile substrate samples, it appears that there has been a differential response of the organisms from the shallow and deep environments. A plausible explanation for the comparatively restricted movement of the organisms from the shallow site sample is that this environment is characterized by higher levels of wave turbulence so that it may not be necessary for species to maintain a high level of mobility in order to colonize or feed. In the relatively quiescent deep water site this may not have been a viable alternative, hence the higher level of mobility of the observed indigenous specimens.

In nearshore environments the mobile species would be expected to form the major assemblage component inhabiting newly formed allochthonous sediment substrates that have developed in response to natural processes such as storm events and that have been deposited in deeper than normal water depths. They would also be among the members of a pioneer community that would initially inhabit the dredged bottoms of harbours and estuaries in temperature environments. Finally, these species would rank among those forms having a relatively better chance of burrowing upward to the sediment surface following burial in the upper layers of sediment.

Conclusion

Comparison of in situ sterile substrate and tank experiment data indicates that the transport-susceptible calcareous rotaloid Foraminifera are also the most active crawling species within the total population. The differential

results obtained for *Elphidium incertum/clavatum* Gp. suggests a reduction of activity for this species in deeper environments. The observed arenaceous species tend to be less active than calcareous forms which may also be indicative of the typically unperturbed conditions of their offshore life zone.

References

- Albani, A.D. and Johnson, K.R.
1975: Resolution of foraminiferal biotopes in Broken Bay, N.S.W.; J. Geol. Soc. Aust., v. 22, p. 435-446.
- Arnold, Z.M.
1974: Field and laboratory techniques for the study of living Foraminifera, in Foraminifera, R.H. Hedley and C.G. Adams, editors; Academic Press, London, 276 p.
- Bock, W.D.
1976: Distribution and significance of Foraminifera in the MAFLA Area; Marit. Sediments, Spec. Pub. No. 1, Pt. A, p. 221-238.
- Buzas, M.A.
1969: On the quantification of biofacies; in Proceedings of the North Am. Paleo. Convention, Pt. B, p. 101-116.
- Grabert, B.
1971: Zur Eignung von Foraminiferen als Indikatoren für Sandwanderung; Sonderdr. Deutsch. Hydr. Z., v. 24, p. 1-14.
- Haake, W.H.
1962: Untersuchungen an der Foraminiferen-fauna in Wattgebiet zwischen Langeogg und dem Festland; Meyniana, v. 12, p. 25-64.
- Hazel, J.E.
1972: On the use of cluster analysis in biogeography; Syst. Zool., v. 21, p. 240-242.
- Muller, P.H.
1976: Sediment production by shallow-water benthic Foraminifera at selected sites on Oahu, Hawaii; Marit. Sediments Spec. Pub. No. 1, Pt. A, p. 263-266.

- Murray, J.W.
1973: Distribution and ecology of living benthic Foraminiferids; Crane, Russask & Co., New York, 274 p.
- Parks, J.M.
1970: Fortran IV Program for Q-Mode cluster analysis on distance function with printed dendrogram; State Geol. Surv., Univ. Kansas, Computer Contr. 46, 36 p.
- Phleger, F.B.
1976a: Benthic Foraminiferids as indicators of organic production in marginal marine areas; Marit. Sediments Spec. Pub. No. 1, Pt. A, p. 107-118.
1976b: Foraminiferal and ecological processes in St. Lucia Lagoon, Zululand; Marit. Sediments Spec. Pub. No. 1, Pt. A, p. 195-204.
- Richter, G.
1965: Zur Okologie der Foraminiferen III - Verdriftung und Transport in der Gezeitenzone; Natur. Mus., Frankfurt., v. 95, p. 51-62.
- Schafer, C.T.
1976: In situ environmental responses of benthonic Foraminifera; in Report of Activities, Part C, Geol. Surv. Can., Paper 76-1C, p. 27-32.
- Schafer, C.T. and Prakash, A.
1968: Current transport and deposition of foraminiferal tests, planktonic organisms and lithogenic particles in Bedford Basin, Nova Scotia; Marit. Sediments, v. 4, p. 100-103.
- Schafer, C.T., Godden, C.A., and Payzant, P.
1975: A portable underwater video-recorder; Proceedings, Offshore Technology Conf., Houston, Texas, p. 725-729.
- Schafer, C.T. and Cole, F.E.
1976: Foraminiferal distribution patterns in the Restigouche Estuary; Marit. Sediments Spec. Pub. No. 1, Pt. A, p. 1-24.
- Scott, D.B., Medioli, F.S., and Schafer, C.T.
Temporal changes in foraminiferal distributions in Miramichi River Estuary, New Brunswick; Can. J. Earth Sci. (in press).
- Sen Gupta, B.K. and Kilbourne, R.T.
1976: Depth distribution of benthonic Foraminifera on the Georgia Continental Shelf; Marit. Sediments, Spec. Pub. No. 1, Pt. A, p. 25-38.
- Shepard, F.P.
1963: Submarine geology; Harper and Row, New York, 557 p.
- Vilks, G., Schafer, C.T., and Walker, D.A.
1975: The influence of a causeway on oceanography and Foraminifera in the Strait of Canso, Nova Scotia; Can. J. Earth Sci., v. 12, p. 2086-2102.

Project 770036

P.J. Kurfurst
Terrain Sciences Division

This project was initiated in spring 1977 as a part of a detailed study of the proposed route of the Polar Gas pipeline. The main objective was to study and to describe the process of rock heave in massive rocks in the central Arctic along the proposed pipeline route and its effect on the pipeline.

A five-week field program was carried out during summer 1977 on Somerset, Cornwallis, Bathurst, Melville, and adjacent islands (Fig. 6.1). A two-fold approach was used in the field: (a) general observations along the length of the proposed pipeline route and (b) detailed study and measurements at specific sites at each island studied. Selection of sites was based on aerial photography evaluation and helicopter reconnaissance flights and traverses.

General studies consisted mainly of determination of rock types present and their performance and of study of fractures in rock masses, their frequency, distribution, orientation, and dimensions. Detailed studies of specific sites also included surveying and instrumentation of frost heaved blocks of massive rock and determination and description of the process of rock heave and differential rock heave encountered.

Although no final conclusion can be drawn at this stage, the preliminary field observations indicate that the process of rock heave is taking place frequently in all types of rocks in the Arctic Islands studied. The construction and operation of a chilled gas pipeline could lead to rapid changes in thermal regime, which in turn could increase the amount of rock heaving, produce extensive ice lensing and movement of rock masses, and result in differential movement, buckling, and eventual rupture of the pipeline. More detailed and extensive studies are planned especially for Somerset Island, where rock heave commonly occurs both in sedimentary rocks and igneous rocks of the Canadian Shield.

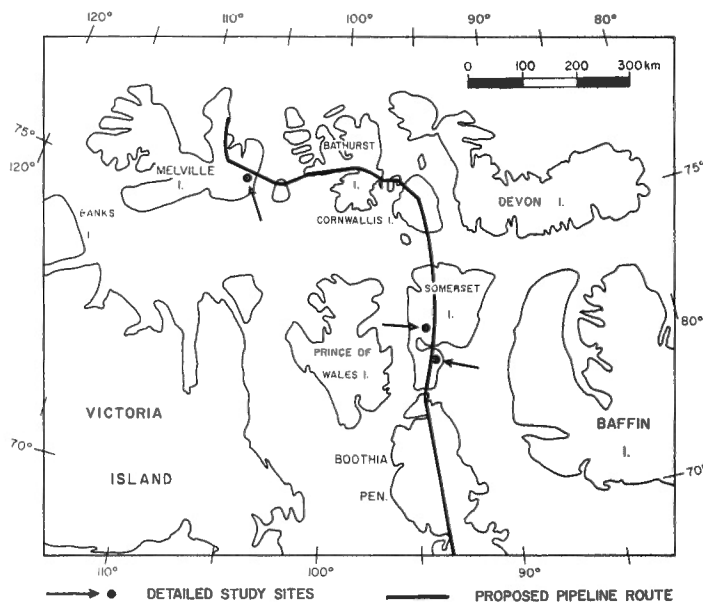


Figure 6.1. General location of study area.

7. EVALUATION OF REGIONAL OCCURRENCE OF GROUND ICE AND FROZEN GROUND, MACKENZIE VALLEY, DISTRICT OF MACKENZIE¹

Project 740046

J.A. Heginbottom, P.J. Kurfurst, and J.S.O. Lau
Terrain Sciences Division

Introduction

This investigation is part of a wide-ranging study into the occurrence and distribution of ground ice and frozen ground in the Mackenzie Delta area and Mackenzie Valley north of Fort Simpson. Special emphasis has been placed on near-surface soils. In order to assess this information all the geotechnical data available were assembled in the Mackenzie Valley Geotechnical Data Bank (Lawrence, 1974a; Lau and Lawrence, 1976a). Since the late 1960's approximately 11 600 boreholes have been drilled for geotechnical purposes in the Mackenzie Valley, Mackenzie Delta, and Beaufort Sea. Borehole logs and laboratory test records with varying degrees of detail are available for these boreholes. The holes were drilled principally for the following purposes:

- 1) investigation of alignment and construction for the Mackenzie and Dempster highways, carried out by the Department of Public Works and its consultants;
- 2) investigations of alignment for several proposed gas and oil pipeline routes, carried out by gas and oil consortia; and
- 3) investigations carried out by the Department of Indian Affairs and Northern Development as part of an inventory of granular construction materials in Mackenzie Valley.

Mackenzie Valley Geotechnical Data Bank

The data bank consists of 11 677 records of borehole information. These records were processed using COBOL programming on a Control Data Cyber 74 computer and are stored on a magnetic tape created at the Departmental Computer Science Centre, Energy, Mines and Resources, Ottawa (Lawrence, 1974b).

Each record in the data bank consists of the following (Proudfoot and Lawrence, 1976):

- 1) a header line which includes 27 variables specifying the location, topography, and technical aspects of each drill site;
- 2) a maximum of 18 lines used to describe soil stratigraphy where up to 29 geotechnical and permafrost characteristics can be recorded; and
- 3) an uncoded comment line where explanatory data can be recorded.

The completeness and accuracy of the data bank information depends to a large degree on the quality of the original records.

A retrieving system using COBOL and FORTRAN programming (Lau and Lawrence, 1976a) can be utilized to retrieve information of permafrost and geotechnical properties from the data bank with respect to various parameters such as topographic position, soil texture, genetic soil type, and season of drilling. Soil moisture and depth relationships (Lawrence, 1975; Lau and Lawrence, 1976a) and winter ground ice distribution (Lau and Lawrence, 1976b) for selected map-areas in the Mackenzie Valley have been studied in detail utilizing the Mackenzie Valley Geotechnical Data Bank.

The objective of this study was to examine the regional distribution of ground ice and frozen ground in the Mackenzie Valley. Unfortunately, the data points stored in the data bank are not distributed evenly across the breadth of the valley but are concentrated largely in a few lines running the length of the valley. These lines follow the alignments of the various proposed highway and pipeline routes that have been investigated in the area. Thus, use of the data bank does not give a true regional picture but instead represents a latitudinal profile from southeast to northwest, parallel to Mackenzie River. The greatest concentrations of data points are shown in Figure 7.1.

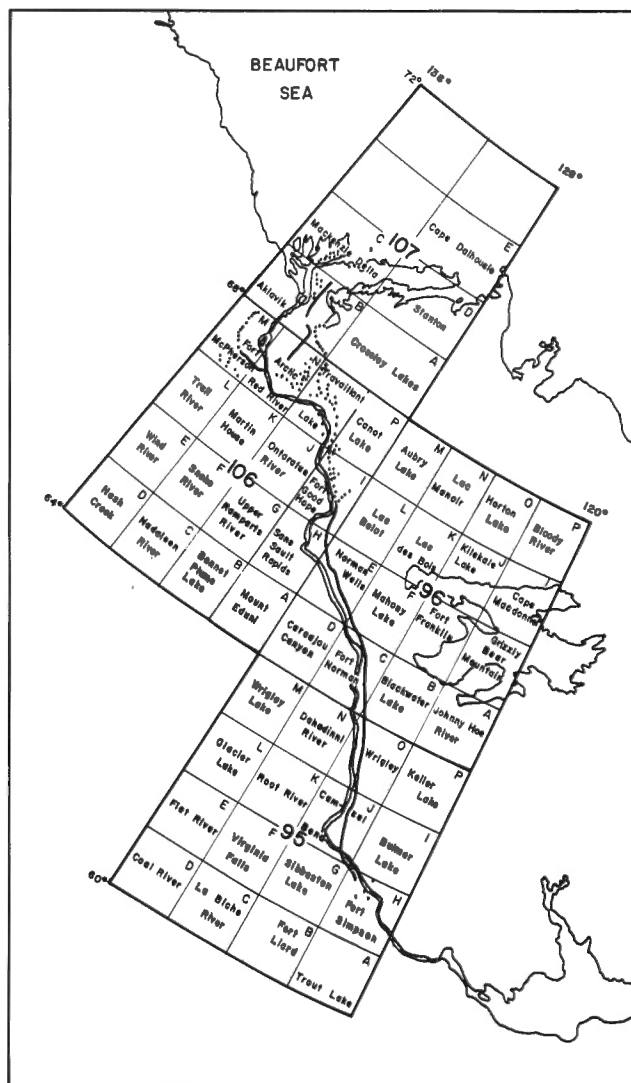


Figure 7.1. The lines and dots show the locations of the greatest concentration of data points in the NTS map-areas covered in the Mackenzie Valley Geotechnical Data Bank.

¹ An extended version of this paper has been accepted for presentation at the 3rd International Conference on Permafrost to be held in Edmonton Alberta, July 10-13, 1978.

In order to examine the variations in ground ice and frozen ground along the profile the complete data set was divided into subsets. For convenience, the National Topographic System (NTS) map-areas were used as a guide in this division, resulting in a total of 28 subsets between map-areas 95 H and 107 C (Fig. 7.1). Fourteen of these subsets contained data from less than 100 boreholes each and were discarded from further analysis.

In addition, data for 121 boreholes from the floor of the Beaufort Sea also were included in the data bank. These were combined into a separate subset within map-area 107C.

In order to consider ground ice and frozen ground as geologic materials, the data within each subset were broken down further by the genesis of the soil material and by the engineering classification of the soils. Fifteen Unified Soil Classification System soil types were encountered in the study area. These were grouped into five major engineering soil groups according to grain size, amount of fines, and liquid limit. Since the soil group containing soil types MH, CH, and OH was encountered in only six map-areas, this group was not used in the statistical analysis. Five classes of soil permafrost and ground ice conditions were identified; they were grouped into three major classes for analysis.

The statistical approach taken was to consider the proportion of 1) frozen soils with visible ice, 2) frozen soils with no visible ice, and 3) unfrozen soils within each map-area, first for each genetic soil class and then for each engineering soil group. Percentages of frozen soils of all

types and frozen soils with visible ice only were plotted (frozen soils of all types include frozen soils with visible ice); the detailed results are shown graphically in Figure 7.2.

Discussion of Results

There is a general increase in amount of frozen ground and ground ice from south to north in Mackenzie Valley. In some parts of upper Mackenzie Valley unfrozen ground predominates, whereas in the delta region frozen ground, commonly with a considerable amount of segregated ice, is ubiquitous.

This general impression is borne out by various detailed studies of ground ice conditions in the region (Judge, 1973; Heginbottom and Kurfurst, 1975) and by the data compiled in the data bank. The amount and rate of this variation, however, differs for each soil type whether genetic or engineering classifications are used. Furthermore, the nature of the change is neither uniform nor consistent.

Engineering Soil Groups

The proportion of frozen soils with visible ice for each engineering soil group is shown in Figure 7.2a (by map-area). Results show the distinctly different behaviour of gravels and sands (groups I and II) from that of fine grained soils and peats (groups III and IV). The distribution curves for both clean, coarse grained soils and coarse grained soils with fines display generally increasing amounts of visible ice with higher latitude.

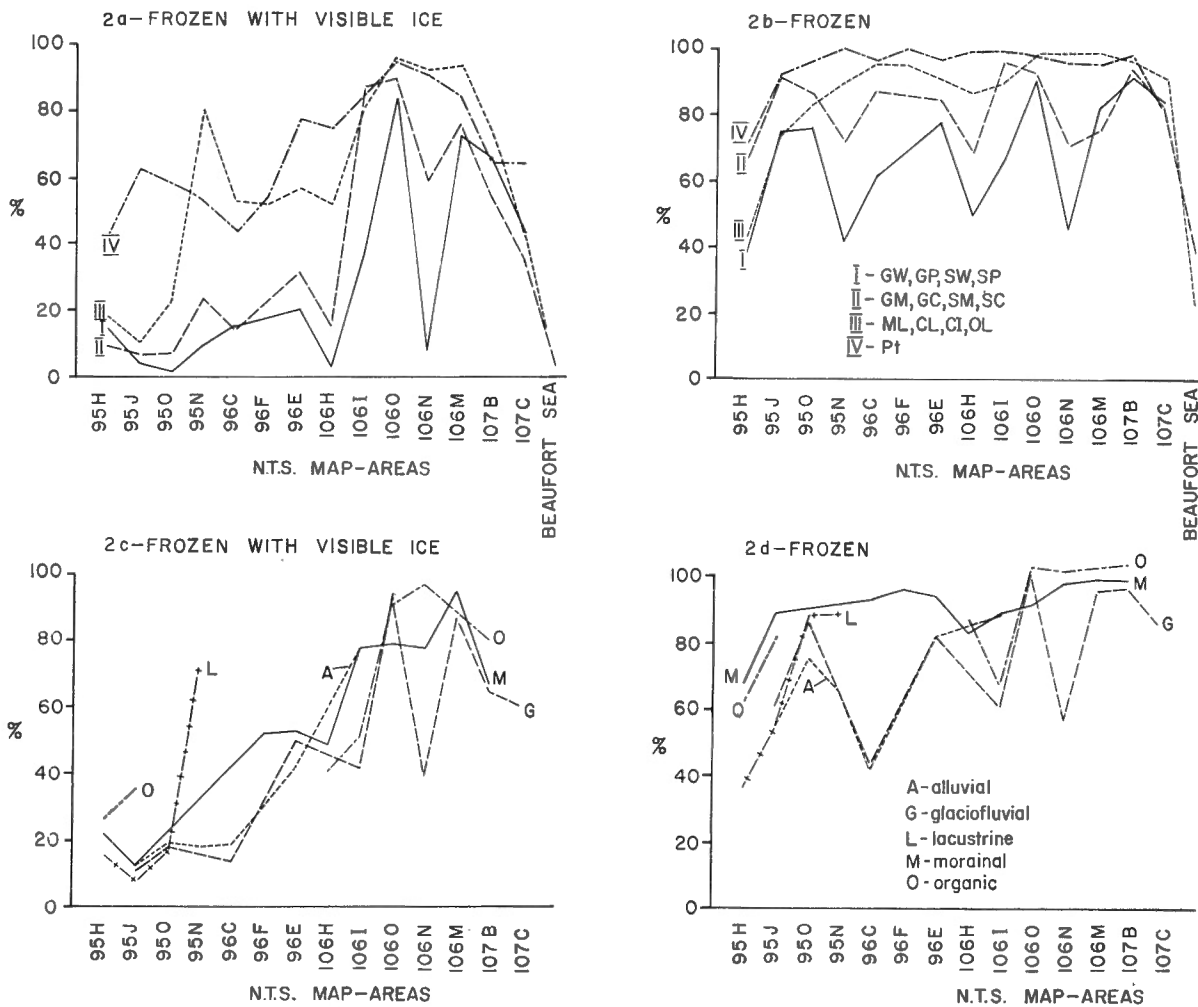


Figure 7.2. Distribution of frozen soils with visible ice and frozen soils of all types by soil type and map-area; 2a, 2b - engineering soil groups; 2c, 2d - genetic soil classes.

The curves for both fine grained soils and peats are similar to those for gravels and sands containing a much higher proportion of frozen soils with visible ice in upper Mackenzie Valley.

The proportion of frozen soils of all types for each engineering soil group is shown in Figure 7.2b (by map-area). The distribution curves for gravels and sands display a slowly increasing trend from south to north, and the curves for fine grained soils and peats show a similar increase with the total amount of frozen soils remaining almost constant at a high level in lower Mackenzie Valley. The curves show a decreasing trend towards the Beaufort Sea which is typical of all soil groups.

Genetic Soil Classes

Figures 7.2c and 7.2d show the proportion of frozen soils with visible ice and frozen soils of all types respectively for each genetic soil class.

Morainal soils derived from Laurentide ice are assumed to be the oldest soils in Mackenzie Valley. These soils are predominantly frozen throughout the region, except in the extreme southeast. The proportion of frozen soils with visible ice ranges from low in the extreme south of Mackenzie Valley to high in the Mackenzie Delta; it drops off sharply towards the Beaufort Sea. The proportion of frozen soils of all types follows a similar pattern, rising from the southern limit of the area, dropping gradually in the central region, and then rising again in the north.

Glaciofluvial soils show a complex and irregular distribution of both frozen soils of all types and frozen soils with visible ice. The proportion of frozen soils with visible ice rises between the southern and central regions. In the northern region, the proportion rises again, then drops off near the coast. The proportion of frozen soils of all types has a similar distribution. It rises gradually from the southern to the central region. In the northern region, the distribution pattern is similar to that of frozen soils with visible ice; near the coast the proportion levels off.

Lacustrine soils are distributed sporadically; they occur in five map-areas in the southern and central regions and in the Mackenzie Delta near the arctic coast. The proportion of frozen soils with visible ice rises sharply within the central region. The distribution of frozen soils of all types appears to be straightforward through upper Mackenzie Valley.

Data on alluvial soils are available mainly from the central region of Mackenzie Valley and in one map-area in each of the southern and northern regions. Frozen soils with visible ice display a normal distribution with a low in the south and a high in the north. The distribution of frozen soils of all types appears to be bimodal.

Organic soils of various ages are present through the length of Mackenzie Valley and are predominantly frozen throughout the area. In the southern and central regions the proportion of frozen soils with visible ice is relatively low and increases significantly in the northern region. This increase is followed by a gradual drop towards the Beaufort Sea. The distribution curve for frozen soils of all types follows a similar pattern.

The general trend of increasing proportions of both visible ice and total ice content in frozen soils from south to north is in good agreement with the general trend of the climatological data available for Mackenzie Valley and the Beaufort Sea (Burns, 1973).

Interpretation of Results

After evaluating all the available data, certain features of distribution of frozen ground and ground ice in Mackenzie Valley become evident. Frozen ground is widespread

everywhere in the valley north of 60°N, and its proportion gradually increases from south to north. The proportion of frozen ground is greater than 50 per cent in all areas and in all genetic classes except for lacustrine soils in the area around Fort Simpson and for alluvial and glaciofluvial soils in the area around Fort Norman. These two anomalies can be attributed to the presence of surficial materials with little or no fines and to the absence of a cover of thick peat or organic soils. These features result in better local drainage conditions.

In soils classified by the Unified Soil Classification System the proportion of frozen ground ranges from 70 to 100 per cent in all areas and for all engineering soil groups except for the following: clean, coarse grained soils in areas around Fort Simpson, Dahadinni River, Sans Sault Rapids, and Arctic Red River; coarse grained soils with fines in areas around Fort Simpson and Sans Sault Rapids; and fine grained soils in the area around Fort Simpson. In the Fort Simpson area, located in the zone of sporadic permafrost, most boreholes were located in recently disturbed terrain along the Mackenzie Highway. In these areas, the amount of frozen ground and ground ice decreased considerably following disturbance of the terrain; thus these results may not be typical of the map-area.

Low values for the Dahadinni River area can be explained by the small number of borehole results available; these boreholes were located predominantly in the well drained, ice free, coarse grained soils of the river terraces.

Data for the Sans Sault Rapids and Arctic Red River areas have been affected by the predetermined location of the majority of boreholes. Detailed investigations carried out for the proposed Mackenzie Valley pipeline route and the pipeline testing facilities, concentrated mainly on the well drained outwash plains and fluvial terraces, which contain low amounts of ground ice, around Sans Sault Rapids. In the Arctic Red River area most data were derived from a detailed study of the granular resources and borrow pits for the Dempster Highway. Because boreholes were located in well drained, coarse grained sediments at high elevation, with little or no excess ground ice, final results tend to be biased towards low values.

The decrease in the proportion of frozen ground and ground ice in the area near the arctic coast probably is controlled by the location of boreholes, because most studies in this area were done in close proximity to the river channels; thus the results reflect the warming influence of Mackenzie River and the massive water body of the Beaufort Sea.

Conclusions

The general impression, substantiated by this study, is that frozen ground is more extensive, occurs at shallower depths, and contains more visible excess ice as one goes from south to north. The greatest change appears to be in the area between Sans Sault Rapids and Travailant Lake, which probably coincides with the boundary between the continuous and discontinuous permafrost zones (Brown, 1967). This is also the area where detailed studies are lacking and where more investigations are needed.

The significant factors controlling the distribution of frozen ground and ground ice in Mackenzie Valley, as determined in this study, appear to be location (latitude), soil texture, surface drainage, surface disturbance, vegetation, and slope aspect. Although the qualitative ranking of these factors varies from site to site, the major controls on permafrost conditions seem to be latitude and soil texture. This is in good agreement with the climatological conditions of Mackenzie Valley, i.e., generally colder and longer winters and the cooler and shorter summers of the northern part, compared to the southern part. There are some anomalies,

however, such as the dry areas around Sans Sault Rapids and Fort Good Hope.

The finer textured soils, such as silts, clays, and clay-silt tills generally contain more moisture and more ice than coarser, sandy, and gravelly soils. There appears to be a clear, positive relationship between natural moisture content and engineering properties of fines.

Although only very general observations of ground surface drainage were made, it can be concluded that poorly drained sites with thick surface peat or organic cover contain more ground ice than adjacent, drier sites.

The effects of vegetation were considered only in terms of its presence or absence as a result of surface disturbance. In such cases the removal of vegetation was found to be a major contributor to the decrease in amount of frozen ground and ground ice.

Differences in slope aspect also were examined. There is strong evidence that south-facing slopes are drier and north-facing slopes are wetter than adjacent level ground. Local lithology, slope angle, and slope aspect, however, can override differences due solely to position on the slope.

References

Brown, R.J.E.

- 1967: Permafrost map of Canada; Geol. Surv. Can., Map 1246A, 1:7.6 million.

Burns, B.M.

- 1973: The climate of the Mackenzie Valley - Beaufort Sea. Volume 1; Dep. Environ., Atmosph. Environ. Serv., Climatol. Stud. no. 24, 227 p.

Heginbottom, J.A. and Kurfurst, P.J.

- 1975: Local variability of ground ice occurrence at selected sites in the Mackenzie Valley; Geol. Surv. Can., Open File 476, 56 p.

Judge, A.S.

- 1973: The thermal regime of the Mackenzie Valley: Observations of the natural state; Environmental-Social Comm., Northern Pipelines, Task Force on Northern Oil Development, Rep. 73-38.

Lau, J.S.O. and Lawrence, D.E.

- 1976a: Review of Mackenzie Valley geotechnical data; in Report of Activities, Part A, Geol. Surv. Can., Paper 76-1A, p. 265-268.

- 1976b: Winter ground ice distribution of selected map-areas, Mackenzie Valley; in Report of Activities, Part B, Geol. Surv. Can., Paper 76-1B, p. 161-168.

Lawrence, D.E.

- 1974a: Geological review of geotechnical data, Mackenzie Valley; in Report of Activities, Part A, Geol. Surv. Can., Paper 74-1A, p. 281.

- 1974b: Geological review of geotechnical data, Mackenzie Valley; Unpubl. rep. to Mackenzie Highway-Environmental Working Group, Dep. Indian Aff. Northern Dev., 63 p.

- 1975: Soil moisture relationships in selected map-areas, Mackenzie Valley, N.W.T.; in Report of Activities, Part B, Geol. Surv. Can., Paper 75-1B, p. 183-184.

Proudfoot, D.A. and Lawrence, D.E.

- 1976: Mackenzie Valley geotechnical data bank tape description manual; Geol. Surv. Can., Open File 350.

Project 730021

R.B. Taylor
Terrain Sciences Division

Introduction

The meteorological data presented in this report were collected during the summer months of 1974-76 in support of a research project which examined coastal processes along northern Somerset Island. The only source of continuous yearly meteorological data along Barrow Strait is from the Resolute Bay meteorological station located on southwestern Cornwallis Island (Fig. 8.1). Because climatic conditions were thought to vary with geographic position and local topography along Barrow Strait, a program to measure meteorological parameters was carried out at the field base camp at Cunningham Inlet, Somerset Island.

The base camp, located at 74°08'N, 93°53'30"W, was situated on a gravel raised beach terrace approximately 9 m above sea level on the western shore of Cunningham Inlet. The meteorological station, adjacent to the base camp, was 1.4 km inland from the northwest headland of Cunningham Inlet (Figs. 8.1, 8.2). A second anemometer was located at the northwest headland approximately 25 m above sea level; this anemometer was set up in 1975 and 1976 to provide a better indication of wind conditions along the exposed northern shore of Somerset Island. Cunningham Inlet, which is approximately 5 km wide at the mouth and 8 km long, is lined on the east and west shores by plateau slopes reaching elevations of 200 m. Because of the protection provided by these high slopes, the climate at the head of the inlet often is less severe than the climate experienced at the more exposed northern end of the inlet.

The field season and duration of observations were mainly from late June to early September, but for 1975 data are only available until August 20. The meteorological observations were collected at least four times daily at 0700, 1200, 1900, and 2300 hours CDT. Because these measurements constitute only a small part of the daily field program, however, some gaps do occur in the information. Observations during the first six hours of each day were limited to those monitored on instruments.

This report is intended as a summary of meteorological observations made during the summers of 1974 to 1976. Also, a comparison of climatic conditions at Resolute Bay and Cunningham Inlet illustrates the similarities and differences of climate at two stations located on either side of Barrow Strait. A climatic summary of daily air temperatures, precipitation, and winds for the Cunningham Inlet station has been prepared and is available upon request to the author.

Air Temperature

Air temperature was recorded continuously on a Short and Mason weekly thermograph in 1974 and on a Bacharach Tempscribe in 1974 and 1976. The mean daily temperature at Cunningham Inlet for July and August, based on data from three summers, was 4.1°C and 3.3°C, respectively (Tables 8.1, 8.2). The maximum recorded temperature was 16.1°C on August 17, 1975, and the minimum was -3.9°C on September 12, 1974 and August 29, 1976 (Table 8.1). Figures 8.3A and 3B illustrate the highest and lowest maximum and minimum temperatures. Unfortunately no records are available for Cunningham Inlet during late August 1975, a time when below normal air temperatures were recorded at Resolute Bay. The coolest summer was 1976 when average temperatures were 1.1°C and 4.6°C below the mean temperatures recorded for July and August, respectively, during the other two summers (Table 8.1). The warmer temperatures recorded in 1974 and 1975 may be partly a function of the

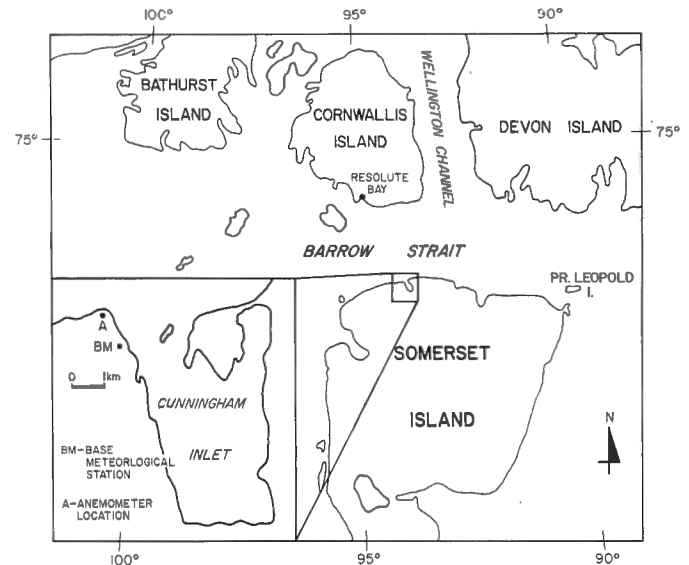


Figure 8.1. Location map.

type of screen used to house the thermometers. During the first two years an unpainted, homemade screen was used whereas in 1976 a regulation Stevenson screen (Fig. 8.2) was borrowed from Polar Continental Shelf Project at Resolute Bay. The warmest summer was in 1975 and followed a very early spring melt at the beginning of June. In 1975, summer temperatures over 10°C, were recorded on 8 days and although the minimum temperatures hovered around 0°C, the frost-free period lasted from July 1 to August 20 at Cunningham Inlet. In contrast, temperatures of 10°C or greater were recorded only on 2 days in 1976, and the longest frost-free period was 16 days from July 17 to August 2. In 1974, temperatures above 10°C were recorded on 8 days, and the frost-free period lasted from July 1 to August 12.

Comparison with Resolute Bay

A comparison of air temperatures recorded at Cunningham Inlet and Resolute Bay (Environment Canada, 1974, 1975, 1976) (Table 8.2, Fig. 8.4) shows that mean temperatures are 1° to 2°C higher at Cunningham Inlet. This difference also may be due to the type of Stevenson screen utilized at Cunningham Inlet. The greatest difference occurs in the mean minimum temperatures at the two stations.

Figure 8.4 illustrates that warming and cooling trends are similar at both stations, and often the maximum air temperatures occur on the same date at both places. Minimum temperatures are lower and commonly occur on different days at Resolute Bay than at Cunningham Inlet. In 1974 similar temperatures were observed at both stations; in 1975 temperatures were higher at Cunningham Inlet; and in 1976 they were usually higher at Resolute Bay. Mean daily temperatures fall below 0°C more often at Resolute Bay, and the frost-free season is much shorter than at Cunningham Inlet. Maximum summer temperatures occur during the last week of July or the first week in August at both stations, with a second peak in temperature around August 15-20.

Table 8.1

Air temperature and precipitation summaries, Cunningham Inlet, NWT, 1974-1976

Year	Month	No. Days of Record	TEMPERATURE (°C)						PRECIPITATION (mm)						
			Mean Daily		Date		Total Amount	No. days with 2.54 mm or more	Heaviest fall in month	No. days with					
			Max.	Min.	Max.	Min.				Snow	Fog				
1974	July	31	6.1	2.8	4.5	10.0	12	0.3	25	20.06	9	8.00	22	3	14
	August	31	5.5	1.4	3.4	15.3	03	-2.2	29	9.67	7	3.30	17	7	12
	Sept.	13	0.4	-1.9	-0.5	3.3	01	-3.9	12	4.95*	4	2.49*	04	8	3
1975	July	31	6.4	2.6	4.5	15.6	29	0.3	17	15.14	10	5.21	31	4	12
	August	20	7.8	3.3	5.6	16.1	17	0.0	20	5.58	6	3.30	07	1	11
1976	July	31	4.9	1.8	3.4	11.1	28	-0.8	01	19.23	8	11.68	02	5	11
	August	31	2.3	-0.4	1.0	6.7	17	-3.9	29	13.93	9	6.35	19	6	12
	Sept.	10	0.1	-1.9	-0.9	1.1	01	-3.1	09	0.25*	2	0.25*	09	3	5

* Instrument unable to measure blowing snow, therefore represents minimum value.

Table 8.2

Comparison of mean air temperatures at Cunningham Inlet and Resolute Bay, NWT (°C)

Month/Station	1974 Average		1975 Average		1976 Average		1974-76 Average	
	Max.	Min.	Max.	Min.	Max.	Min.	Max.	Min.
July Cunningham Inlet	6.1	2.8	6.4	2.6	4.9	1.8	5.8	2.4
Resolute Bay	5.8	0.6	4.9	-0.1	6.4	0.8	5.7	0.4
August Cunningham Inlet	5.5	1.4	7.8	3.3	2.3	-0.4	5.2	1.4
Resolute Bay	5.3	-0.7	4.2	-1.3	2.4	-1.6	3.9	-1.2



Figure 8.2. (A) Meteorological station located at the base camp, Cunningham Inlet (arrow locates rain gauge). (GSC 169681)

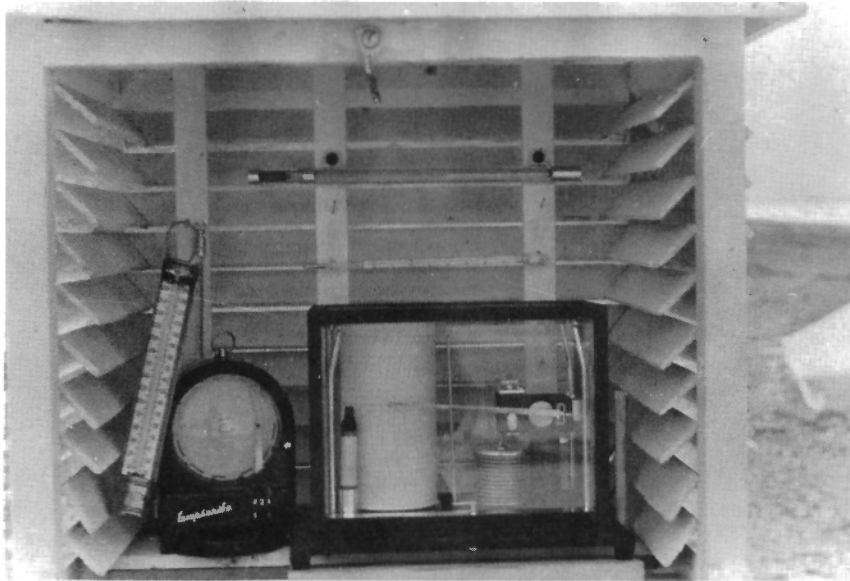


Figure 8.2. (B) Instruments housed in the Stevenson screen at the meteorological station at Cunningham Inlet. (GSC 169684).

Precipitation

Precipitation was monitored continuously at Cunningham Inlet each season. Although the recorded values of rainfall are accurate, those of snowfall are underestimated because of the inability to catch and measure blowing snow in the small gauge (Fig. 8.2A); therefore the percentage rainfall shown in column 6 of Table 8.3 is higher than it should be for the Cunningham Inlet station.

The average amount of precipitation recorded during the months of July and August was 29.7 mm. The most precipitation fell in the summer of 1976 and the least during 1975. Measurable precipitation (2.54 mm or more) was recorded on 16 to 17 days each summer. The heaviest recorded fall of precipitation in one day was 11.68 mm on July 2, 1976. At Cunningham Inlet precipitation generally was greater for July than August.

Snow fell on twice as many days during the summers of 1974 and 1976 than 1975. At Cunningham Inlet, however, the last 10 days of August 1975, which was a period of considerable snowfall at Resolute Bay, were not monitored. Snow may fall during any summer month at Cunningham Inlet, but it does not remain on the ground for any length of time until late August or early September.

Each July and August recorded more than 10 days of fog (Tables 8.1, 8.3). These figures include all fog banks that occurred within some part of Cunningham Inlet and not necessarily just those over the meteorological station.

Comparison of data from Cunningham Inlet and Resolute Bay

A comparison of total summer precipitation for both meteorological stations is presented in Table 8.3. On average, precipitation was 22.5 mm more each summer at Resolute Bay than at Cunningham Inlet. Some of this difference results from an inability to measure the amount of blowing snow at Cunningham Inlet. Only in 1976 were more days of rainfall recorded at Cunningham Inlet than at Resolute Bay; however, the total amount of summer precipitation was still greater at Resolute Bay. When a large low pressure system was situated over Barrow Strait and considerable precipitation fell at Resolute Bay, precipitation also would fall at Cunningham Inlet. The amount of precipitation that fell at each station, on the same date, varied as did the date on which maximum seasonal precipitation was recorded.

Columns 2 and 3 of Table 8.3 illustrate that although precipitation fell on more than half of the days on record, only 25 to 35 per cent of these days recorded measurable precipitation (2.54 mm or more). The large number of days with trace precipitation may be a function of the coastal location of both stations, where fog and drizzle often occur especially after the sea ice breaks up in Barrow Strait. Both stations had similar fog records, but Resolute Bay experienced a few more days of fog than did Cunningham Inlet during two of the three years. In fact, fog occurred at both stations on the same date an average of 17 days each summer (Table 8.3). Fog is common along the north coast of Somerset Island, but often it did not extend landward south of the weather station which was 1.4 km inland from Barrow Strait.

Sunshine

The amount of sunshine at Cunningham Inlet was recorded only during summer 1976 using a modified Campbell-Stokes sunshine recorder. July was the sunniest month with 57 per cent of the total possible sunshine recorded. Twenty-four hours of sunshine were recorded on July 26 and 28 which were also days of maximum air temperature (Fig. 8.4C) at Cunningham Inlet. August and the beginning of September had very little sunshine, less than 16 per cent of the possible duration of sunshine (Table 8.4).

A comparison of sunshine records collected at Resolute Bay over the same period indicates that similar conditions existed at both stations in July, but differences arose during

Table 8.3

Summer precipitation at Cunningham Inlet and Resolute Bay, NWT, 1974-76

	(1)	(2)	(3)	(4)	(5)	(6)	(7)	(8)	(9)	(10)
Days of Available Data	Days with Precipitation	Days with Precipitation more than trace	Total Amount (mm)	Rainfall (mm)	Rainfall as % of Total	Maximum in one day (mm)	Date of Maximum Fall	No. Days of Fog	No. Days Fog Occurred at both stations	
1974 (July 1 - Sept. 13) Cunningham Inlet	75	42	34.68	25.58	73.7	8.00	July 22	29	18	
Resolute Bay	75	54	63.24	45.96	72.7	15.49	July 22	31		
1975 (July 1 - August 20) Cunningham Inlet	51	29	20.70	19.6	94.6	5.21	July 31	23	15	
Resolute Bay	51	40	46.73	42.41	90.8	7.11	Aug. 9	30		
1976 (July 1 - Sept. 10) Cunningham Inlet	72	32	33.37	28.88	86.5	11.68	July 2	28	17	
Resolute Bay	72	44	46.23	19.81	42.8	9.65	Aug. 19	26		

Table 8.4

Amount of sunshine, Cunningham Inlet and Resolute Bay¹, NWT, 1976

Location	Observation Period	Duration (hours)	Total Possible Hours	% of Possible Duration	Maximum Sunshine in one day		No. Days with no Sunshine
					Hours	Date	
Cunningham Inlet	July 3-31	394.5	744	57.8	24.0	26, 28	1
Resolute Bay		406.0		59.4	24.0	26, 27	1
Cunningham Inlet	Aug. 1-31	101.6	648	15.7	14.4	11	8
Resolute Bay		139.0		21.4	15.6	27	7
Cunningham Inlet	Sept. 1-8	18.1	126.6	14.2	6.9	01	3
Resolute Bay		46.4		36.6	11.1	05	0

¹ Fisheries and Environment Canada, 1976.

the rest of the season. A large, long-lasting high pressure system over the study area (Fig. 8.5) accounts for the similarity of conditions in July, and a series of high and low pressure systems caused more variable sunshine at both stations in August. In the latter case the local configuration of open water - sea ice - land with respect to the wind direction would be responsible for the cloud cover (B. Taylor-Alt, pers. comm., 1977). During August and early September, Resolute Bay received more total sunshine and had fewer days with no sunshine than did Cunningham Inlet.

Winds

Wind direction and speed were monitored at Cunningham Inlet using two rotating cup anemometers; one was located at base camp, the other on the northwest headland of the inlet. Both were mounted on posts approximately 2 m above the ground. Wind speed was recorded continuously 24 hours a day, but wind direction was documented only when the anemometers were visited. Wind direction was determined using a large flag. Although wind speed and direction data were collected, particularly during storms, the present summary is based on measurements taken four times daily.

Wind Direction

The prevailing wind direction recorded at Cunningham Inlet was from the west-northwest (Table 8.5); the next largest number of observations was from the northwest. Slightly more than 40 per cent of all winds recorded at Cunningham Inlet originated from these two directions.

For coastal process studies it is useful to know the direction of strong winds. Over the three summers the most frequent direction of winds 20 mph or greater was from the northwest quadrant, but when wind data for each year are examined the direction of winds greater than 20 mph varies. For example in 1975 most strong winds blew from the south, whereas in 1974 and 1975 some easterly winds were strongest.

Wind Velocity

Wind velocity data collected over the three summers are summarized in Table 8.6. During 1974 and 1975, 75 per cent of all winds were less than 13 mph compared to 57 per cent in 1976 when winds were slightly stronger. Only 4 per cent of the winds were stronger than 20 mph; the maximum wind velocity recorded at Cunningham Inlet was 32.8 mph from the west-northwest on July 13, 1976. Occurrences of

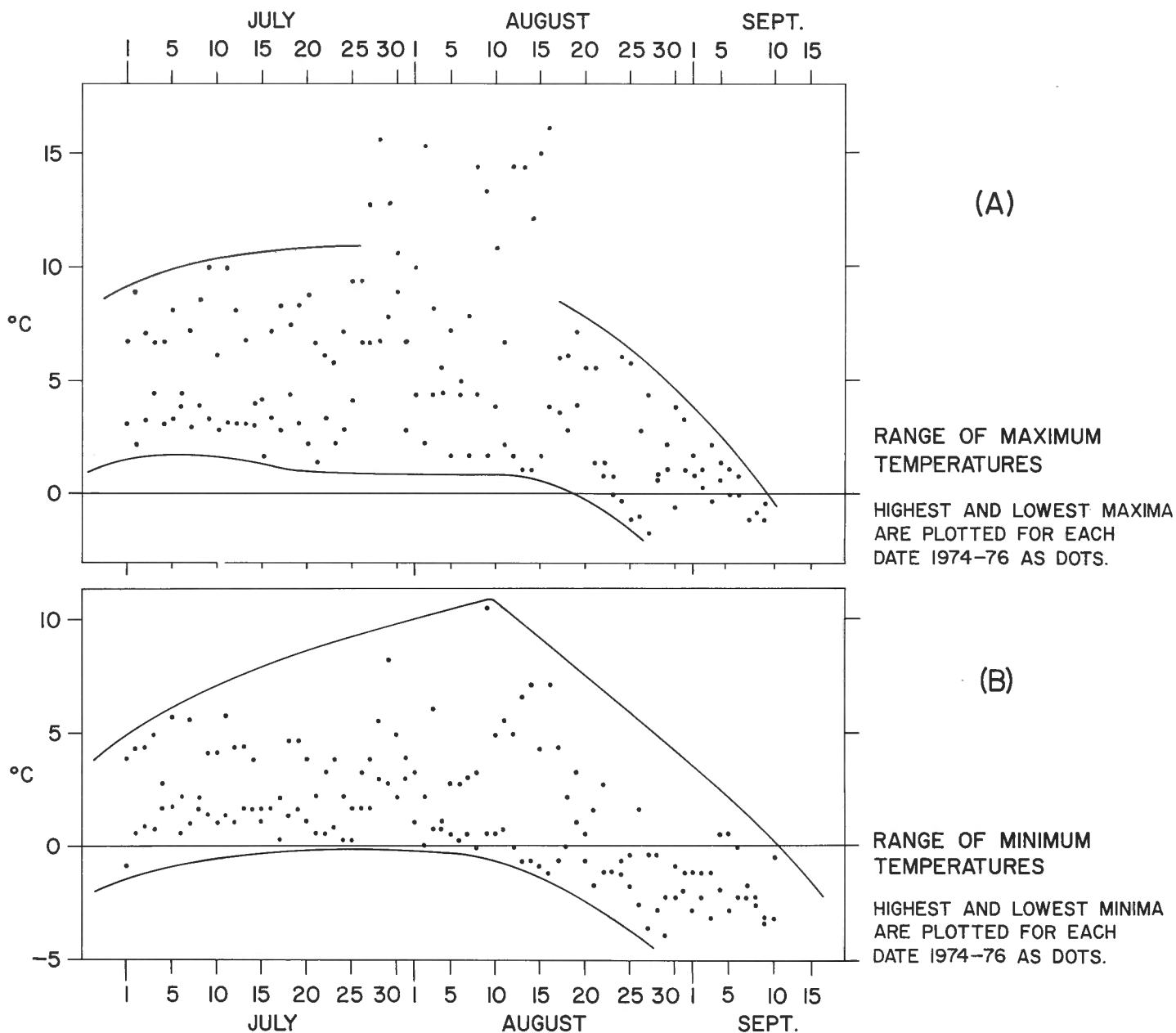


Figure 8.3. Maximum and minimum summer temperatures, Cunningham Inlet, Northwest Territories, 1974-1976.

Table 8.5
Summary of wind direction, Cunningham Inlet, NWT, 1974-1976

Year/Month	No. of Observations	N	NNE	NE	ENE	E	ESE	SE	SSE	S	SSW	SW	WSW	W	WNW	NW	NNW	Calm	Prevailing Wind
1974 July	124	12	1	1	1	1	1	3	7	4	4	11	24	28	28	13	10	3	WNW
August	124	9	1	2	1	3	6	3	4	10	4	8	15	23	17	12	5	5	WNW
September	52	6	3	8	4	-	-	-	1	-	-	-	1	6	9	10	2	2	Variable
% Frequency of observations		9.0	1.6	3.7	1.6	1.3	2.3	1.3	2.3	6.0	2.7	1.6	6.3	13.3	19.0	13.0	10.7	3.3	WNW
1975 July	124	10	5	3	1	3	-	-	2	11	-	3	1	21	24	29	7	4	NW
August	80	5	2	-	3	3	-	1	-	13	4	1	2	11	10	20	7	1	NW
% Frequency of observations		7.4	3.4	1.5	0.5	2.9	-	0.5	0.9	11.8	1.9	1.9	1.5	15.7	16.7	24.0	6.8	2.5	NW
1976 July	124	12	1	5	1	3	1	6	10	-	1	1	1	4	35	28	11	4	WNW
August	124	-	2	-	-	1	-	10	6	6	2	6	-	8	39	37	10	3	WNW
September	40	4	1	3	3	2	4	3	5	4	-	-	-	-	3	4	-	4	Variable
% Frequency of observations		5.6	1.4	2.8	1.4	1.7	2.9	3.1	8.7	3.5	1.0	2.4	0.3	4.2	26.7	23.9	7.3	3.8	WNW
Total number of observations		58	16	23	10	15	13	14	34	52	15	16	23	84	168	157	67	26	WNW
% Frequency of all observations (792) 1974-1976		7.3	2.0	2.9	1.3	1.9	1.6	1.8	4.3	6.6	1.9	2.0	2.9	10.6	21.2	19.8	8.4	3.3	WNW

winds of 20 mph or greater numbered 2 to 3 in July and August of 1974 and 1975 and numbered 10 in 1976. Calm conditions at Cunningham Inlet represent only 3 per cent of all observations. The average wind velocity, as a mean of the grouped data of 792 observations, was 9.7 mph.

Comparison of data from North Coast and Base Camp

Observations made in 1974 indicated that winds on the north coast were often much stronger than those recorded at base camp 1.4 km inland. To determine if there was a difference in velocity and if so, how much, anemometer readings were made at both locations in 1975 and 1976.

In 1975, 92 per cent of the winds were stronger at the coast; only on a few occasions were winds stronger at base camp, but the difference was less than 1 mph. The ratio of mean wind speed at the coast to that at base camp was 1.23. The differences in wind speed between the two localities were least on days of shifting winds and greatest during periods of strong winds blowing from one direction.

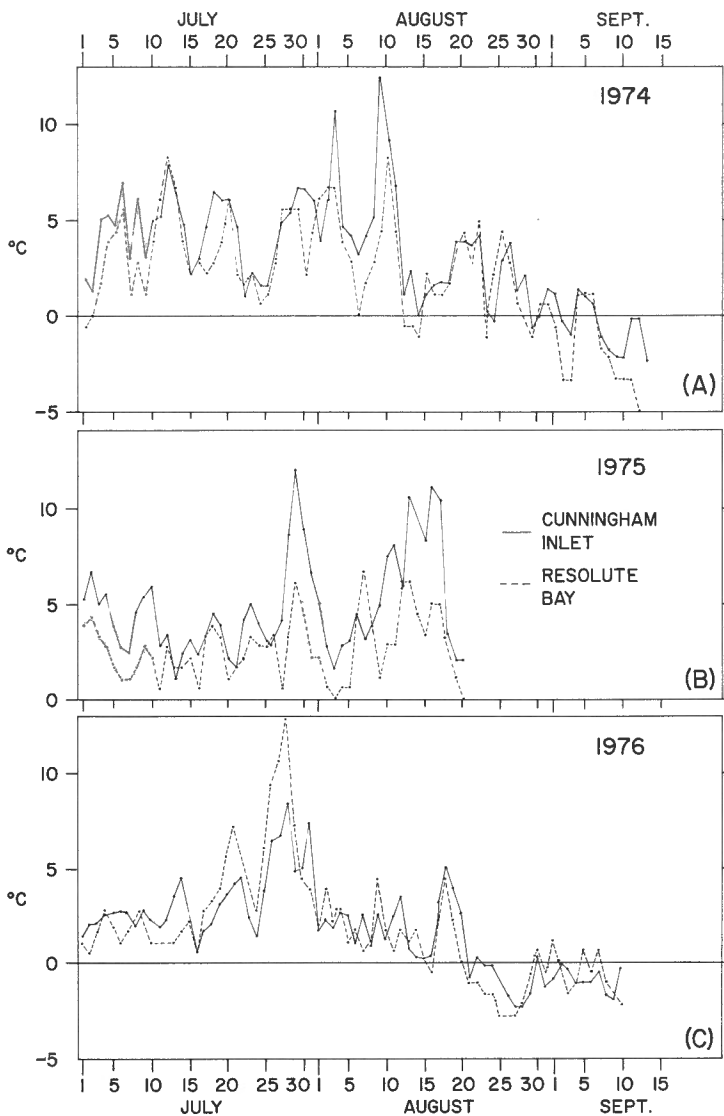


Figure 8.4. Mean daily air temperatures, at Cunningham Inlet and Resolute Bay, Northwest Territories, 1974-1976.

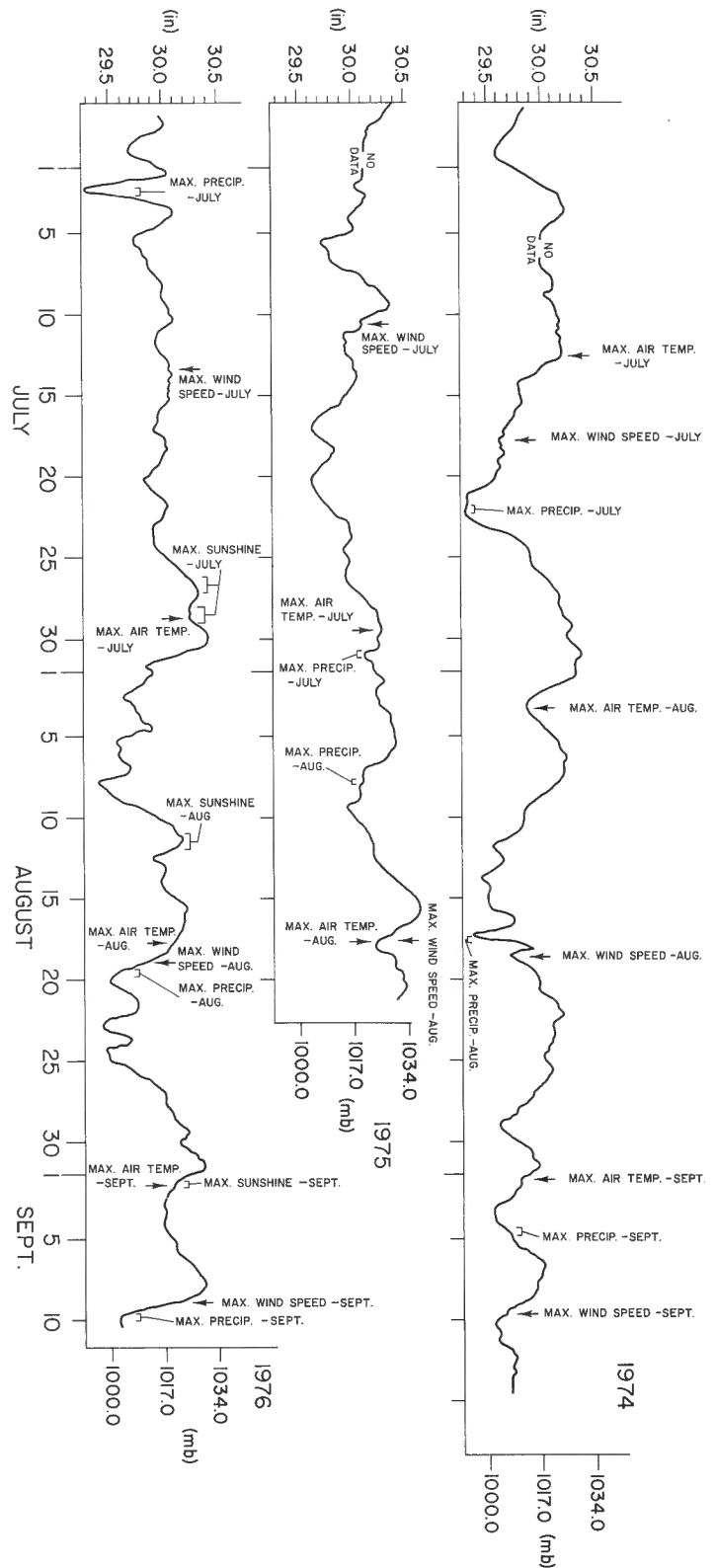


Figure 8.5. Barometric pressure and significant climatic occurrences, Cunningham Inlet, Northwest Territories, 1974-1976.

Table 8.6

Summary of wind velocity, Cunningham Inlet, NWT, 1974-1976

Year/Month	No. Observations	Velocity (mph) no. of occurrences				Monthly Mean Velocity
		Calm	1 - 12.9	13 - 19.9	20 - 39	
1974 July	124	3	97	27	3	9.2
August	124	5	100	17	2	7.9
September	52	2	34	13	3	9.7
% Frequency of observations		3.3	75.0	19.0	2.7	
1975 July	124	4	88	30	2	9.6
August	80	1	62	14	3	9.1
% Frequency of observations		2.4	73.6	21.6	2.4	
1976 July	124	3	90	21	10	9.6
August	124	4	49	62	9	13.4
September	40	4	24	8	3	8.9
% Frequency of observations		3.8	56.8	31.7	7.7	
Total number of observations (792)		26	538	192	35	
% Frequency of all observations 1974-76		3.3	68.0	24.3	4.4	

Table 8.7

Comparison of wind data for Resolute Bay and Cunningham Inlet, NWT, 1974-1976

Year/Month	Days of Available Data	Prevailing Wind Direction	Mean Monthly Velocity (mph)	Occurrence of Winds ≥ 20 mph				Maximum Hourly Velocity		
				N	NNW-W	NNE-E	Other	Velocity	Direction	Date
1974-July										
Cunningham Inlet	31	WNW	9.2	-	1	-	2	22.5	WSW	17
Resolute Bay	31	WNW	14.5	4	7	3	15	40.0	ESE	21
1974-August										
Cunningham Inlet	31	WNW	7.9	-	-	1	1	22.8	E	18
Resolute Bay	31	SE	14.2	1	2	14	9	45.0	ESE	19
1975-July										
Cunningham Inlet	31	NW	9.6	-	2	-	4	22.5	W	10
Resolute Bay	31	WNW	11.7	7	4	3	4	37.0	N	14
1975-August										
Cunningham Inlet	20	NW	9.1	-	2	-	5	23.9	SSW	17
Resolute Bay	20	SE	11.2	-	3	2	9	31.0	ESE	11
1976-July										
Cunningham Inlet	31	WNW	9.6	-	8	-	3	32.8	WNW	13
Resolute Bay	31	N	13.2	7	6	10	4	49.0	E	02
1976-August										
Cunningham Inlet	31	WNW	13.4	-	11	-	4	28.8	SSE	18
Resolute Bay	31	WNW	16.1	13	6	10	4	47.0	NNW	03

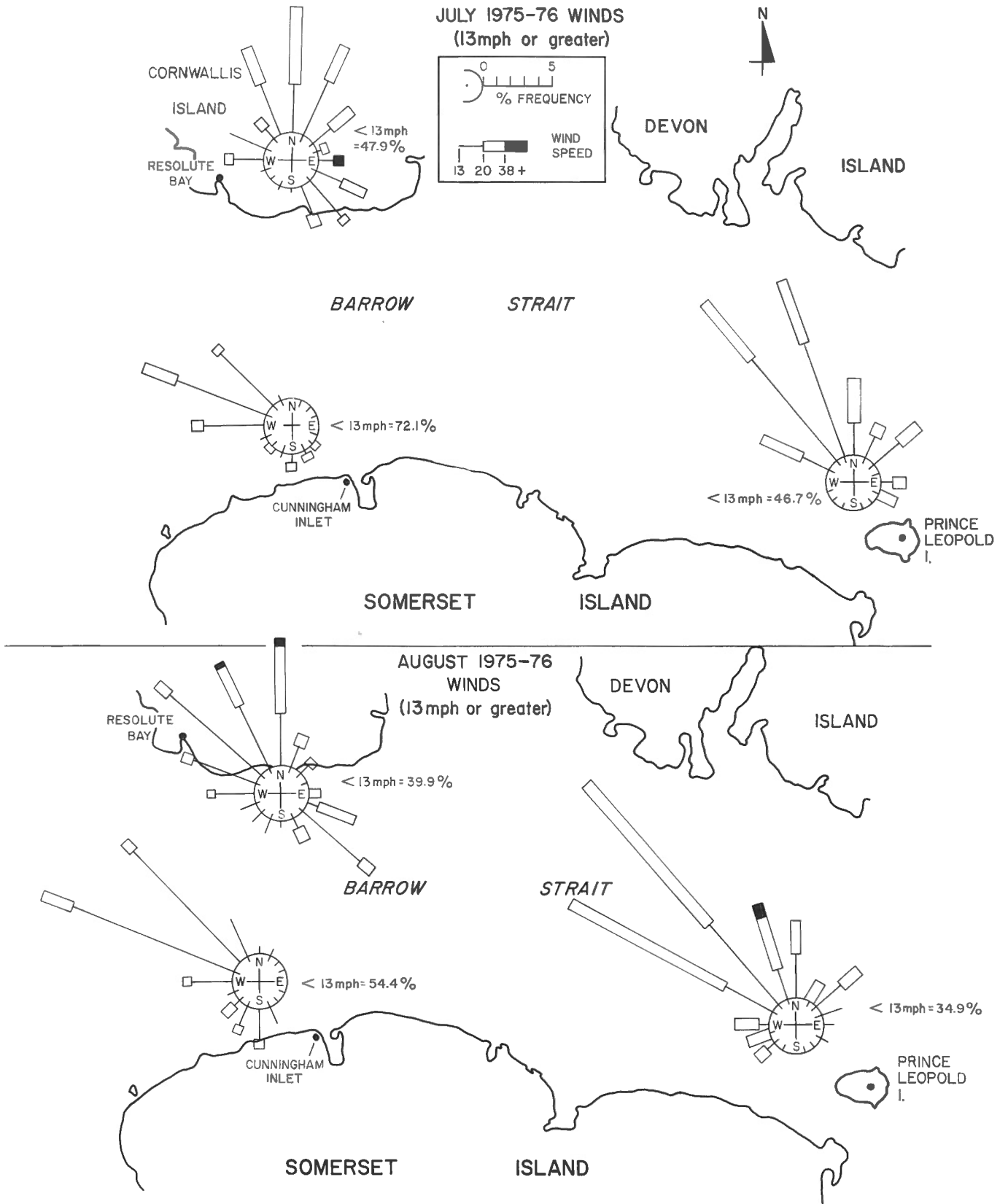


Figure 8.6. Wind rose diagrams for July and August 1975 and 1976 for three stations on Barrow Strait.

In 1976 only 66 per cent of the winds were stronger at the coast than at base camp. Furthermore wind direction differed at the two sites on two occasions, but these occurred during winds of less than 3 mph; generally wind direction seldom changed within short distances inland from the coast.

Using all the wind data collected for 1975 and 1976, the ratio of mean wind speed at the coast to that at camp was 1.10. For winds less than 20 mph the ratio was 1.08; and for winds of 20 mph or greater from the north to west direction the ratio was 1.18. Winds blowing at more than 20 mph from the south were slightly stronger at base camp than on the coast.

It is evident that even though winds are slightly stronger on the coast, the difference is only significant during periods of strong winds at which time winds on the coast could be calculated from the base camp wind data by multiplying by a constant of 1.18 to 1.23.

Comparison of data from Cunningham Inlet and Resolute Bay

In 1974 wind speeds, on average, were 5.8 mph greater at Resolute Bay than at Cunningham Inlet, whereas in 1975 and 1976 the winds were only 2.6 mph stronger at Resolute Bay. The larger difference in wind speed during 1974 is due to the absence of wind data from the north coast of Somerset Island, which was incorporated into the calculations for 1975 and 1976 for Cunningham Inlet. The number of occurrences of winds more than 20 mph (Table 8.7) was greater at Resolute Bay, and the maximum wind speed there each summer, except in 1975, was greater than 39 mph (Table 8.7). Some of the high winds recorded at Resolute Bay, however, are due to local conditions. Only in August 1974 did maximum wind velocity and same wind direction occur during the same storm at both stations, otherwise maximum reported winds at both stations occurred on different dates and from different directions. An examination of prevailing monthly wind direction indicates relatively similar winds from the west-northwest to northwest at both places in July but considerable differences exist for August. In August 1974 and 1975 winds were from the northwest quadrant at Cunningham Inlet and from the southeast at Resolute Bay. Wind rose diagrams for July and August 1975 and 1976 were drawn based on wind observations from three stations along Barrow Strait in order to illustrate the summer wind pattern (Fig. 8.6). The third station monitored was situated on Prince Leopold Island at approximately 250 m elevation (Nettleship, pers. comm., 1976); therefore the wind speeds are stronger than would be experienced at sea level. It is evident that of all the climatic parameters monitored at Cunningham Inlet and Resolute Bay, wind characteristics differed the most.

Barometric Pressure

A barograph was used during the three seasons to measure tendencies in air pressure and to monitor pressure systems moving through the study area and their relationship to storms experienced along the coast. The barographs used were not calibrated with barographs at the weather station in Resolute Bay, hence absolute comparisons cannot be made. The resultant barometric data for the three summers are shown in Figure 8.5 together with other related climatic occurrences.

Summary and Conclusions

Based on information collected over three summers some generalizations can be made about the climate at Cunningham Inlet. Furthermore, it is now possible to comment on the usefulness of Resolute Bay records in describing the climate on northern Somerset Island.

Summer air temperatures at Cunningham Inlet ranged from -3.9° to 16.1°C, with a mean of 3° to 4°C. The

warmest period each summer appears to occur in the last week of July or the first week of August. More than ten days of fog or precipitation occurred each month, and the average summer precipitation was 29.6 mm. The coolest, wettest summer during the period studied was in 1976, and the warmest was in 1975. On northern Somerset Island spring melt did not occur until late June to early July in 1974 and 1976, but in 1975 the rivers had peaked and the snow had melted by mid to late June.

Slightly more than 40 per cent of all winds recorded each summer at Cunningham Inlet blew from the northwest quadrant. No winds were recorded here over 33 mph, and 50 per cent to 75 per cent of all winds were less than 13 mph. Although winds more than 20 mph most frequently were from the west-northwest, it was found that these strong winds could originate from several directions. Calm periods were rare at Cunningham Inlet, occurring only 3.3 per cent of the time.

In the past, climatic records from Resolute Bay have been used by researchers to determine the climate on adjacent islands including northern Somerset Island. Warming and cooling trends in air temperature are very similar at both stations; therefore, even though temperatures averaged 1° to 2°C higher on Somerset Island, air temperature data from Resolute Bay in most cases would characterize the temperature at Cunningham Inlet. Precipitation usually falls at both stations on the same date, but the amounts are different and the date of maximum precipitation rarely coincides.

At Resolute Bay and Cunningham Inlet, wind direction is similar in July but not in August. This is not necessarily a monthly phenomenon but is thought to be related to sea ice cover and to air pressure systems over Barrow Strait. Wind speeds are much greater at Resolute Bay during the entire summer. Whereas winds over 33 mph were not observed at Cunningham Inlet (Table 8.6) winds stronger than this were experienced an average of 5 times at Resolute Bay during the summers of 1974-76 and each of the previous five summers.

It is suggested, therefore, that the above differences in wind and precipitation data should be taken into account when applying data from Resolute Bay to northern Somerset Island.

Acknowledgments

The author is indebted to several persons including R. Wahlgren, R. Featherstone, and S. Morison who aided in the collection of field data. Polar Continental Shelf provided logistics and some meteorological instruments during the three seasons. Climatic records for Resolute Bay, Northwest Territories for 1972-1976 were provided by the Meteorological Applications Branch of Atmospheric Environment Service, Toronto. Appreciation is also extended to B. Taylor-Alt for comments on the paper.

References

- Environment Canada
1974: Monthly record, meteorological observations in Canada, June to September; Atmos. Environ. Serv., Environ. Can., 4 v., 180 p.
- 1975: Monthly record, meteorological observations in Canada, June to September; Atmos. Environ. Serv., Environ. Can., 4 v., 180 p.
- Fisheries and Environment Canada
1976: Monthly record, meteorological observations in Canada, June to September; Atmos. Environ. Serv., Fish. Environ. Can., 4 v., 180 p.

EMR Research Agreement 1135-D13-4-190/73

D.C. Ford¹ and H.P. Schwarcz²
Terrain Sciences Division

The dating and stable isotopic analysis of speleothem has been continued to extend our record of temperature and glacial activity in Canada during the past 350 000 years. Recent work on this project was focused on Vancouver Island where an extensive series of caves was sampled for speleothem. Paleomagnetic studies of speleothem from Vancouver Island and the Rocky Mountains have been initiated. Both $^{230}\text{Th}/^{234}\text{U}$ and $^{231}\text{Pa}/^{235}\text{U}$ dating are being applied to speleothem samples through alpha-particle spectrometry. Analyses of stable isotope profiles were made from the Vancouver Island suite of samples. Fluid inclusion studies of speleothem have begun using the direct analysis of $^{18}\text{O}/^{16}\text{O}$ ratios through fluorination of water liberated by crushing of speleothem. An attempt is being made to improve the uranium series dating of molluscs, through beneficiation of the molluscan tests.

Results from some of these investigations recently have been published (e.g., Ford et al., 1976; Harmon et al., in press; Schwarcz et al., 1976).

Results

Vancouver Island

Two collections of speleothem were made from caves on Vancouver Island. The $^{230}\text{Th}/^{234}\text{U}$ dating technique was used to date samples from Euclataws, Main, and Lower Main caves (Horne Lake Provincial Park) and from Cascade Cave (near Port Alberni). Analysis of the first collection (made in April 1975) is now complete, and work is approximately 70 per cent completed in dating the October 1976 collection.

Stable isotope analysis ($^{18}\text{O}/^{16}\text{O}$ and $^{13}\text{C}/^{12}\text{C}$) of dated speleothems for equilibrium deposition began in late 1976. Core samples have been taken for fluid inclusion analysis in order to derive absolute temperatures of deposition, but they will not be processed until the speleothems showing isotopic equilibrium deposition are analyzed.

A full report on the genesis and development of the Euclataws Main Cave system recently has been submitted to the Parks Branch, British Columbia (Ford, 1976), and a further report on the Riverbend-Lower Main System is in preparation.

Horne Lake Provincial Park Caves

Samples taken from Euclataws, Main, and Lower Main caves all show extremely low uranium concentrations (≤ 0.03 ppm). These values are some of the lowest ever encountered in speleothem work. At this level, interferences from reagent blank concentrations, memory effects, and background levels become very important, thus imposing large error limits on computed ages. Examples of these ages are given in Table 9.1, although quoted errors are based on counting statistics only. Samples 75100-2 and -3 illustrate this problem by the age inversion based on the stratigraphy of the stalagmite. Some speleothem portions (75100-1, 75102-1, 75103C-1) show evidence of uranium loss because $^{230}\text{Th}/^{234}\text{U}$ ratios are well in excess of unity. This loss is probably due to recrystallization from multicrystalline calcite to a single-crystal form as is clearly seen in sample 75103C-1. Recent acquisition of new low-background detectors, use of specially purified reagents, and more precise measurement of reagent

blank activities will permit reanalysis of suitable samples in an attempt to determine accurate ages. Speleothems collected from Main and Lower Main caves were found to be generally porous and leached of uranium. One sample, 75151-1, appears to have been leached during formation. It is anticipated that samples from Riverbend Cave similarly will be low in uranium because the cave lies near Euclataws.

Cascade Cave, Port Alberni

More success has been had in dating speleothems from Cascade Cave near the west coast of the island. About ten times more uranium occurs in most samples, and radiometric ages show excellent agreement, both in terms of the internal stratigraphy of one specimen and between samples. A well defined growth period for four speleothems is seen to have commenced between 53 000 and 58 000 years B.P., terminating in some cases as late as 33 000 years B.P. These dates are in good agreement with the apparent timing of a mid-Wisconsinan interstadial at approximately 60 000 to 45 000 years B.P., indicated by stage 3 in the foraminiferal isotope record (Shackleton and Opdyke, 1973) and presumably correlative with the Port Talbot interstadial (Terasmae and Dreimanis, 1976). This adds to the existing evidence of full glacial conditions both before and after this period, because speleothem growth cannot occur when groundwater movement is terminated due to deep permafrost. The samples show no evidence of surficial re-solution, so the caves probably remained vadose and largely devoid of percolation water during these periods. Because no speleothem has yet been found dating from the Sangamon interglacial (95 000 to 125 000 years B.P.; Shackleton and Opdyke, 1973), it is tentatively proposed that this represents the principal period of solutional genesis of Cascade Cave when calcite deposits, if formed, were easily removed or buried by river and sediment action.

Analysis of growth layers in two speleothems from Cascade Cave (samples 75123, 75125) has shown sample 75125 to be unsuitable for paleotemperature studies due to ^{18}O calcite enrichment by evaporation of water and to ^{13}C calcite enrichment by rapid degassing of CO_2 from the drip water. Both trends indicate nonequilibrium deposition. Preliminary data from growth layers of sample 75123 suggest equilibrium deposition, and a $\sigma^{18}\text{O}$ profile of the sample will be determined shortly. Sample 75125 was collected from the wall of a fossil stream passage, a site where draughts are present now and probably were present during formation. Sample 75123, on the other hand, was collected from a restricted alcove adjacent to a well aerated chamber and so may be more suitable for isotopic studies.

Oxygen Isotopic Analysis of Fluid Inclusions

Work is continuing on the analysis of inclusions of water trapped in speleothem. These inclusions represent the drip or seepage water from which the speleothem grew. Isotopic analysis of this water, together with analysis of the enclosing calcite, will allow determination of the temperature of calcite formation using the calcite-water geothermometer. Until now, the waters have been analyzed only for their deuterium/hydrogen ratios, and the $^{18}\text{O}/^{16}\text{O}$ ratios have been inferred from the known relation between oxygen and hydrogen isotope ratios for meteoric waters. However, an

¹ Department of Geography, McMaster University, Hamilton, Ontario.

² Department of Geology, McMaster University, Hamilton, Ontario.

Table 9.1

Vancouver Island Speleothems

Sample No.	Cave	Height above base (cm)	U (ppm)	Yields %		$\frac{^{234}\text{U}}{^{238}\text{U}}$	$\frac{^{230}\text{Th}}{^{232}\text{Th}}$	$\frac{^{230}\text{Th}}{^{234}\text{U}}$	AGE $\times 10^3$ years B.P.	COMMENTS
				U	Th					
75100-1	Euclataws	0-4	0.01	68	34	1.434	39	1.362	>300	Preferential leaching of U
75100-3	"	4-7	0.01	47	53	2.053	>1000	0.046	5.1 \pm 2.4	Dubious - low U
75100-2	"	11-12	0.02	33	25	1.100	2.7	0.313	40.5 \pm 11.2	"
75101-6	"	-	0.03	35	61	1.241	>1000	0.143	16.6 \pm 5.8	"
75102-1	"	composite	0.01	38	14	2.030	14.4	5.166	>300	Stalactite - U leached
75103C-1	"	35-38	0.01	66	29	1.023	35.1	>10	>300	U leached
75103A-3	"	2-5	0.01	35	55	3.286	>1000	0.278	34.0 \pm 8.9	Dubious - low U
76002-1	"	flowstone	0.01	34	14	1.571	3.0	0.330	42.4 \pm 9.6	
75123-1	Cascade	0-0.5 (base)	0.15	53	64	1.531	29.4	0.411	55.5 \pm 2.9	
75123-2A	"	6-9 (top)	0.09	46	67	1.829	11.6	0.362	47.0 \pm 4.2	
75125-3	"	3-5 (top)	0.25	58	12	1.957	3.6	0.274	33.8 \pm 3.2	
75125-4	"	1-3 (mid)	0.39	35	8	1.224	1.3	0.338	44.1 \pm 9.8	
75125-6	"	0-1 (base)	0.15	62	18	1.817	20.8	0.383	50.3 \pm 5.4	
76013C-1	"	(subbase)	0.11	28	14	1.638	10.7	0.399	53.2 \pm 5.9	underlies 75125
75126-1	"	0-3 (base)	0.09	51	50	1.578	4.5	0.100	13.0 \pm 1.3	
75126-2	"	15-20 (top)	0.07	63	44	1.713	2.7	0.110	12.5 \pm 2.0	
75127-1	"	0-2 (base)	0.11	46	20	1.716	7.0	0.135	15.5 \pm 2.5	
75127-2	"	2-4 (mid)	0.09	50	21	1.651	3.4	0.145	16.9 \pm 3.1	
75151-1	Main	0-2 (base)	0.06	47	9	1.150	5.8	0.825	175.9 \pm 91.1	modern speleothem (U leaching while forming?)
76008-1	Cascade	0-1 (base?)	0.08	66	49	1.835	59.2	0.429	57.9 \pm 4.1	
76008-2	"	9-10 (top?)	0.06	37	39	1.629	5.5	0.387	51.3 \pm 5.0	portions of loose flow-stone fragments growth direction uncertain
76010-2	"	10-11 (mid?)	0.07	40	24	1.741	12.6	0.434	59.0 \pm 5.1	
76011-1	"	0-2 (base)	0.08	36	21	1.618	16.9	0.425	57.7 \pm 4.7	
76011-2	"	5-7 (top)	0.08	35	44	1.400	4.0	0.439	60.7 \pm 5.9	
76012-1	"	0-2 (base)	0.18	49	35	1.938	4.6	0.181	21.2 \pm 1.4	
76012-2	"	12-15 (top)	0.16	42	60	1.969	2.2	0.151	17.5 \pm 1.2	

attempt is being made now to determine the oxygen isotopic compositions directly by reacting the waters with bromine pentafluoride to liberate oxygen, converting the oxygen to CO₂, and analyzing on a mass spectrometer. This procedure permits the analysis of as little as 1 mg of water; this is the amount of water liberated by the crushing of about 1 g of typical speleothem. During the past year, the writers have been experimenting with the analysis procedure and adapting it to specific needs and are now at the point of being able to make routine speleothem analyses.

Caves of the Western Cordillera

In co-operation with Dr. R.S. Harmon a synthesis of dates on speleothems formed in caves along the western North American Cordillera over the past 350 000 years has been completed. Periods of intense glaciation are recognizable by the absence of appreciable deposition of travertine and hiatuses in the growth of individual speleothems. These interruptions presumably are due to freezing of water sources and to lowering of biotic activity in the overlying soil. From this synthesis periods of cool climate can be recognized at the following intervals: (Ka = 1000 years B.P.) 345-320 Ka, 275-240 Ka, 180-155 Ka, and 90-20 Ka. The intensity of the warm intervals, as inferred from the aggregate frequency of speleothem growth during the interval, appears to have decreased from 350 000 years B.P. to the present.

Paleomagnetic Studies of Speleothem

Unoriented, trial samples of flowstone from various localities were cut into one inch cubes and spun on a PAR magnetometer at the University of Toronto. Low, but measurable intensities were observed (about 10^{-7} oe g⁻¹). Subsequent natural remanent magnetism studies on oriented samples from caves in the Rockies have shown good directional groupings for coeval samples ($\alpha_{95} < 10^\circ$ for ten specimens), despite low intensities. This work was carried out on a cryogenic magnetometer, also at the University of Toronto. So far no stability measurements have been made, but the close site and time groupings are encouraging. Additional material is being collected, oriented in the field by means of a compass-aligned tripod (for flowstones) or a special aluminum plate (for stalagmites). Dating of the speleothems will be done by Th/U and Pa/U methods, as previously described.

Mollusc Dating

A sample of fossil marine pelecypod, *Mya truncata*, from a raised marine deposit on Ellesmere Island was submitted to our laboratory by W. Blake, Jr. of Terrain Sciences Division. Dating was attempted, and an apparent age of 12 000 years B.P. was obtained. This result is much younger than a series of ¹⁴C ages from the same deposit, the youngest of which was 27 700 ± 460 years (Blake, 1975, 1976). In the light of uncertainties in the dating of fossil molluscs (see Kaufmann et al., 1971) it is clear that the Th/U

date is incorrect. Typically Th/U ages on molluscs are younger than ¹⁴C ages due to postmortem uptake of uranium from groundwater. The high ²³⁴U/²³⁸U ratio (1.63) strongly suggests some uptake of continent-derived uranium (because seawater uranium has a ratio of 1.15). At present experimentation is being done on methods of separating out of the whole mollusc a pure fraction of primary, unaltered aragonite, free of any postmortem contaminant.

References

- Blake, W., Jr.
1975: Radiocarbon age determinations and postglacial emergence at Cape Storm, southern Ellesmere Island, Arctic Canada; Geogr. Ann., Ser. A, v. 57, p. 1-71.
1976: Quaternary geochronology, Arctic Islands; in Report of Activities, Part A, Geol. Surv. Can., Paper 76-1A, p. 259-264.
- Ford, D.C.
1976: The Euclataws-Main Cave systems of Horne Lake Cave Provincial Park, Vancouver Island; rep. to Parks Branch, Govt. British Columbia, 25 p.
- Ford, D.C., Harmon, R.S., Schwarcz, H.P., Wigley, T.M.L., and Thompson, P.
1976: Geohydrologic and thermometric observations in the vicinity of the Columbia Icefields, Alberta and British Columbia, Canada; J. Glaciol., v. 16, p. 219-230.
- Harmon, R.S., Thompson, P., Schwarcz, H.P., and Ford, D.C.
Late Pleistocene paleoclimates of North America as inferred from isotope studies of speleothems; Quat. Res. (in press).
- Kaufmann, A., Broecker, W.S., Ku, T.-L., and Thurber, D.L.
1971: The status of U-series methods of mollusk dating; Geochim. Cosmochim. Acta, v. 35, p. 1155-1183.
- Schwarcz, H.P., Harmon, R.S., Thompson, P., and Ford, D.C.
1976: Stable isotope studies of fluid inclusions in speleothems and their paleoclimatic significance; Geochim. Cosmochim. Acta, v. 40, p. 657-665.
- Shackleton, N.J. and Opdyke, N.
1973: Oxygen isotope and paleomagnetic stratigraphy of equatorial Pacific core V23-238: Oxygen isotope temperatures and ice volumes on 10⁵ year scale; Quat. Res., v. 3, p. 39-55.
- Terasmae, J. and Dreimanis, A.
1976: Quaternary stratigraphy of southern Ontario; in Quaternary Stratigraphy of North America, ed. W.C. Mahaney; Dowden, Hutchinson and Ross, Stroudsburg, p. 51-63.

EMR Research Agreement 1135-D13-4-145/76

J. Brian Bird¹
Terrain Sciences Division

A brief visit was made in 1975 to the Kivitoo Peninsula, on the east coast of Baffin Island, (Fig. 10.1), to examine landform modification under periglacial conditions. Field studies were continued in summer 1976 and were concentrated on the geomorphic processes active along the coast and on the role of snow in terrain development.

Shoreline Investigations

The dynamics and rates of shoreline modification in arctic environments are inadequately known both in construction of theoretical models and in their application to resource development. In Canada there is a fundamental contrast between western Arctic shores, where massive ground ice and fine unconsolidated sediments are major components of marine cliffs and depositional beach forms are widespread, and the eastern Arctic, where cliffs and talus slopes are characteristic and coarse sediments dominate the beaches. Special elements in coastal processes in the eastern Arctic include the presence of an ice foot, low energy wave conditions for a large part of the year due to sea ice, and great seasonal variability of the shore environment depending on the distribution of sea ice (McCann, 1973).

The coasts of the eastern Arctic adjacent to the Labrador Sea, Davis Strait, and Baffin Bay are developed in rocks of the Canadian Shield and are dominated by high cliffs and rock forelands; coastal lowlands are few. A conspicuous exception to the general pattern is on either side of Home Bay, Baffin Island, where low forelands, separated by fiord troughs, are covered with marine, glacial, and fluvio-glacial deposits (Andrews et al., 1975; Feyling-Hanssen, 1976).



Figure 10.1. Location map.

¹ Dept. of Geography, McGill University, 805 Sherbrooke St. W., Montreal, P.Q. H3A 2K6



Figure 10.2. Beach and gullied cliff, Kivitoo Peninsula, August 1976. A small fan, developed from a mudflow on the cliff face, temporarily buries part of the beach.

During low sea level phases in the late Quaternary, the forelands apparently extended eastwards as part of the relatively wide, and today, shallow, continental shelf (Løken and Hodgson, 1971) and to some degree were glacier free. The forelands are surrounded in part by cliffs eroded in unconsolidated sediments. The cliffs at present are retreating rapidly as indicated (in the case of the Kivitoo area) by the destruction of prehistoric Eskimo house sites.

Coastal Morphology – The Cliffs

Kivitoo Peninsula, the foreland on the southeast side of Home Bay (Fig. 10.1), is ringed by cliffs from near the former Kivitoo settlement at the entrance of Kagitokuluk Fiord for 27 km to Narpaing Fiord. The cliffs vary in height, increasing from 5 to 8 m in the vicinity of Kangeeak Point to more than 20 m at the northwest corner of the peninsula. They are developed in a variety of unconsolidated materials including sorted sands, silts and clays, pebbles, cobbles, and boulders. Bedding commonly is obscured along the cliff face; where visible it is generally horizontal with local tilting and minor faulting and occasional conspicuous unconformities. Andrews et al. (1975) have identified several units in the sediments and interpreted them as a succession of glacial (till) and elevated interglacial/interstadial marine beds dating back to the last interglacial or earlier. No massive ground ice, either in the form of wedges or horizontal sheets, has been observed in the cliffs.

In detail, the morphology of the cliff face is highly varied. At some localities, usually where the cliff is formed in mixed, coarse sediments with a sandy matrix, the face is a single linear slope, from crest to beach, unbroken by gullies

or slump features and with an angle of 38 to 44 degrees. At other localities the slope angle is more variable (range 30 to more than 65 degrees, major grouping ~39 degrees). The face morphology is less uniform, and it is broken by gullies and earthflow features. The base of the cliff is steepened in places but is nowhere vertical or (wave) notched. In some areas gullies are spaced uniformly along the cliff and apparently are developed by moisture from the cliff face. Elsewhere gullies are associated with surface fissures developed in an elevated marine terrace to the rear of the cliff. The fissures, which are 10 to 50 cm deep, extend to the crest of the cliff where a gully starts; in one sector of 13 consecutive gullies, 12 were linked to fissures. Gully erosion results from water led off the terrace in the fissure during the spring and from large boulders that are concentrated in the fissures and that slide down the cliff face as retreat occurs. Moisture seepage in late summer along the cliff face also is associated with earthflows, mudflows, and rivulet erosion.

Markers and cliff crest lines, surveyed in 1976, eventually will enable the rate of cliff retreat to be determined; preliminary observations indicate retreat of approximately 0.5 to 1.0 m per year in the most vulnerable sectors by a combination of 1) concentrated debris slides initiated by falling boulders; 2) sheet debris slides where desiccation and removal of the sand matrix by gravity and wind leaves larger particles unsupported; and 3) earthflows and mudflows located in gullies.

The active transfer season for debris across the cliff face reaches a maximum of about 125 days in the north and northwest of the peninsula. Snowbanks bury the cliff face for much of the summer in the eastern parts of the peninsula; in the vicinity of Kangeeak Point some snowbanks are quasi-permanent. The distribution of late-surviving snowbanks is associated with extreme shallow offshore conditions; in these cases the banks are resting on an ice foot which is not easily removed by wave action. Further examination will reveal the relationship of the snow to the cliff and particularly whether they are frozen together at the interface. Northeast of the former Kivitoo settlement, where late snowbanks are widespread, melting snow saturates the cliff face as the ground thaws, and small mudflows are common in the latter part of the summer.

The Beach

A beach separates the base of the cliff from the sea, and it is unusual for waves to reach the foot of the cliff. Beaches have an average width above the high tide mark of 10 m and a variable slope averaging 5 degrees; the normal tidal range at spring is 1.5 m. The composition of the beach differs from sector to sector with a uniform grade size predominating at some sites and a mixture at others. The dominant beach materials are commonly cobbles (subrounded to rounded) with small boulders (subrounded) and a few large subangular boulders (more than 1.5 m diameter) (Fig. 10.2). Sand is rarely present on the beach although it forms a high proportion of the cliff material. Inspection offshore shows that sand is widely distributed 1 m and more below low water (or 1.75 m below sea level), and therefore it must be transferred rapidly across the beach from the cliff to deeper water.

The beach profile is normally straight with a berm restricted to the widest beaches (at the northwest end) and to wide gaps (valleys) in the cliffs. At a few points, double (stepped) berms were observed suggesting that the profile may be in a dynamic state and is combed down and then built up at different periods. Except for two small fans no unreworked cliff material was found on the beaches below the berm.

There is little direct evidence in the beach profile of the action of sea ice; apart from the morphologically graded nature of the profile and the rounding of the finer material, there is little evidence of sediment transfer, especially in the form of longshore drifting. Large boulders accumulate at or just below low water, a process that is suggestive of the growth of incipient boulder barricades; large boulders also are concentrated at the headlands. It was not evident, however, to what degree headlands are preserved by the presence of boulders offshore, providing protection against ice and wave action.

It is suggested (Fig. 10.3) that longshore movement is minimal, and it follows that the dynamic transfer of debris off the beach, enabling cliff retreat to continue at a high rate, must be found in movement of sediments to inshore and offshore zones.

Wave Action on the Beach

Two processes associated with waves and sea ice are responsible for redistributing sediments on the beach. Wave action clearly is restricted by sea ice conditions. Fast ice and close pack ice are present until late June and do not permit inshore wave activity. Conditions in the open sea period, which prevail from then until late October, are highly variable from year to year. When heavy pack ice is present throughout the summer (e.g., 1973), it is unlikely that any significant wave action occurs on the outer coast of the Kivitoo Peninsula. In contrast, during a season in which there is little pack ice either inshore or in Davis Strait (e.g., 1975), long swell waves generated in the open ocean arrive for days at a time, and beach material is in constant motion in the surf. Even under these conditions much of the wave energy is dissipated in the shallow offshore waters before reaching the beach. This is particularly evident in the vicinity of Kangeak Point where the water may be less than 5 m deep for more than 1 km offshore.

A 'normal' season falls between these extremes and resembles the 1976 season when pack ice was present off the coast throughout July and August. For the first part of the summer the sea was open, and ice remained off the coast giving clear water near the beach; however, there was little wave action. In the second month the ice cover was up to 4/10 within 5 km of the shore, and waves were effectively dampened.

The roundness of cobbles and fine beach material may be explained by their original roundness in the cliff beds and by the action of surf spread over a long period. The transfer of cliff debris from the rear of the beach is explained less easily, as grading to the local profile occurs for all material except the largest boulders within the period of an annual cycle. To analyze this, conditions prior to breakup, and particularly the role of the ice foot, will have to be examined.

The peninsula is drained by several streams which rise in the Kivitoo Hills and flow to the northeast. For the upper and middle part of their courses the streams flow in shallow

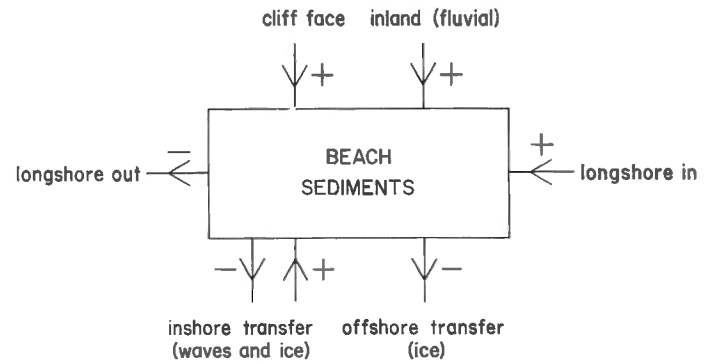


Figure 10.3. A model of beach sediment transfer.

depressions and shallow channels on the surface of the plateau. Near the sea the streams become entrenched into the foreland, the valley sides are steep (more than 25 degrees), and the channels are choked with coarse sediment including large boulders. Although the watersheds are small (the largest is 38 km² and the majority are less than 10 km²), stream competency and capacity are temporarily high during the spring runoff when the snowpack over the entire foreland melts essentially at the same time. The stream load is derived primarily from the sides of the lower, entrenched valleys where the erosional processes closely resemble those acting on the marine cliffs. The coarse component of the load that reaches the sea is deposited as an underwater boulder delta off the stream mouth. The deltas are small in terms of the material eroded to form the valleys, and it is assumed that the finer material becomes incorporated in the sea bed directly offshore.

It is proposed in continuing studies to concentrate on the properties of the cliff sediments, the relationship between permafrost and soil moisture distribution near the cliff face, the initial protective and subsequent sediment transport role of the ice foot, and the frequency of exceptional environmental events especially the incidence of storms on open beaches.

References

- Andrews, J.T., Szabo, B.J., and Isherwood, W.
1975: Multiple tills, radiometric ages, and assessment of the Wisconsin glaciation in eastern Baffin Island, NWT, Canada: A progress report; *Arct. Alp. Res.*, v. 7, p. 39-59.
- Feyling-Hanssen, R.W.
1976: The stratigraphy of the Quaternary Clyde Foreland formation, Baffin Island, illustrated by the distribution of benthic foraminifera; *Boreas*, v. 5, p. 77-94.
- Løken, O.H. and Hodgson, D.A.
1971: On the submarine geomorphology along the east coast of Baffin Island; *Can. J. Earth Sci.*, v. 8, p. 185-195.
- McCann, S.B.
1973: Beach processes in an arctic environment; in *Coastal Geomorphology*, ed. D.R. Coates; Binghamton, N.Y., 404 p.

Project 730092

Frances J.E. Wagner
Atlantic Geoscience Centre, Dartmouth

In May 1974, during the cruise of *C.S.S. Dawson*, samples were collected from 62 stations in Chaleur Bay. Sediments were obtained using standard Shipek and Van Veen grab samplers (Schafer et al., 1974), and the material was examined for its faunal content. This paper presents some observations on the relationship of molluscan species and assemblages to measured environmental parameters.

Molluscs were present at 56 of the 62 stations at depths ranging between 17 and 110 m (Fig. 11.1). The bottom sediment types and their areal and depth distribution in this part of the bay have been detailed by Schafer (1976, p. 19-23), and watermass distributions may be inferred from Loring and Nota (1973) and Schafer and Cole (in press).

Fifty-one species of molluscs have been identified, comprising 33 pelecypods and 18 gastropods. In several instances specimens could be identified to the generic level only, and there were frequent cases where fragments were recovered that were unidentifiable. Total mollusc data were analyzed using Q-mode cluster analysis and the Jaccard's coefficient of association (Bonham-Carter, 1967) based on the presence or absence of species in each sample. This method classifies the samples into groups based on the similarity of their species composition. Twenty-four species were used in the analysis, these being the species that were present at three or more stations. This selection criterion removed seven stations and 27 rare forms from consideration so that the analysis performed was based on 24 species from 49 stations. The samples were clustered by the unweighted pair-group method (Sokal and Sneath, 1963). At about the 0.05 level of similarity two major groups are evident, each of which can be divided into subgroups. The subgroups are designated Biotope 1A and 1B, and 2A and 2B respectively

(Fig. 11.2). On the basis of an intuitive evaluation of the species involved in the major groups, the poorly associated stations 10, 15, 39, 17 and 63 have been assigned to Biotope 1A and stations 16, 57 and 8 have been defined as Biotope 1C. Figure 11.1 shows the areal distribution of the biotopes. Stations initially eliminated from the computer analysis have been referred to the appropriate biotopes on the basis of species present and geographic location.

Biotope 1A, 1B and 1C are restricted essentially to areas of sand or gravelly sand bottom, and Biotope 2A and 2B are characteristic of substrates consisting of clayey silt or silty clay. These divisions are also related to depth because the coarser sediments are found primarily in the shallower areas on both sides of the bay, with finer sediments confined to the deeper, mid-bay area. Biotope 2A shows a relationship to bottom areas that are in contact with comparatively warm ($>1^{\circ}\text{C}$) Atlantic bottom water (Schafer and Cole, in press).

The species composition of each biotope is summarized in Table 11.1. The shallower, coarser-bottomed area supports a relatively ubiquitous and diverse fauna compared with the deeper fine sediment substrates. Forty-four species (29 pelecypods and 15 gastropods) were identified from the former in contrast with 15 species (13 pelecypods and 2 gastropods) from the latter. Only eight species, all pelecypods, were found in both coarse and fine sediments. These are *Clinocardium ciliatum* (Fabricius), *Liocyma fluctuosa* (Gould), *Macoma calcarea* (Gmelin), *Mya truncata* Linné, *Nuculana minuta* (Fabricius), *Panomya arctica* (Lamarck), *Periploma fragile* (Totten) and *Serripes groenlandicus* (Bruguière).

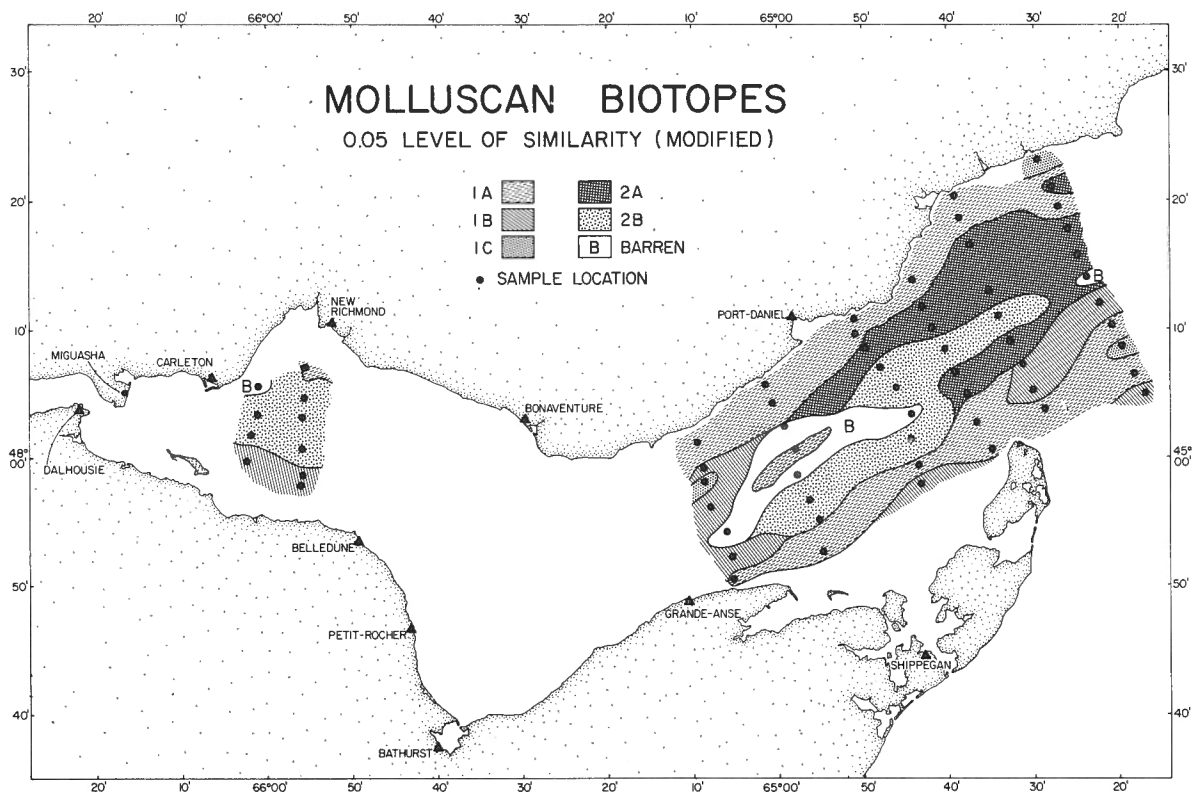


Figure 11.1. Station locations and molluscan biotopes, Chaleur Bay.

Table 11.1

Species characteristic of the molluscan biotopes, Chaleur Bay.

SAND AND GRAVELLY SAND		SILT AND CLAY		
BIOTOPE 1A 18-85 m 12 STATIONS	BIOTOPE 1B 22-70 m 11 STATIONS	BIOTOPE 1C 17-85 m 3 STATIONS	BIOTOPE 2A 48-110 m 11 STATIONS	BIOTOPE 2B 19-86 m 11 STATIONS
<p>Macoma calcarea (3) *</p> <p>Serripes groenlandicus (1)</p> <p>Clinocardium ciliatum (5)</p> <p>Chlamys islandica (5)</p> <p>Cyclocardia borealis (3)</p> <p>Cerastoderma pinnulatum (3)</p> <p>Placopecten magellanicus (3)</p> <p>Ensis directus (2)</p> <p>Mytilus edulis (2)</p> <p>Mya arenaria (1)</p> <p>Tachyrhynchus erosus (1)</p> <p>Liocyma fluctuosa (3)</p> <p>Nuculana minuta (1)</p> <p>Periploma fragile (1)</p> <p>Astarte undata (10)</p> <p>Lepeta caeca (6)</p> <p>Aporrhais occidentalis (5)</p> <p>Astarte striata (4)</p> <p>Astarte subaequilatera (3)</p> <p>Crenella glandula (3)</p> <p>Oenopota turricula (3)</p> <p>Astarte borealis (2)</p> <p>Margarites costalis (2)</p> <p>Beringius ossiani (1)</p> <p>Crassostrea virginica (1)</p> <p>Crepidula fornicata (1)</p> <p>Lunatia sp. (1)</p> <p>Lyonsia arenosa (1)</p> <p>Macoma balthica (1)</p> <p>Nucula tenuis (1)</p> <p>?Solaria varicosa (1)</p> <p>Tellina agilis (1)</p> <p>Velutina undata (1)</p>	<p>M. calcarea (9)</p> <p>S. groenlandicus (4)</p> <p>C. ciliatum (1)</p> <p>C. islandica (2)</p> <p>C. borealis (1)</p> <p>C. pinnulatum (1)</p> <p>P. magellanicus (1)</p> <p>E. directus (1)</p> <p>M. edulis (1)</p> <p>M. arenaria (2)</p> <p>Hiatella arctica (2)</p> <p>Puncturella noachina (1)</p> <p>Mya truncata (1)</p> <p>Colus stimpsoni (2)</p> <p>Margarites groenlandicus (1)</p> <p>Moellieria costulata (1)</p>	<p>T. erosus (1)</p> <p>H. arctica (1)</p> <p>P. noachina (1)</p> <p>Panomya arctica (3)</p> <p>Acmaea testudinialis (1)</p> <p>?Anomia simplex (1)</p> <p>Crenella faba (1)</p> <p>Spisula polynyma (1)</p>	<p>M. calcarea (1)</p> <p>S. groenlandicus (1)</p> <p>L. fluctuosa (1)</p> <p>N. minuta (2)</p> <p>P. fragile (6)</p> <p>M. truncata (1)</p> <p>P. arctica (1)</p> <p>Yoldia limatula (2)</p> <p>Nuculana tenuisulcata (6)</p> <p>Calliostoma occidentale (1)</p> <p>Megayoldia thraciaeformis (1)</p> <p>Natica clausa (1)</p>	<p>M. calcarea (1)</p> <p>S. groenlandicus (1)</p> <p>C. ciliatum (1)</p> <p>Nuculana pernula (2)</p> <p>Yoldia sp. (2)</p> <p>Buccinum tenue (1)</p>

*(3) indicates the number of stations within the biotope at which species is present.

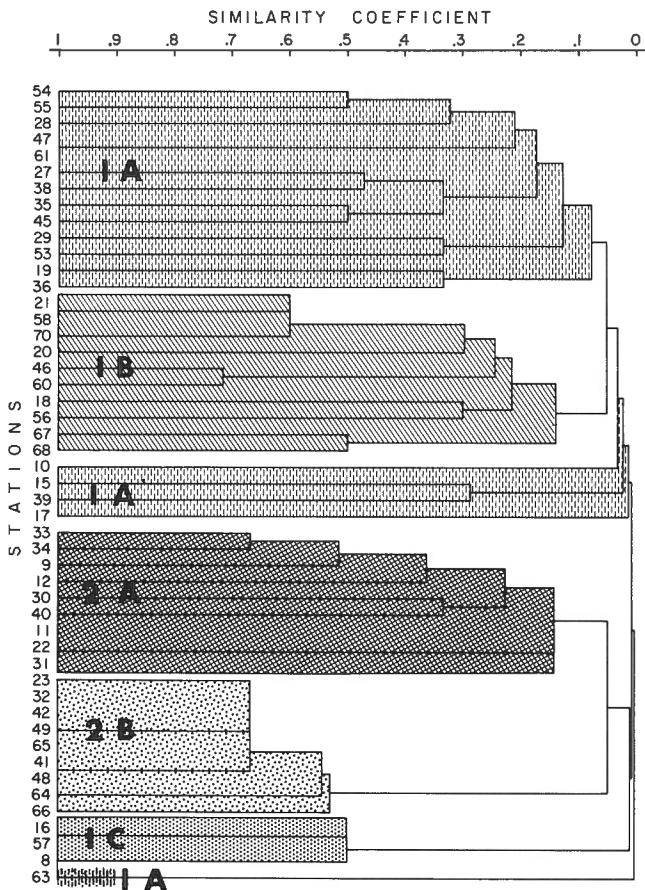


Figure 11.2. Dendrogram showing the similarity of grab samples based on the Jaccard's Coefficient and the cluster groups used to define the five molluscan biotopes in Chaleur Bay.

The index species for Biotope 1A is *Astarte undata* Gould. This species was present at only 53 per cent of the stations, but it was restricted to this biotope. *Lepeta caeca* (Müller) and *Aporrhais occidentalis* Beck were also restricted to Biotope 1A and were present at 32 per cent and 26 per cent of the stations respectively. Half of the remaining 30 species in this biotope each occurred at only one station. Nineteen species were unique to the biotope. Biotope 1A spans a depth range of 18 to 85 m. However, two Biotope 1A stations, at 75 m and 85 m respectively, yielded only incomplete and, therefore, probably not in situ specimens. Thus they may suggest a deeper, lower limit for the biotope than is actually the case.

Although *Macoma calcaria* (Gmelin) is present as a minor constituent in Biotopes 1A, 2A and 2B, it is the predominant species in Biotope 1B where it is present, both living and dead, at 82 per cent of the stations. Of the other 15 species, only *Serripes groenlandicus* (Bruguière) was found at more than two stations in this biotope. Most species showed only single-station occurrences, and only three species were restricted to the biotope. The depth range for this biotope is from 22 to about 70 m.

The three stations in Biotope 1C are represented by a total of eight species. The stations are widely separated areally and are located in depths of 17, 32 and 85 m. The predominant species is *Panomya arctica* (Lamarck), the only species common to all three stations. Although this species also was found in Biotope 2A, the species associated with it, the generally shallower depth range and the type of bottom sediment of Biotope 1C reflects a fairly close affinity with Biotope 1B.

Periploma fragile (Totten) and *Nuculana tenuisulcata* (Couthouy) were each found at 6 of the 11 stations in Biotope 2A and co-occurred at three of them. Eight of the remaining 10 species represent singular occurrences. *N. tenuisulcata* is one of the four species apparently confined to this biotope. Depth range for Biotope 2A is between 48 and 110 m.

The index species for Biotope 2B is *Yoldia limatula* (Say), a species that was present as a minor constituent in Biotope 2A. Two localities had specimens that were identifiable as *Yoldia* sp.; these might or might not be *Y. limatula*. A total of seven species (including *Yoldia* sp.) are recorded in Biotope 2B and three of these are unique to the biotope. Species indicative of this biotope were collected over a water depth range of 19 to 86 m, between 19 and 30 m for the stations in the New Richmond area and 60 to 86 m in the eastern part of the bay.

The index species for the Chaleur Bay biotopes have been reported from similar ecological niches elsewhere on the east coast of North America. Three species, namely *Astarte undata*, *Macoma calcaria* and *Periploma fragile*, are index species also for biotopes in Bay of Fundy (Wagner, 1977). In Fundy, they, as well as *Panomya arctica* and *Yoldia limatula*, occur under conditions of depth and substrate comparable to those recorded for them in Chaleur Bay. Wagner (1977) did not find the other Chaleur Bay index species, *Nuculana tenuisulcata*, in any of the samples she examined from Bay of Fundy. Only *Y. limatula* was reported (Wagner, 1976) from the shallow (maximum depth sampled = 11 m) Miramichi estuary.

Of the 32 named species in Biotope 1A five are within 4° of latitude of their northern limit at Chaleur Bay, and another five are within 4° of their southern limit. Chaleur Bay marks the actual northern limit of two of the former. The index species, *A. undata*, is at about the midpoint of its range. Geographic ranges, and some ecological data, are derived from Abbott (1974), Bousfield (1960), Morris (1973) and Ockelmann (1958). Three of the 16 species in Biotope 1B approach their northern limit, but none comes within 6° of its southern limit. *M. calcaria*, index species for this biotope, is closer to the southern limit than to the midpoint of its range. The index species for Biotope 1C, *P. arctica*, is also south of the midpoint of its range at Chaleur Bay. One of the eight species associated with this biotope is about 4° from its southern limit, and another one is at its northern limit. Of the two index species for Biotope 2A, *N. tenuisulcata* is halfway between the midpoint and northern limit of its range, and *P. fragile* is just about at the midpoint of its range. Twelve species characterize this biotope. Two of the twelve are at their northern limit, and Chaleur Bay is about 4° from the southern limit of two other species. Biotope 2B has six species of which one, the index species, *Y. limatula* is at its northern limit and another is near its southern limit.

A biometrical analysis has been employed using the median-of-midpoints method (Schenck and Keen, 1937) to determine temperature differences, if any, between the biotopes. This involves calculations based on the midpoint of the geographic range of each species in an assemblage. Ideally, a sample should comprise at least 50 species. A smaller number could result in an error of possibly as much as two degrees of latitude. Schenck and Keen later elaborated on this technique (1940), and in their Figure 2 illustrated the discrepancies between the actual latitude of collection and the calculated median latitude for a series of 28 shore collections and five shallow dredgings along the Pacific coast of North America. Dredged collections showed a higher (colder) latitude than shore collections from the same latitude. They also (1940) tested the method using a distribution list of molluscs from the western North Atlantic Ocean and they considered the results to be valid in spite of the greater trend of the eastern coast of North America away from a north-south orientation.

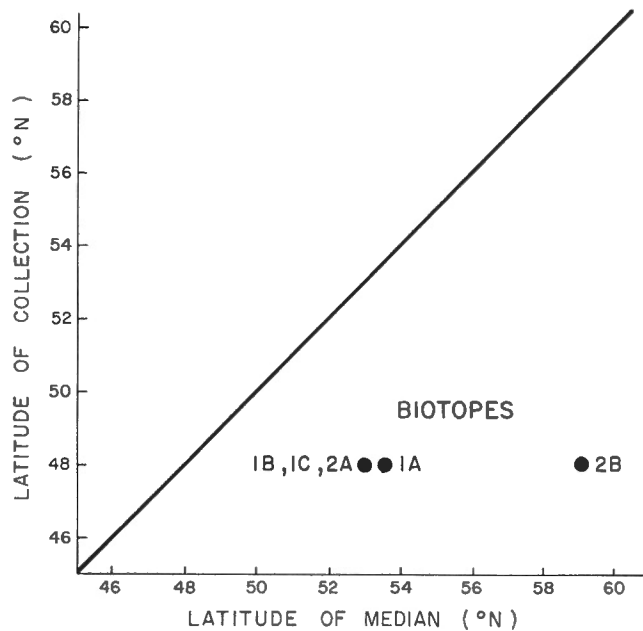


Figure 11.3. Plot of the median latitudes of the molluscan biotope assemblages versus latitude of collection.

Results of the application of the median-of-midpoints method to each of the Chaleur Bay biotopes are summarized in Figure 11.3. None of the biotopes comprised shore collections and none met the minimum standard of 50 species. However, all results are consistent in showing median latitudes farther north than the latitude of collection, i.e. the normal situation for offshore collections. A latitude of 53°N was indicated for Biotopes 1B, 1C and 2A, and 53.5°N for Biotope 1A. These four biotopes are, therefore, essentially the same with regard to temperature. Biotope 2B, however, has a calculated latitude of 59°N, a full 11 degrees farther north than the latitude of collection. Thus it shows a definitely colder aspect than the other biotopes. Even assuming an error such that the warmer biotopes would be up to two degrees farther north and Biotope 2B as much as two degrees farther south than indicated, the latter is still significantly colder than the others. This biotope may, therefore, reflect the cold Gaspé current waters (near 0°C in summer) that have been observed by Loring and Nota (1973, Fig. 9) in the Gulf of St. Lawrence between about 80 and 100 m and in eastern Chaleur Bay at depths between about 60 and 80 m by Schafer and Cole (in press). The depth range for Biotope 2B in the eastern part of the bay is 60 to 86 m. Apparently this cold layer comes much closer to the surface in the channel farther west because the stations of Biotope 2B in the New Richmond area range in depth between 19 and 30 m. Although Biotope 2A in eastern Chaleur Bay includes the 60 to 80 m depth range, 73 per cent of the stations are deeper than 80 m and they are shown by the median latitude to be associated with the less cold waters underlying the cold-water mass.

Conclusions

1) Five molluscan biotopes have been recognized in Chaleur Bay. Although there is some overlap of depth ranges, the biotopes show a relationship with the type of substrate, water depth, and with certain water-mass characteristics.

2) Index species can be identified for each biotope. *Astarte undata*, *Macoma calcarea*, and *Panomya arctica* are the index species for Biotopes 1A, 1B and 1C respectively. Biotope 2A is characterized by two index species, namely *Nuculana tenuisulcata* and *Periploma fragile*. The index species for Biotope 2B is *Yoldia limatula*.

3) Analysis of the faunas by the median-of-midpoints method suggests that Biotope 2B represents considerably colder conditions than are indicated for the other biotopes, apparently reflecting the upwelling of the cold Gaspé current water into Chaleur Bay.

References

- Abbott, R.T.
1974: American seashells; New York, Van Nostrand Reinhold Company, 2nd ed.
- Bonham-Carter, C.F.
1967: Fortran IV program for Q-mode data cluster analysis of non-quantitative data using IBM 7090/7094 computers; State Geol. Survey, Univ. Kansas Computer Contrib. 17, 13 p.
- Bousfield, E.L.
1960: Canadian Atlantic sea shells; Nat. Mus. Canada, 72 p., 13 pl.
- Loring, D.H. and Nota, D.J.G.
1973: Morphology and sediments of the Gulf of St. Lawrence; Fish. Res. Bd., Can., Bull. 182, 147 p.
- Morris, P.A.
1973: A field guide to shells of the Atlantic and Gulf coasts and the West Indies; Boston, Houghton Mifflin Company, 330 p., 76 pl.
- Ockelmann, W.K.
1958: The zoology of East Greenland: Marine Lamelli-branchiata; Medd. om Grønland, v. 122, no. 4, 256 p., 3 pl.
- Schafer, C.T.
1976: Distribution of foraminifera in Chaleur Bay, New Brunswick-Quebec; in Report of Activities, Part C, Geol. Surv. Can., Paper 76-1C, p. 19-23.
- Schafer, C.T. and Cole, F.E.
Distribution of foraminifera in Chaleur Bay; Geol. Surv. Can., Paper (in press).
- Schafer, C.T., Cranston, R.E., Staufbergen, N., McKeown, D.L., Sherin, A., and Kingston, P.F.
1974: Cruise Report No. 74-013, C.S.S. DAWSON; Bedford Inst. Oceanogr.
- Schenck, H.G. and Keen, A.M.
1973: An index-method for comparing molluscan faunules; Proc. Am. Philos. Soc., Proc., v. 77, no. 2, p. 161-182.
1940: Biometrical analysis of molluscan assemblages; Soc. Biogéographie, v. 7, p. 379-392, 2 pl.
- Sokal, R.R. and Sneath, P.A.
1963: Principles of numerical taxonomy; London, W.H. Freeman and Co., 359 p.
- Wagner, F.J.E.
1976: Mollusc distributions, Miramichi estuary, New Brunswick; in Report of Activities, Part C, Geol. Surv. Can., Paper 76-1C, p. 45.
1977: Mollusc distribution, Bay of Fundy area, New Brunswick and Nova Scotia; in Report of Activities, Part B, Geol. Surv. Can., Paper 77-1B, p. 97-98.

Project 720084

R.L. Grasty
Resource Geophysics and Geochemistry Division

In the last few years several large scale uranium reconnaissance programs have commenced in various parts of the world. Many thousands of line kilometres of high sensitivity gamma-ray spectrometer surveys are now being flown annually for the purpose of delineating areas favourable for uranium exploration. In these surveys, considerable emphasis has been placed on the calibration and standardization of the different systems involved (IAEA, 1976; Darnley, 1977). In particular the Geological Survey of Canada has constructed large concrete calibration sources and utilizes a calibration strip in order that the airborne count rates can be converted to equivalent ground concentrations of potassium, uranium, and thorium (Grasty and Darnley, 1971; Grasty and Charbonneau, 1974). The calibration procedure using the concrete calibration sources is essentially the same as that adopted by Adams and his co-workers for a laboratory gamma-ray spectrometer (Adams et al., 1958; Adams, 1964). The equations relating the background corrected count rates in the three radio-element windows, K, U, and T to the potassium, uranium, and thorium content, K_{conc} , U_{conc} and T_{conc} are given by:

$$T_{conc} = T/k_1 \dots\dots\dots (1)$$

$$U_{conc} = (U - \alpha T)/k_2 \dots\dots\dots (2)$$

$$K_{conc} = (K - \beta T - \gamma (U - \alpha T))/k_3 \dots\dots\dots (3)$$

where k_1 , k_2 and k_3 are the three sensitivities, measured in terms of counts per unit concentration of the respective radio-element. These sensitivities are derived from flights over the calibration strip. The constants, α , β , and γ , are commonly called the stripping ratios.

These equations assume that a uranium source will have no contribution to the thorium window and also that a potassium source will have no contribution to either the uranium or the thorium windows. In reality, there are ^{214}Bi gamma-rays at 2.20 MeV and 2.45 MeV, in the uranium decay chain which result in gamma-rays being detected in the thorium window from a uranium source. For a thorium window 400 KeV wide and centred on the 2.61 MeV thallium peak and a uranium window 200 KeV wide on the 1.76 MeV ^{214}Bi peak, approximately five per cent of the number of counts detected in the uranium window over a pure uranium source will appear in the thorium window. In normal circumstances this correction is small, but for rocks with high uranium-to-thorium ratios considerable errors can arise in the estimation of the thorium concentration.

For portable gamma-ray spectrometers utilizing single crystals the effect of potassium in the uranium window can be neglected. However, for an airborne system with multiple crystal arrays and associated problems of detector gain matching, the resolution can be degraded to the extent that some counts from a potassium source can appear in the uranium window. It should also be noted that the potassium count rate is normally an order of magnitude higher than that in the uranium window and consequently even a small percentage can be significant.

Nowadays many airborne systems are utilizing more than one window for the measurement of uranium. Foote and Humphrey (1976) use multiple windows above 1.0 MeV to reduce the errors due to poor counting statistics that occur when using only the conventional single uranium window at 1.76 MeV. They report an increase in accuracy of 10 per cent in the measurement of uranium.

Since the Geological Survey is planning to have a multiple channel system operational in 1977 and will have the capability of utilizing several windows for the measurement of uranium, and in view of the approximations involved in the present method of calibration, it was decided to develop a general calibration procedure which would satisfy the requirements of multi-uranium and thorium windows and would correct for interference between any of the windows. The technique developed was essentially the same as that applied by Hurley (1956) to the laboratory analysis of potassium, uranium and thorium.

Irrespective of the number of windows used, they can be grouped into three sets relating to each of the radio-elements. For instance the counts recorded in the 0.61 MeV and 1.12 MeV ^{214}Bi windows can be added to the counts in the 1.76 MeV window to give the total number of counts for the uranium window. For a fixed detector source configuration the measurements in each of the three windows will be linearly related to the three radio-element concentrations. Consequently it is a simple matter to formulate a general set of equations relating the count rates in each window to the radioactive concentration of the ground.

For a measurement on the calibration pads and using a similar notation to that used previously, the equations are:

$$K = \epsilon_{KK} K_{conc} + \epsilon_{KU} U_{conc} + \epsilon_{KT} T_{conc} + B_K \dots (4)$$

$$U = \epsilon_{UK} K_{conc} + \epsilon_{UU} U_{conc} + \epsilon_{UT} T_{conc} + B_U \dots (5)$$

$$T = \epsilon_{TK} K_{conc} + \epsilon_{TU} U_{conc} + \epsilon_{TT} T_{conc} + B_T \dots (6)$$

B_K , B_U and B_T are the background count rates arising from the radioactivity of the ground surrounding the pads, the radioactivity of the aircraft and equipment plus the contribution from cosmic radiation and the radioactivity of the air. The ϵ_{ij} 's are constants to be determined and give the count rate in window I per unit concentration of element J.

In terms of the more conventional calibration method, the constants ϵ_{KK} , ϵ_{UU} and ϵ_{TT} are the potassium, uranium, and thorium sensitivities, equivalent to k_1 , k_2 and k_3 in equations (1), (2) and (3). The stripping ratios are given by:

$$\alpha = \epsilon_{UT}/\epsilon_{TT} \dots\dots\dots (7)$$

$$\beta = \epsilon_{KT}/\epsilon_{TT} \dots\dots\dots (8)$$

$$\gamma = \epsilon_{KU}/\epsilon_{UU} \dots\dots\dots (9)$$

Because of the interference between all the windows, it is necessary to define three new constants. For convenience the notation has been adopted in which:

- α is the thorium into uranium stripping ratio
- a is the reversed stripping ratio, uranium into thorium
- β is the thorium into potassium stripping ratio
- b is the reversed stripping ratio, potassium into thorium
- γ is the uranium into potassium stripping ratio
- g is the reversed stripping ratio, potassium into uranium

These new constants, a , b and g are given by:

$$a = \epsilon_{TU}/\epsilon_{UU} \dots\dots\dots (10)$$

$$b = \epsilon_{TK}/\epsilon_{KK} \dots\dots\dots (11)$$

$$g = \epsilon_{UK}/\epsilon_{KK} \dots\dots\dots (12)$$

Each of the equations (4), (5) and (6) have four unknowns and consequently from measurements on all five calibration pads these four unknowns can be evaluated. This can be achieved using a standard linear least squares technique to derive the various ϵ_{Tj} values.

For an airborne system, the pads cannot be considered infinite in size and consequently the sensitivity factors cannot be applied to airborne data. In addition they have been calculated at ground level, which is only applicable to a ground instrument. In order to derive the sensitivities for an airborne system, flights must be made over the calibration strip.

For a measurement over the test strip, the background corrected count rates in the three windows are related to the corrected count rates, T_C , U_C and K_C by the equations:

$$T = T_C + aU_C + bK_C \dots\dots\dots(13)$$

$$U = \alpha T_C + U_C + gK_C \dots\dots\dots(14)$$

$$K = \beta T_C + \gamma U_C + K_C \dots\dots\dots(15)$$

These corrected count rates are proportional to the ground concentration of the strip.

Solving these equations for T_C , U_C and K_C we get:

$$T_C = \frac{T(1 - g\gamma) + U(b\gamma - a) + K(ag - b)}{A} \dots(16)$$

$$U_C = \frac{T(g\beta - \alpha) + U(1 - b\beta) + K(b\alpha - g)}{A} \dots(17)$$

$$K_C = \frac{T(\alpha\gamma - \beta) + U(a\beta - \gamma) + K(1 - a\alpha)}{A} \dots(18)$$

where A has the value

$$A = 1 - g\gamma - a(\alpha - g\beta) - b(\beta - \alpha\gamma)$$

These equations reduce to the standard stripping equations similar to equations (1), (2) and (3) when a, b and g equal zero.

From these equations the airborne data can be unfolded to give the corrected count rates in the three windows. It is then a simple matter to derive the radio-element sensitivities of the airborne system, since the ground concentration of the strip is known.

In the particular case of the airborne systems involved in Canada's Federal-Provincial Uranium Reconnaissance Program, only a high energy thorium window at 2.61 MeV is used and it can be assumed that potassium has no influence on the thorium window. Consequently both ϵ_{TK} in equation (6) and b in equation (11) will be zero. Calibration pad data from these systems are evaluated accordingly.

Table 12.1 shows the results of the pad analysis for two airborne systems, one with good resolution and one with poor resolution. An advantage of this particular procedure is that the value of the potassium into uranium coefficient is a good indicator of the system resolution. A system with poor resolution, either because of poor detector alignment or because of bad crystals shows a high potassium into uranium coefficient. The particularly high value indicated suggests that the spectrum for this system may have shifted relative to the windows. It should be pointed out that at present no analyses have been carried out on the accuracy of the various coefficients.

Due to scattering in the air of the high energy 2.61 MeV ^{208}Tl gamma-rays into the uranium window, the value of the stripping ratio should be adjusted for the particular height of the airborne measurement as has been described by Grasty (1976). Similarly, if multi-uranium or thorium channels are used, it may be necessary to correct some of the calibration

Table 12.1
Calibration results*

Calibration Coefficient	System with good resolution	System with poor resolution
Thorium into uranium (α)	0.46	0.42
Thorium into potassium (β)	0.51	0.48
Uranium into potassium (γ)	0.97	0.95
Uranium into thorium (a)	0.07	0.12
Potassium into uranium (g)	0.03	0.40
*For the particular energy windows		
Potassium	- 1.37-1.57 MeV	
Uranium	- 1.66-1.86 MeV	
Thorium	- 2.41-2.81 MeV	

coefficients for aircraft altitude. The program to evaluate the various calibration coefficients may be obtained by writing to the author.

Acknowledgments

The technique described in this paper originated from discussions with Jim Lindow and Bob Fowler of Geometrics, who had described a similar procedure in a company report. John Carson provided the results of measurements on the calibration pads.

References

Adams, J.A.S.
1964: Laboratory γ -ray spectrometer for geochemical studies; in *The Natural Radiation Environment*, p. 485-497, Univ. Chicago Press, Adams, J.A.S. and Lowder, W.M. (ed.).

Adams, J.A.S., Richardson, J.E., and Templeton, C.C.
1958: Determination of thorium and uranium in sedimentary rocks by two independent methods; *Geochim. Cosmochim. Acta*, v. 13, p. 270-279.

Darnley, A.G.
1977: The advantages of standardizing radiometric exploration measurements, and how to do it; *Can. Min. Metall. Bull.*, v. 71, p. 91-95.

Foote, R.S. and Humphrey, N.B.
1976: Airborne radiometric techniques and applications to uranium exploration; in *Exploration for Uranium Ore Deposits*, International Atomic Energy Agency, Vienna, p. 17-34.

Grasty, R.L.
1976: A calibration procedure for an airborne gamma-ray spectrometer; *Geol. Surv. Can., Paper 76-16*, p. 1-9.

Grasty, R.L. and Charbonneau, B.W.
1974: Gamma-ray spectrometer calibration facilities; in *Report of Activities, Part B*, *Geol. Surv. Can., Paper 74-1B*, p. 69-71.

Grasty, R.L. and Darnley, A.G.
1971: The calibration of gamma-ray spectrometers for ground and airborne use; *Geol. Surv. Can., Paper 71-17*, 27 p.

Hurley, P.M.
1956: Direct radiometric measurement by gamma-ray scintillation spectrometer; *Geol. Soc. Am. Bull.*, v. 67, p. 395-404.

IAEA
1976: Radiometric reporting methods in uranium exploration; *Technical Report No. 174*, International Atomic Energy Agency, Vienna, 57 p.

Project 730004

A.K. Sinha

Resource Geophysics and Geochemistry Division

Introduction

Several geophysical techniques utilizing artificial (man-made) plane electromagnetic waves have been introduced in the past fifteen years. Of these, the most important ones are the very low frequency (VLF) method (Paterson and Ronka, 1971) and the E-Phase technique (Barringer, 1971). The VLF method uses very low frequency (15-25 kHz) transmissions from powerful naval transmitters which are used for submarine communications. The E-Phase technique, on the other hand uses two or three frequencies from the VLF range to the broadcast band (BCB). Thus, besides the VLF transmitters, military transmitters (50-100 kHz), navigational transmitters (200-400 kHz) and broadcast transmissions (500 kHz - 1.5 MHz) may be used in this system. A unique feature of this system is that electric rather than the magnetic field is used. The normal electric field in free space is vertical but the presence of any body with finite resistivity produces a horizontal component of the electric field thereby introducing a tilt to the wave front. This wave tilt may be measured continuously from an aircraft and the changes in the measured wave tilt may be correlated with changes in the lithology of the ground below.

There are two main flaws in the interpretation scheme presently employed for the interpretation of airborne E-Phase data. Firstly, the altitude of the aircraft (generally 60-100 m) is not taken into consideration and, secondly, the influence of displacement currents are ignored. It was shown in previous studies (Sinha, 1976, 1977) that while the effects of these factors may be ignored at low frequencies and for conducting ground, the errors may become serious when the ground is resistive (e.g. permafrost terrain) and when high frequencies from broadcast stations are used. A technique for correcting these effects was outlined in these papers. The present paper provides several master charts or correction diagrams so that anyone may obtain the correct values of the ground parameters using these and the wave tilt values from airborne E-Phase surveys.

Basic Theory

The wave tilt is defined as the ratio of the horizontal to the vertical electric field just above the surface of the ground. Thus

$$\text{Wave Tilt} = \text{WT} = \frac{E_x}{E_z} \Big|_{z=0} \quad (1)$$

Assuming a time dependence of $\exp(i\omega t)$, the wave tilt at an altitude of 'h' over a homogeneous earth (Norton, 1937) may be written as

$$\text{WT} = \frac{v \sqrt{1-v^2}}{1-\gamma_0 h v \sqrt{1-v^2}} \quad (2)$$

where

$$v = \gamma_0 / \gamma_1, \quad h = \text{altitude in metres, } i = \sqrt{-1},$$

$$\gamma_0 = (-\omega^2 \mu \epsilon_0)^{\frac{1}{2}} = \text{propagation constant of air,}$$

$$\gamma_1 = (i\omega \mu \sigma_1 - \omega^2 \mu \epsilon_1)^{\frac{1}{2}} = \text{propagation constant of the medium,}$$

$$\epsilon_0 = \text{permittivity of air } (8.854 \times 10^{-12} \text{ F/m}),$$

$$\epsilon_1 = \text{permittivity of the medium,}$$

$$\sigma_1 = \text{conductivity of the medium,}$$

$$\mu = \text{permeability of the medium and air.}$$

It may be shown easily that

$$\gamma_1^2 / \gamma_0^2 = \epsilon_1 - \frac{i\sigma_1}{\omega \epsilon_0} \quad (3)$$

where

$$\epsilon_1 = \epsilon_1 / \epsilon_0 = \text{the dielectric constant of the medium.}$$

Using equation (2), several diagrams were plotted to illustrate the influence of altitude, frequency values, and the electrical parameters of the ground on the wave tilt (Sinha, 1977). The correction diagrams and their use are described in the next section.

Use of Correction Diagrams

The E-Phase system measures only the quadrature part of the wave tilt since it is very difficult to measure the in-phase part from an airborne platform. Hence, any correction scheme should consider the quadrature part of the wave tilt only. In the correction scheme that has been devised, quadrature parts of the wave tilt are needed at least at two frequencies. Figure 13.1 shows a typical correction diagram where the two frequencies are taken to be 50 kHz and 15 kHz respectively. The ratios of the quadrature part of the wave tilt are plotted along the ordinate while the quadrature part of the wave tilt at the lower frequency is plotted along the abscissa. Figure 13.1 is drawn for an altitude of 60 m and six resistivity and dielectric constant values of the ground as shown in the diagram. As expected, the resolution between the curves improves with increasing resistivity.

Figures 13.2 and 13.3 illustrate the correction diagrams when the altitudes are 80 m and 100 m respectively. Figures 13.1 through 13.3 are similar except for the high resistivity lines. That indicates that the influence of altitude is small in the VLF and lower LF range although the displacement current effects (different ϵ_1/ϵ_0 lines) are quite strong. Figure 13.4 illustrates the correction diagram for an altitude of 100 m when the two frequencies are 80 kHz and 15 kHz. Figures 13.5, 13.6, and 13.7 represent correction diagrams when the frequencies are 200 kHz and 20 kHz, a typical combination for E-Phase surveys for three altitude values of 60, 80 and 100 m respectively. Since the upper frequency is higher for the last three diagrams, the altitude effect is considerably larger since it is controlled both by the altitude and the displacement current contributions. Figure 13.8 shows the correction diagram for the frequency combination of 300 and 20 kHz for an altitude of 100 m. It is interesting that as the higher frequency is increased, the range of variation of the ratio of wave tilt values increases sharply and the ratios become increasingly negative for large resistivity values. Similar curves may be generated for any other combination of altitude and frequency to suit a particular survey.

From the correction diagrams, it is clear that if the wave tilt values are obtained at two different frequencies (E-Phase normally provide data at three frequencies), a more correct estimate of the ground resistivity may be obtained using appropriate correction diagrams. What is more, we may also get an idea about the dielectric constant of the ground from these diagrams. This is especially useful when surveying over frozen ground (permafrost terrain), since these terrains provide very good E-Phase anomalies because of their high resistivities. Since dielectric constants are related to the ice-content of the ground, the E-Phase data may also be used to sense remotely the ice content of a permafrost terrain from an aircraft.

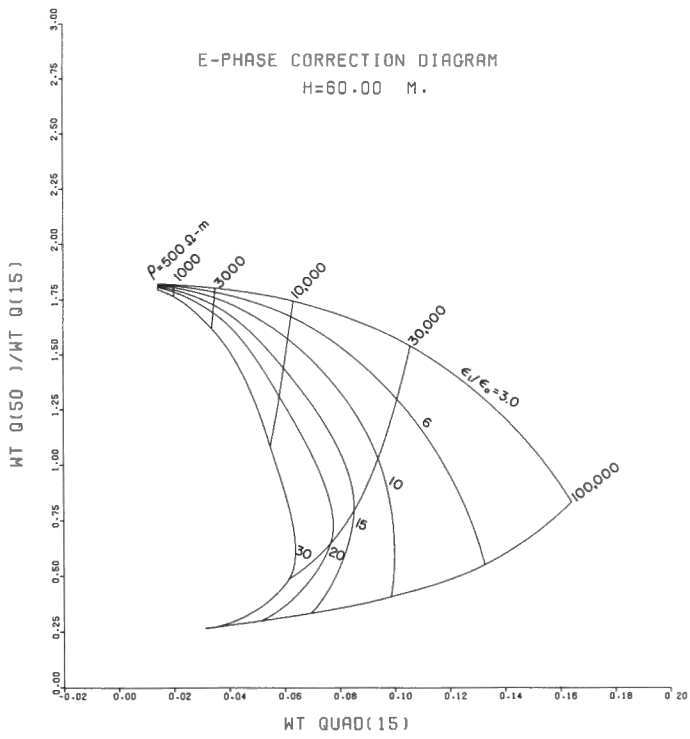


Figure 13.1. Correction diagram for E-Phase for an altitude of 60 m and frequency combinations of 50 and 15 kHz.

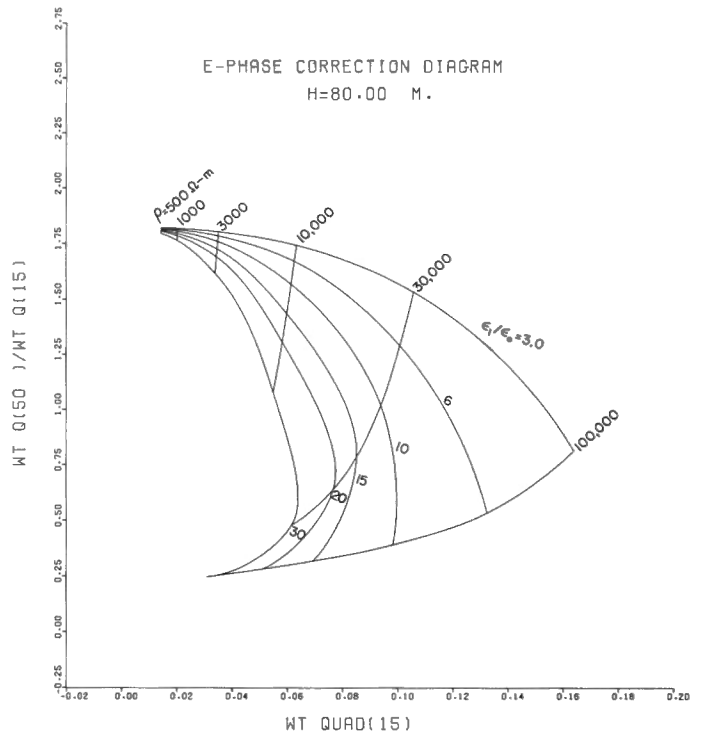


Figure 13.2. Correction diagram for E-Phase for an altitude of 80 m and frequency combinations of 50 and 15 kHz.

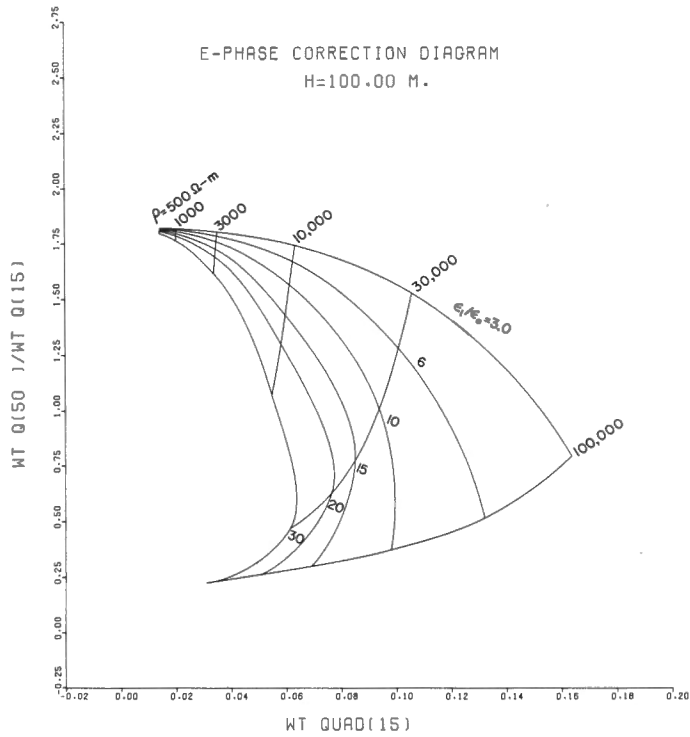


Figure 13.3. Correction diagram for E-Phase for an altitude of 100 m and frequency combinations of 50 and 15 kHz.

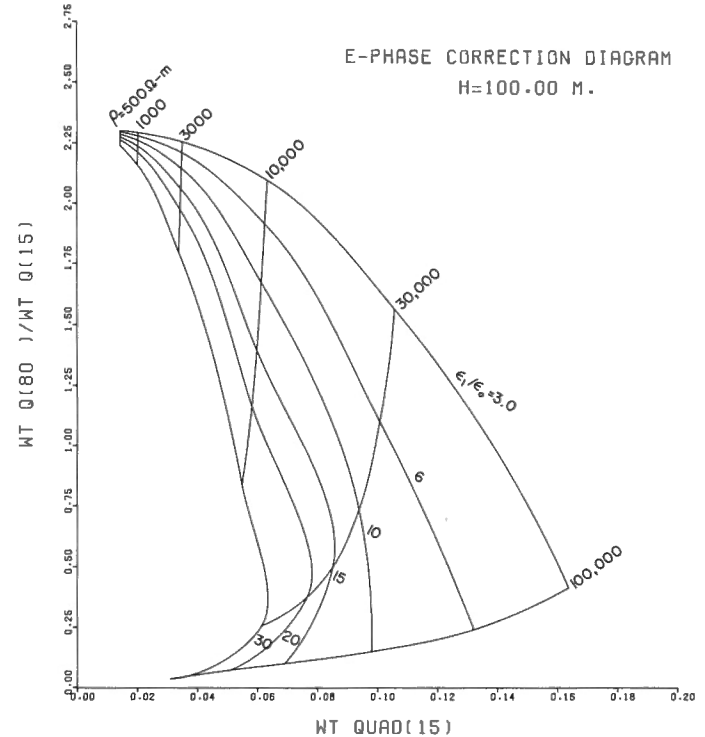


Figure 13.4. Correction diagram for E-Phase data for frequency combinations of 80 and 15 kHz at an altitude of 100 m.

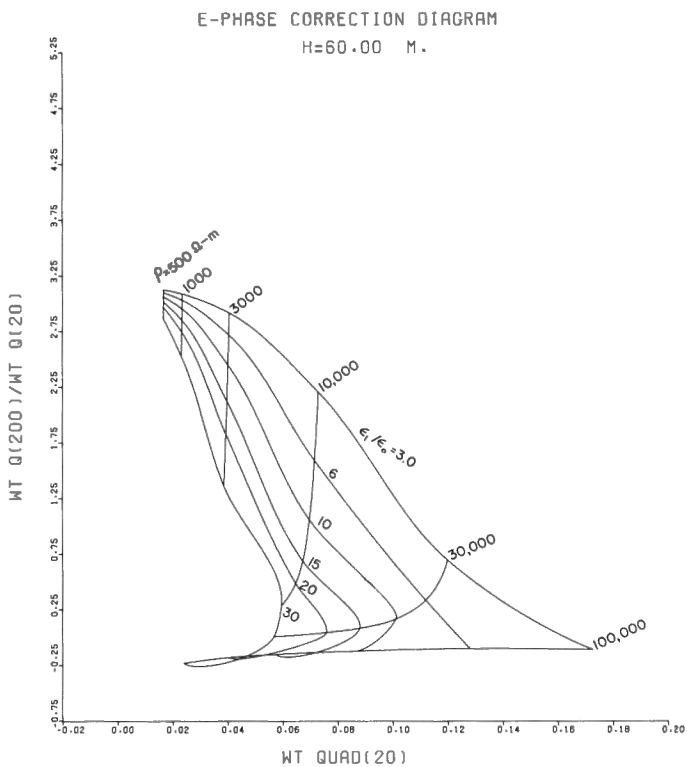


Figure 13.5. Correction diagram for E-Phase data for frequency combinations of 200 and 20 kHz for an altitude of 60 m.

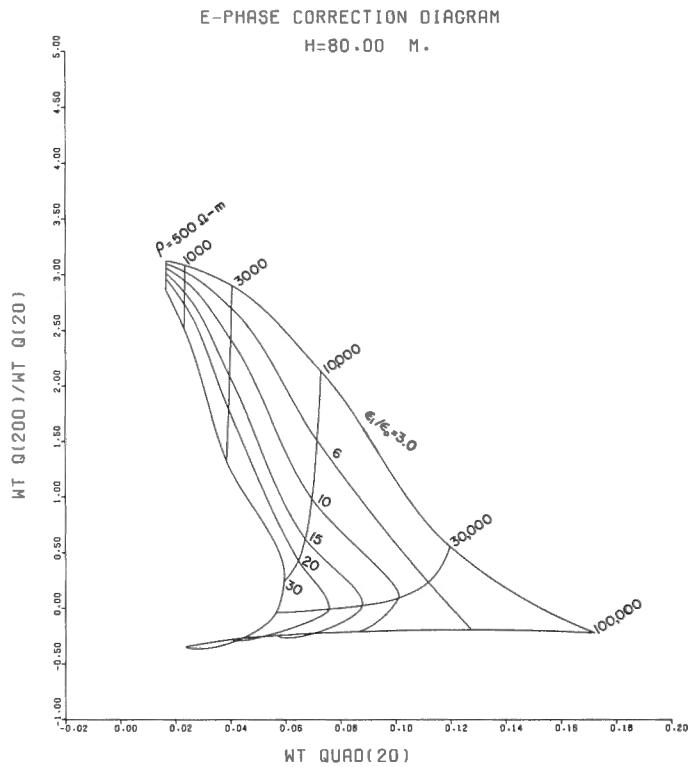


Figure 13.6. Correction diagram for E-Phase for an altitude of 80 m and frequency combinations of 200 and 20 kHz.

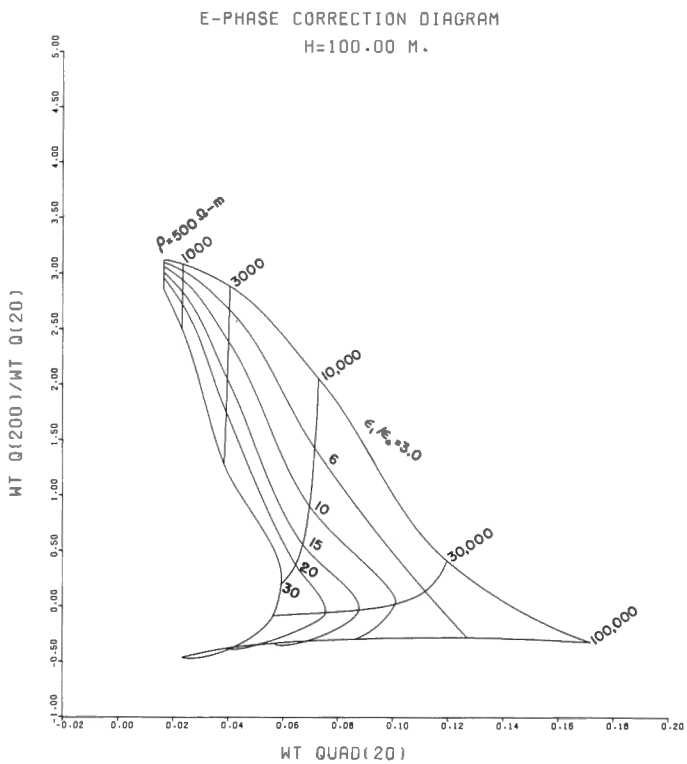


Figure 13.7. Correction diagram for E-Phase for an altitude of 100 m and frequency combinations of 200 and 20 kHz.

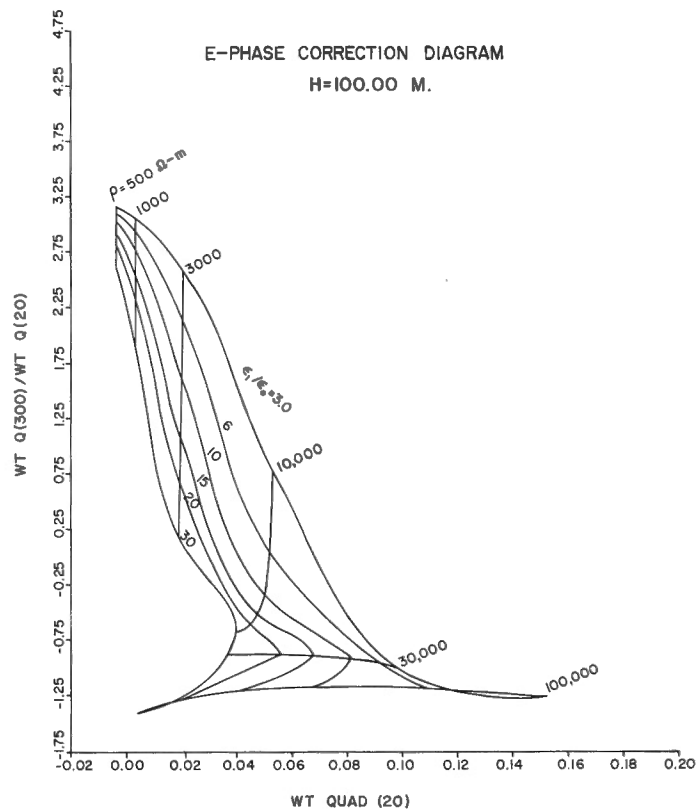


Figure 13.8. Correction diagram for E-Phase for an altitude of 100 m and frequency combinations of 300 and 20 kHz.

References

Barringer, A.R.

1971: Airborne exploration; Min. Mag., v. 124, no. 3, p. 1-6.

Norton, K.A.

1937: The propagation of radio waves over the surface of the earth and in the upper atmosphere, Part II; Proc. of the Institute of Radio Engineers (IRE), v. 25, no. 9, p. 1203-1236.

Paterson, N.R. and Ronka, V.

1971: Five years of surveying with the very low frequency electromagnetic method; Geoexploration, v. 9, no. 1, p. 7-26.

Sinha, A.K.

1976: A technique for obtaining correct ground resistivity from airborne wave tilt measuring systems; in Report of Activities, Part B, Geol. Surv. Can., Paper 76-1B, p. 281-283.

1977: Influence of altitude and displacement currents on plane-wave EM fields; Geophysics, v. 42, no. 1, p. 77-91.

Project 710036

F.G. Young
Institute of Sedimentary and Petroleum Geology, Calgary

Introduction

Upper Lower Cretaceous (Aptian and Albian Stages) and possibly lowest Upper Cretaceous (Cenomanian Stage) rocks in northern Yukon Territory comprise a very thick flysch sequence which thins rapidly eastward and changes facies to bedded ironstone and shale in northwestern District of Mackenzie. Field studies of these rocks by the writer have been carried out sporadically for the last eight field seasons, and have been concentrated in the northern Richardson Mountains (Fig. 14.1). Sufficient data have been gathered to define stratigraphic units in this sequence and to construct a sedimentological model. This paper summarizes knowledge of the stratigraphy and sedimentology of the sequence to date.

The mountainous area in which the flysch sequence outcrops is structurally complex, thus hindering determination of the stratigraphic sequence. The western limit of the study area is bounded by the north-trending Blow Fault Zone (Young, 1974) east of which is the associated Rapid Fault Array (Norris, 1974; Yorath and Norris, 1975). East of the fault array, broad northeast-trending folds, cut by steeply dipping, northeast-trending faults, are the dominant structural elements. Mackenzie Delta delimits the eastern margin of the outcrop area. Total width of the study area is 65 km (40 miles).

Brief descriptions and interpretations of the Aptian-Albian flysch division in the study area have been published previously (Young, 1972, 1973, 1974; Young et al., 1976). Jeletzky (1971, 1972, 1974, 1975a, b) has described the stratigraphy, lithology, and paleontology of these rocks to the southwest.

Not only the structural complications but also the lack of stratigraphic markers and near-absence of fossils have created great difficulties in unravelling the flysch stratigraphy. Microfossil recoveries are extremely sparse and practically useless for age determinations (T.P. Chamney and J.H. Wall, pers. comm.). Palynological analysis is similarly impractical because of the sparse and blackened nature of all palynomorphs, with the exception of those from samples along the eastern margin of the outcrop area (W.W. Brideaux, pers. comm.). The rare ammonites and pelecypods that have been found provide the only biostratigraphic data.

Stratigraphy

The northwestern Richardson Mountains can be subdivided into four structural blocks which are convenient for describing the flysch and ironstone stratigraphy. Each block is separated from its neighbour by a major, north-trending vertical fault (Fig. 14.1). From west to east these blocks are named the Skull Ridge (A), Rapid Creek (B), Mount Davies Gilbert (C), and Big Fish River (D) structural blocks. The mid-Cretaceous stratigraphy within each block is fairly consistent, and differs in important respects from that of other blocks.

In the following paragraphs the stratigraphy of each block is described briefly, using informal stratigraphic units. The problems of correlation and facies changes are discussed at the end of this section.

Skull Ridge Block

Recent field work has resulted in the establishment of the stratigraphic sequence and approximate thickness of the flysch sequence in this area. The total thickness of strata between the top of the Upper sandstone division and the base of the Boundary Creek Formation is approximately 4000 m (13 200 ft), as determined from a combination of direct measurements and graphic calculations based on structural data and airphoto mapping.

Stratigraphic units recognized in the flysch sequence of the Skull Ridge block include, from base to top: the lower shale unit, the conglomerate and sandstone unit, the upper shale unit, and the turbiditic sandstone and shale unit.

The lower shale unit conformably overlies calcareous sandstone and bioturbated mudstone of the Upper sandstone division and consists predominantly of grey-black, brittle shale, with quartz sandstone and ironstone in the basal third of the unit. It ranges in thickness from 370 to 730 m (1200–2400 ft) and is generally poorly exposed. The relatively resistant quartz sandstone and ironstone member varies from 40 to 200 m (130–650 ft) in thickness, and contains rare beds of chert-pebble conglomerate and diamictite.

The imposing conglomerate and sandstone unit of Skull Ridge (Young, 1973; Young et al., 1976) overlies conformably the lower shale unit. The contact is abrupt where the 60 m (200 ft) thick conglomerate tongue overlies the shale, but is more gradational elsewhere. The thickness of this unit is now known to be 2100 m (7000 ft). It can be subdivided into four members subequal in thickness in the immediate area of Skull Ridge including, from base to top: a basal conglomerate-sandstone, a lower sandstone, a middle pelite, and an upper sandstone.

Clastic rocks of the conglomerate-sandstone member are notably rich in chert and lithic clasts, and are commonly carbonaceous. The ammonite *Sonneratia* sp. was collected from this member, and identified by J.A. Jeletzky (pers. comm., 1972) who assigned it an early Early Albian age. This member grades into the flaggy sandstones of the lower sandstone member, which is approximately 700 m (2300 ft) thick. Coalified plant remains, current lineations, and parallel lamination are common characteristics of these sandstone beds (Fig. 14.2). Very thin bedded siltstone and shale form a minor part of this member, but are rarely exposed. The middle pelite member is also only sparsely exposed, but debris on hillslopes indicates the abundance of siltstone and dark grey shale. The upper sandstone member consists of thin to medium bedded sandstone rhythmically interbedded with shale and siltstone (Fig. 14.3). Ripple lamination and flute-casts are common in these rocks, which are probably turbiditic in origin.

The upper shale unit of the flysch sequence is known to the writer only in the lower end of Purkis Creek valley, north of Skull Ridge. Because of tectonic disturbance, its thickness can be only roughly estimated, and is in the order of 1000 m (3300 ft). This unit consists of silt-laminated, dark grey shale, with minor very fine grained sandstone. Black sooty shale predominates in the upper third of the unit.

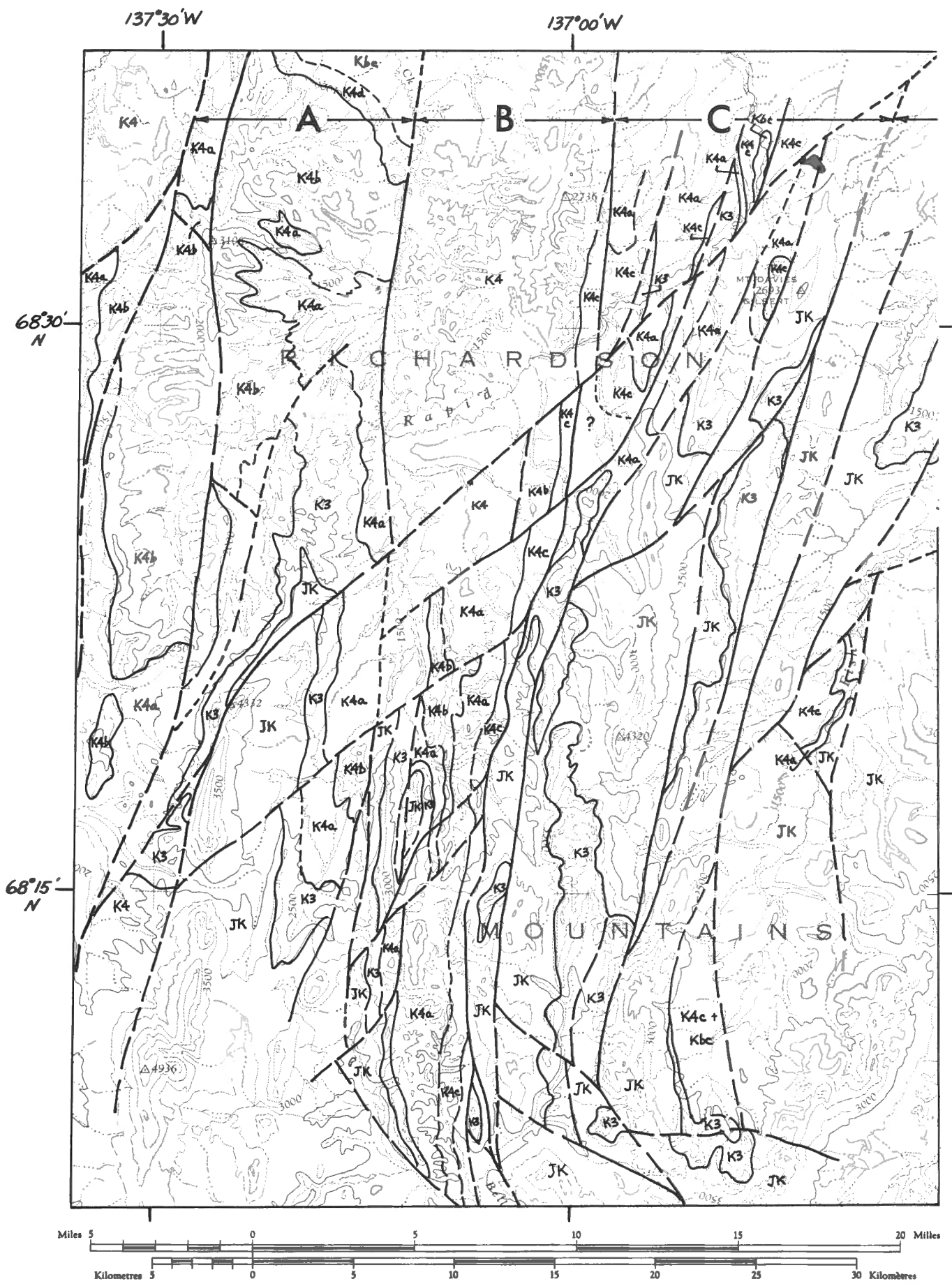
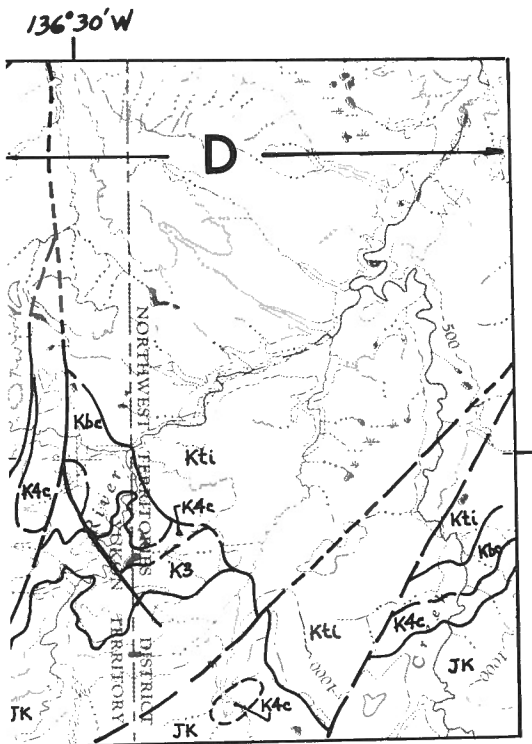


Figure 14.1. Geological map showing distribution of mid-Cretaceous units in northwestern Richardson Mountains.



----- Fault (defined, approximate, assumed)

CRETACEOUS AND TERTIARY
UPPER CRETACEOUS

- Kti Tent Island Formation (and younger)
- Kbc Boundary Creek Formation

LOWER CRETACEOUS

- K4d Upper shale unit
- K4c Bedded ironstone & shale unit
- K4b Conglomerate & sandst. unit (A); turbidite sandstone unit (B)
- K4a Lower shale unit
- K3 Upper sandstone division

K4 Aptian-Albian Flysch, undivided

JURASSIC AND LOWER CRETACEOUS

- JK Sedimentary rocks older than K3

- A - Skull Ridge block
- B - Rapid Creek block
- C - Mount Davies Gilbert block
- D - Big Fish River block

The upper shale unit is overlain abruptly by the turbiditic sandstone and shale unit, 85 m (280 ft) thick, which in turn grades into dark grey, reddish-weathering chippy shale, recognizable as Boundary Creek Formation. These contact relations suggest that the turbiditic sandstone unit may be related more to the Boundary Creek Formation than to the Albian flysch division.

Rapid Creek Block

The Rapid Creek block is a narrow, north-trending structural element, drained by the upper tributaries of Rapid Creek (Fig. 14.1). Except for a narrow belt of outcrops formed by the Upper sandstone division and underlying Upper shale-siltstone division along its western flank at the south end, only the thick mid-Cretaceous flysch sequence occurs in this block, and, in general, dips steeply eastward.

In ascending order, the sequence consists of the lower shale unit, the turbidite sandstone unit, the bedded ironstone and shale unit, and the upper shale unit. In the southern part of the block, the turbidite unit grades laterally into shale, resulting in a very thick lower shale unit.

The appearance of grey-black, brittle, ferruginous shale above generally bioturbated silty mudstone defines the basal contact of the lower shale unit of the flysch sequence on the upper member of the Upper sandstone division. At or near the base of the lower shale unit is a quartz sandstone and ironstone member, as in the Skull Ridge block. It ranges up to 150 m (490 ft) in thickness, and contains fine grained quartz arenite, siltstone, shale, and rare chert-grit diamictite. In the Bell River headwaters, some of the arenaceous beds contain blue and green phosphate minerals as cements. Sideritic ironstone and carbonaceous films are common also in this member.

At the north end of the block an upper tongue of the lower shale unit above the turbidite sandstone unit contains minor thin beds of sandstone, but becomes less arenaceous and silty southward, and combines with the lower tongue to form a single brittle shale unit about 1600 m (5300 ft) thick at the southern end of the block. In this area the upper 200 m (680 ft) of the unit contain abundant laminae and very thin beds of siltstone.

The turbidite sandstone unit attains a thickness of 700 m (2300 ft) in the northern end of the block, but thins and becomes mainly siltstone and shale (Fig. 14.4) toward the south end. Arenaceous rocks of this unit are characteristically chert rich and dark coloured (Young, 1973).

The bedded ironstone and shale unit gradationally overlies the lower shale, and it occurs along the entire eastern margin of the Rapid Creek block. A complete section is available only at the south end, however, where it is 1000 m (3300 ft) thick. The shale in this unit is typically very brittle, splintery, dark grey, and pyritic. Irregular laminae of spherulitic pyrite and siderite are common in this rock. The ironstone is mainly argillaceous microcrystalline siderite, and forms thin, laterally extensive beds. Phosphate mineralization was observed near the top of the unit at the south end of the block. A chemical analysis of a typical specimen from this facies is given in Table 14.1.

The recessive, upper shale unit overlies the bedded ironstone and shale only at the south end of the block. Here several hundred metres of medium grey, non-brittle shale occur below the eastern bounding fault.

Mount Davies Gilbert Block

Mid-Cretaceous rocks outcrop only at the north end of this block, in the vicinity of Rapid Creek. The stratigraphic units and their thicknesses are transitional between the thick flysch sequence immediately to the west and the thin ironstone-shale sequence characteristic of the block to the east.

Table 14.1

Chemical analyses of Albian ironstone

Structural Block	Sample No.	Fe ₂ O ₃ ^T	MnO	CaO	SiO ₂	Al ₂ O ₃	FeO	P ₂ O ₅	CO ₂	Other	H ₂ O ^T	Total
Rapid Creek	121YA-8	32	4	20	20	3	20.5	18	9.6	4.7	3.6	100.4
Mount Davies Gilbert	142YA-28	24	0.5	16	23	3	15.4	15	12.9	3.9	2.4	99.0
	142YA-32	41	2	3	12	1	17.2	27	1.8	4.6	6.6	97.0
	142YA-33	32	3.5	13	26	2	0.7	12	5.4	1.2	5.3	100.1
	142YA-34	35	3.5	18	13	2	0	18	1.8	0.8	7.3	99.4
	142YA-35	32	4	6	26	0.9	13.7	21	3.4	5.2	4.1	101.3
	Average		32.8	2.7	11.2	20	1.8	9.4	18.6	5.1	3.1	5.1
Big Fish River	20YA-4	38	8	9	9	2.5	31.6	7	25	2.4	2.5	100.0
	16YAb-19	30	5	17	11	3	23.2	13	18.7	2.4	3.1	101.4
	108YA-1	39	6	6	14	3	34	4	24	4.0	2.4	99.4
	108YA-4	27	3.5	10	21	5	18.4	18	8	4.9	4	99.8
	108YA-9	42	3	4.5	14	3	35	4	26	3.9	2.7	100.0
	Average		35.2	5.1	9.3	13.8	3.3	28.4	9.2	20.3	3.5	2.9

Note: Fe₂O₃^T means total Fe calculated as Fe₂O₃

H₂O^T means total H₂O

Other includes TiO₂, K₂O, MgO, and Na₂O

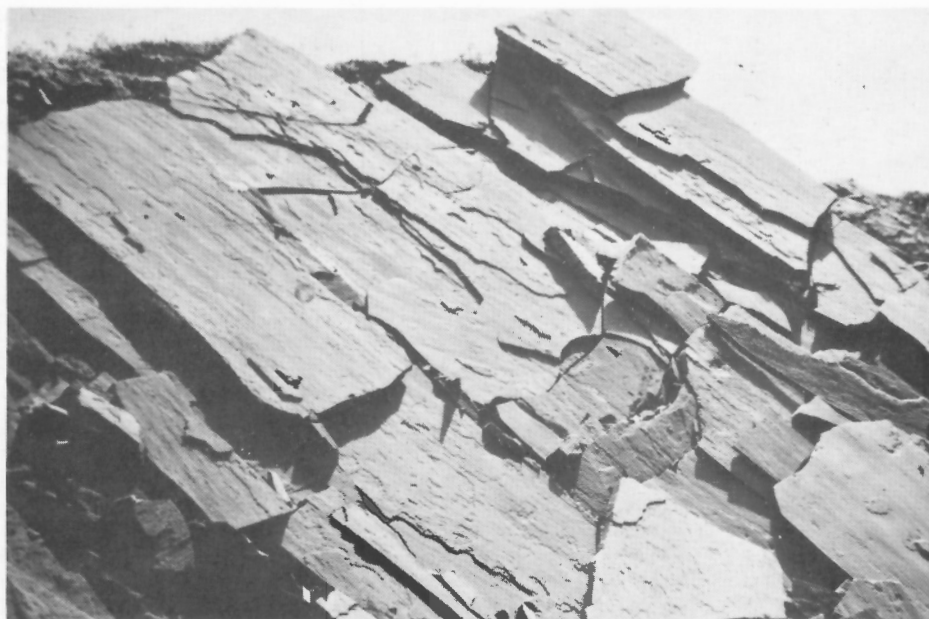


Figure 14.2. Primary parting lineations in flaggy sandstone of conglomerate-sandstone member, Albian flysch division, Purkis Creek area.

In ascending order, the mid-Cretaceous sequence consists of the lower and upper members of the Upper sandstone division [upper member previously called concretionary silty mudstone division (Young, 1972)], lower shale unit, bedded ironstone and shale unit, and Boundary Creek Formation.

The upper member of the Upper sandstone division is characterized by bioturbated, concretionary, dark grey shale and siltstone. It thickens from about 90 m (295 ft) near Mount Davies Gilbert to approximately 300 m (985 ft) on Rapid Creek just 5.5 km (3.5 miles) southwest.

The base of the Albian flysch-equivalent sequence is marked by the presence of chert-pebble diamictite or pebbly mudstone. Regional correlations suggest this contact may be unconformable in this structural block, especially toward the east.

The lower shale unit is 260 m (850 ft) thick near Mount Davies Gilbert, and thickens abruptly to approximately 550 m (1800 ft) a few kilometres westward (Fig. 14.2). It too is burrowed in part in its basal 60 m (197 ft), but is largely devoid of biogenic structures above this level. It is characterized by brittle, dark grey shale and mudstone, with rare "floating" chert pebbles, some of which are 40 to 50 mm in diameter. Siltstone is common in the basal 30 m (98 ft), and is notably ferruginous and dark blue weathering in the western part of the block. Flat clay-ironstone concretions are sparse throughout the unit. A 10 cm thick (3.9 in.) light green clay bed occurs about halfway through the unit in two sections studied, and may represent a volcanic ash fall.

The bedded ironstone and shale unit overlies conformably the lower shale unit, and is 350 m (1145 ft) thick, including a 95 m (310 ft) thick, siltstone-rich member at its base. This unit exhibits an interesting array of rock types, mineral varieties, and diagenetic phenomena in this structural block (see below). No fossils have yet been found from this unit in this area.

Ironstone comprises about 15 per cent of the unit of which shale is the major constituent. Lenticular beds of intraformational conglomerate, diamictite, and breccia, up to 3 m (10 ft) thick, are relatively rare. Shale with rare to

minor ironstone occurs in tongues up to 25 m (82 ft) thick between zones much richer in ironstone. At the top of the bedded ironstone and shale unit, small cycles, 6 to 10 m (20–33 ft) thick, are formed by upward increases in the abundance and bed-thickness of ironstone.

Big Fish River Block

In the Big Fish River area, the Aptian-Albian sequence is relatively thin and non-flyschoid in character. The Albian Stage is represented entirely by the bedded ironstone and shale unit, which, in many places, lies unconformably above the lower part of the Upper sandstone division, or even older strata (Fig. 14.5). However, at sections exposed in the gorge of Big Fish River at Latitudes 68°27'N and 68°20'N, the sequence is complete, and bedded ironstone overlies conformably the argillaceous upper member of the Upper sandstone division. The thickness of the concretionary mudstone of the upper member is 152 m (500 ft) and 122 m (400 ft) respectively at these localities. On Boundary Creek, just 4 km (2.5 miles) north of the first locality, however, the upper member is absent, and sandy shale of the bedded ironstone and shale unit rests disconformably upon a 1 m (3.3 ft) thick bed of ferruginous regolith formed on shallow marine quartz arenite of the Upper sandstone division.

In the area of Little Fish Creek near Latitude 68°27'N, the bedded ironstone and shale unit lies disconformably on the Husky Formation, a bioturbated siltstone unit of Late Jurassic to earliest Cretaceous age. The basal bed of the Albian unit is typically dark green due to the presence of glauconite pellets, and commonly contains chert pebbles and coalified wood fragments.

The bedded ironstone and shale unit in the Big Fish River block ranges in thickness from 60 m (200 ft) at the south end to 105 m (350 ft) at the north. In all sections the basal member is a grey-black, brittle, ferruginous shale or argillite. In the lower part of the overlying ironstone-shale member, marine fossils including gastropods, ammonites, and pelecypods are present. Identified forms include *Inoceramus* ex gr. *I. anglicus-cadottensis* and the ammonite *?Sonneratia* n. sp. A (identified by J.A. Jeletzky, internal report), indicative of an Early Albian age.

Correlations and Facies Changes

Correlations within any structural block are fairly straightforward. However, correlations of sequences between adjacent blocks are more speculative, owing to a lack of fossils and distinctive marker beds, and the great variation in thickness from east to west. The similar stratigraphic positions of the conglomerate and sandstone unit and the turbidite sandstone unit, respectively, in the Skull Ridge and Rapid Creek structural blocks, suggest that they are correlative. Their abrupt basal contacts form a horizon used as a rough stratigraphic datum. The shaly sequence below this level is similar in both areas, and may be equivalent to the lower shale unit of the Mount Davies Gilbert block. The presence of *?Sonneratia* n. sp. A in the lower part of the



Figure 14.3. Sequence of rhythmically interbedded sandstone, shale and siltstone of probable turbidite origin, upper sandstone member of conglomerate and sandstone unit. Beds are overturned and face left.

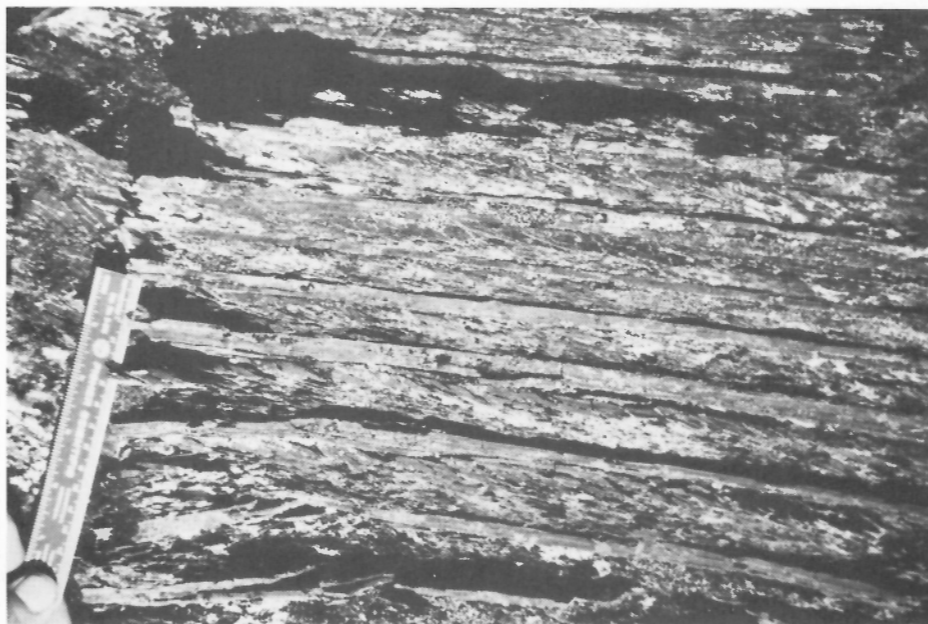


Figure 14.4. Rhythmically interbedded siltstone and cleaved shale at distal end of Albian turbidite tongue, lower shale unit of Rapid Creek block, north-central Richardson Mountains.

conglomerate and sandstone unit of the Skull Ridge block and in the lower part of the bedded ironstone and shale unit of the Big Fish River block allows a correlation between these remotely spaced structural blocks. This correlation, as well as the gradual disappearance eastward of turbiditic sandstones which is matched by an increase in ironstone and shale, suggests that the turbidites grade laterally into the ironstone and shale. This transition is accomplished through a series of steps, which are illustrated in the stratigraphic profile (Fig. 14.5).

Poorly sorted conglomerate and medium grained carbonaceous sandstone in the conglomerate and sandstone unit of the Skull Ridge block grade rapidly eastward into very fine to fine grained turbiditic sandstone and interbedded shale of

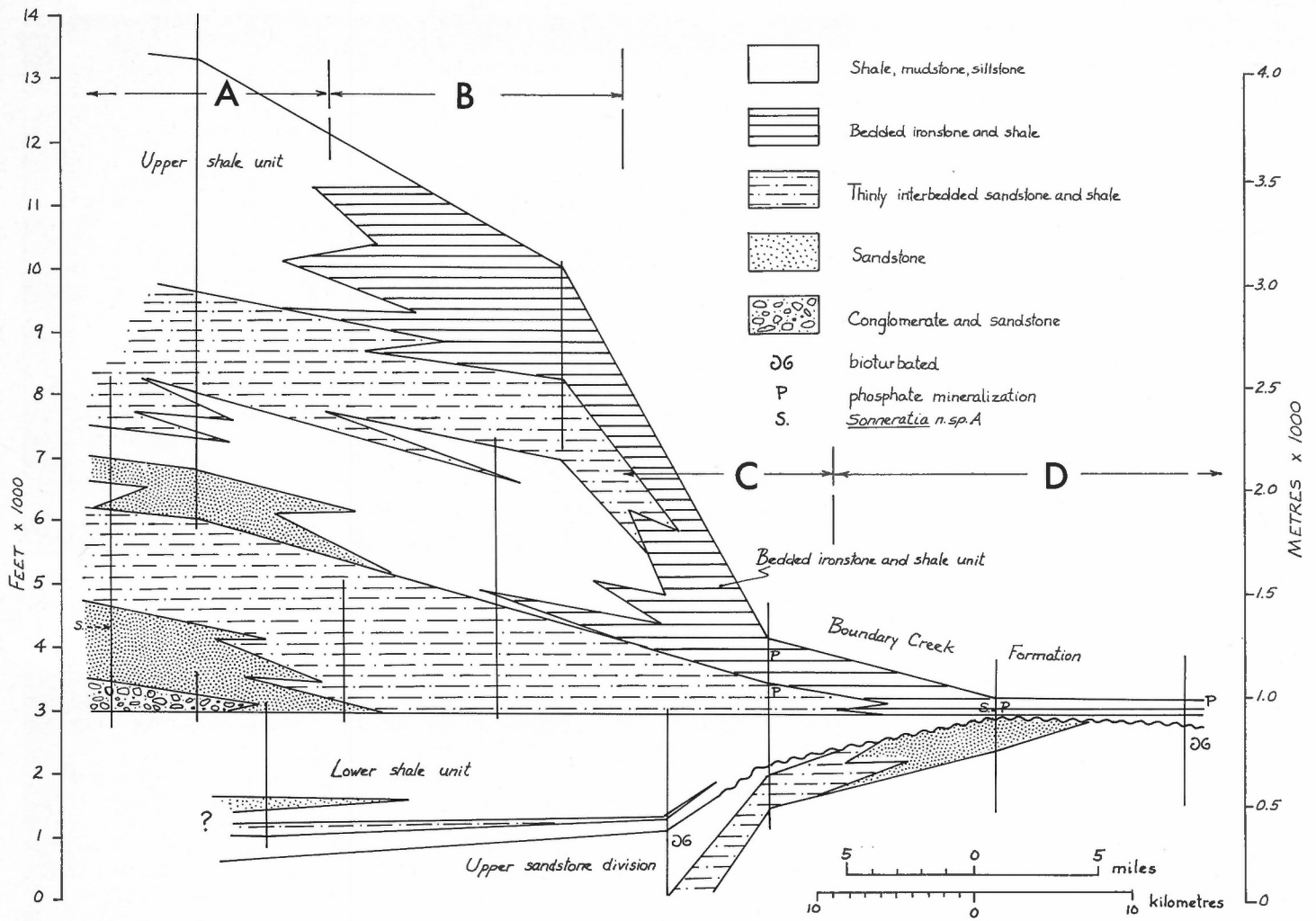


Figure 14.5. East-west stratigraphic profile of mid-Cretaceous units in northern Richardson Mountains. Letters refer to structural blocks denoted on Figure 14.1.

Figure 14.6.

Resistant ironstone beds with interbedded brittle shale, upper Big Fish River area.



the turbidite sandstone unit in the Rapid Creek block. The sandstone beds become thinner eastward, lose their flute- and groove-casts, and grade into laminated siltstone and ironstone beds of the basal part of the bedded ironstone and shale unit in the Mount Davies Gilbert block. Eastward in the Big Fish River area, siltstone and ironstone pass laterally into shale and ironstone beds, and the ironstone becomes increasingly predominant eastward.

The pelitic upper portion of the flysch sequence of the Skull Ridge block grades southeast and eastward into ferruginous shale and bedded ironstone. Hence, the latter facies constitutes a distal facies with respect to both turbidites and associated pelites, and is assumed to have been deposited in relatively deep water.

Sedimentology of the Phosphatic Ironstone

Phosphatic ironstone beds are an important component of the bedded ironstone and shale unit, and form a minor part of the quartz sandstone and ironstone member of the lower shale unit. The ironstone occurs primarily as thin beds, each being separated from succeeding beds by a thin layer or bed of ferruginous, brittle shale (Fig. 14.6).

In the Mount Davies Gilbert block, the ironstone includes compact microcrystalline siderite, medium grained to pebbly ironstone-intraclast wackestones and packstones, and pyrite-phosphate rock. All these varieties are phosphatic, with phosphate minerals appearing within mud matrix, as sparry replacement cements, and in veinlets and open fractures. The textures of the conglomerates and breccias can only be appreciated on freshly slabbed surfaces, owing to the dark bluish grey weathering patina appearing on all outcrops.

Intraclasts are generally subangular bits of dark grey microcrystalline ironstone, although tan-coloured microcrystalline fragments, possibly rich in phosphate, also occur rarely. Size sorting is generally poor. Some of the packstones display good to excellent microvuggy porosity, whereas others show complex replacement textures by siderite and phosphate minerals, particularly childrenite.

Lenses of ironstone-clast conglomerate were observed associated with overturned slump-folds, and are probably debris flows impelled by downslope creep. Clasts in these conglomerates are mainly angular, highly variable in size, and in jumbled orientations. Axial planes on most slump-folds are overturned toward the east.

Ironstone beds increase in abundance northeastward, and form a maximum of approximately 37 per cent of the section in the Boundary Creek-Big Fish River area. In this area, the ironstone is principally microcrystalline siderite, occurring in hard, thin to medium beds. The thickest ironstone bed observed to date is 70 cm (27.6 in.) thick, observed in the middle course of Big Fish River. Beds are commonly banded internally due to slight colour variations or the presence of layers of pyrite or siderite.

The brittle nature of microcrystalline ironstone evidently developed soon after deposition, as fractures and brecciation of ferruginous laminae appear within undisturbed shale beds. This brecciation undoubtedly led to the formation of ironstone intraclasts, which were reworked by bottom currents in the area of Mount Davies Gilbert. Fractures of various ages are lined commonly with quartz and/or phosphate minerals, and some are still partly open.

Economic Geology

The bedded ironstone and shale unit and the quartzose sandstone member of the lower shale unit are interesting not only from a sedimentological viewpoint, but also because of their iron, manganese and phosphate contents, and the host of curious and unique mineral species found in them.

Semi-quantitative chemical analyses of a suite of ironstone samples supplied by the writer were carried out in the laboratories of the Geological Survey in Ottawa. The results of these analyses are shown in Table 14.1, and arranged according to the structural block from which samples were derived. As can be seen from the average values determined for each block, the amount of total iron, reported as ferric oxide equivalent, increases but slightly from west to east. Manganese is richer in the Big Fish River area, but silica and phosphate are distinctly higher in proportion in the Rapid Creek-Mount Davies Gilbert area. Because ferrous oxide and carbon dioxide are more abundant in the Big Fish River samples than in the Mount Davies Gilbert samples, it seems likely that siderite (iron carbonate) is more abundant in the Big Fish area.

Some mineral claims have been staked by Welcome North Mines Limited on Rapid Creek and Big Fish River but, compared with other iron deposits, this formation is definitely of low grade. The high phosphorous content would necessitate its removal before submitting an ore-concentrate to steel-making processes. Nevertheless, the volume of low grade iron-formation in the area is impressive.

A rough calculation of reserves in the Rapid Creek-Big Fish River area was made, using an average composition of 33% Fe₂O₃, 14% P₂O₅, and 5% MnO, a specific gravity of 3.4, and a subsurface limit of 1000 m (3300 ft). This yielded approximately 27 x 10⁹ metric tonnes (30 x 10⁹ tons) of ironstone, of which about 10¹⁰ metric tonnes (11 x 10⁹ tons) would be Fe₂O₃ equivalent. Nearby drilling for petroleum may prove up more ironstone immediately east of the outcrop area and ironstone at the surface in the Rapid Creek Block was ignored in the calculations.

Phosphate content of the ironstones is also of interest, although undoubtedly subeconomic at the present time. Unlike the iron content, phosphorous content is highly variable from sample to sample, so that values of phosphate ranging between 25 and 30 per cent might be concentrated in certain groups of beds. The prime interest at present is in the excellent phosphate mineral specimens prized by mineralogists and rockhounds. Mineralogists of the Royal Ontario Museum have collected extensively from the Rapid Creek and Big Fish River outcrops, and have reported the presence of the minerals lazulite, brazilianite, augelite, wardite, childrenite, ludlamite, vivianite, and arrojadite (Sturman and Mandarino, 1975). New minerals named and described already from these localities include kulanite (Mandarino and Sturman, 1976), baricite (Sturman and Mandarino, 1976), maricite (Sturman et al., 1977), and penikisite (Mandarino et al., 1977).

Of interest to petroleum explorationists is the good to excellent microvuggy porosity and abundant open fractures in intraclastic ironstones of the Mount Davies Gilbert area. This porosity enhances the attractiveness of the numerous anticlines north and northwest of Mount Davies Gilbert as hydrocarbon traps. Because of the blackened state of palynomorphs in this area, it is likely that only natural gas would be found here.

Acknowledgments

I am grateful to T.P. Poulton, Geological Survey of Canada, for providing an operational base and considerable helicopter time during the 1976 field season. Similar appreciation is extended to A.E. Calverley, Petro-Canada Exploration Inc., who kindly invited me to join his field party in 1977. Discussions held with G.A. Gross, D.K. Norris, J.A. Jeletzky, and R.L. Christie on various aspects of this stratigraphic sequence have been most helpful. Finally, the cheerful assistance provided by numerous student-helpers over the years is gratefully acknowledged.

References

- Jeletzky, J.A.
1971: Stratigraphy, facies and paleogeography of Mesozoic rocks of northern and west-central Yukon; in Report of Activities, Part A, Geol. Surv. Can., Paper 71-1A, p. 203-221.
1972: Stratigraphy, facies and paleogeography of Mesozoic and Tertiary rocks of northern Yukon and northwestern District of Mackenzie; Geol. Surv. Can., Open File 82.
1974: Contribution to the Jurassic and Cretaceous geology of northern Yukon Territory and District of Mackenzie, Northwest Territories; Geol. Surv. Can., Paper 74-10.
1975a: Sharp Mountain Formation (new): a shoreline facies of the Upper Aptian-Lower Albian flysch division, eastern Keele Range, Yukon Territory; in Report of Activities, Part B, Geol. Surv. Can., Paper 75-1B, p. 237-244.
1975b: Jurassic and Lower Cretaceous paleogeography and depositional tectonics of Porcupine Plateau, adjacent areas of northern Yukon and those of Mackenzie District; Geol. Surv. Can., Paper 74-16.
- Mandarino, J.A. and Sturman, B.D.
1976: Kulanite, a new barium iron aluminum phosphate from the Yukon Territory, Canada; Can. Mineral., v. 14, p. 127-131.
- Mandarino, J.A., Sturman, B.D., and Corlett, M.I.
1977: Penikisite, the magnesium analogue of kulanite from Yukon Territory, Canada; Can. Mineral., v. 15, p. 393-395.
- Norris, D.K.
1974: Structural geometry and geological history of the northern Canadian Cordillera; in Proc. of the 1973 National Convention, A.E. Wren and R.B. Cruz, eds., Can. Soc. Exploration Geophysicists, Calgary, p. 18-45.
- Sturman, B.D. and Mandarino, J.A.
1975: Phosphate minerals from the Yukon Territory, Canada; in Abstracts with programs, Joint Mtg. of Geol. Soc. Am. (North-Central Sect.), Geol. Assoc. Can., and Mineralogical Assoc. Can., Waterloo, p. 865-866.
1976: Baričite, the magnesium analogue of vivianite, from Yukon Territory, Canada; Can. Mineral., v. 14, p. 403-406.
- Sturman, B.D., Mandarino, J.A., and Corlett, M.I.
1977: Maričite, a sodium iron phosphate from the Big Fish River area, Yukon Territory, Canada; Can. Mineral., v. 15, p. 396-398.
- Yorath, C.J. and Norris, D.K.
1975: The tectonic development of the southern Beaufort Sea and its relationship to the origin of the Arctic Ocean Basin; in Yorath, C.J., E.R. Parker, and D.J. Glass, eds., Canada's Continental Margins and Offshore Petroleum Potential, Can. Soc. Petrol. Geol., Mem. 4, p. 589-612.
- Young, F.G.
1972: Cretaceous stratigraphy between Blow and Fish Rivers, Yukon Territory; in Report of Activities, Part A, Geol. Surv. Can., Paper 72-1A, p. 229-235.
1973: Mesozoic epicontinental, flyschoid and molassoid depositional phases of Yukon's north slope; in Proc. Symp. on the Geology of the Canadian Arctic, J.D. Aitken and D.J. Glass, eds.; Can. Soc. Petroleum Geologists, Calgary, and Geol. Assoc. Can., p. 181-201.
1974: Cretaceous stratigraphic displacements across Blow Fault Zone, northern Yukon Territory; in Report of Activities, Part B, Geol. Surv. Can., Paper 74-1B, p. 291-296.
- Young, F.G., Myhr, D.W., and Yorath, C.J.
1976: Geology of the Beaufort-Mackenzie Basin; Geol. Surv. Can., Paper 76-11.

Project 740030

J. Wm. Kerr

Institute of Sedimentary and Petroleum Geology, Calgary

During the summers of 1975 and 1976, the writer did bedrock mapping on Somerset Island and Boothia Peninsula (Kerr and de Vries, 1976, 1977; Reinson et al., 1976; Miall and Kerr, 1977). In the course of that work, he made observations on many mounds and other small topographic features. Nearly all those observed appear to be simple erosional remnants, felsenmeer-mantled bedrock highs controlled by the interplay of periglacial weathering and erosional processes on bedrock. Three small mounds (Fig. 15.1), on which additional controls are suggested, are described here.

On northwestern Somerset Island, a small buckle occurs in the Proterozoic Hunting Formation (Fig. 15.2), and is attributed to frost heaving. The formation is thick bedded dolomite about 1000 m (3280 ft) thick that strikes northwest and dips uniformly northeast at 15 degrees. The formation is tilted regionally but not internally folded, indicating that the buckle did not form by regional tectonic deformation. It apparently formed by frost heaving. According to J. Veillette, (pers. comm., 1977), tilted beds present good conditions for infiltration of water down bedding planes, and buildup of ground ice to cause buckling of the overlying beds. Using the UTM co-ordinate system, this buckle is located in Zone 15X at 422250mE, 8181750mN. Using the co-ordinate system outlined by Norris (1972), it is located at +4.3X; -5.6Y on Airphoto A16194-211.

A small tor-like bedrock knob on eastern Somerset Island (Fig. 15.1, Loc. 2) is located at UTM Zone 15X, 534950mE; 8132200mN, and an Airphoto A16331-79 is at +7.4X; -1.75Y. It outcrops on the top of a moderate-size hill that is several hundred feet across and 50 or so feet high.

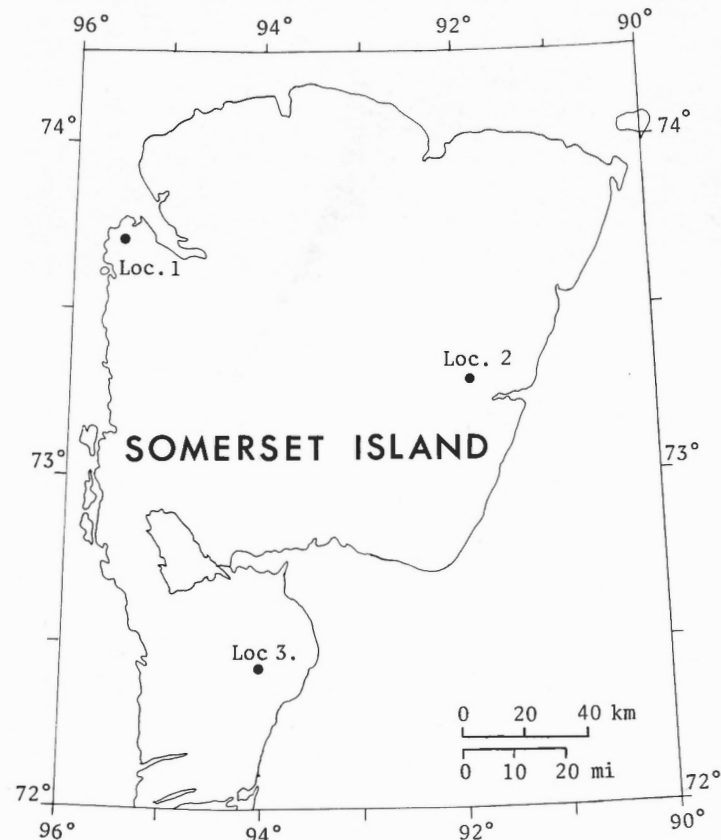


Figure 15.1. Index map of Somerset Island showing the locations mentioned in text.

From another bedrock outcrop nearby at lower elevation on the side of the same hill, the regional bedding was determined as striking north and dipping west at 5 degrees. The bedding in the knob in question, however, dips steeply to the west at 60 degrees (Fig. 15.3). A dislocation or displacement of some type therefore occurs between the two outcrops. This knob (Fig. 15.3) is in a region of gently dipping to horizontal Silurian limestone of the Read Bay Formation, and both outcrops are parts of that formation. A few near-vertical normal faults cross this region, but generally they do not produce steep dips. Moreover, it seems unlikely that there is a fault between the outcrops, because most faults in this region are long features, and therefore readily traceable and mappable on aerial photographs. No such lineament intersects the hill on which the knob occurs. It seems most reasonable, therefore, to conclude that the dislocation that produced the steep dip of the knob (Fig. 15.3) was due to either a glacial shove phenomenon or possibly to frost heaving. Glacial shoving may have buckled up the bedrock, perhaps in some way selectively buckling it up on the mound because it projects upward and the nearly horizontal beds at the top could be caught up by ice. The author can think of no other likely explanations.

On southern Somerset Island (Fig. 15.1, Loc. 3), another unusual carbonate bedrock mound exists (Fig. 15.4). This is a bedrock outcrop which, in its upper part, dips 45 degrees to



Figure 15.2. Frost-heaved outcrop of the Hunting Formation. View to the southeast along strike. Dip to the left (NE) at 15 degrees. Person provides scale. GSC Photo 199292.

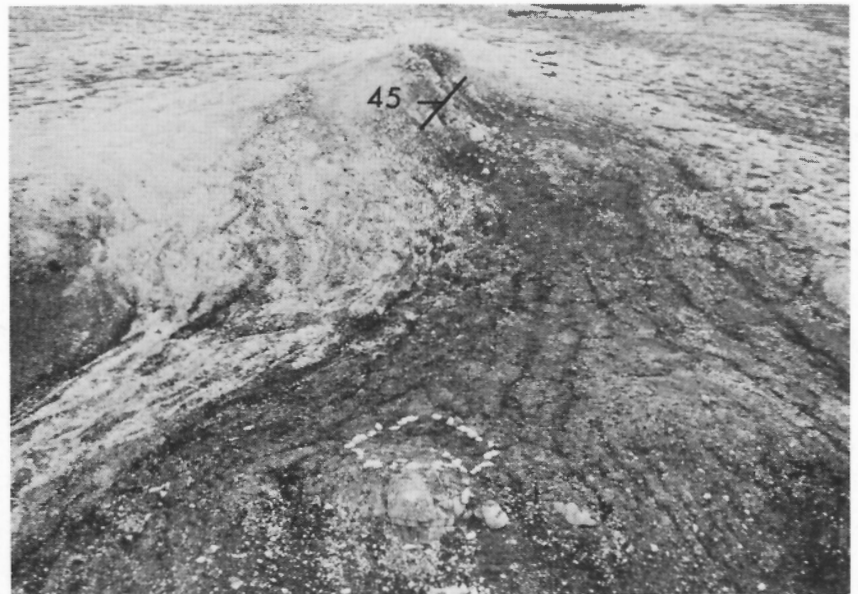


Figure 15.3.

Outcropping of the Read Bay Formation on eastern Somerset Island that may be glacially deformed bedding. View is to the north. The outcrop dips to the left (W) at 68 degrees. The regional dip in this region is 5°W. GSC Photo 199294.

Figure 15.4.

Outcropping of the Lang River Formation on southern Somerset Island. View is to the north. Tent ring in the foreground is 4 m (12 ft) in diameter. GSC Photo 199293. Located at UTM Zone 15x; 463900ME; 8037250mN.



the northwest. A prominent dislocation occurs between the top and lower part of this bedrock mound, for the lower part dips 24 degrees northwest. Interpretation of this exposure is uncertain. It may be due to faulting or to glacial or frost-heaving action. In this region faults are common and there are steep dips in places, although in most places the bedrock is nearly horizontal. Because of the thick alluvial cover in the vicinity, faults are not readily traceable, and a fault could well intersect the mound in question.

In both cases of possible glacial shove cited above (Figs. 15.3, 15.4), it is not possible to trace bedding planes continuously into completely exposed well-understood bedding, so the interpretation of both is rather tenuous. The writer suggests that the dislocation on eastern Somerset Island probably resulted from glacial shove with the ice moving westward. The knob on southern Somerset Island may be due to glacial shove, but could be due to faulting.

In eastern Somerset Island where the suggested glacially shoved knob occurs, Netterville et al. (1976) indicated a terrain of hummocky carbonate bedrock (their area Ia), containing numerous bedrock basin lakes interspersed with weathered bedrock cored knobs mantled by rubble. Dyke

(1976) interpreted this hummocky terrain as the product of glacial erosion, rather than primarily subaerial weathering. Hence, the knobs are not true tors, which are bedrock features that are a residual of differential weathering and mass movement. The present explanation of the bedding distortion (Fig. 15.3) as due to glacial ice would support Dyke's interpretation of the hummocky bedrock terrain as the product of glacial erosion.

One and possibly two knobs (Figs. 15.3, 15.4), in which deformed bedrock outcrops, suggest deformation by glacial ice. This implies that an ice sheet covered part or all of Somerset Island, as is also evident from the apparently ubiquitous distribution of erratics (Craig, 1964; Netterville et al., 1976; Dyke, 1976). In both cases, the shove is toward the west. This conflicts with evidence from striae on southern Somerset Island, which show an eastward flow (A.S. Dyke, pers. comm., 1977). The hypothesis can be tested by searching for more such knobs and recording the direction of displacement. The writer concurs with Dyke (1976) that the larger mounds on Somerset Island, which are rubble mantled and not obviously of stack type, are bedrock cored and due mainly to erosional processes, primarily glacial.

Acknowledgments

I am grateful to A.S. Dyke, O.L. Hughes, and R.W. Klassen for constructive criticism of this paper.

References

Craig, B.G.

1964: Surficial geology of Boothia Peninsula and Somerset, King William, and Prince of Wales Islands, District of Franklin; Geol. Surv. Can., Paper 63-44.

Dyke, A.S.

1976: Tors and associated weathering phenomena, Somerset Island, District of Franklin; in Report of Activities, Part B, Geol. Surv. Can., Paper 76-1B, p. 209-216.

Kerr, J.Wm. and de Vries, C.D.S.

1976: Structural geology of Somerset Island, District of Franklin; in Report of Activities, Part A, Geol. Surv. Can., Paper 76-1A, p. 493-495.

1977: Structural geology of Somerset Island, and Boothia Peninsula; Report of Activities, Part A, Geol. Surv. Can., Paper 77-1A, p. 107-111.

Miall, A.D. and Kerr, J. Wm.

1977: Phanerozoic stratigraphy and sedimentology of Somerset Island and northeastern Boothia Peninsula; in Report of Activities, Part A, Geol. Surv. Can., Paper 77-1A, p. 99-106.

Netterville, J.A., Dyke, A.S., Thomas, R.D., and Drabinsky, K.A.

1976: Terrain inventory and Quaternary geology, Somerset, Prince of Wales, and adjacent islands; in Report of Activities, Part A, Geol. Surv. Can., Paper 76-1A, p. 145-154.

Norris, D.K.

1972: A method for determination of geographic position; in Report of Activities, Part B, Geol. Surv. Can., Paper 72-1B, p. 124, 125.

Reinson, G.E., Kerr, J. Wm., and Stewart, W.D.

1976: Stratigraphic field studies, Somerset Island, District of Franklin (58B to F); in Report of Activities, Part A, Geol. Surv. Can., Paper 76-1A, p. 497-499.

Project 670016

J. Wm. Kerr

Institute of Sedimentary and Petroleum Geology, Calgary

An unusual sea stack (Fig. 16.1) was observed on northwestern Devon Island in the course of a bedrock study in 1971. It is located 1.45 km (0.9 mile) northeast of the coast of Prince Alfred Bay (Fig. 16.2, Loc. 4). Judging from the 1:250 000 topographic map of the area, it was estimated to be at about 100 m (350 ft) above sea level, and plotting in a Zeiss stereotopograph by G. Mizerovsky gave an elevation of 108 ± 5 m (354 ± 16 ft).

The pinnacle has a characteristic sea stack form and is associated with former marine beaches. The work of waves on a shoreline seems to be the only means of developing such a feature.

The stack stands about 5.5 m (18 ft) above the surrounding terrain (Fig. 16.1) and is the only stack in the region. It is located at 505600mE, 8460200mN in UTM Zone 15X. On aerial photograph A16147-164 it occurs at -6.1X; -3.8Y, using the grid system described by Norris (1972).

The stack is a slender pinnacle and is narrower at the base than at the top. The surrounding terrain is a plateau of rather flat to gently rolling topography, with shallow, narrow stream valleys. Nearly all of the land surface nearby is felsenmeer of the underlying bedrock. Small frost shattered bedrock outcrops project out of the felsenmeer in places on the uplands, but all other large outcrops are restricted to stream valleys.

The stack occurs in a bedrock unit of thick undivided Devonian carbonates (Morrow and Kerr, 1975). In the vicinity of the stack this unit is thick bedded dolomite, commonly with steep jointing. It occurs in a gentle syncline, where the beds at the stack are close to horizontal. The stack is composed of dolomite similar to the surrounding bedrock, but

is highly jointed and probably sheared. It probably is in a fault zone or major joint zone. Since no lineament was observable on the ground or on aerial photographs, displacement, if present, was minor. The resistant nature of the stack probably is due to silicification in this incipient shear zone.

It generally has been considered that most of the islands in the central Canadian Arctic were covered by ice and depressed below sea level during late Pleistocene (Wisconsin) time, and that the ice retreated in Holocene time, which began about 10 000 years ago. Since the region was subjected to Wisconsin glaciation, the stack must have developed after the disappearance of ice from that location in Holocene time.

It does not seem likely that this stack developed simply by solution because the process is too slow. Smith (1972) concluded that denudation by removal of dissolved solids from limestone in northwestern Somerset Island is about 2 mm per 1000 years. If this is representative of Holocene rates, only about 2 cm of denudation would have occurred by that process operating alone. It is equally unlikely that the stack formed by normal erosional processes on land.

Raised beaches formed on the Arctic Island during the Holocene in the period of upward rebound which followed the breakup and disappearance of the Innuitian Ice Sheet (Blake, 1970). Prominent raised beaches occur inland from the present shoreline of Prince Alfred Bay, and features that appear to be raised beaches occur close below the stack. The stack is regarded here as the highest indication of the upper limit of postglacial marine submergence on the east side of Prince Alfred Bay.



Figure 16.1. A sea stack near Prince Alfred Bay on northwestern Devon Island. GSC Photo 199291. It is located at Locality 4 (Fig. 16.2).

The minimum upper marine limit on parts of Devon Island now has been established as follows (Fig. 16.2); all elevations are approximate.

1. Head of Barrow Harbour (Grosswald, 1973) 125 m (410 ft)
2. Northwest of Stewart Point (Grosswald, 1973) 150 m (492 ft)
3. Southern Sheil's Peninsula (Grosswald, 1973) 150 m (492 ft)
4. East of Prince Alfred Bay (this report) 108 m (354 ft)
5. Norfolk Inlet (Blake, 1975) 123 m (405 ft)
6. Cape Hawkes (Blake, 1975) 120 + m (400 ft)
7. Wellington Channel (Roots, 1963, p. 177) 91 m (300 ft)
8. Eastern Jones Sound (Barr, 1971) 76 m (250 ft)

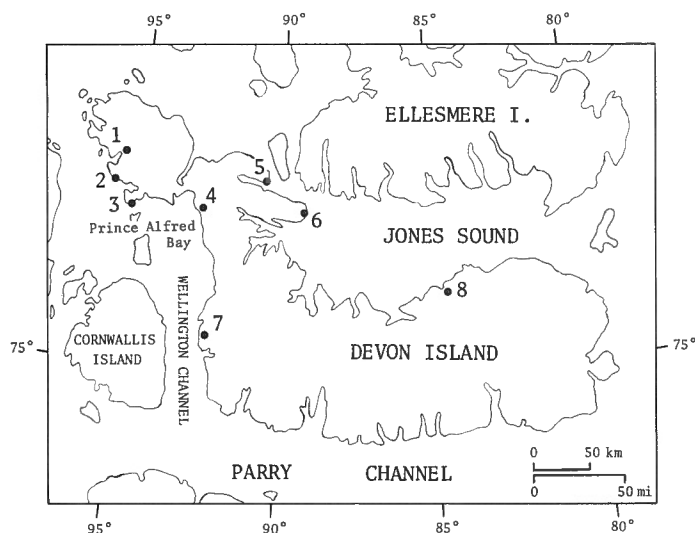


Figure 16.2. Index map of Devon Island showing localities mentioned in the text.

The marine limit appears to ascend westward on Devon Island as pointed out by Grosswald (1973). The sea stack near Prince Alfred Bay (Loc. 4) at about 108 m (345 ft) above sea level is compatible with the earlier observations. It confirms the data derived from raised beaches, which indicate that northwestern Devon Island has emerged a greater amount than eastern Devon Island. The pattern of differential uplift on Devon Island is similar to the situation in southern Ellesmere Island, where Blake (1970) reported that a pumice level, representing a time horizon in the sediments of the raised beaches, ascends westward.

Acknowledgments

I am grateful to W. Blake Jr., O.L. Hughes, G. Mizerovsky (Mrs.), and G.D. Osborne for help and constructive comment on this paper.

References

- Barr, W.
1971: Postglacial isostatic movements in northeastern Devon Island; a reappraisal; *Arctic*, v. 24, p. 249-268.
- Blake, W., Jr.
1970: Studies of glacial history in Arctic Canada I: Pumice, radiocarbon dates, and differential post-glacial uplift in the eastern Queen Elizabeth Islands; *Can. J. Earth Sci.*, v. 7, no. 2, pt. 2, p. 634-664.
1975: Radiocarbon age determinations and post-glacial emergence at Cape Storm, southern Ellesmere Island, Arctic Canada; *Geograf. Annual.*, Ser. A., *Phys. Geogr.*, Svenska Sällskapet För Anthropologi Och Geographi, v. 57A, no. 1-2, p. 1-71.
- Morrow, D.W. and Kerr, J. Wm.
1975: Stratigraphy and sedimentology of lower Paleozoic formations near Prince Alfred Bay, Devon Island (59B); *Geol. Surv. Can.*, Open File Report 255 and Bull. 254 in press.
- Grosswald, M.G.
1973: Reconnaissance glacial geology, Southwestern Grinnell Peninsula, Devon Island, District of Franklin; in Report of Activities, Part A, *Geol. Surv. Can.*, Paper 73-1A, p. 199-200.
- Norris, D.K.
1972: A method for determination of geographic position; in Report of Activities, Part B, *Geol. Surv. Can.*, Paper 72-1B, p. 124-125.
- Roots, E.F.
1963: Devon Island Physiography in *Geology of the north-central part of the Arctic Archipelago, Northwest Territories*, Y.O. Fortier et al.; *Geol. Surv. Can.*, Mem. 320, p. 164-179.
- Smith, D.I.
1972: The solution of limestone in an arctic environment in *Polar Geomorphology*, Price R.J. and Sugden, D.E., eds.; *Inst. Brit. Geogr.*, Spec. Publ. 4, p. 187-200.

Project 690005

D.K. Norris

Institute of Sedimentary and Petroleum Geology, Calgary

Introduction

Northern mainland and offshore Canada embraces the Western Canada Sedimentary Basin in Yukon Territory and Northwest Territories and the contiguous continental shelf of southern Beaufort Sea. The area can be divided into a number of physiographic elements. Those elements in which hydrocarbons have been discovered or in which the sedimentary successions are prospective are included in Figure 17.1. Flanking the Kazan Region of the Canadian Shield are the relatively undeformed strata underlying the Interior Plains. They are joined on the west and north by the deformed bedrock successions beneath the Cordilleran Region, Yukon Coastal Plain, Mackenzie Delta and Arctic Continental Shelf. The Cordilleran Region, moreover, embraces prospective, folded and faulted rocks of the Old Crow Plain, Eagle Plain and Liard Plateau. Beneath the continental shelf is a seaward-thickening blanket of (Neogene) sediments younger than the bedrock succession of the mainland.

Exploration for hydrocarbons in the area began in 1920 with the discovery of oil in a Middle Devonian reef at Norman Wells on the Mackenzie River (Fig. 17.1). The relative inaccessibility of the region combined with the hostile climate which prevails for more than half of the year seriously inhibited the growth of hydrocarbon exploration. Even in the momentous search for additional oil reserves during the Second World War (Canol Project), activity was confined largely to the main river courses. The advent of the helicopter in the 1950's, however, rendered virtually all parts of the region accessible. Geological mapping was extended throughout the northern mainland and regional syntheses of the structural and stratigraphic framework became possible.

The Sedimentary Wedge

The rock succession in this part of the northern mainland and adjacent continental shelf is in the form of an eastward-tapering and northward-truncated wedge, ranging in age from Proterozoic to Tertiary, and comprising two superposed, genetically and compositionally distinct, stratigraphic assemblages. The lower, Proterozoic to Lower Cretaceous miogeoclinal-platform and eugeoclinal assemblage thickens westward beneath the Interior Plains from its zero edge against the Canadian Shield to approximately 10 km at the eastern margin of the Cordilleran Region. Within the Cordillera, the composite, restored section would appear to have been more than twice as thick. The overlying, Lower Cretaceous and younger, exogeoclinal assemblage is the syn- and post-orogenic suite of rocks derived from deformed and uplifted areas farther west in the Cordilleran Region.

Many unconformities within this wedge attest to a long, regionally episodic history of orogeny and epeirogeny from the Proterozoic to the Tertiary. Although commonly they are disconformities, as beneath the Interior Plains, locally the unconformities are spectacularly angular, as in parts of the Cordilleran Region. Periods of deformation, uplift and differential erosion identified by these unconformities doubtless led to breaching of many hydrocarbon reservoirs so that the potential of the area is limited largely to the less-deformed rocks beneath the Interior Plains, Mackenzie Delta and Arctic Continental Shelf. Drilling experience during the past two decades lends support to this conclusion.

Potential Reservoir Rocks

The potential reservoir rocks for hydrocarbons in the northern mainland and offshore Canada range in age from Early Cambrian to Tertiary (Neogene) (Table 17.1). They are contained in three sedimentary sequences separated by regional unconformities. The Franklinian platform carbonates are known to contain gas in the southern Interior Plains (e.g. Rabbit Lake and South Island River wells). Moreover, a significant gas discovery was made (Ashland et al. Tedji Lake F-24) in basal Cambrian sandstones, 240 km north of Norman Wells (see Fig. 17.1). Gas continues to be produced in Liard Plateau from Middle Devonian carbonate rocks in the core of large anticlines along the eastern margin of the Cordilleran Region (Beaver River and

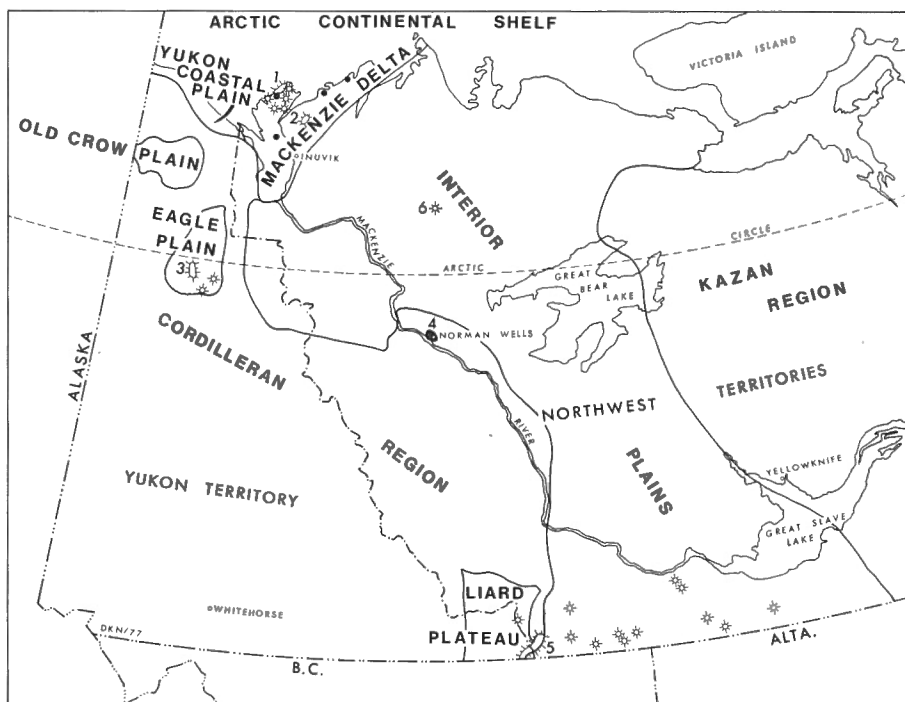


Figure 17.1.

Physiographic elements of northern Canada north of Latitude 60°N (after Bostock, 1970), showing location of principal gas and oil fields:

1. Taglu
2. Parsons
3. Chance
4. Norman Wells
5. Pointed Mountain and Beaver River
6. Ashland et al. Tedji Lake F-24 well

¹ Prepared for the International Soils Congress, Edmonton, Alberta, June 13-25, 1978.

Table 17.1

Potential reservoir rocks
Northern Mainland and Offshore Canada

Sequence	Age	Facies	Arctic Coastal Plain		Arctic Continental Shelf	Interior Plains	Cordillera
			Mackenzie Delta	Yukon Coastal Plain			
Brookian	Neogene	Alluvial-deltaic sand, sandstone, conglomerate	○	○	▼	○	○
	Late Early Cretaceous to Paleogene	Flyschoid sandstone, molassoid sandstone, conglomerate	●	▼	▼	○	○
Ellesmerian	Mississippian to early Early Cretaceous	Platformal carbonates and littoral sandstones; epicontinental sandstone	●	▼	○	○	●
Franklinian	Early Cambrian to Late Devonian	Platformal carbonates, flyschoid sandstone	●	▼	○	●	●

- oil and/or gas discovery
- ▼ prospective facies
- no significant hydrocarbon potential

Pointed Mountain Fields). The Norman Wells Oil Field produces from a Middle Devonian reef, also at the eastern margin of the Cordillera; and oil occurs in the Mackenzie Delta (IOE Mayogiak J-17) in fault-bounded, Devonian carbonate rocks of the Eskimo Lakes Fault Zone. Isolated carbonate masses like those seen in outcrop elsewhere in northern Yukon Territory may occur within the lower Paleozoic graptolitic shale succession beneath the Yukon Coastal Plain. They may be prospective, but could be out of reach of the drill beneath the Arctic Continental Shelf.

Hydrocarbon discoveries in the Ellesmerian Sequence are confined to the northern Cordilleran Region and Mackenzie Delta. In the Eagle Plain, gas and oil are trapped in Mississippian conglomeratic (Chance) sandstones. Gas also occurs in other Mississippian and Permian sandstones (Graham, 1973, p. 179). In the Mackenzie Delta, on the other hand, significant reserves of hydrocarbons have been found associated with porous, nearshore and deltaic sandstone bodies in roll-over anticlines on the seaward, downthrown sides of some components of the Eskimo Lakes Fault Zone. In the Parsons Field (Coté et al., 1975, p. 618), for example, gas, condensate and light oil occur in lower Lower Cretaceous sandstones. These same rocks contain oil in the Shell Kuppik O-13 well 70 km to the west in the middle of the Mackenzie Delta (Young et al., 1976, p. 53). They are prospective for hydrocarbons beneath the delta where they are erosionally truncated down the plunge of Cache Creek Uplift (Norris, 1976, p. 461), as well as in the Yukon Coastal Plain. The southeastward extension of the principal Permian and Triassic reservoirs at Prudhoe Bay, on the other hand, would appear to be absent from the coastal plain and continental shelf of Canada because they have been overstepped by Jurassic strata (Norris, 1974a, p. 38). The Ellesmerian Sequence may underlie much of the Old Crow Plain, however, because it outcrops in the middle of the plain and on its north and east flanks. The hydrocarbon potential of the plain would appear to be small because both source and reservoir beds are so extensively exposed.

Both oil and gas have been discovered in the lower part of the Brookian Sequence beneath the Mackenzie Delta. Shale diapirism, possibly combined with stratigraphic traps and pressure seals (Evans et al., 1975), is an important factor in the trapping of hydrocarbons, as in the Paleogene reservoir sands of the Taglu Gas Field (Fig. 17.1), and in the several wells in which oil has been found along the outer fringe of the subareal Mackenzie Delta (see I.N.A., 1976, p. 13). Many prospective shale diapirs are known from geophysical investigations beneath the Arctic Continental Shelf in Upper Cretaceous and younger, molassoid sediments. Underlying flyschoid, clastic rocks of late Early Cretaceous age are doubtless beyond reach of the drill, but they are prospective where suitably capped by impervious Upper Cretaceous shales beneath Yukon Coastal Plain. In Eagle Plain, moreover, oil is reported from Lower? Cretaceous, porous sandstone in some of the major anticlines traversing the region (Norris, 1974b, p. 348). The hydrocarbon potential of the upper (Neogene) part of the Brookian Sequence, on the other hand, would appear to be limited to the continental shelf where it has not yet been tested.

Drilling Record

Since the year 1920, more than seven hundred wildcat and development wells have been completed in northern mainland and offshore Canada (Table 17.2). Activity reached a peak in 1973 when approximately 83 wells were drilled (I.N.A., 1976, p. 36). As a consequence of this activity, 92 wells have been designated as oil bearing, 53 as gas bearing, and 5 oil and gas fields have been identified (see Fig. 17.1). The bulk of the boreholes are in the relatively accessible parts of the Interior Plains. Exploration on the Arctic Continental Shelf has barely begun, with three wells having been spudded between the outer shelf edge and the proximal Mackenzie Delta.

Table 17.2
Drilling record Northern Mainland and Offshore Canada

Region	Division	No. of Boreholes (to March 31, 1977)			
		Oil	Gas	D&A	Total
Arctic Coastal Plain	Mackenzie Delta (includes Parsons & Taglu gas fields)	10	24	105	139
	Yukon Coastal Plain	0	0	3	3
Arctic Continental Shelf		0	0	3*	3
Interior Plains	(includes Norman Wells oil field)	74	12	475	561
Cordilleran	Eagle Plain (includes Chance gas field)	4	4	21	29
	Old Crow Plain	0	0	0	0
	Liard Plateau (includes Beaver River and Pointed Mountain gas fields)	0	9	10	19
TOTALS:		92	53	609	754

* Suspended

Hydrocarbon Resources

For the purposes of evaluating the hydrocarbon resources, the region can be divided into two parts (E.M.R., 1977), the one embracing the Mackenzie Delta and the Arctic Continental Shelf, and the other the Interior Plains, the Cordilleran Region and Yukon Coastal Plain.

The Mackenzie Delta and Arctic Continental Shelf between the Alaska border and Victoria Island experienced geological and geophysical activity beginning in the 1960's, with the first hydrocarbon discovery being in Lower Cretaceous sandstones beneath Atkinson Point, on the southern shore of the Beaufort Sea. There followed many significant discoveries and a variety of estimates of the hydrocarbon potential. It would appear, however, that there are about 6.5 trillion cubic feet of gas and 400 million barrels of liquid hydrocarbons proven to date (E.M.R., 1977, p. 31). The resource of the region in all likelihood will be predominantly gas. Because of the deltaic nature of the Brookian sequence, it is expected that there will be a large number of modest-sized pools. In addition, the fields may be broken into many pools by abundant, down-to-basin faults with normal stratigraphic separations. Moreover, numerous reservoirs may be stacked one above another (E.M.R., 1977).

Some 650 wells have been drilled in the Interior Plains, the Cordilleran Region and the Yukon Coastal Plain since the discovery of the Norman Wells Oil Field in 1920. A number of modest gas finds have been made. They include the Beaver River and Pointed Mountain Fields in Liard Plateau, the Chance Field in southern Eagle Plain, and numerous cased gas wells in the southern Interior Plains. No additional oil fields have been found, although a significant heavy oil show was discovered in lower Paleozoic rocks in the Mackay Range 85 km southeast of Norman Wells. The only oil reserves in the region are those of the Norman Wells Field which are estimated at 50 million barrels recoverable (E.M.R., 1977, p. 29). Gas reserves, moreover, are estimated at one trillion cubic feet (E.M.R., 1977).

Acknowledgments

The writer is indebted to G.K. Williams and R.M. Procter of the Geological Survey of Canada for providing valuable comment on the manuscript.

References

- Bostock, H.S.
1970: Physiographic regions of Canada; Geol. Surv. Can., Map 1254A.
- Coté, R.P., Lerand, M.M., and Rector, R.J.
1975: Geology of the Lower Cretaceous Parsons Lake gas field, Mackenzie Delta, Northwest Territories in Canada's Continental Margins and Offshore Petroleum Potential, C.J. Yorath, E.R. Parker and D.J. Glass, eds.; Can. Soc. Petrol. Geol., Mem. 4, p. 613-632.
- Energy, Mines and Resources, Canada
1977: Oil and natural gas resources of Canada, 1976; Rept. EP77-1.
- Evans, C.R., McIvor, D.K., and Magara, K.
1975: Organic matter, compaction history and hydrocarbon occurrence - Mackenzie Delta, Canada in Proc. 9th World Petrol. Congr.; v. 2, p. 149-157.
- Graham, A.D.
1973: Carboniferous and Permian stratigraphy, southern Eagle Plain, Yukon Territory, Canada in Proc. Symposium on the Geology of Arctic Canada, J.D. Aitken and D.J. Glass, eds.; Geol. Assoc. Can. and Can. Soc. Petrol. Geol., p. 159-180.
- Indian and Northern Affairs, Canada
1976: Report on the activities in 1975 of the oil and gas industry in the Yukon Territory and Northwest Territories; compiled by the Northern Natural Resources and Environment Branch.
- Norris, D.K.
1974a: Structural geometry and geological history of the northern Canadian Cordillera in Proc. 1973 National Convention, A.E. Wren and R.B. Cruz, eds.; Can. Soc. Explor. Geophys., p. 18-45.
1974b: Structural and stratigraphic studies in the northern Canadian Cordillera; in Report of Activities, Part A, Geol. Surv. Can., Paper 74-1A, p. 343-349.
1976: Structural and stratigraphic studies in the northern Canadian Cordillera; in Report of Activities, Part A, Geol. Surv. Can., Paper 76-1A, p. 457-466.
- Young, F.G., Myhr, D.W., and Yorath, C.J.
1976: Geology of the Beaufort-Mackenzie Basin; Geol. Surv. Can., Paper 76-11.

Introduction

The sharp rise in demand for U as an energy fuel has led to an intensified search for U ore deposits. The depletion of surface ore deposits is forcing man to develop methods of prospecting which can detect U ore at depth. The fact that U and Th generate He makes He a tracer for U and Th deposits. To measure fractions of ppm of He with precision requires a mass spectrometer at the present time. Using mass spectrometers Clarke and Kugler (1973), Clark et al. (1977), Pogorski et al. (1976), Goldak (1974) and Dyck (1973, 1976) have shown that the He concentration is markedly higher in and near U mineralization. Older mass spectrometers are too heavy (over 200 kg) and require too much power to be useful as field instruments for exploration. Ereemeev et al. (1973) describe a truly portable He detector that can be carried by a man. However, its sensitivity is only 50 ppm, not considered sufficient for near surface samples such as soil gases and lake waters. Recently Reimer (1976) has assembled a portable unit which can be put in a truck for field measurements of He.

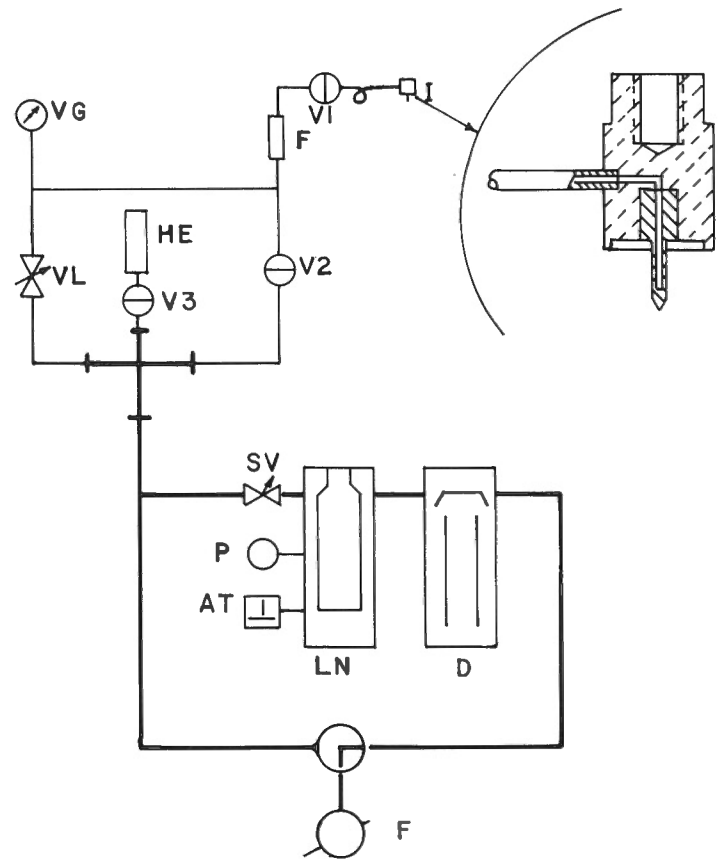
This paper describes a He analysis system using a commercially available He leak detector with an appropriate inlet system for the analysis of water samples and soil gases in a field camp. The system described below was chosen because of its light weight and compactness (60 kg vs over 200 kg of other leak detectors currently on the market), air cooled diffusion pump, low power requirement, relatively low cost, and high sensitivity.

Description of He Detector and Inlet System

The He analyzer and sample inlet system assembly is shown in Figure 18.1. It consists of an Alcatel ASM-10 He leak detector and a home-made stainless steel inlet system. This system is made up of Alcatel "O" ring flanges, stainless steel Nupro bellows valves, and 1/4 inch swagelock connections with teflon seals. The ASM-10 is essentially a compact, light-weight vacuum system with a mass spectrometer tuned to mass 4. The assembly is ready for measurements about one hour after start up. It is protected from sudden air bursts by the solenoid valve (SV) and against filament burnout by the automatic cut off element or triode pressure gauge (T) which switches the filament current off when the pressure in the analyzer (A) rises above 10^{-4} torr. The unit is tuned and calibrated to He using atmospheric air and the standard He leak (HE). A gas sample is admitted to the evacuated inlet system via V1 using a cap punching device (I) illustrated in the cross-section detail in Figure 18.1. This puncher is normally attached to a portable drill stand with the spring reversed so it forces the puncher down on the sample bottle. The heart of this puncher is a hollow case hardened steel needle which is sealed with a rubber septum. This septum also provides the seal between the metal bottle cap and needle when the puncher is forced through the cap into the bottle.

Sample Collection, Storage, and Analysis

Water samples are collected in 310 cm³ soft glass bottles similar to those used in the soft drink industry. A 4.0 cm³ aliquot is removed from the bottle by lowering a 4.0 cm³ plunger into the neck of the bottle displacing said volume exactly. The bottle is then capped with a metal cap and a bottle capper available from Homebrew retailers, and stored two days or more prior to analysis. It was found that



- | | |
|--|---------------------------|
| F - filter | SV - solenoid valve |
| I - sample inlet | LN - liquid nitrogen trap |
| P - pirami gauge | HE - standard helium leak |
| D - diffusion pump | VG - rough vacuum gauge |
| R - roughing pump | |
| V1, V2, V3 - high vacuum valves | |
| AT - analyzer and triode vacuum gauge | |
| VL - leak valve in the 10^{-3} lusec range | |

Figure 18.1 Schematic of the Alcatel ASM-10 helium leak detector and GSC inlet system.

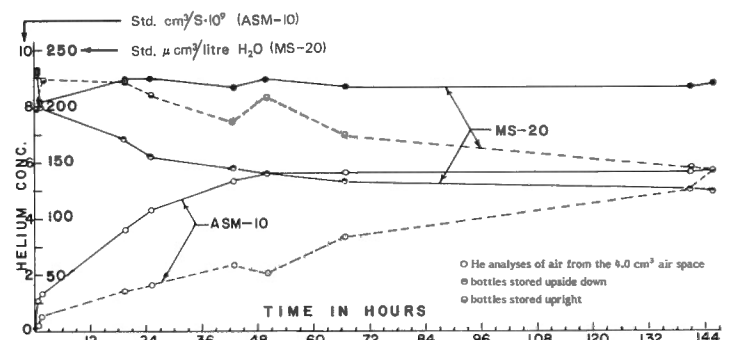


Figure 18.2 Equilibrating time of 4.0 cm³ atmospheric air and 306 cm³ water containing excess He in a 310 cm³ (10 oz) soft drink bottle. Filled and partially filled circles - He analyses of water using the MS-20.

by storing the bottles upside down equilibrium between the He in the water and the He in the 4.0 cm³ air space was reached sooner than when stored right side up (see Fig. 18.2). He losses were found to be lower in bottles stored upside down. Presumably He escapes easier through the bottle cap seal when air is on both sides of the cap. As shown in Figure 18.2 equilibrium is reached in about two days. No doubt the air-water equilibrium could be achieved sooner with a shaker. The presence of 4.0 cm³ of atmospheric air results in the "contamination" of the He in a water sample. One litre of water in equilibrium with air at STP contains about 18 std cm³ of air. A 310 cm³ sample of water therefore contains about 6 std cm³ of dissolved air at equilibrium. But this air has a He concentration of only 2 ppm instead of the 5 ppm found in atmospheric air. Hence there is nearly twice as much He in the 4 cm³ air space as there is in the water at equilibrium. In terms of concentrations in the bottle one can show, using the Bunsen coefficient for He in water (0.0087 at ~20°C and 1 atmosphere) that, if for example the He concentration of the water in the bottle was twice that found at equilibrium with air i.e. 90 μ cm³/litre instead of 45 μ cm³/litre, μ the concentration of He in the 4 cm³ air space would be 7.2 ppm instead of 5.2 ppm, or only 38 per cent higher.

The Alcatel unit reads He as a leakage rate in standard cubic centimetres per second. At an analyzer air pressure of 1×10^{-4} torr, as recorded by the triod vacuum gauge, the unit reads 3.5×10^{-9} std cm³/s. This reading is reproducible within 0.2×10^{-9} std cm³/s, or 6 per cent, from day to day with periodic recalibration. To convert instrument readings to absolute He concentrations the unit was calibrated using the gas analysis facility (MS-20) described by Dyck et al. (1976). Two such calibration curves are shown in Figure 18.3. For these calibrations He was bubbled through water in a 20 litre bottle and mixed thoroughly. Different aliquots of this water were then put into glass bottles in pairs. Both bottles were then filled with air equilibrated water; one was then capped and the other had 4.0 cm³ of water removed before it was capped. After equilibrium was established, as determined by a timed test (Fig. 18.2), the filled bottle was analyzed on the MS-20 and the air in the other bottle was read on the AMS-10. To facilitate the admittance of the bottled air to the AMS-10, a bottle cap punching device, constructed in the Instrument Shop of the Geological Survey of Canada and described above was used. When inlet and analyzer systems are evacuated V1 and V2 are closed and the cap puncher is forced through the cap of a sample bottle. After 3 seconds V1 is opened momentarily and then closed again. After adjusting the analyzer pressure with the V1 valve to 1×10^{-4} torr, the He leak rate is read off the meter and recorded. The atmospheric air or background reading is then subtracted from the sample reading and this net sample leak rate converted to standard microcubic centimetres of He per litre of water using Figure 18.3. The whole operation is rather simple and fast. By reading atmospheric air between samples, it was found that the instrument drift could amount to as much as 0.2×10^{-9} std cm³/s during the course of a day. Hence using net rather than total standard cubic centimetres/second resulted in greater precision. This value of 0.2×10^{-9} std cm³/s can be taken as the analytical precision of the instrument and amounts to about 7 μ cm³/litre as shown in Figure 18.3. The two calibration graphs shown were obtained on May 20, 1977 and August 11, 1977. They illustrate an appreciable drift both in slope (sensitivity) and intercept. This intercept should ideally have a value of about 45, the equilibrium He concentration of water (Weiss, 1971). The observed intercept variation of $\pm 10 \mu \text{ cm}^3/\text{litre}$ about this value in the first two calibration runs suggests a practical long term detection limit of $10 \mu \text{ cm}^3/\text{litre}$.

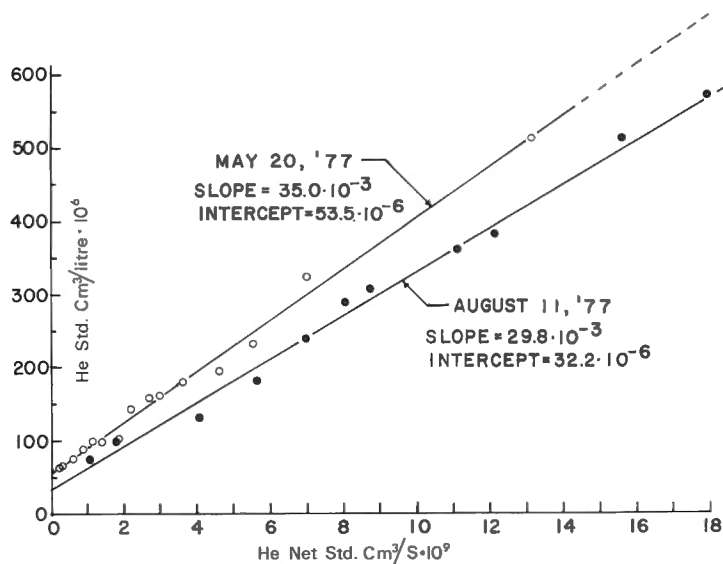


Figure 18.3 Calibration curves of ASM-10. Net ASM-10 readings, i.e. air sample reading minus atmospheric air reading, vs He concentration as determined with the MS-20.

As the sampling and analytical precision tests in Table 18.1 show, this bias is hardly significant for some ground waters. The results shown in Table 18.1A were obtained from a suite of samples collected from the tap of a domestic well just outside of Ottawa. This well was known to contain much higher than background He from an earlier survey (Dyck, 1976). The Table 18.1A results for the ASM-10 were obtained with an air space of 10 cm³. This volume was chosen in the earlier experiments but later was reduced to 4.0 cm³ because of too great a dilution effect in samples near the equilibrium concentration. The results from the two laboratory He solutions shown in Table 18.1 gave similar precisions to the well water samples on the MS-20 but widely divergent precisions on the ASM-10. It is not known where this bias originates. The microcubic centimetre/litre results are derived from the MS-20 which is calibrated independently using atmospheric air. Both instruments change in sensitivity with time as a result of filament aging and amplifier gain changes. Errors due to the degassing of samples during handling are always made as are volume and pressure measurement errors. It is hoped that higher precision will be obtained as the instrument and procedures are evaluated more carefully.

During the 1977 field season the He analyzer was shipped by air to a field camp in the Key lake area, Saskatchewan and set up in the mobile trailer. Electrical power was obtained from a 3000 watt MacCulloch gasoline driven generator. Liquid nitrogen was brought in by plane in 150 litre pressurized containers. The unit performed well during the analysis of several hundred samples. It can be stated here that lake bottom water samples in the area investigated during June and July contain, as a rule, equilibrium He concentrations but were found to rise to detectable levels - up to 96 μ cm³/litre in one instance. This He value was found 12 km from the known U deposits in the area and is believed to reflect geological structure rather than U mineralization. In the mineralized area only several tens of microcubic centimetre/litre above equilibrium were detected in lake bottom water samples. Such low levels relative to the equilibrium value of 45 μ cm³/litre make a sensitive and reliable instrument for U prospecting imperative.

Table 18.1

Sampling and analytical precision tests of ASM-10 and MS-20
 Units are standard $\mu\text{ cm}^3/\text{s} \cdot 10^9$ for ASM-10 and standard cm^3/litre for MS-20

A. Domestic well May 4, 1977			B. Laboratory He solutions				
			May 11, 1977		Aug. 11, 1977		
ASM-10 net 10 cm^3 air space		MS-20	ASM-10 net	MS-20	ASM-10 net	MS-20	
Upright bottles	Upside down bottles	Full bottles	Upside down 4.0 cm^3 air space	Full bottles	Upside down 4.0 cm^3 air space	Full bottles	
16.4	17.6	1040	3.6	157	6.3	182	
16.4	17.4	1210	3.5	166	6.3	213	
16.5	17.4	1180	3.8	162	6.3	213	
15.8	18.5	1180	3.5	168	6.4	213	
16.6	17.5	1210	3.6	172	6.4	209	
17.4	17.6	1210	3.9	157	6.3	213	
16.9	18.4	1220	3.4	172	6.4	211	
16.7	17.7	1220	3.5	174	6.3	205	
			4.1	154	6.3	221	
			3.2	162	6.2	205	
			2.8	157	6.3	207	
			2.8	166	6.2	209	
\bar{x}	16.71	17.76	1184	3.48	163.9	6.31	208.4
S	.530	.437	60.2	.393	6.79	.067	9.40
p*	6%	5%	10%	23%	8%	2%	9%

p* = precision = $2S \times 100 / \bar{x}$

Acknowledgment

The authors wish to acknowledge the assistance of the Geological Survey's Instrument Shop staff in the construction of parts of the inlet system in particular the bottle cap punch for the sample inlet.

References

- Clarke, W.B., Top, Z., Beavan, A.P., and Gaudhi, S.S.
 1977: Dissolved helium in lakes: Uranium prospecting in the Precambrian terrain of central Labrador; *Econ. Geol.*, v. 72, p. 233-242.
- Clarke, W.B. and Kugler, G.
 1973: Dissolved helium in ground water: A possible method for uranium and thorium prospecting; *Econ. Geol.*, v. 68, p. 243-251.
- Dyck, W.
 1973: The use of simple volatile compounds in mineral exploration: in Report of activities, Part B, *Geol. Surv. Can.*, Paper 73-1B, 2 p.
 1976: The use of helium in mineral exploration; *J. Geochem. Explor.*, v. 5, p. 3-20.
- Dyck, W., Pelchat, J.C., and Meilleur, G.S.
 1976: Equipment and procedures for the collection and determination of dissolved gasses in natural waters; *Geol. Surv. Can.*, Paper 75-34, 12 p.
- Eremeev, A.N., Sokolov, V.A., Solovov, A.P., and Yanitskii, I.N.
 1973: Application of helium surveying to structural mapping and ore deposit forecasting; in *Geochemical Exploration 72 I.M.M.*, London, p. 183-193.
- Goldak, G.R.
 1974: Helium-4 mass spectrometry for uranium exploration; *AIME Ann. Meet. Paper 74-L-44*, Feb. 1974, 12 p.
- Pogorski, L.A., Quirt, G.S., and Blascheck, A.
 1976: A new exploration tool for locating uranium deposits; *Chemical Projects Ltd.*, Technical Paper CPL-6/76, 27 p.
- Reimer, G.M.
 1976: Design and assembly of a portable helium detector for evaluation as a uranium exploration instrument; *US Geol. Surv. Open File Report 76-398*, 17 p.
- Weiss, R.F.
 1971: Solubility of helium and neon in water and seawater; *J. Chem. Eng. Data*, v. 16, no. 2, p. 235-241.

Project 700025

D.J. Tempelman-Kluit and R.G. Currie
Regional and Economic Geology Division, Vancouver

Introduction

Surface rock samples were collected for the study of the minor element geochemistry from part of the Yukon Crystalline Terrane in 1971 and 1972 during a regional geologic reconnaissance. A synthesis of the results of this mapping is given in Tempelman-Kluit (1976) and the minor element geochemistry is detailed in Tempelman-Kluit and Currie (in press). The petrology, setting, and minor element geochemistry suggest that the Nisling Range alaskite with its cogenetic subvolcanic and volcanic rocks has potential for uranium concentrations. The 550 samples of these rocks have therefore been analyzed recently for uranium and this is a report of the uranium content of this suite.

Geology

The Nisling Range alaskite is an Eocene leucogranite with associated acid volcanics found in the southwest part of the Yukon Crystalline Terrane (Fig. 19.1). It forms discordant, high level plutons intruded into Late Precambrian to mid-Paleozoic metamorphic rocks. Extensive swarms of dykes, associated with the alaskite, are localized by north-trending fractures that transect older Cordilleran trends. Explosive acid volcanics, also associated with the alaskite, lie on a surface of low relief which was later tilted towards the northeast. This has permitted deeper erosion on the southwest so that the plutonic rocks of this assemblage are generally exposed southwest of the associated volcanics. The volcano-plutonic suite has genetic affiliations with the Coast Plutonic belt and marks the imprint of that tectonic element on the Yukon Crystalline Terrane.

The Nisling Range alaskite (TGAL)¹ is a medium grained miarolitic granite made up of euhedral and subhedral perthitic potash feldspar (50%), euhedral smoky quartz (30%), and anhedral interstitial albite (15%). Biotite and purple fluorite are accessory minerals. Biotite granite (TG) is gradational with, and similar to, the alaskite, but is equigranular, rarely miarolitic and contains more biotite. It is interpreted as the more hypabyssal equivalent of the alaskite. The alaskite locally grades into feldspar porphyries (TFP) which are its subvolcanic and volcanic relatives. These porphyries contain euhedral andesine, hornblende and quartz phenocrysts in an aphanitic to very fine grained quartzo-feldspathic groundmass. The Mount Nansen Group (TMN) includes intermediate to acid tuff and breccia, the products of explosive volcanism. The explosive rocks contain fragments of, in places grade into, and elsewhere are cut by, feldspar porphyries demonstrating a close genetic relationship. Casino volcanics (TVA) are acid breccias like those of the Mount Nansen, but separated physically; some of these rocks are breccia pipes (Godwin, 1976). The varicoloured tuff (TVR) is a kaleidoscopic assemblage of welded tuff and ignimbrite.

¹ The mnemonics indicate map units (see Table 19.3) as used in Tempelman-Kluit (1976) and Tempelman-Kluit and Currie (in prep).

Because they include only fine grained tuffs they are interpreted as the distal equivalent of the Mount Nansen Group. The alaskite and its related volcanics are Eocene as indicated by K-Ar and Rb-Sr ages of 52 to 67 m.y. from intrusive and extrusive phases of this consanguinous suite.

Nisling Range alaskite is geochemically interesting because its concentrations of zinc, lead, molybdenum, and tungsten are higher than most rocks in Yukon Crystalline Terrane. The Mount Nansen Group similarly has higher silver and arsenic levels than other rocks in the region. Metal partitioning between the extrusive and intrusive phases of this cogenetic suite has concentrated the zinc, copper, mercury, arsenic, and silver in the volcanics of the Mount Nansen Group and the lead, molybdenum, and tungsten in the plutonic alaskite.

At least three porphyry molybdenum-copper occurrences with economic potential (Casino, Mount Cockfield, Mount Nansen) are enclosed by the alaskite-Mount Nansen suite, and the small, but rich, gold-silver veins at Mount Nansen and Freegold Mountain are genetically related to the Mount Nansen Group. The Mount Nansen Group is the equivalent of the Sloko Group (Souther, 1971) and the Skukum Group (Wheeler, 1961). Both these assemblages are closely associated with plutonic rocks like the alaskite.

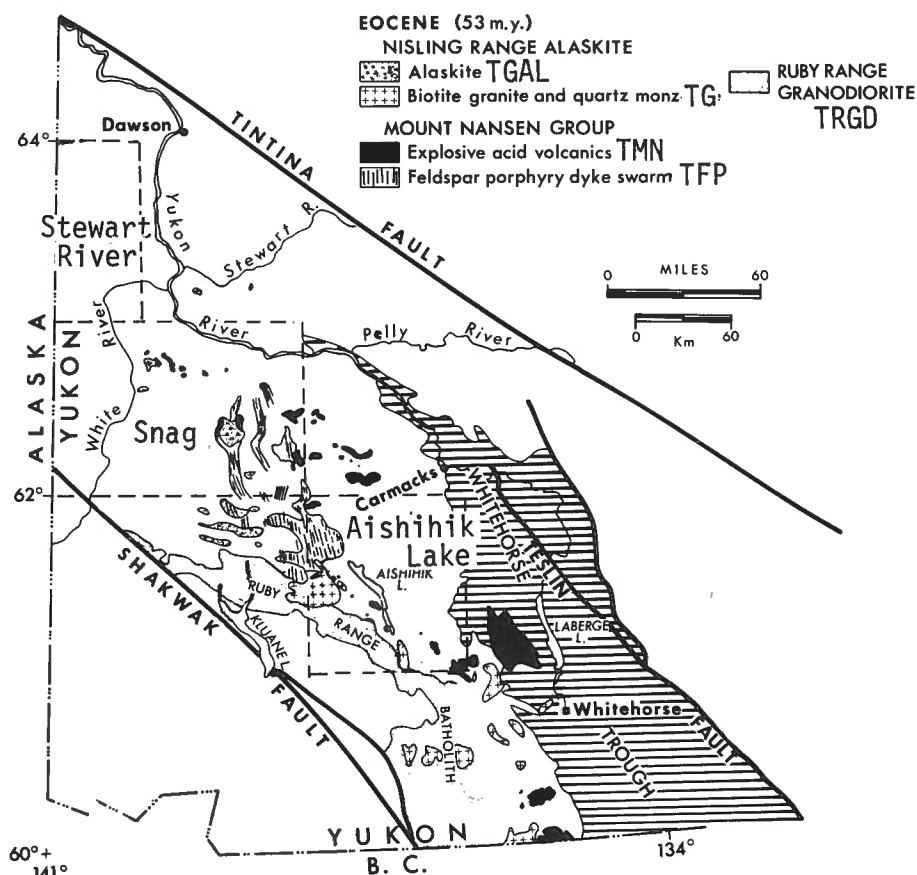


Figure 19.1. Distribution of the early Eocene Nisling Range alaskite with its subvolcanic dyke swarms and explosive volcanic rocks (Mount Nansen Group). The Ruby Range Batholith, part of the Coast Plutonic belt is made up of granodiorite that yields the same K-Ar ages as the alaskite.

Table 19.1

Samples with more than 8.0 ppm uranium

Rock Unit	Rock Type	Easting	Northing	Minor Element Geochemistry (ppm)								
				Zn	Cu	Pb	Mo	Hg	W	Ag	As	U
TMN	AEXV	348300	6873570	24	6	18	1	5	2	0.4	3.0	9.2
TMN	AEXV	349000	6873300	23	4	16	1	5	2	0.6	7.0	9.6
TVR	BSLT	425700	6811250	61	53	6	1	5	2	0.6	2.0	10.6
TFP	FLST	650750	6928850	34	13	15	2	5	2	0.3	7.0	13.9
TFP	FLST	617750	6939750	6	3	7	1	5	2	0.1	3.0	8.8
TFP	FPPP	531250	6969700	21	2	3	2	10	2	0.3	3.0	8.3
TFP	FPPP	358300	6857750	38	2	18	1	5	2	0.1	2.0	10.2
TFP	FPPP	351870	6844170	26	9	6	1	5	2	0.5	1.0	10.9
TFP	GRNT	650700	6928950	34	11	15	7	5	2	0.5	45.0	10.6
TGAL	GRNT	608350	6924200	87	8	10	2	10	2	0.2	2.0	8.0
TGAL	GRNT	559180	6956600	24	2	13	1	5	4	0.3	2.0	8.2
TVA	IEXV	560450	6970350	64	30	14	1	10	2	0.2	1.0	16.3
TFP	IMIV	644950	6880750	19	4	7	1	10	2	0.3	1.0	8.2
TFP	MNZN	650750	6928750	37	6	21	4	5	2	0.4	3.0	12.1
TG	QZMZ	355000	6809450	158	6	14	1	5	2	0.4	1.0	10.1
TMN	RYLT	354500	6808900	20	6	14	2	5	2	0.4	1.0	9.6
TFP	RYLT	358200	6846700	128	2	11	1	5	5	0.4	0.5	9.9
TVR	RYLT	390100	6840800	22	2	6	1	5	2	0.6	4.0	11.1
TFP	RYLT	540180	6936200	9	50	14	140	5	2	0.5	3.0	10.8
TVR	RYLT	390300	6839500	29	4	7	1	10	2	0.3	1.0	8.8
TFP	TUFF	358250	6846700	190	3	21	1	5	2	0.4	1.0	8.5
TFP	TUFF	352200	6846500	75	5	7	1	5	2	0.8	3.0	8.2
TVA	TUFF	566500	6964400	41	2	9	2	5	5	0.4	0.5	19.6
TVR	TUFF	392250	6847800	54	2	81	1	10	2	0.9	1.0	9.7
TVR	TUFF	414620	6822830	44	1	11	1	115	2	0.4	1.0	8.5
TMN	TUFF	382650	6806750	68	128	9	1	10	2	0.6	8.0	11.1

Table 19.2

Statistical Parameters				
Group	Number of samples	Mean ppm	95% confidence limits on mean	Standard deviation
Total	550	4.10	3.90 - 4.30	2.39
Rock Unit				
Varicoloured acid tuffs (TVR)	116	3.19	2.77 - 3.62	2.30
Explosive volcanics (TMN)	197	3.68	3.42 - 3.94	1.84
Nisling Range granites (TG)	16	4.20	3.04 - 5.35	2.17
Feldspar porphyry (TFP)	141	4.80	4.38 - 5.21	2.51
Casino volcanics (TVA)	26	5.32	3.63 - 7.01	4.19
Nisling Range alaskite (TGAL)	46	5.38	4.89 - 5.87	1.65
Rock Type				
Andesite	28	2.55	1.97 - 3.13	1.50
Basalt	38	3.40	2.74 - 4.07	2.03
Intermediate extrusive	35	3.44	2.42 - 4.46	2.97
Dyke	17	3.81	2.76 - 4.85	2.04
Tuff	122	4.16	3.70 - 4.62	2.57
Feldspar porphyry	69	4.17	3.67 - 4.67	2.08
Rhyolite	32	5.23	4.27 - 6.18	2.66
Acid extrusive	31	5.42	4.61 - 6.22	2.20
Granite	25	6.16	5.49 - 6.82	1.62

Table 19.3

This table lists the map-unit mnemonics used in text and illustrations (from Tempelman-Kluit and Currie, in prep.)

MNEMONIC	MAP UNIT
PPSQR	Kluane schist, staurolite quartz biotite schist (Aishihik L.)
PPSBQ	Biotite schist (Aishihik L., Snag)
PPMH	Amphibolite in Aishihik L. map-area PLUS amphibolites in PPSBQ
PPC	Marble (Stewart R., Aishihik L.)
PPC+	PLUS marbles in PPSBQ and PPQC
PPQC	Nasina quartzite, grey graphitic quartzite and slate (Stewart R., Snag)
PPGDN	Pelly gneiss, biotite granodiorite gneiss (Snag, Stewart R.)
PPGD	Foliated biotite granodiorite (Snag, Stewart R.)
PPSQM	Klondike schist, quartz muscovite schist (Snag, Stewart R.)
PPSN	Schist gneiss, biotite quartz schist and gneiss (Snag, Stewart R.)
PPM	Amphibolite (Snag, Aishihik L.)
PPPS	Phyllite (Snag)
PPSB	Schist (Snag)
PPT	Argillaceous chert (Snag)
PT	Chert and metachert (Stewart R.)
PPTI	Hornfels (Snag)
PMUB	Dunite (Snag, Stewart R.)
PMB	Gabbro (Snag)
PMPR	Peridotite (Snag)
TRVB	Lewes River Group, basalt (Aishihik L.)
TRGDMA	Hornblende granodiorite (Klotassin Suite in southeastern Snag)
TRGDMS	Hornblende granodiorite (Klotassin Suite in Aishihik L.)
TRGDMT	Hornblende granodiorite (Klotassin Suite between Donjek and Yukon rivers in Snag)
TRGDMW	Hornblende granodiorite (Klotassin Suite west of White River in Snag and Stewart R.)
TRGDM	All rocks of the Klotassin suite together
TRQM	Pink quartz monzonite (Snag, Aishihik L.)
MQMP	Porphyritic quartz monzonite (Snag, Aishihik L.)
KG	Coffee Creek granite (Snag, Aishihik L.)
MGDB	Nisling Range granodiorite (Snag)
PPQMM	Foliated muscovite quartz monzonite (Stewart R.)
TG	Nisling Range granite (Aishihik L.)
LMMZ	Hornblende monzonite (Stewart R.)
LMQM	Quartz monzonite (Snag, Stewart R.)
LMMZP	Porphyritic monzonite (Snag, Stewart R.)
TGAL	Nisling Range alaskite (Snag, Aishihik L.)
TFP	Feldspar porphyry (Aishihik L.)
TMN	Mount Mansen Group, explosive acid volcanic rocks (Snag, Aishihik L.)
TCGG	Granite conglomerate (Snag)
JL	Laberge Group, conglomerate, sandstone, shale (Aishihik L.)
TCGQ	Quartzite conglomerate (Snag)
LTSP	Sandstone (Snag)
LKT	Tantalus Formation, conglomerate, sandstone, shale (Aishihik L.)
ETCCG	Sandstone and conglomerate (Stewart R.)
ETVRP	Rhyolite porphyry (Stewart R.)
TVR	Varicoloured acid tuff (Aishihik L.)
ETCV	Carmacks Group, tholeiitic basalt (Snag, Aishihik L., Stewart R.)
LTVD	Donjek volcanics, tholeiitic basalt (Snag)
TLR	Little Ridge volcanics, tholeiitic basalt (Aishihik L.)
TQVBO	Columnar basalt, olivine basalt (Stewart R.)
QTVBO	Olivine basalt (Snag)
TVA	Casino volcanics, acid volcanic breccia and tuff (Snag)
TV	Undifferentiated volcanics (Aishihik L.)
LTVR	Felsic volcanics (Snag)
PMV	Volcanic rocks (Snag)
PMS	Sedimentary rocks (Snag)
PV	Sheared greenstone (Snag, Stewart R.)

Quartz Monzonite, Midnight Mine, Washington	12.4 ppm
Loon Lake Batholith, Washington	5.1 ppm
Quartz Monzonite, Sherwood Mine, Washington	9.3 ppm
Granite, Sherwood Mine, Washington	7.0 ppm
Granodiorite, Sherwood Mine, Washington	5.3 ppm
Horsethief Batholith, British Columbia	10.5-30.5 ppm
Quartz Monzonite, Vahalla Intrusion, Beaverdell, British Columbia	6.9 ppm
Japanese intrusives without related uranium deposits	2.6 ppm
Japanese intrusives related to Tertiary sedimentary uranium deposits	4.9 ppm

Conclusions

The geochemistry confirms what was expected, namely that the alaskite has a comparatively high uranium background of 5.4 ppm. It does not help in assessing the possibilities for occurrences of uranium within these rocks or the related volcanics. The uranium geochemistry does not pinpoint specific prospecting targets, but it helps identify the Nisling Range alaskite as a potential uranium source rock.

The suggestion that uranium may have been leached from the high background alaskite and concentrated in the continental Tertiary sedimentary rocks of Yukon Crystalline Terrane, made by Smee at the Whitehorse Geoscience Forum (December 1976), bears consideration. Specific rock units that warrant investigation in this light are the Tertiary sandstone and conglomerate found as comparatively restricted erosional remnants in Snag, Stewart River, and Carmacks map-areas in the lowest part of the Carmacks Group (i.e. map-units TCCG, TCGQ, LTSP, ETCCG of Tempelman-Kluit, 1974a, b).

In this volcano-plutonic suite uranium is concentrated in the intrusive rocks and depleted in the extrusives. Lead, molybdenum, and tungsten show the same tendency to be enriched in the plutonic rocks, but zinc, copper, mercury, silver, and arsenic show the reverse and are concentrated in the volcanics.

References

Garrett, R.G.

- 1971: Molybdenum, tungsten and uranium in acid plutonic rocks as a guide to regional exploration, southeast Yukon; Can. Min. J., v. 92, no. 4, p. 37-40.

Godwin, C.I.

- 1976: Casino, Y.T., a porphyry copper-molybdenum deposit; Can. Inst. Min. Metall., Spec. Vol. 15.

Levinson, A.A.

- 1974: Introduction to Exploration Geochemistry; Applied Publishing Ltd., Calgary, 612 p.

Souther, J.G.

- 1971: Geology and mineral deposits of Tulsequah map-area, British Columbia; Geol. Surv. Can., Mem. 362, 84 p.

Tempelman-Kluit, D.J.

- 1974a: Carmacks map-area, Y.T.; Geol. Surv. Can., Open File 200.

- 1974b: Reconnaissance geology of Aishihik Lake, Snag and part of Stewart River map-areas, west-central Yukon; Geol. Surv. Can., Paper 73-41 97 p.

- 1976: The Yukon Crystalline Terrane: Enigma in the Canadian Cordillera; Geol. Soc. Am., Bull., v. 87, p. 1343-1357.

Tempelman-Kluit, D.J. and Currie, R.G.

- Reconnaissance rock geochemistry of Aishihik Lake, Snag and Stewart River map-areas in the Yukon Crystalline Terrane; Geol. Surv. Can. (in prep.).

Wheeler, J.O.

- 1961: Whitehorse map-area, Yukon Territory; Geol. Surv. Can., Mem. 312, 156 p.

Project 750059

J. Rimsaite

Regional and Economic Geology Division

Further studies of secondary uranium- and lead-bearing minerals from the oxidation zone of uranium deposits in northern Saskatchewan (Rimsaite, 1976) revealed the occurrence of hydrous uranyl carbonates, a lead molybdate, and two unidentified uranium-bearing compounds X-1 and X-2. This report presents a brief description and mode of occurrence of these mineral aggregates. Because much of the radioactive material is amorphous to X-rays, or metamict, the author examined all samples under petrographic microscope in oil immersion mounts, in autoradiographs of thin sections, and, when sufficient material was available, by X-ray diffractometer, applying glyceration and heat treatments.

Hydrous Uranyl Carbonates in the Rabbit Lake Uranium Deposit

In addition to secondary uranium-bearing sulphate, oxide and silicate minerals (Rimsaite, 1977) two rare uranyl carbonates bayleyite and liebigite, were found in the pit of the Rabbit Lake uranium mine during the 1977 field investigation. These uranyl carbonates occur as brightly-coloured coatings on wet, weathered surfaces of dark grey chloritic metasediments exposed in the northern wall of the pit at the fourth level.

Bayleyite

$Mg_2.UO_2(CO_3)_3.18H_2O$; GSC XRD powder pattern No. 57279. Wet bayleyite is apple-green in colour and crystallizes as globular aggregates of prismatic crystals, <1mm in length, forming bright green deposits on wet walls of the pit. In dry atmosphere, bayleyite dehydrates and disintegrates to fine grained powder consisting of yellowish specks, < 1 μm in size. Bayleyite has low refractive indices, $\alpha = 1.454$, $\beta = 1.492$, $\gamma = 1.502$, and characteristic high birefringence of 0.048. These data are consistent with published values. Rapid disintegration to powder in dry atmosphere probably accounts for its rare occurrence in nature. Properties and occurrences of bayleyite in Arizona, Morocco and Utah have been described by: Axelrod et al. (1951); Branche et al. (1951); and by Stern and Weeks (1952). To the author's knowledge, this is the first reported occurrence of bayleyite in Canada.

Liebigite

$Ca_2.UO_2(CO_3)_3.10H_2O$; GSC XRD powder pattern No. 57276. Liebigite is associated with bayleyite and occurs as grass-green crusts on wet walls of the pit. It has a fairly high birefringence of 0.037, and somewhat higher refractive indices than bayleyite, $\alpha = 1.500$, $\beta = 1.502$, and $\gamma = 1.532$. In the samples from the Rabbit Lake uranium deposit, liebigite is more abundant than bayleyite which is consistent with observations by Axelrod et al. (1951) in other occurrences.

Wulfenite and Unidentified Secondary Uranium-Bearing Compounds X-1 and X-2 in the Cluff Lake Deposit

The secondary uranium- and lead-bearing mineral aggregates were observed in thin section of a brightly-coloured uranium ore collected in 1975 from the oxidation zone at ore body 'N' of the Cluff Lake uranium deposit. The specimen was taken in the trench, just above the groundwater level. The distribution of the radioactive mineral aggregates

(Figs. 20.1a, 20.1b, 20.2) and their relative sequence of crystallization are as follows: remnant pitchblende grains (P), 1-2 mm in diameter, are pseudomorphously replaced by kasolite (K), which in turn is replaced by compound X-1(1). All these mineral aggregates are embedded in fine grained speckled, fibrous and botryoidal aggregates of uranophane and amorphous compound X-2(2). Wulfenite (W) occurs as vein and vug fillings in the groundmass composed of compound X-2(2). Portions of these aggregates were removed from the thin section and identified by X-rays by A.C. Roberts. Spots used for X-ray identification are marked with mineral symbols on the thin section and on its autoradiograph (Figs. 20.1a and 20.1b).

Kasolite

$PbO.UO_3.SiO_2.H_2O$ is red-brown translucent in thin section and pseudomorphously replaces black-opaque pitchblende. Kasolite has markedly lower reflectivity than the associated pitchblende.

Compound X-1

This mineral is speckled, mottled, translucent brown and pseudomorphously replaces kasolite grains. The X-ray powder pattern of aggregate X-1 is hazy and has six strongest lines with the following spacings and intensities: 7.90Å, 3.39s, 6.56m, 4.77m, 3.20m and 2.90m.

Compound X-2

This mineral is one of the major components in the thin section. It is bright yellow-green in colour and surrounds as well as partly replaces earlier radioactive minerals (Figs. 20.1b and 20.2). It appears amorphous in oil immersion mounts and it is amorphous to X-rays.

Wulfenite

$PbMoO_4$ occurs in fine grained bright red to opaque aggregates forming red translucent patches, 2 mm in length, in a yellow-green groundmass composed of micaceous phyllosilicates, quartz, and compounds X-1 and X-2. An occurrence of wulfenite in British Columbia has been reported by Traill (1970).

On the basis of isotopic analysis of lead in secondary radioactive minerals from the Rabbit Lake deposit (Rimsaite, 1977) it is assumed that the lead in the secondary minerals at the Cluff Lake uranium deposit is also mainly radiogenic.

The occurrence of secondary lead- and lead-uranium-compounds in this uranium deposit infers liberation of the radiogenic lead and uranium from decomposing pitchblende during its replacement by secondary minerals. The liberated lead crystallizes with the uranium as kasolite in an early secondary paragenesis and without uranium as wulfenite in the late paragenesis. Isotopic analysis of uranium and lead in conjunction with electron microprobe analyses are needed to determine processes of the removal and redistribution of the radiogenic lead and uranium. This study indicates that only a portion of the uranium is removed from the oxidation zone the other part remains in the form of uranyl-bearing compounds.

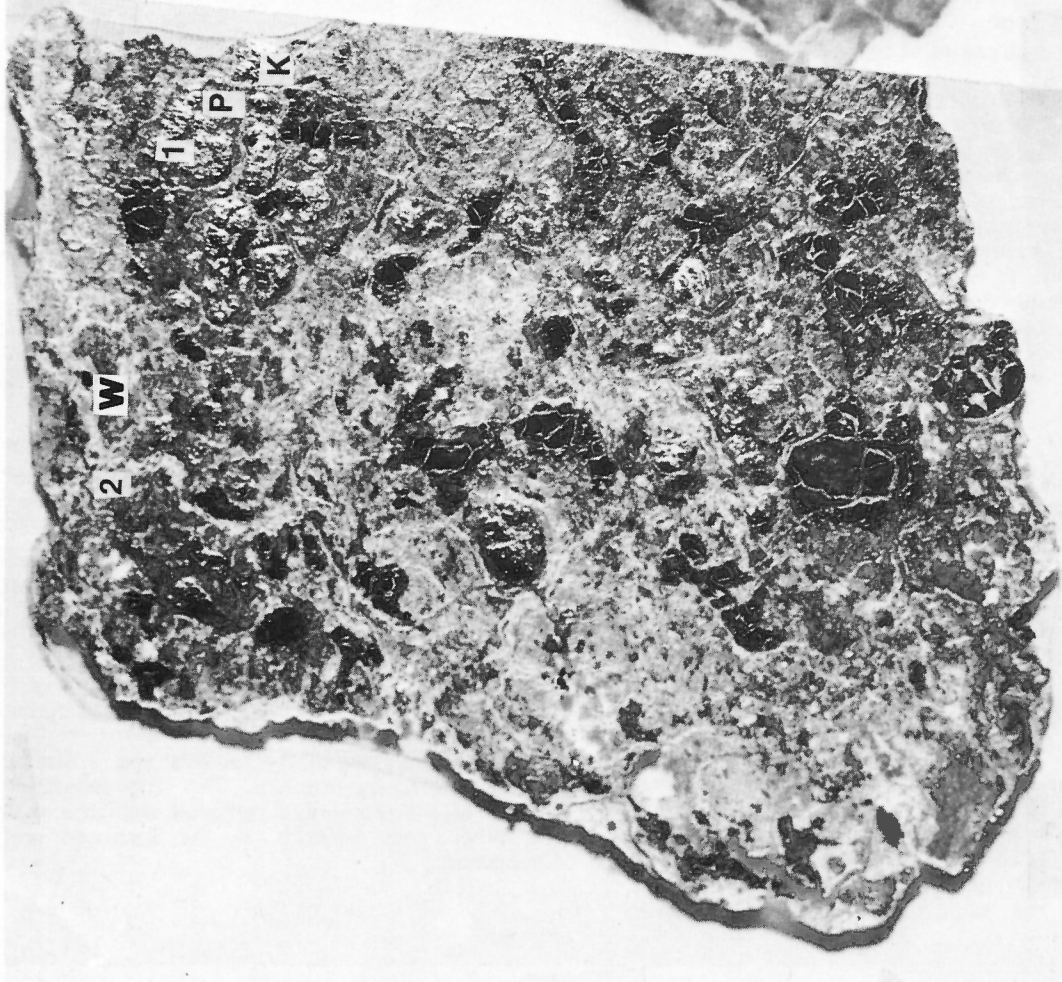


Figure 20.1a. Thin section of oxidized uranium ore showing the distribution of pitchblende (P) and of secondary compounds: kasolite (K), compounds X-1(1), and X-2(2), and wulfenite (W) (x 6.5; GSC 202203-N).

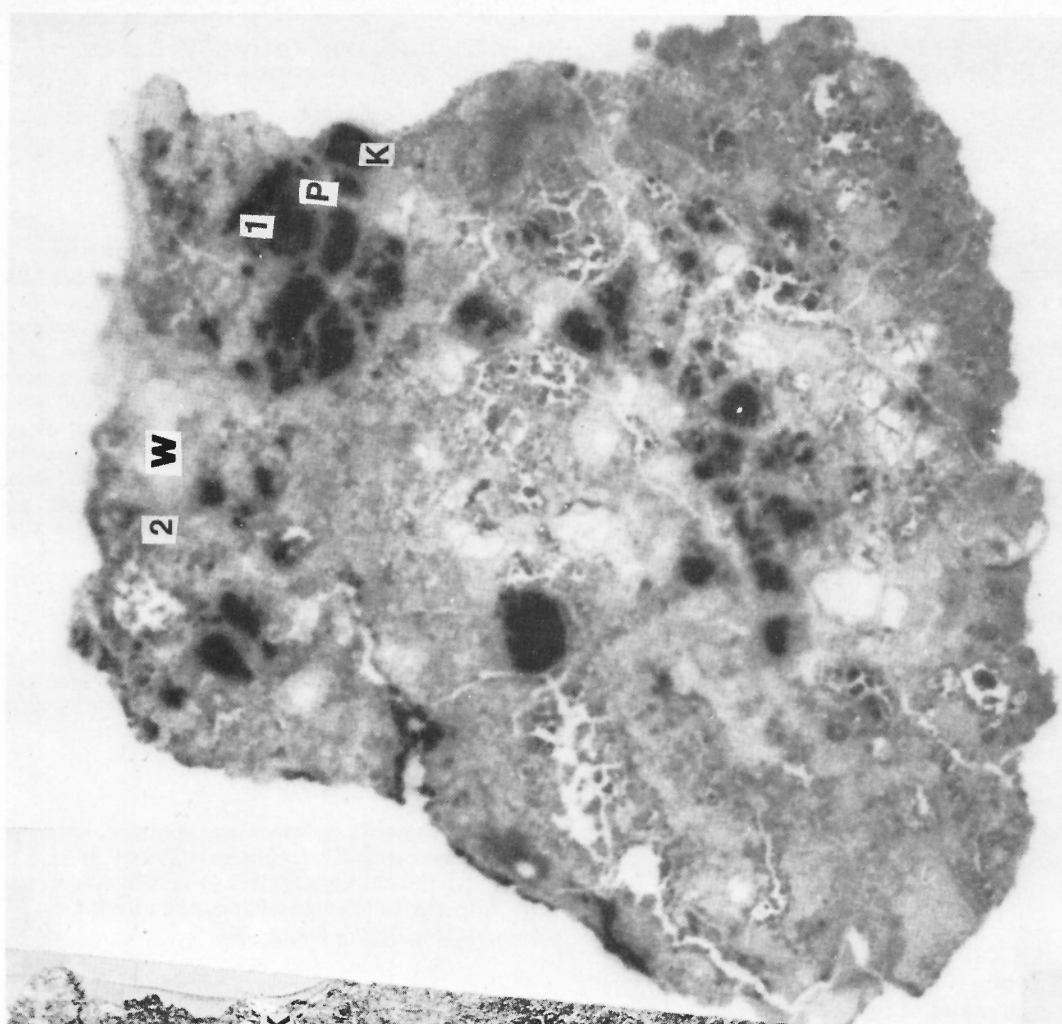


Figure 20.1b. Autoradiograph of thin section of oxidized uranium ore in Figure 20.1a showing the distribution of strongly radioactive compounds (black); pitchblende (P), kasolite (K), and aggregate X-1(1) in less radioactive matrix (grey) composed of aggregate X-2(2). White areas are non-radioactive wulfenite (W), quartz, and micaceous phyllosilicates (x 6.5).

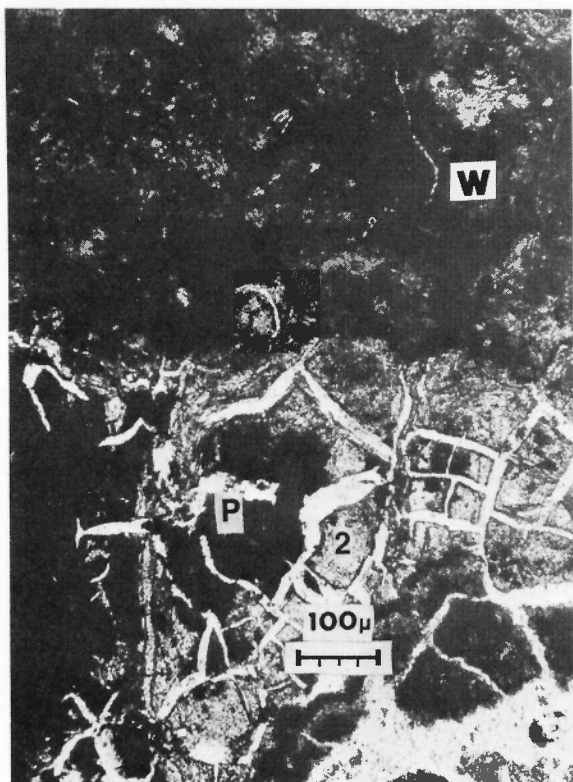


Figure 20.2.

Fine grained, semi-opaque wulfenite aggregates (W) in groundmass composed of compound X-2(2), hematite and quartz, with opaque remnants of partly resorbed pitchblende (P). White areas are fractures. Transmitted light, enlarged from Figure 20.1a. GSC XRD powder pattern numbers of aggregates identified in this thin section are as follows: uraninite (pitchblende) 57145; kasolite 57149; unidentified compound X-1 57146 and 57148; unidentified (amorphous) compound X-2 57144, and wulfenite 57143.

Acknowledgments

The author is very grateful to A.C. Roberts of Central Laboratories and Administrative Services Division, Geological Survey of Canada, for X-ray identification of the uranyl-carbonates and the other aggregates, and to Gulf Minerals Canada Limited, Uranerz Canada Limited and AMOK Limited for their permission to collect specimens in the mining localities.

References

- Axelrod, J.M., Grimaldi, F.S., Milton, C., and Murata, K.J.
 1951: The uranium minerals from Hillside Mine, Yavapai County, Arizona; *Am. Miner.*, v. 36, no. 1-2, p. 1-22.
- Branche, C., Chervet, J., and Guillemin, C.
 1951: Nouvelles espèces uranifères françaises; *Soc. Fr., Mineral. Cristallog.*, Bull., v. 74, p. 458-461.

Rimsaite, J.

1976: Progressive alteration of pitchblende in an oxidation zone of uranium deposits; 25th Internat. Geol. Cong., Sydney, Australia; Abstracts, v. 2, p. 594-595.

1977: Mineral assemblages at the Rabbit Lake uranium deposit, Saskatchewan; in Report of Activities, Part B, Geol. Surv. Can., Paper 77-1B, p. 235-246.

Stern, T.W. and Weeks, A.D.

1952: Second occurrence of bayleyite in the United States; *Am. Mineral.*, v. 37, no. 11-12, p. 1058-1060.

Traill, R.J.

1970: A catalogue of Canadian minerals; Geol. Surv. Can., Paper 69-45, p. 617.

NOTES ON A REPORT EVALUATING THE REGIONAL MINERAL POTENTIAL
(NON-HYDROCARBON) OF THE WESTERN ARCTIC REGION,
YUKON AND NORTHWEST TERRITORIES

G.B. Leech
Regional and Economic Geology Division

In connection with land claim negotiations on behalf of the Inuvialuit Nunangat, the native people of the western Canadian Arctic; the Committee for Original Peoples' Entitlement (COPE) requested that the Department of Energy, Mines and Resources provide it with an evaluation of the mineral potential of the region to which the Inuvialuit claim land rights. This region extends from longitude 110°W to longitude 141°W and its irregularly-shaped southern boundary lies mainly between latitudes 68°N and 69°N.

A report dealing with the non-hydrocarbon mineral potential of this region was prepared by members of the Economic Geology Subdivision of the Geological Survey in response to the COPE request. The report that was provided to COPE will be released late in 1977 as Open File 492.

This report provided an initial qualitative evaluation of a large region in which mineral discoveries are sparse and geological information is generally at only a reconnaissance level. Because of these factors, and because of the short time available in which to make the evaluations, it is only a preliminary assessment of this large region.

The report considers 17 commodities ranging from base metals to aggregate (construction) materials with principal attention devoted to lead and zinc. Small-scale maps illustrate the distribution of mineral occurrences and outline areas that are considered to be relatively favourable, in comparison with the rest of the region, for the occurrence of lead, zinc, copper and uranium.

Project 700041

J.L. Jambor¹ and J.M. Beaulne¹
Regional and Economic Geology Division

Introduction

Several large porphyry copper-molybdenum deposits, with aggregate reserves in excess of two billion tonnes grading more than 0.4 per cent copper-equivalent, are tightly clustered within an area of less than 4 km radius in the central part of Highland Valley, B.C., about 370 km northeast of Vancouver. Only two of the largest deposits are currently in production (Lornex and Iona, Fig. 22.1). In 1976, Lornex Mining Corp. milled approximately 43 000 tonnes per day having an average grade of 0.511 per cent copper and 0.016 per cent molybdenum (Lornex Mining Corp. Ltd., Annual Report, 1976); open-pit reserves at Lornex are more than 450 million tonnes grading 0.41 per cent copper and 0.015 per cent molybdenum (Waldner et al., 1976). The 1976 daily milling rate at Bethlehem Mining Corp. exceeded 19 000 tonnes grading 0.44 per cent copper; the ore was drawn from the Iona and Jersey deposits, whose open-pit reserves are approximately 41 million tonnes averaging 0.46 per cent copper (Bethlehem Copper Corp., Annual Report, 1976; Northern Miner, March 3, 1977). Bethlehem's J.A. deposit, if mined by underground methods, would yield about 120 million tonnes grading 0.51 per cent copper and 0.027 per cent molybdenum (Bethlehem Copper Corp., Annual Report, 1976). Valley Copper, the largest of the unexploited deposits, has reserves of about 800 million tonnes grading 0.48 per cent copper (Osatenko and Jones, 1976). The Highmont deposits are the most molybdenum-rich in the region; open-pit reserves at Highmont No. 1 deposit are about 111 million tonnes grading 0.287 per cent copper and 0.042 per cent MoS₂, and reserves in the No. 2 deposit are 24 million tonnes grading 0.273 per cent copper and 0.093 per cent MoS₂ (Reed and Jambor, 1976).

The Highmont, Lornex, and Valley Copper deposits were examined and sampled extensively during parts of three field seasons in order to study the mineralogy and hydrothermal alteration of the deposits. This note summarizes one aspect of a more detailed account (Jambor and Beaulne, in prep.) of the area which encompasses Highmont, Lornex, and Valley Copper.

The geology of the Highland Valley is discussed by McMillan (1976), and the local geology of the Highmont, Lornex, and Valley Copper properties has been presented most recently by Reed and Jambor (1976), Waldner et al. (1976), and Osatenko and Jones (1976). The porphyry deposits occur in the core of the Upper Triassic Guichon Creek batholith. Highmont and Lornex have the Skeena granodiorite phase of the batholith as principal host rocks, whereas Valley Copper is almost entirely in a slightly younger granodiorite to quartz monzonite known as the Bethsaida phase.

Regional Sulphide Zoning

The term "region" here denotes the area shown in Figure 22.4. Delineation of sulphide zonal patterns in the region is based on megascopic examination of about 100 000 m of drill core, supplemented by reflected-light studies of about 700 polished sections.

The major deposits have mappable pyritiferous peripheral zones but these do not have the high concentrations of pyrite which are typical of haloes around most porphyry deposits. Overall sulphide abundance at Highmont averages less than 1 per cent, whereas that at Valley Copper

is probably close to 1 per cent. Sulphide content of the Lornex ore zone has been estimated by Waldner et al. (1976) to be 1 to 1.5 weight per cent. Parts of the Lornex ore zone contain appreciable amounts of pyrite, thus accounting for higher sulphide abundances even though copper grade is less than that at Valley Copper; the latter deposit does not contain significant amounts of pyrite in its copper zone.

Sulphide ratios within the region were categorized as follows: (1) bornite zone: bornite present, but pyrite and chalcopyrite absent or very sparse. Zones of this category occur only at Highmont. (2) Bornite > chalcopyrite and (3) chalcopyrite > bornite: these categories reflect the predominance of one sulphide over the other, with the implication that both minerals are common and that pyrite is absent. (4) Bornite = chalcopyrite: proportions of the two minerals are approximately equal; rather than an obvious equality, this category was most commonly accepted because of uncertainty as to whether bornite or chalcopyrite was the more abundant. (5) Bornite + chalcopyrite: this category was generally used where sulphides are extremely sparse and a meaningful ratio either was not determinable or, in a few other cases, where the data obtainable were inadequate for a

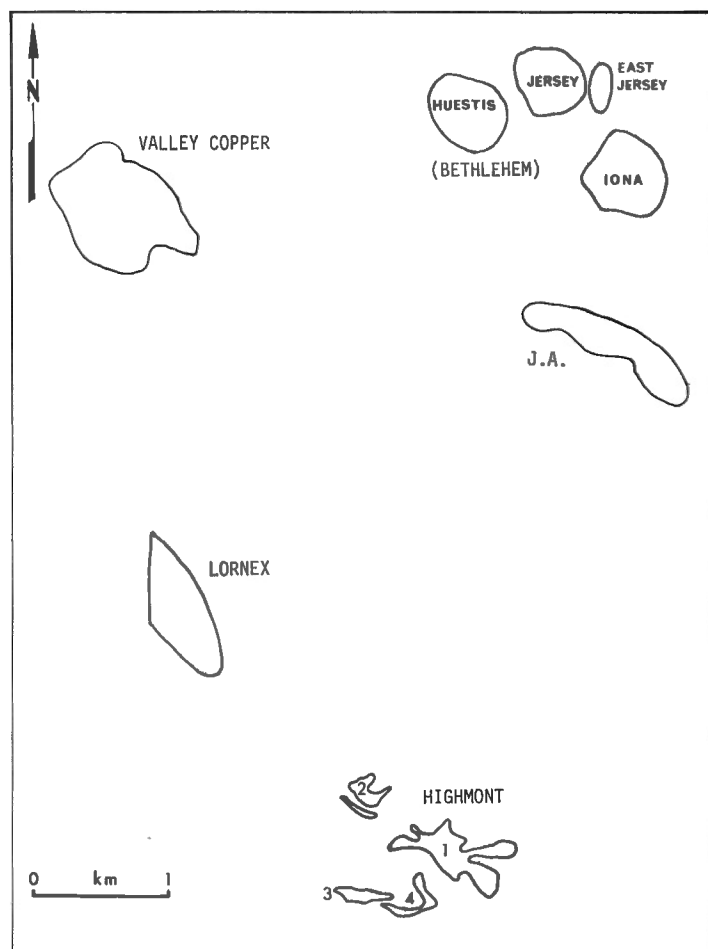


Figure 22.1. Relative positions of the major Highland Valley porphyry copper-molybdenum deposits. The area is about 30 km southeast of Ashcroft and about 50 km southwest of Kamloops.

¹ Present address: CANMET, 555 Booth Street, Ottawa

more precise classification. (6) Pyrite + chalcopyrite: pyrite abundances throughout the area are generally extremely low; thus, zones referred to as pyritiferous are intended to signify only that pyrite is present. However, chalcopyrite exceeds pyrite in the Valley Copper and Highmont ore zones, and in nearly all of the Lornex orebody. (7) Pyrite + chalcopyrite + bornite: this combination is extremely rare in the Valley Copper orebody, and is uncommon at Lornex. In contrast, several large zones in the category have been mapped at Highmont, but large parts of these have pyrite contents amounting to a very low percentage of total sulphide. Pyrite and bornite are generally antithetic except where sulphide content is less than 0.1 per cent of the rock.

Inclusion of a sulphide in any of the last three divisions (i.e., 5, 6, and 7) indicates that the mineral was observed persistently, even though its amount may have been small. These divisions therefore reflect more the frequency of occurrence of a sulphide rather than its relative abundance. In cases where a sulphide mineral lacked continuity in occurrences, its sporadic presence has been indicated by the symbol \pm . Discontinuous sulphides typically constitute only a fraction of a percentage of total sulphide.

The sulphide zones at Highmont have been given by Reed and Jambor (1976), and those for Lornex and Valley Copper are shown in Figures 22.2 and 22.3. At Valley Copper, a well-defined chalcopyrite-rich zone surrounds the bornite core and is in turn ringed by a pyritiferous zone in which sulphides are less than one volume per cent of the rock. The pyrite halo at Lornex is shown as a zone of pyrite + chalcopyrite (Fig. 22.2). Although both minerals decrease with distance from the orebody, the gradational decline in chalcopyrite is more rapid so that pyrite exceeds chalcopyrite in at least the outer half of this zone. The much greater width of the pyritiferous zone relative to that given by Waldner et al. (1976) probably reflects the different criteria used to delimit the outer boundary. Of principal concern here is the fact that the pyrite haloes for Lornex and Valley Copper show appreciable offset (Fig. 22.4). The significance of this offset is discussed in succeeding text.

Hydrothermal Biotite Alteration

The character and distribution of hydrothermal biotite alteration at Highmont were discussed by Reed and Jambor (1976). This type of alteration has also been mapped, by the present writers, for the Lornex and Valley Copper deposits. Intense biotite alteration overlaps and encompasses most of the copper zone at Valley Copper, and a broad aureole of weaker biotite alteration surrounds this core and gradually declines in intensity outward from it. Much of the hydrothermal biotite in the upper part of the Lornex deposit has been destroyed by superimposed phyllic, argillic, and propylitic hydrothermal alterations, but thin section studies indicate that the outer limit of hydrothermal biotitization probably did not extend more than about 100 m beyond the ore zone. The western part of the Lornex ore zone and biotite halo terminate against a major north-striking structure, the Lornex fault. Figure 22.5 shows that the biotite haloes for Lornex and Valley Copper apparently have been offset in a right-lateral direction, similar to that noted for the pyrite zones.

Lornex Fault

The Lornex fault bisects the region and truncates the Lornex orebody. McMillan (1971, 1976) and Waldner et al. (1976) have concluded that movement along the fault was right-lateral and reverse. The amounts of pre-ore versus post-ore movements had not been established, but geological contacts along this segment of the fault indicate a cumulative right-lateral offset of 5 to 6 km (McMillan, 1976).

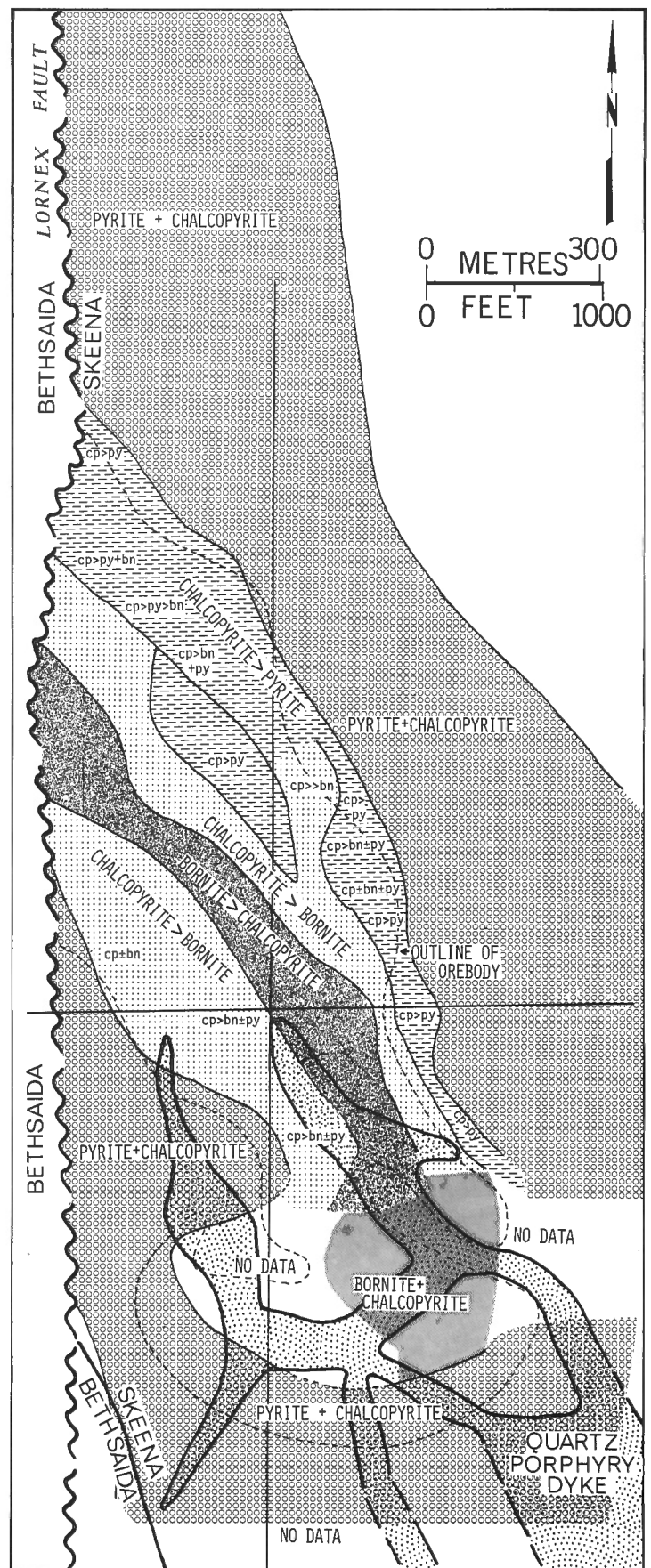


Figure 22.2. Sulphide zones at Lornex, projected to original bedrock surface (1375-1525 m). Geology is from Waldner et al. (1976) for the 1370-m level.

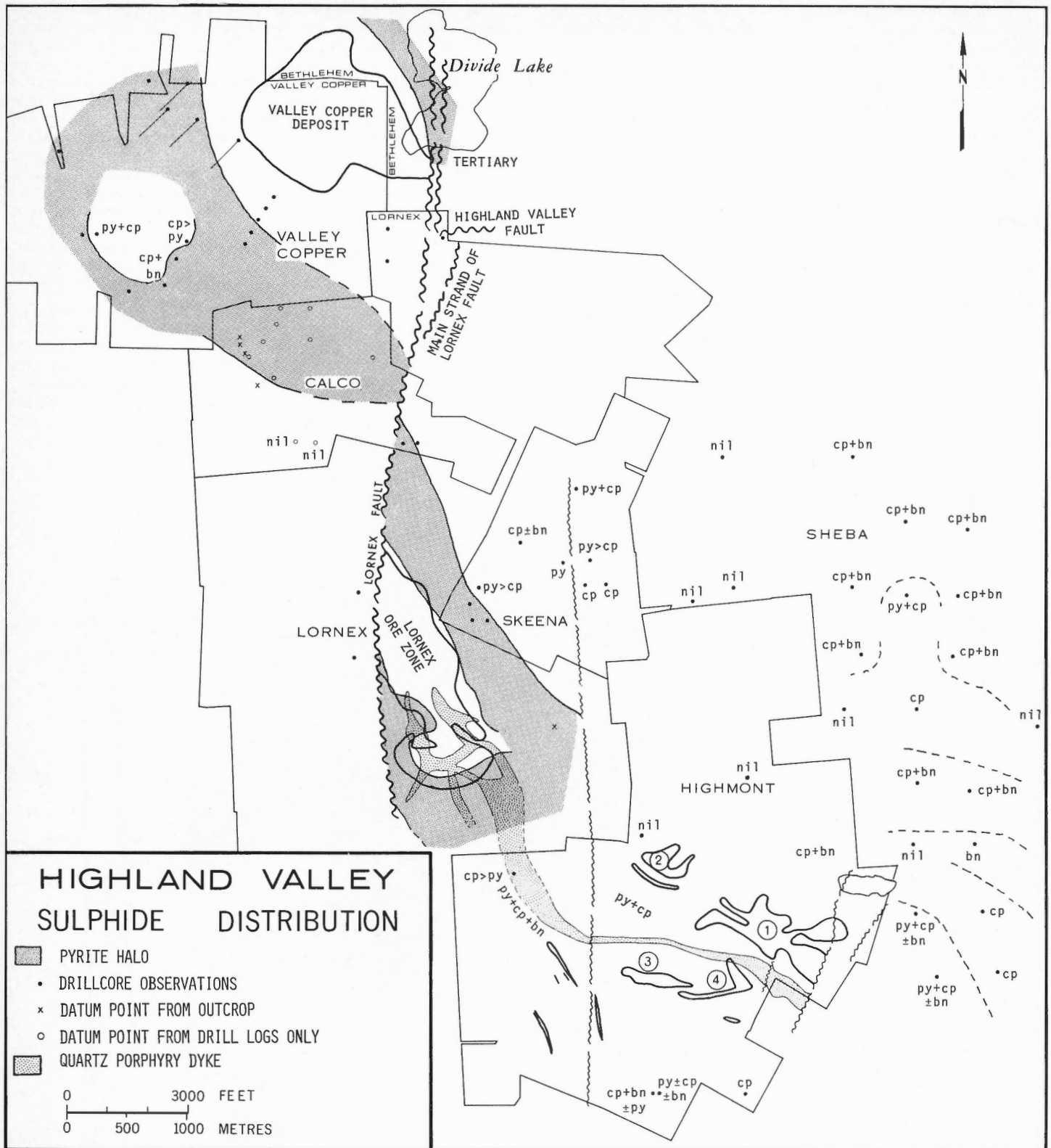


Figure 22.4. Regional sulphide variations in the southwestern part of central Highland Valley. Details for the Nos. 1 to 4 Highmont deposits are given in Reed and Jambor (1976), and the Lornex ore zone and Valley Copper deposit are shown in Figures 22.2 and 22.3. Sulphides in the Sheba drillholes are mostly at, or close to, background levels. The zone of chalcopyrite + bornite northeast of Highmont No. 1 deposit is based on results from several drillholes in this area. In the almost circular area about a km southwest of the Valley Copper deposit, pyrite decreases and copper sulphides increase; this area is considered to merit further exploration. The offset part of the Lornex ore zone is interpreted to abut the western side of the labelled main strand of the Lornex fault. The position of the main strand is not known exactly, but it is interpreted to be east of the drillhole near the Highland Valley fault. Dots represent the collar sites of drillholes.

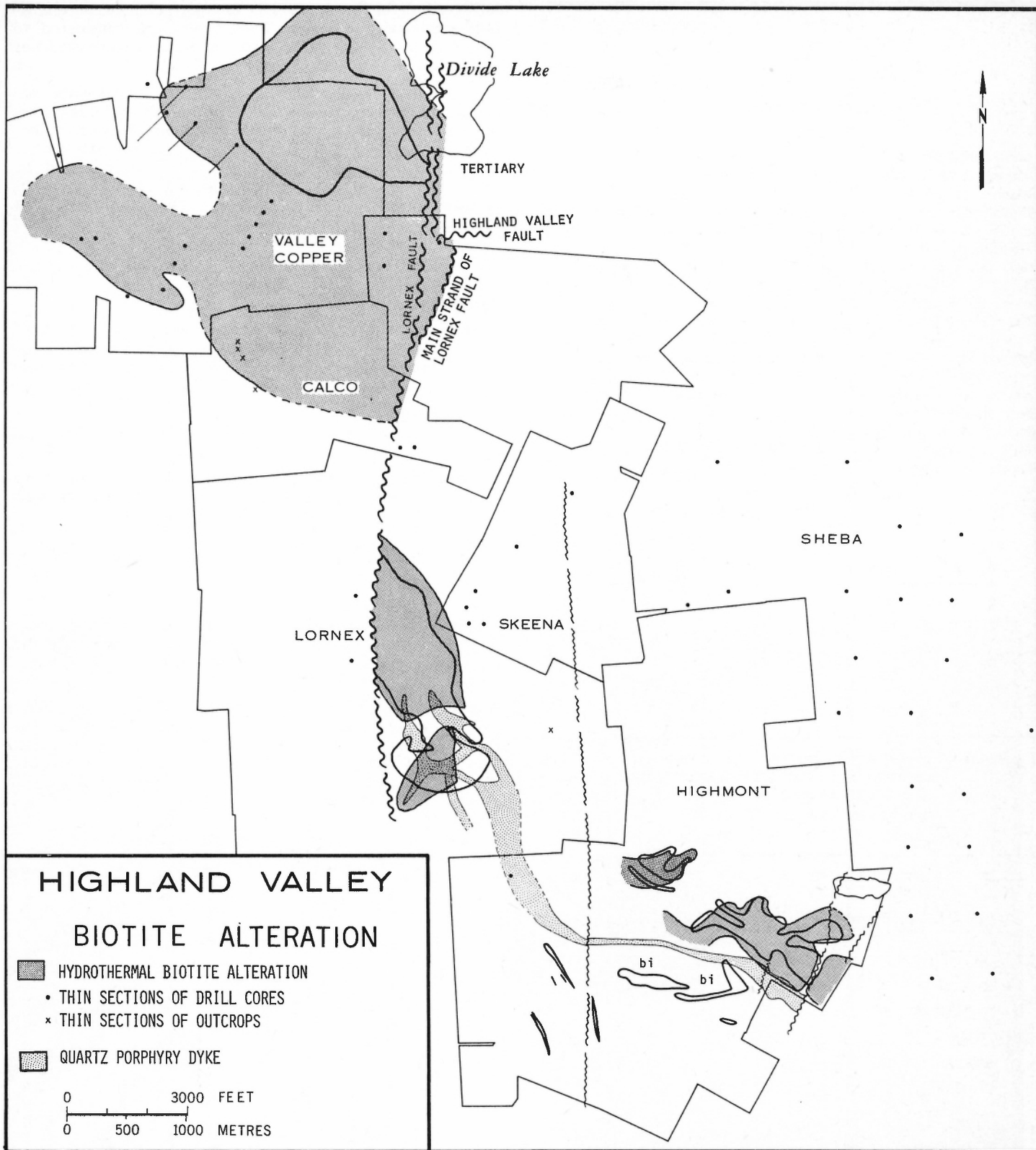


Figure 22.5. Regional distribution of hydrothermal biotite alteration in the southwestern part of central Highland Valley. Data for Highmont are from Reed and Jambor (1976), who noted that hydrothermal biotite (bi) is present also in the sulphide deposits south of the porphyry dyke which extends to Lornex. Dots represent collar sites of drillholes.

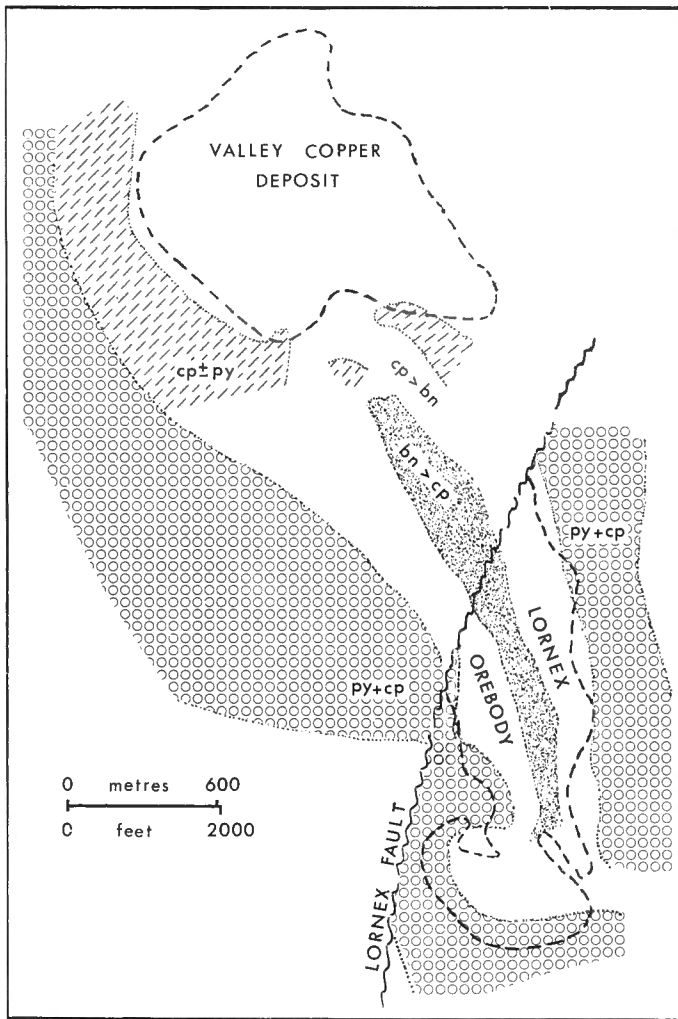


Figure 22.6. Restoration showing the interpreted relative positions of the Lornex and Valley Copper deposits and continuity of sulphide zones across the Lornex fault.

reflects progressive declines in intensity of potassic alteration and copper grades. These traits are considered to constitute valid criteria for assessing exploration possibilities in the Highland Valley.

Although megascopic identification of hydrothermal biotite in Highland Valley rocks is possible with practice, reliable identification requires microscopic study; thin sections are essential if alteration is weak. To evaluate biotite alteration, rocks with seemingly fresh mafics should be sought because overprinting by phyllic and argillic alterations destroys the hydrothermal biotite. Such overprinting is extensive in the Valley Copper and Lornex copper zones and has partly masked the well-developed biotite alteration in these deposits.

References

- Jambor, J.L. and Beaulne, J.M.
Sulphide zones and hydrothermal biotite alteration at porphyry copper-molybdenum deposits, Highland Valley, B.C.; Geol. Surv. Can. (in prep.).
- McMillan, W.J.
1971: Valley Copper; B.C. Dep. Mines Pet. Resour., Geology, Exploration and Mining, 1970, p. 354-369.
1976: Geology and genesis of the Highland Valley ore deposits and the Guichon Creek batholith; Can. Inst. Min. Met., Spec. Vol. 15, p. 85-104.
- Osatenko, M.J. and Jones, M.B.
1976: Valley Copper; Can. Inst. Min. Met., Spec. Vol. 15, p. 130-134.
- Reed, A.J. and Jambor, J.L.
1976: Highmont: linearly zoned copper-molybdenum deposits and their significance in the genesis of the Highland Valley ores; Can. Inst. Min. Met., Spec. Vol. 15, p. 163-185.
- Waldner, M.W., Smith, G.D., and Willis, R.D.
1976: Lornex; Can. Inst. Min. Met., Spec. Vol. 15, p. 120-129.

Project 750063

W. Blake, Jr.
Terrain Sciences Division

Part of the 1977 field season was devoted to investigating glacial features in the vicinity of Cape Herschel and Pim Island, on the east-central coast of Ellesmere Island (Figs. 23.1, 23.2). The Cape Herschel station of the "North Water Project" (Müller et al., 1975) was utilized for the duration of our stay, and a period of exceptionally good weather between July 15th and 25th facilitated field observations and travel.

Cape Herschel is the easternmost promontory of Johan Peninsula, and together with Pim Island, which is separated from Johan Peninsula by Rice Strait, it juts out into Smith Sound at the entrance to Kane Basin. The eastern side of Pim Island is only 40 km from the nearest point on the Greenland coast. The highest points on Cape Herschel and Pim Island are approximately 285 m and 550 m a.s.l., respectively. Both areas consist for the most part of massive red granite, gneissic in places (Christie, 1962) and physiographically they are plateaus with undulating surfaces surrounded by steep slopes or cliffs to the sea. Holocene marine deposits were not discovered above approximately 85 to 90 m a.s.l. in the vicinity of Cape Herschel or in the valley south of the abandoned R.C.M.P. Post at Alexandra Fiord.

The most striking feature of Cape Herschel and Pim Island is that they have been overridden and deeply sculptured by glacier ice flowing from north to south. Roches moutonnées abound, their polished, striated, and grooved north sides and plucked south sides showing clearly the direction in which the ice moved. In fact, the highest points on both Cape Herschel and Pim Island are fine examples of this type of landform. Figures 23.3 to 23.8 illustrate some of the well developed features which have resulted from glacial sculpturing. On a larger scale, steep yet rounded slopes are present on the northeast side of Cape Herschel for instance, but the southeast side, overlooking Herschel Bay, is dominated by cliffs. Striae with the same orientation are displayed near Cape Herschel on Christie's (1962) map, however, the sense of ice movement is not indicated. On the "Glacial Map of Canada" the direction of ice flow is given as northward by a striae symbol on Pim Island (Prest et al., 1968), but in view of the observations made in 1977 this must be modified.

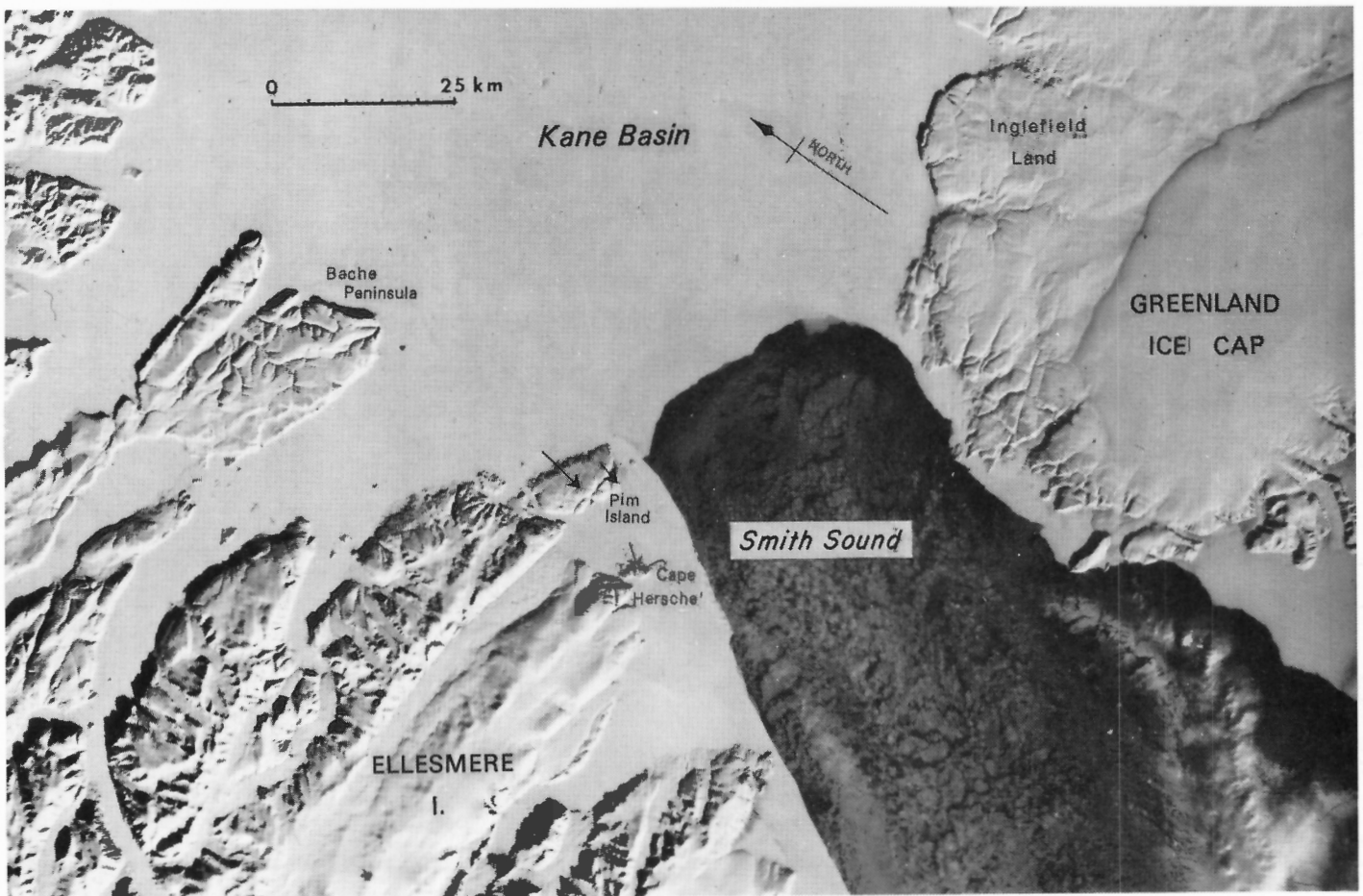


Figure 23.1. LANDSAT image showing Smith Sound and southern Kane Basin. Black arrows indicate direction of ice flow across Pim Island and Cape Herschel. Note the development of the North Water on April 4, 1973 (image E-10255-18054, spectral band 7).

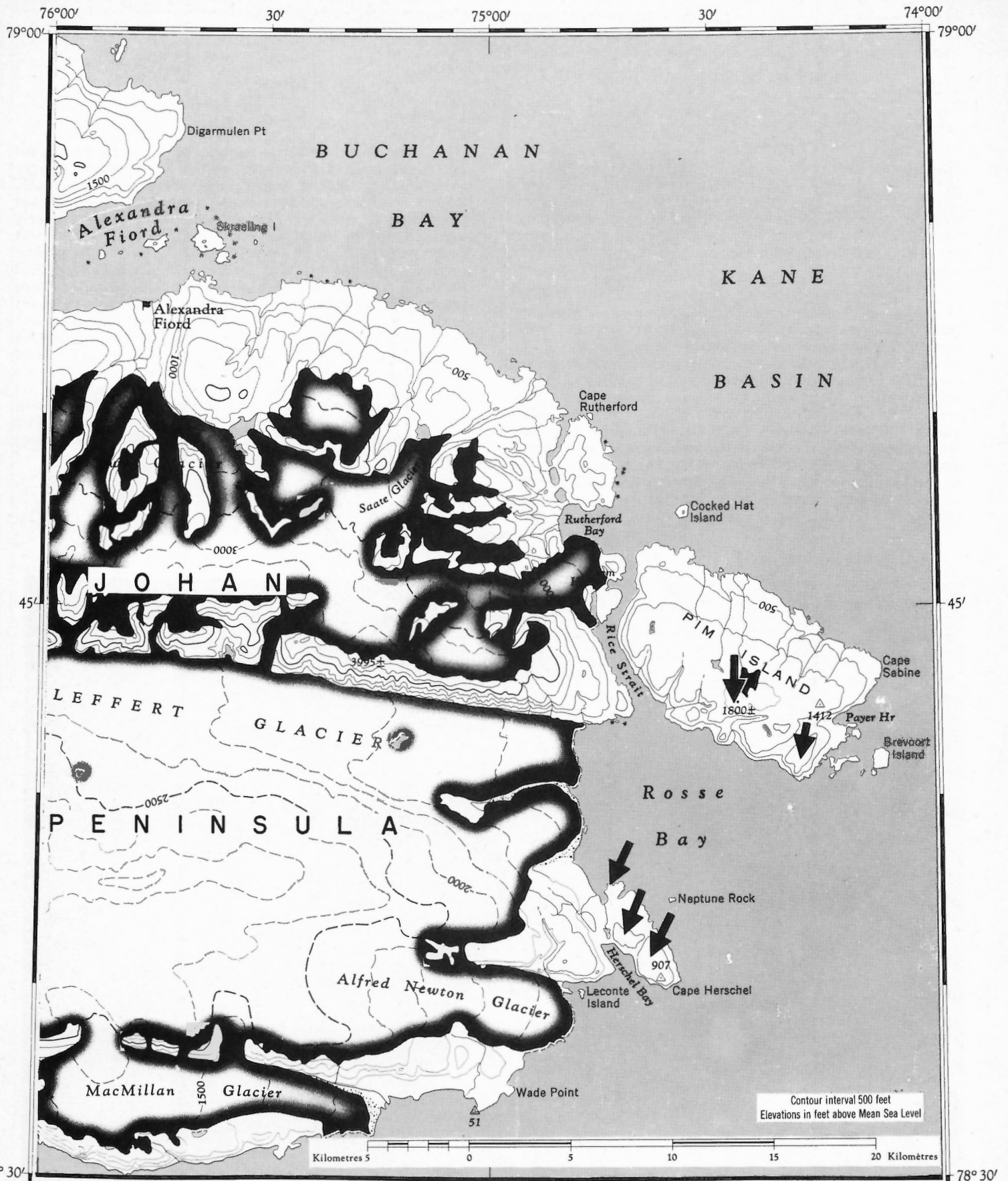


Figure 23.2. Location map of features and sites referred to in the text. Black arrows indicate how the ice, which formerly flowed out of Kane Basin, moved across Pim Island and Cape Herschel at right angles to the present-day direction of flow of Leffert and Alfred Newton glaciers. Base map is 1:250 000 NTS map-sheet 39F and 39E, Ekblaw Glacier (1967).



Rocks below Cambridge
Cape Herschel,
July 77

Figure 23.3.
Glacially sculptured and polished granite below the limit of postglacial marine submergence near Cape Herschel base. Note the rounded contours of the rock surface on the left (northeast) and the plucked lee side to the right (southwest), the direction in which the ice was flowing. Reproduced with permission from a drawing by John Leaning, July 20, 1977.



Figure 23.4. Striated granite surface on the side of a through-valley on the plateau near Cape Herschel, at an elevation of approximately 180 m a.s.l. Ice motion was toward the south-southwest, from right to left in the photograph. July 17, 1977 (GSC-203240).



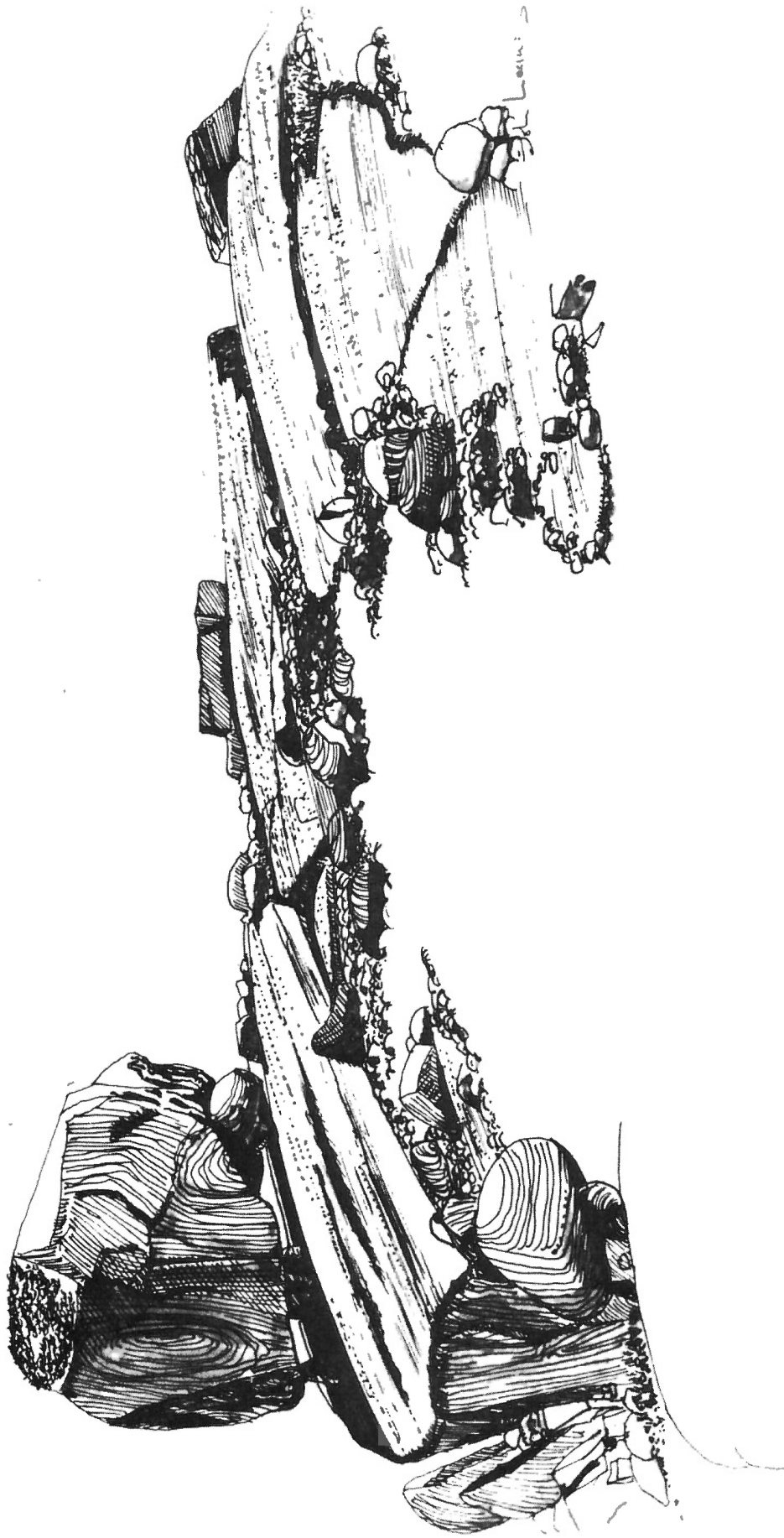
Figure 23.5. Striated and polished granite outcrop on the summit of the plateau above Cape Herschel, at an elevation of approximately 280 m. View toward the northwest. Note the plucked lee side side toward the south-southwest (left), the direction in which the ice moved across this plateau. July 17, 1977 (GSC-203238).



Figure 23.6. View west at a glacially sculptured bedrock knob, with a perched boulder, on the plateau of Pim Island near its southeast corner, elevation circa 440 m a.s.l. This striated granite outcrop displays the typical rounded stoss side (to the right) and plucking on the lee side (left). Ice formerly flowed across the plateau of Pim Island from north to south, precisely at right angles to the present day direction of flow of Leffert Glacier (arrow), seen in the distance across Rosse Bay. July 21, 1977 (GSC-203241).



Figure 23.7. View east across the summit plateau of Pim Island, from the highest point at approximately 550 m a.s.l. Note the smoothed rock boss in the foreground. The plucked lee side to the right (south), the direction in which the ice flowed, is over 3 m high. July 22, 1977 (GSC-203242).



Rocks about
Cape Herschel.
Ellomere. July 72.

Figure 23.8.
Striated granite and perched boulders on the Cape Herschel plateau, elevation circa 200 m.
Ice flowed from left to right, toward the south-southwest.
Reproduced with permission from a drawing by John Leaning, July 21, 1977.

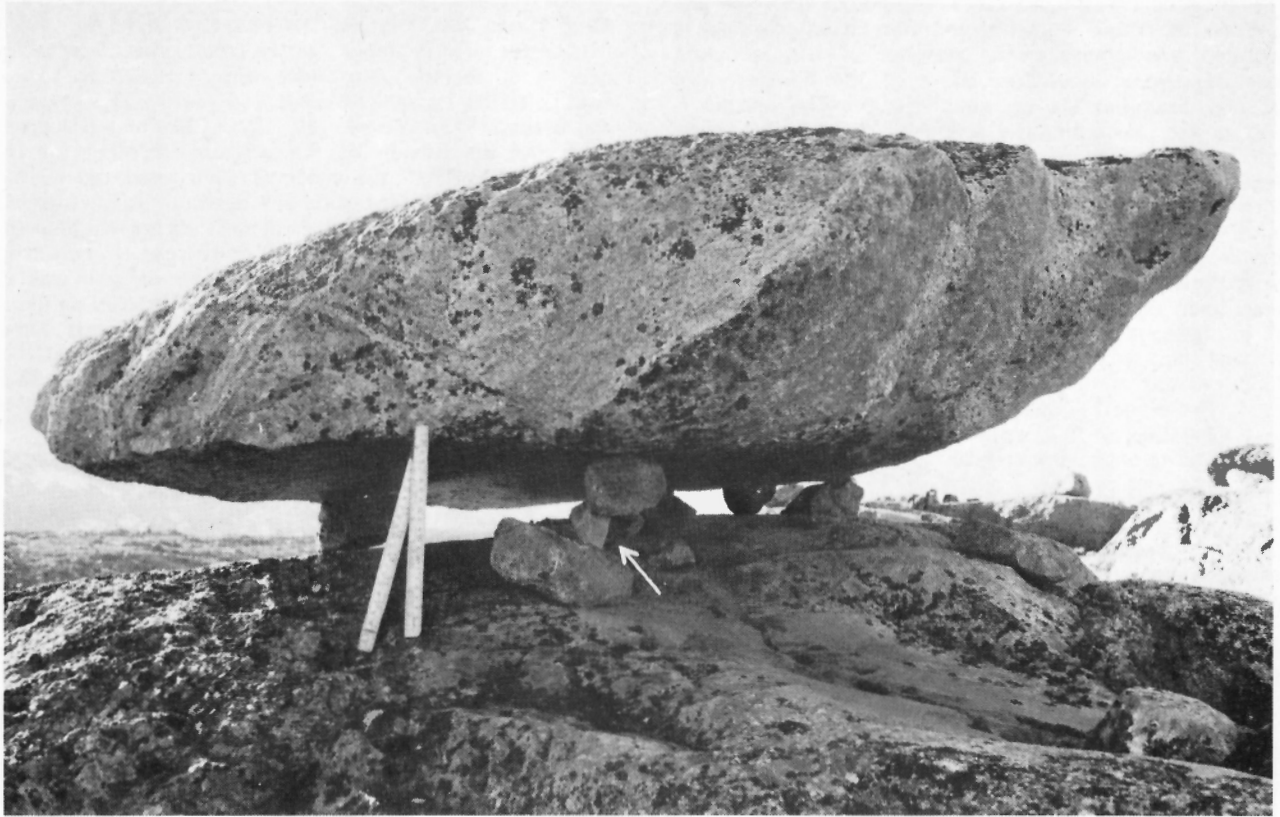


Figure 23.9. Perched boulder of grey granite on red granite bedrock, Cape Herschel plateau. This erratic measures 145 x 180 cm and is 25 to 40 cm thick (the length of the vertical rule is 22 cm). It is balanced on five supports, and at the corner nearest the observer the support is a stack of three angular cobbles, the middle one of which (arrow) is grey limestone-dolomite. July 17, 1977 (GSC-203239).



Figure 23.10. Detail of striated and polished granite surface near the highest point of Pim Island. The direction of ice flow is away from the observer (toward the south). Note the absence of differential weathering at the contacts with the aplite dyke. July 22, 1977 (GSC-203243).

In addition to the features carved in bedrock the landscape on the Cape Herschel and Pim Island plateaus is characterized everywhere by the presence of till, including thousands of erratic boulders. Many of the boulders are perched, and examples are shown in Figures 23.8 and 23.9. The erratics are predominantly sedimentary rocks which do not outcrop nearer than Alexandra Fiord, about 30 km to the northwest of Pim Island, or on Bache Peninsula, approximately the same distance to the north. Rock types present include all of those grouped by Christie (1962) under the Proterozoic and Lower Paleozoic category — dolomite (in part stromatolitic), limestone, limestone-dolomite breccia, sandstone, and conglomerate — as well as a considerable variety of igneous and metamorphic rocks. In addition, fragments of marine mollusc shells were found in till at high elevations on the summit plateaus of Cape Herschel and Pim Island. These shell fragments are also a type of erratic, like those Christie (1967) described from Bache Peninsula at elevations of up to approximately 460 m.

The fact that Pim Island and Cape Herschel have been overridden by southward-flowing ice is of considerable importance to a proper understanding of the glacial history of the entire region (cf. recent reviews by Andrews and Miller, 1976; Weidick, 1976a, b; Paterson, 1977; Paterson et al., 1977). Flow toward the south, and in the case of Cape Herschel toward the south-southwest, could not have been accomplished unless Smith Sound were filled by an outlet glacier draining from Kane Basin. This relatively shallow body of water, in which depths over 500 m are common only near its junction with Smith Sound¹, must have been filled completely with ice which originated from both the Greenland Ice Sheet and the Innuitian Ice Sheet (cf. Blake, 1970). Presumably the Humboldt Gletscher, which is today about 90 km wide at its snout (over twice the width of Smith Sound at Pim Island) and is the sole outlet glacier entering the eastern side of Kane Basin, was the main drainageway for Greenland ice. To the west, valley glaciers in the numerous fiords which indent the Ellesmere Island coast funnelled ice into Kane Basin from the Innuitian Ice Sheet. The volume of ice flowing southward was apparently such that it could impinge on, and inundate, Pim Island and Cape Herschel. Although Pim Island rises close to 1200 m above the deepest parts of Smith Sound, because of the constricted width of the Sound as compared to Kane Basin (40 km as opposed to approximately 100 km), there was no place for the ice to escape except over the adjacent landmasses. In fact, the force of the ice flowing out of Kane Basin was sufficiently great to deflect the ice streams entering from the Ellesmere side, hence the south-southwestward direction of flow across Cape Herschel.

Not only is the wealth of glacial sculpture on Cape Herschel and Pim Island impressive, but the freshness of all features — the incredible array of perched boulders (Figs. 23.8, 23.9), and the lack of differential weathering along the contacts between rocks of different grain size (Fig. 23.10) provide convincing evidence that the ice which eroded and polished these rocks flowed out of Kane Basin in late Wisconsin time. If the carving of these textbook glacial features had been accomplished during an earlier glaciation, say during early Wisconsin time (> 50 000 years ago?) then it would be reasonable to expect destruction of fine striae and polished surfaces, the development of weathering pits, and the toppling over of precariously perched boulders; however, none of this has happened.

Relatively little is known of the absolute chronology of glacial events around Kane Basin. A number of radiocarbon age determinations from Inglefield Land, Greenland, have been published by Nichols (1969) and Tedrow (1970). The oldest Holocene materials — both peat and marine shells — reported by Nichols (1969) are 7800 ± 200 years old

(L-1091A and L-1091E, respectively). On the Ellesmere side of Kane Basin the only radiocarbon date available for raised marine features is one on marine pelecypods collected in 1968 near the former Alexandra Fiord R.C.M.P. Post by R.L. Christie; its age is 6220 ± 140 years (GSC-1348; Lowdon and Blake, 1973). A new collection of *Macoma calcarea* shells from the distal side of the moraine forming the head of Herschel Bay is in the order of 9000 years old (GSC-2516). This is the first radiocarbon age determination obtained from the shores of Smith Sound. Additional dates will help to fill in details of the pattern of ice retreat. However, the distribution of moraines suggests that ice still was flowing into the low-lying pass between Cape Herschel peninsula and the higher land of Johan Peninsula to the west some 9000 years ago. Much of the Cape Herschel plateau, including features such as those illustrated in Figures 23.4, 23.5, 23.8 and 23.9 probably has been ice-free for approximately the same length of time.

Acknowledgments

Excellent base camp facilities and helicopter support were made available by T. Frisch, Regional and Economic Geology Division, and Twin-Otter support was provided by the Polar Continental Shelf Project (G.D. Hobson, Director). I also am indebted to T. Frisch and W.C. Morgan for much valuable information on bedrock geology. R.J. Richardson assisted in the field, and John Leaning, who joined us for the stay at Cape Herschel, kindly supplied the drawings reproduced as Figures 23.3 and 23.8. B.G. Craig and D.A. Hodgson reviewed the manuscript.

References

- Andrews, J.T. and Miller, G.H.
1976: Quaternary glacial chronology of the eastern Canadian Arctic: A review and a contribution on amino acid dating of Quaternary molluscs from the Clyde cliffs; in Quaternary Stratigraphy of North America, ed. W.C. Mahaney; Dowden, Hutchinson & Ross, Inc., Stroudsburg, Pa., p. 1-32.
- Blake, W., Jr.
1970: Studies of glacial history in Arctic Canada. I. Pumice, radiocarbon dates and differential post-glacial uplift in the eastern Queen Elizabeth Islands; *Can. J. Earth Sci.*, v. 7, p. 634-664.
- Christie, R.L.
1962: Geology, Alexandra Fiord, Ellesmere Island, District of Franklin; *Geol. Surv. Can.*, Map 9-1962.
1967: Bache Peninsula, Ellesmere Island, Arctic Archipelago; *Geol. Surv. Can.*, Mem. 347, 63 p.
- Lowdon, J.A. and Blake, W., Jr.
1973: Geological Survey of Canada radiocarbon dates XIII; *Geol. Surv. Can.*, Paper 73-7, 61 p.
- Müller, F., Blatter, H., and Kappenberger, G.
1975: Temperature measurement of ice and water surfaces in the North Water area using an airborne radiation thermometer; *J. Glaciol.*, v. 15, p. 241-250.
- Nichols, R.F.
1969: Geomorphology of Inglefield Land, North Greenland; *Medd. Grønland*, v. 188, no. 1, 109 p.
- Paterson, W.S.B.
1977: Extent of the Late-Wisconsin glaciation in north-west Greenland and northern Ellesmere Island: a review of the glaciological and geological evidence; *Quat. Res.*, v. 8, p. 180-190.

¹ See Pelletier (1966), who described Kane Basin as a drowned watershed from which ice flowed both north and south. Also Chart 896, "Arctic Bathymetry north of 72°, 0° to 90° West", Canadian Hydrographic Service, 1967.

- Paterson, W.S.B., Koerner, R.M., Fisher, D., Johnsen, S.J., Clausen, H.B., Dansgaard, W., Bucher, P., and Oeschger, H.
1977: An oxygen-isotope climatic record from the Devon Island ice cap, Arctic Canada; *Nature*, v. 266, p. 508-511.
- Pelletier, B.R.
1966: Development of submarine physiography in the Canadian Arctic and its relation to crustal movements; in *Continental Drift*, ed. G.D. Garland; Roy. Soc. Can., Spec. Publ. 9, p. 77-101.
- Prest, V.K., Grant, D.R., and Rampton, V.N.
1968: Glacial map of Canada; *Geol. Surv. Can.*, Map 1253A.
- Tedrow, J.C.F.
1970: Soil investigations in Inglefield Land, Greenland; *Medd. Grønland*, v. 188, no. 3, 93 p.
- Weidick, A.
1976a: Glaciation and the Quaternary of Greenland; in *Geology of Greenland*, ed. A. Escher and W.S. Watt; *Grønlands Geol. Undersøgelse*, p. 430-458.
1976b: Glaciation of northern Greenland – new evidence; *Polarforschung*, 46 Jahrgang, p. 26-33.

AUTHOR INDEX

Bracketed numbers refer to individual reports within this publication

	Page		Page
Beaulne, J.M. (22)	101	Manchester, K.S. (2)	9
Bird, J. Brian (10)	53	Mitchell, W. (3)	13
Blake, W. Jr. (23)	107	Norris, D.K. (17)	81
Cole, F.E. (1)	1	Overton, A. (4)	19
Currie, R.G. (19)	89	Pelchat, J.C. (18)	85
Dyck, W. (18)	85	Perry, J. (3)	13
Ford, D.C. (9)	49	Rimsaite, J. (20)	95
Fowler, G.A. (2)	9	Robbins, D. (3)	13
Ghent, E.D. (3)	13	Schafer, C.T. (1)	1
Grasty, R.L. (12)	61	(2)	9
Heginbottom, J.A. (7)	35	(5)	27
Jambor, J.L. (22)	101	Schwarcz, H.P. (9)	49
Kerr, J.Wm. (15)	75	Sinha, A.K. (13)	63
(16)	79	Simony, P.S. (3)	13
Kurfurst, P.J. (6)	33	Taylor, R.B. (8)	39
(7)	35	Tempelman/Kluit, D.J. (19)	89
Lau, J.S.O. (7)	35	Wagner, F.J.E. (1)	1
Leech, G.B. (21)	99	(11)	57
		Wagner, J. (3)	13
		Young, F.G. (14)	67
		Young, J.A. (5)	27